Development of ^{99m}Tc Agents for Imaging Central Neural System Receptors

IAEA
International Atomic Energy Agency

DEVELOPMENT OF ^{99m}Tc AGENTS FOR IMAGING CENTRAL NEURAL SYSTEM RECEPTORS

The following States are Members of the International Atomic Energy Agency:

AFGHANISTAN
ALBANIA
ALGERIA
ANGOLA
ARGENTINA
ARMENIA
AUSTRALIA
AUSTRIA
AZERBAIJAN
BANGLADESH
BELARUS
BELGIUM
BENIN
BOLIVIA
BOSNIA AND HERZEGOVINA
BOTSWANA
BRAZIL
BULGARIA
BURKINA FASO
CAMEROON
CANADA
CENTRAL AFRICAN
  REPUBLIC
CHILE
CHINA
COLOMBIA
COSTA RICA
CÔTE D'IVOIRE
CROATIA
CUBA
CYPRUS
CZECH REPUBLIC
DEMOCRATIC REPUBLIC
  OF THE CONGO
DENMARK
DOMINICAN REPUBLIC
ECUADOR
EGYPT
EL SALVADOR
ERITREA
ESTONIA
ETHIOPIA
FINLAND
FRANCE
GABON
GEORGIA
GERMANY
GHANA
GREECE

GUATEMALA
HAITI
HOLY SEE
HONDURAS
HUNGARY
ICELAND
INDIA
INDONESIA
IRAN, ISLAMIC REPUBLIC OF
IRAQ
IRELAND
ISRAEL
ITALY
JAMAICA
JAPAN
JORDAN
KAZAKHSTAN
KENYA
KOREA, REPUBLIC OF
KUWAIT
KYRGYZSTAN
LATVIA
LEBANON
LIBERIA
LIBYAN ARAB JAMAHIRIYA
LIECHTENSTEIN
LITHUANIA
LUXEMBOURG
MADAGASCAR
MALAYSIA
MALI
MALTA
MARSHALL ISLANDS
MAURITIUS
MEXICO
MONACO
MONGOLIA
MOROCCO
MYANMAR
NAMIBIA
NETHERLANDS
NEW ZEALAND
NICARAGUA
NIGER
NIGERIA
NORWAY
PAKISTAN
PANAMA
PARAGUAY

PERU
PHILIPPINES
POLAND
PORTUGAL
QATAR
REPUBLIC OF MOLDOVA
ROMANIA
RUSSIAN FEDERATION
SAUDI ARABIA
SENEGAL
SERBIA AND MONTENEGRO
SEYCHELLES
SIERRA LEONE
SINGAPORE
SLOVAKIA
SLOVENIA
SOUTH AFRICA
SPAIN
SRI LANKA
SUDAN
SWEDEN
SWITZERLAND
SYRIAN ARAB REPUBLIC
TAJIKISTAN
THAILAND
THE FORMER YUGOSLAV
  REPUBLIC OF MACEDONIA
TUNISIA
TURKEY
UGANDA
UKRAINE
UNITED ARAB EMIRATES
UNITED KINGDOM OF
  GREAT BRITAIN AND
  NORTHERN IRELAND
UNITED REPUBLIC
  OF TANZANIA
UNITED STATES OF AMERICA
URUGUAY
UZBEKISTAN
VENEZUELA
VIETNAM
YEMEN
ZAMBIA
ZIMBABWE

The Agency's Statute was approved on 23 October 1956 by the Conference on the Statute of the IAEA held at United Nations Headquarters, New York; it entered into force on 29 July 1957. The Headquarters of the Agency are situated in Vienna. Its principal objective is "to accelerate and enlarge the contribution of atomic energy to peace, health and prosperity throughout the world''.

TECHNICAL REPORTS SERIES No. 426

DEVELOPMENT OF ^{99m}Tc AGENTS FOR IMAGING CENTRAL NEURAL SYSTEM RECEPTORS

INTERNATIONAL ATOMIC ENERGY AGENCY
VIENNA, 2004

FOREWORD

Radiopharmaceuticals that bind to central neural system (CNS) receptors in vivo are potentially useful for understanding the pathophysiology of a number of neurological and psychiatric disorders, their diagnosis and treatment. Carbon-11 labelled compounds and positron emission tomography (PET) imaging have played a vital role in establishing the usefulness of imaging the dopaminergic, cholinergic, serotonergic and benzodiazapine receptors, and relating the receptor density to disease status.

Since the use of ^{11}C agents is constrained due to their 20 min half-life, various radiohalogenated analogues based on the structure of ^{11}C compounds have been successfully developed, providing comparable information. Iodine-123 is the most widely employed of these radioisotopes; it has a longer, 13 h, half-life. Through the use of ^{123}I, there has been a steady growth in CNS receptor imaging studies employing single photon emission computerized tomography (SPECT). SPECT, as compared with PET, has slightly inferior image resolution but has the advantage of being readily available worldwide. However, the ^{123}I radiopharmaceutical is expensive and the distribution system outside of the major markets is not well developed for its supply on a routine basis.

The ideal radioisotope for SPECT imaging is ^{99m}Tc, due to its low cost per dose, availability through commercially available generator systems and physical decay characteristics. Over 80% of all diagnostic nuclear medicine imaging studies worldwide are conducted using this radioisotope.

Development of ^{99m}Tc radiopharmaceuticals for imaging CNS receptors is therefore of considerable importance.

On the basis of the recommendations of a consultants meeting, the International Atomic Energy Agency (IAEA) initiated in 1996 a Co-ordinated Research Project (CRP) on Development of Agents for Imaging CNS Receptors based on ^{99m}Tc. At that time there were no ^{99m}Tc CNS receptor imaging radiopharmaceuticals available even though work on development was being pursued in a few laboratories. The CRP, in which ten laboratories from Asia, Europe and Latin America participated, was concluded in 2001. Four Research Co-ordination Meetings (RCMs) to review the results were held: in Dresden, Athens, Montevideo and at IAEA headquarters in Vienna. There was considerable collaboration and co-operation between the participating laboratories.

The results of the work carried out in the participating laboratories under the CRP are described in this report. It is expected that these will be useful for radiopharmaceutical scientists worldwide who are working on the

development of ^{99m}Tc radiopharmaceuticals in general and ^{99m}Tc CNS agents in particular.

The IAEA wishes to thank all the participants for their co-operation. D.V.S. Narasimhan of the Division of Physical and Chemical Sciences was the IAEA officer responsible for this report.

CONTENTS

CHAPTER 10. LABELLING OF CENTRAL NEURAL SYSTEM
RECEPTOR LIGANDS WITH THE *fac*-[Tc(CO)$_3$]$^+$ MOIETY . .
R. Alberto, J. Bernhard, J. Wald

CHAPTER 11. DEVELOPMENT OF NOVEL MIXED LIGAND
TECHNETIUM COMPLEXES FOR IMAGING 5-HT$_{1A}$
NEURAL SYSTEM RECEPTORS . . . .
A.S. León, A. Rey, E.T. León, M. Pagano, J. Gigilio, E. Manta,
M.L. Mallo

PART I

OVERVIEW OF THE
CO-ORDINATED RESEARCH PROJECT

Chapter 1

RESULTS AND ACHIEVEMENTS

1.1. INTRODUCTION

It is generally acknowledged that diagnostic nuclear medicine, compared with other imaging modalities, has as its major strength the ability to measure or estimate organ function and to probe the biochemical processes which underlie diseases. While the pre-eminence of nuclear medicine in functional imaging is beginning to be eroded by magnetic resonance imaging (MRI), its unique ability to provide information on biochemical processes remains a strong asset. This is especially true when information is required on the relationships between the densities of low capacity, high specificity receptors and disease status. High specific activity radiopharmaceuticals are ideal non-invasive probes of such receptor systems, especially for receptors in the central neural system (CNS).

The CNS receptor related diseases are epilepsy (benzodiazepin receptor), Alzheimer's disease (cholinergic receptor), Parkinson's disease (dopaminergic receptor), and depression and other psychiatric diseases (serotonergic receptor). Positron emission tomography (PET) using ^{11}C and ^{18}F labelled radiopharmaceuticals has led the way in studies of receptor imaging, and has provided much useful information on neurophysiology and neuropharmacology.

There is considerable interest in discovering and developing new ^{99m}Tc radiopharmaceuticals for imaging CNS receptors. Technetium-99m should significantly reduce the cost of performing such imaging studies and should allow many more nuclear medicine centres access to receptor imaging radiopharmaceuticals. Currently, there are no commercially available ^{99m}Tc CNS receptor imaging radiopharmaceuticals in use. There are significant technical hurdles to overcome. While PET radioisotopes and ^{123}I can be attached to targeting molecules by a simple covalent bond, technetium is a second row transition metal, so it needs to be bound to a metal-binding organic molecule (a chelating agent) to be attached to a targeting molecule. The combination of technetium with a chelating agent (called the technetium chelate) is generally large in size, so it will often change considerably the physical and biochemical properties of the targeted molecule to which it is attached. However, in the last few years considerable progress has been made in labelling ligands specific to various receptor systems with ^{99m}Tc. Recently, the successful development of ^{99m}Tc-TRODAT as a radioligand for the dopamine transporter has shown the

feasibility of imaging specific transporters in the brain with radiotracers based on ^{99m}Tc.

A consultants meeting held in Vienna in July 1995 recommended organization of a Co-ordinated Research Project (CRP) aimed at developing ^{99m}Tc CNS receptor imaging agents. In 1996, ten research groups from Asia, Europe and Latin America participated in this initiative. During the course of the CRP four Research Co-ordination Meetings (RCMs) were held: in November 1996 in Germany, September 1998 in Greece, April 2000 in Uruguay and December 2001 in Austria. This report summarizes the work carried out by different research groups during the CRP. The research projects presented by the participants included the development and evaluation of the serotonin receptor ligands 5-HT$_{1A}$ and 5-HT$_{2A}$, benzodiazepinic receptor ligands and dopamine receptor ligands, and the study of novel cores for Tc labelling, as well as molecular modelling.

After two years of work on these topics, it was recommended at the 1998 RCM to focus on the serotonergic receptors, owing to their implication in neurological disorders such as anxiety, depression, schizophrenia and Alzheimer's disease. WAY 100635, a potent antagonist of pre- and post-synaptic 5-HT$_{1A}$ receptors, with residue 1-(2-methoxyphenyl)piperazine known to have a high affinity to this receptor's subtype, was selected as the prototypic compound for the design of potential radiopharmaceuticals.

Using the WAY 100635 molecule (1-(2-methoxyphenyl)piperazine), known to have specificity for the serotonin receptor, as the lead structure, the participants successfully synthesized several ligands for incorporating ^{99m}Tc, pursued different approaches for ^{99m}Tc labelling of these ligands, including the mixed ligand approach, bifunctional chelate approach and carbonyl approach, and achieved good results. The participants synthesized the corresponding rhenium complexes for characterizing the ^{99m}Tc compounds used as standard in analytical systems and for estimating receptor affinity in vitro, and established in vitro receptor assays for determining their affinity and specificity. Several ^{99m}Tc compounds developed exhibited good in vitro receptor binding. These techniques can be readily adopted for ^{99m}Tc labelling and evaluation of several other CNS receptor avid molecules. Establishing in vivo affinity and selectivity of selected compounds was also attempted. Many compounds showed significant brain uptake and evidence of receptor binding in animal models. However, it was clear that more extensive studies in animal models, probably in higher species, will be needed to correlate the in vitro data to predict their in vivo behaviour in humans. Such facilities and resources are not readily available to the group at present but could be pursued in future.

Three different approaches were used to attach the technetium to the pharmacophore moiety of WAY 100635, namely the mixed ligand complex

approach (2 + 1 + 1, 3 + 1, 4 + 1), tetradentate N_2S_2 chelates and the Tc-tricarbonyls. One group also carried out molecular modelling and the results were taken into account for the fine tuning of the molecular structures of the ligands.

Synthetic procedures for ligands bearing the selected pharmacophore were developed and optimized by most of the participants. High purity compounds adequate for carrier and tracer level preparation were successfully obtained, as described in detail in the individual reports.

A series of Re and ^{99}Tc complexes was synthesized with the various ligands. The complexes were characterized by elemental analysis, IR and NMR spectroscopy. Moreover, selected compounds were characterized by X ray crystallographic analysis. Almost all complexes were successfully prepared at tracer level and characterized by comparative high performance liquid chromatography (HPLC) using the Re and ^{99}Tc complexes as reference.

The in vitro affinity of the rhenium and some ^{99}Tc complexes was determined using hippocampal homogenates. Synthesized ^{99m}Tc complexes were evaluated in experimental animals.

The compounds can be divided into five categories:

(1)   Mixed ligand complexes using the 3 + 1 combination,
(2)   Mixed ligand complexes using the 4 + 1 combination,
(3)   Mixed ligand complexes using the 2 + 1 + 1 combination,
(4)   Complexes using tetradentate ligands,
(5)   Tricarbonyl complexes.

1.1.1.   Mixed ligand complexes using the 3 + 1 combination

A series of mixed ligand oxotechnetium-99m complexes carrying the 1-(2-methoxyphenyl)piperazine moiety has been synthesized. For structural characterization and for in vitro binding assays, the analogous oxorhenium or oxotechnetium-99 complexes were prepared. All oxorhenium analogues showed an affinity for the 5-HT$_{1A}$ receptor binding sites with 50% inhibitory concentration (IC$_{50}$) values in the nanomolar range. Most of the ^{99m}TcO[SN(R)S]/[S] complexes showed a significant brain uptake in rats. The regional distribution in rat brains is inhomogeneous, but the ratio between areas rich and poor in 5-HT$_{1A}$ receptor was not high. One representative of this type of complex was evaluated in monkeys with single photon emission computerized tomography (SPECT).

1.1.2. Mixed ligand complexes using the 4 + 1 combination

Technetium and rhenium complexes carrying the 1-(2-methoxy-phenyl)piperazine moiety have been synthesized using the 4 + 1 mixed ligand approach. In vitro binding studies demonstrated the high affinity for 5-HT$_{1A}$ receptors of the technetium and rhenium complexes. The IC$_{50}$ values are in the subnanomolar range. Technetium-99m complexes showed a moderate brain uptake in rats. Although the regional distribution is inhomogeneous, only small ratios between areas rich and poor in 5-HT$_{1A}$ receptor could be observed.

1.1.3. Mixed ligand complexes using the 2 + 1 + 1 combination

Rhenium and technetium complexes carrying the 1-(2-methoxy-phenyl)piperazine moiety have been synthesized and evaluated. In vitro affinity of the rhenium complex was low. The ^{99m}Tc complex demonstrates a low uptake in rat brains. Accumulation of the radioactivity was not homogeneous in brain regions. Areas rich in 5-HT$_{1A}$ receptors, such as the hippocampus, showed low concentrations of radioactivity. Additionally, a SPECT study in monkeys was carried out.

1.1.4. Complexes using tetradentate ligands

A series of oxorhenium and oxotechnetium diaminodithiol (N$_2$S$_2$) complexes was synthesized and evaluated in vitro. Affinities of the complexes were in the nanomolar range. An in vivo distribution in rats demonstrated the capability of the ^{99m}Tc complexes to penetrate the blood–brain barrier in a significant percentage.

A complex carrying the intact lead compound WAY 100635 was synthesized at tracer level using the monoamide monoaminethiol (MAMA) chelating unit. The labelling procedure is quantitative. The in vivo distribution in rats showed a moderate brain uptake. A SPECT study in rabbits was carried out.

1.1.5. Tricarbonyl complexes

Many efforts were made to find an improved system or alternative methods for the labelling of various CNS receptor binding agents based on the *fac*-[Tc(CO)$_3$]$^+$ fragment. One of the most important achievements is the final formulation of a kit useful for the preparation of [^{99m}Tc(OH$_2$)$_3$(CO)$_3$]$^+$ without the requirement of using free CO.

Several new chelating systems were tested and 1-(2-methoxy-phenyl)piperazine (*o*-MPP) was attached to selected systems. The attachment of *o*-MPP to a HYNIC chelating unit resulted in a ^{99m}Tc tricarbonyl complex with low brain uptake and low concentration in the hippocampus.

For imino-pyridine derivatives of *o*-MPP, a strong dependence on IC_{50} values of the chain length spacer was observed. This was also true for *o*-MPP bearing cyclopentadienyl derivatives.
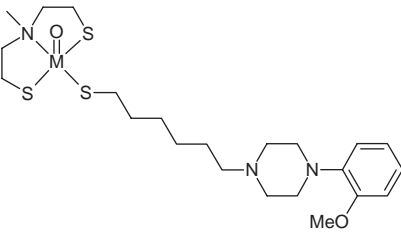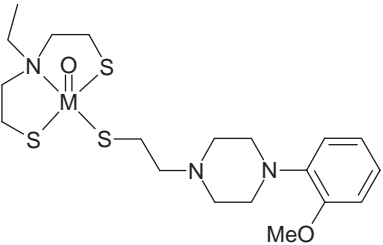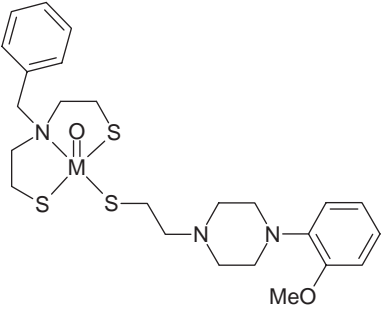
A summary of the in vitro and in vivo results of the most relevant compounds reported by participants of the CRP is presented in Table 1.1, where ID stands for injected dose.

1.2. ACHIEVEMENTS OF THE CO-ORDINATED RESEARCH PROJECT

(a) The CRP provided an opportunity for the participants to study the feasibility of developing ^{99m}Tc complexes for imaging CNS receptors. For many of the participants this was the first opportunity of working in a very challenging field, which has been attracting the attention of the radiopharmacy scientific community.

(b) Co-operation and collaboration were established between many of the participants, including both information and ligand exchange. Technical assistance in the implementation of procedures for complex synthesis and quality control procedures is also an outcome. This collaboration is expected to continue in the future.

(c) The development of technology for the synthesis, radiolabelling and quality control of potential CNS receptor ligands was successfully achieved by many of the participants. In vivo and in vitro biological techniques, relevant for studying the biological efficacy of receptor imaging agents, were also established.

(d) The improvement of the capabilities of participating groups in all the procedures needed for the development of novel radiopharmaceuticals is considered one of the most important achievements of the CRP. These skills can be applied to the design of potential radiopharmaceuticals for other types of CNS receptors and also to new fields of interest in radio-pharmacy.

(e) Most of the participants generated good quality scientific data that were presented in meetings and published in international journals.
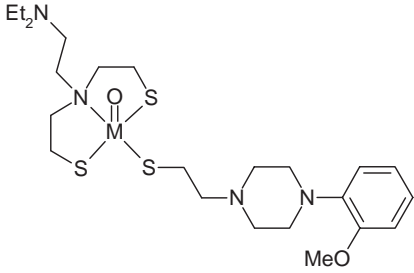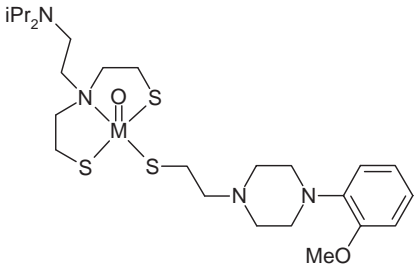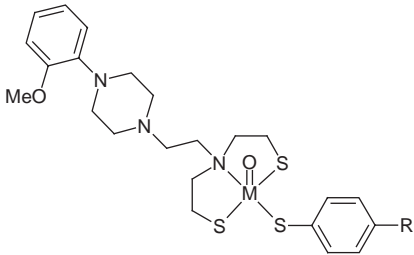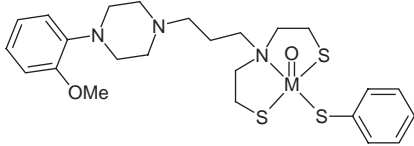
TABLE 1.1. SUMMARY OF IN VITRO AND IN VIVO RESULTS OF THE MOST RELEVANT COMPOUNDS REPORTED BY PARTICIPANTS OF THE CRP (5-HT$_{1A}$/IC$_{50}$ values)

Complex	IC$_{50}$ (nM)	Brain uptake in rats (% ID/g)	Reported from
3 + 1 complexes			
	—	0.12	Cuba
	0.13 (Tc) 0.24 (Re)	0.22	Germany
	31	0.413 (% ID/organ)	Greece
	23.2	1.77 (mice)	China
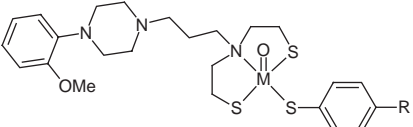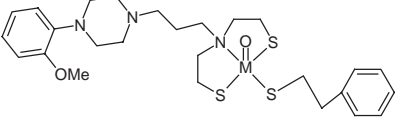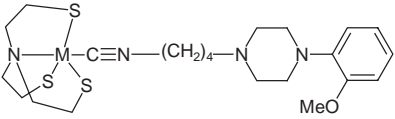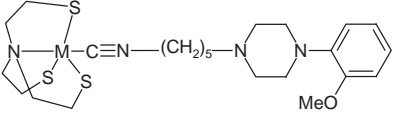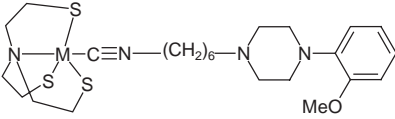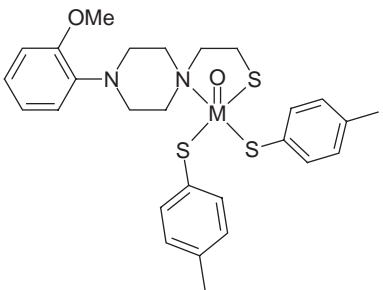
TABLE 1.1. SUMMARY OF IN VITRO AND IN VIVO RESULTS OF THE MOST RELEVANT COMPOUNDS REPORTED BY PARTICIPANTS OF THE CRP (5-HT$_{1A}$/IC$_{50}$ values) (cont.)

Complex	IC$_{50}$ (nM)	Brain uptake in rats (% ID/g)	Reported from
Et$_2$N structure (MeO)	67	1.6 (mice)	Uruguay
	98.7	1.6 (mice)	China
iPr$_2$N structure (MeO)	45	0.9 (mice)	Uruguay
MeO structure, R	R = H / 22	1.31 (% ID/organ)	Greece
	R = MeO / 20	0.78 (% ID/organ)	Greece
OMe structure	6	0.47 (% ID/organ)	Greece
	6	0.6 (mice)	Uruguay
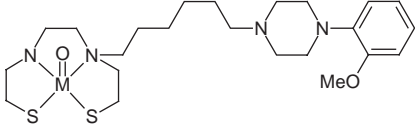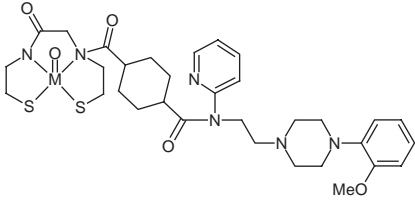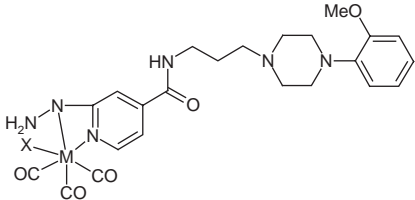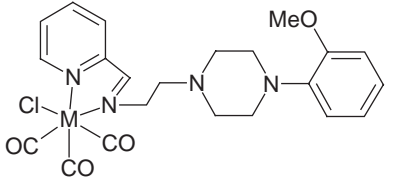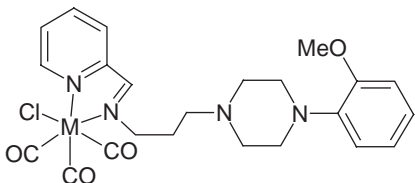
TABLE 1.1. SUMMARY OF IN VITRO AND IN VIVO RESULTS OF THE MOST RELEVANT COMPOUNDS REPORTED BY PARTICIPANTS OF THE CRP (5-HT$_{1A}$/IC$_{50}$ values) (cont.)

Complex	IC$_{50}$ (nM)	Brain uptake in rats (% ID/g)	Reported from
	R = MeO — 5.8 Me — 12 Et — 26.6 n-Bu — 103 Cl — 21 3-Br — 26	(% ID/organ) 0.41 0.42 0.36 — 0.53 0.62	Greece
	12	0.24 (% ID/organ)	Greece
4 + 1 complexes			
	0.29	0.32	Germany
	0.62	0.29	Germany
	4.5	0.18	Germany
2 + 1 + 1 complexes			
		0.153	Greece
	106	0.105	Cuba
	106	0.08	Hungary
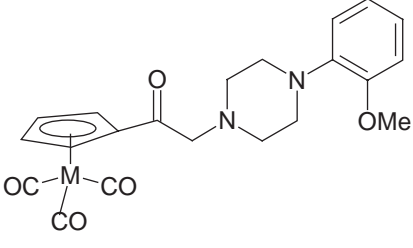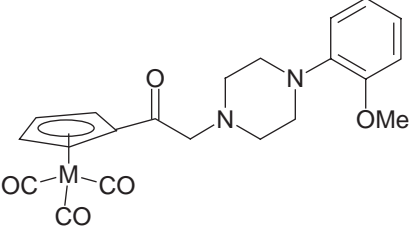
TABLE 1.1. SUMMARY OF IN VITRO AND IN VIVO RESULTS OF THE MOST RELEVANT COMPOUNDS REPORTED BY PARTICIPANTS OF THE CRP (5-HT$_{1A}$/IC$_{50}$ values) (cont.)

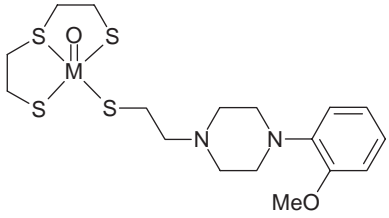| Complex	IC$_{50}$ (nM)	Brain uptake in rats (% ID/g)	Reported from
Tetradentate N$_2$S$_2$ complexes			
	1.29	0.52	Germany
	—	0.17	Republic of Korea
Tricarbonyl complexes			
	—	0.11	Greece
	630	0.04	Germany/ Switzerland
	5	0.1	Germany/ Switzerland

TABLE 1.1. SUMMARY OF IN VITRO AND IN VIVO RESULTS OF THE MOST RELEVANT COMPOUNDS REPORTED BY PARTICIPANTS OF THE CRP (5-HT$_{1A}$/IC$_{50}$ values) (cont.)

Complex	IC$_{50}$ (nM)	Brain uptake in rats (% ID/g)	Reported from
	6	—	Switzerland
	600	—	Switzerland

1.3. SCIENTIFIC CONCLUSIONS AND RECOMMENDATIONS

(1) Reliable and reproducible methods for the derivatization and labelling of various Tc based CNS receptor ligands have been developed. These methods can be adapted to further pharmacophores considered to be important for SPECT imaging of brain receptors.

(2) Series of Tc and Re complexes have been synthesized and characterized in macroscopic amounts.

(3) In general, the complexes showed nanomolar and subnanomolar affinities to the target receptors. The affinities of the studied complexes for 5-HT$_{1A}$ receptors were comparable to those of lead structures. The higher receptor affinities of some compounds went along with higher affinities for other types of receptors, resulting in lower selectivity and high non-specific receptor binding.

(4) Most complexes were successfully synthesized at tracer level (^{99m}Tc) and characterized by comparative HPLC studies. Evaluation in experimental

animals of the complexes prepared at tracer level showed a high structure dependent brain uptake in rats. The brain uptake values in rats of some of these complexes were comparable to reported values of ^{99m}Tc-TRODAT.

(5)   Although the brain uptake values and affinities were comparable to those of lead structures, they suffer from insufficient selective localization in brain areas rich in 5-HT_{1A} receptors.

(6)   From data obtained so far there is no clear relationship between affinity and brain uptake, although the compounds meet the requirements of sufficient lipophilicity.

(7)   In order to obtain Tc based CNS receptor binding ligands, the following main results have to be achieved:

— Significant increase of brain uptake for candidates with a high receptor affinity;

— Insight into fundamental structure–activity relationships, to guide the design of receptor ligands with sufficient brain uptake;

— Systematic knowledge about the species dependence as well as about the metabolic behaviour evident in later in vivo validation of promising candidates.

(8)   A systematic study of the influence of diverse chelates on affinity, selectivity and brain uptake is required, since a clear but not rational difference was observed in the behaviour of receptor ligands labelled with homologous receptor targeting domains.

(9)   All experimental effort should be accompanied to a greater extent by, or be fully based on, predictions from computational chemistry.

(10)   Although the ultimate goal of developing ^{99m}Tc agents for imaging CNS receptors could not be fully achieved, important data and technology have been compiled that serve as a useful base for further rational design of this kind of radiopharmaceutical.

1.4.   PUBLICATIONS AND PRESENTATIONS ORIGINATING FROM THE CO-ORDINATED RESEARCH PROJECT

ALBERTO, R., et al., First application of *fac*-[^{99m}Tc(OH$_2$)3(CO)$_3$]$^+$ in bioorganometallic chemistry: Design, structure and in vitro affinity of a 5-HT_{1A} receptor ligand labelled with ^{99m}Tc, J. Am. Chem. Soc. **121** (1999) 6076–6077.

BERGMANN, R., et al., Assessment of the in vitro and in vivo properties of a ^{99m}Tc-labelled inhibitor of the multidrug resistant gene product P-glycoprotein, Nucl. Med. Biol. **27** (2000) 135–141.

CHAPTER 1

BODO, K., et al., "Kozponti idegrendszeri receptorok vizsgalatara alkalmas [99mTc]-mal jelzett uj radiofarmakonok kutatasa", paper presented at 11th Congr. of the Hungarian Soc. Nuclear Medicine, Bukfurdo, 1997.

BODO, K., et al., "Preparation and biodistribution study of a novel brain 5-HT$_{1A}$ receptor imaging agent", paper presented at EAMN Congr., Paris, 2000.

BODO, K., et al., "Az agyi 5-HT$_{1A}$ receptor lekepzesere alkalmas uj radioligand eloallitasa es biologiai vizsgalata", paper presented at 12th Congr. of the Hungarian Soc. of Nuclear Medicine, Gyula, 2001.

BODO, K., et al., "Biodistribution study of [99mTc]-labelled serotonin 1A receptor imaging agent", paper presented at RRC Congr., Drezda, 2001.

BOUZIOTIS, P., et al., Novel oxorhenium and oxotechnetium complexes from an aminothiol[NS]/thiol[S] mixed ligand system, Chem. Eur. J. **7** (2001) 3671–3680.

BOUZIOTIS, P., et al., Synthesis and structural characterization of two cis-dioxor-henium(V) ReO$_2$[SN][P] mixed ligand complexes, Inorg. Chim. Acta **320** (2001) 175–177.

DREWS, A., et al., Synthesis and biological evaluation of technetium(III) mixed-ligand complexes with high affinity for the cerebral 5-HT$_{1A}$ receptor and the alpha1-adrenergic receptor, Nucl. Med. Biol. **29** (2002) 389–398.

FEI, L., HE, Y., ZHIFU, L., Synthesis and biodistribution of 5-HT$_{1A}$ receptor imaging agents with [99mTc], J. Isot. **14** 3–4 (2001) 129–135.

FEI, L., HE, Y., ZHIFU, L., Progress in development of WAY analogues in central nervous system 5-hydroxytryptamine receptor imaging agents, J. Isot. **14** 1 (2001) 41–49.

FEI, L., HE, Y., ZHIFU, L., Synthesis, characterization and biodistribution evaluation of [99mTc]/Re [SNS/S] mixed ligand complexes derived from WAY 100635, J. Lab. Comput. Radiopharm. (in press).

GEETHA, R., et al., Synthesis of SNS tridentate ligand and mixed ligand technetium complex (3 + 1 combination) for CNS serotonin receptor imaging, Ind. J. Nucl. Med. **15** (2000) 133–134.

GEETHA, R., et al., "Piperazino compounds labelled with [99mTc] as probable agents for the central nervous system receptor imaging", paper presented at 5th Int. Symp. on Innovation in Pharmaceutical Sciences and Technology, Mumbai, 2003.

HEIMBOLD, A., et al., A novel Tc-99m radioligand for the 5-HT$_{1A}$ receptor derived from Desmethyl-WAY-100635 (DWAY), Eur. J. Nucl. Med. **29** (2002) 82–87.

HEIMBOLD, A., et al., Synthesis, biological and autoradiographic evaluation of a novel Tc-99m radioligand derived from WAY 100635 with high affinity for the 5-HT$_{1A}$ receptor and the alpha1-adrenergic receptor, Nucl. Med. Biol. **29** (2002) 375–387.

HOEPPING, A., et al., TROTEC-1, a new high-affinity ligand for labelling of the dopamine transporter, J. Med. Chem. **41** (1998) 4429–4432.

HOEPPING, A., et al., Novel rhenium complexes derived from a-tropanole as potential ligands for the dopamine transporter, Bioorg. Med. Chem. **6** (1998) 1663–1672.

HOEPPING, A., SPIES, H., JOHANNSEN, B., Retropane — A new rhenium complex as a potential ligand of the dopamine transporter, Biol. Med. Chem. Lett. **6** (1996) 2871–2874.

HU, J., HE, Y., WANG, Y., XIAO, L., Development of ^{99m}Tc labelled central nervous system (CNS) receptor imaging agents, J. Isot. **11** (1998) 184–188.

HU, J., HE, Y., WANG, Y., XIAO, L., "Design and synthesis of new neutral Re(V)O complex derived from benzamides", Isotopes (Proc. 3rd Int. Conf. Vancouver, 1999), (STEVENSON, N.R., Ed.), World Scientific Publishing, Singapore (1999) 40–42.

HU, J., HE, Y., WANG, Y., XIAO, L., Synthesis and biological evaluation of ^{99m}Tc labelled benzamides for dopamine D2 receptor imaging, J. Isot. **13** (2000) 193–198.

JOHANNSEN, B., PIETZSCH, H., Development of technetium-99m-based CNS receptor ligands: Have there been any advances?, Eur. J. Nucl. Med. **29** (2002) 263–275.

JOHANNSEN, B., SPIES, H., Advances in technetium chemistry towards ^{99m}Tc receptor imaging agents, Transition Met. Chem. **22** (1997) 318–320.

JOHANNSEN, B., et al., Technetium (V) and rhenium (V) complexes for 5-HT$_{2A}$ serotonin receptor binding: Structure-affinity considerations, Nucl. Med. Biol. **23** (1996) 429–438.

JOHANNSEN, B., et al., Structural modification of receptor-binding technetium-99m complexes in order to improve brain uptake, Eur. J. Nucl. Med. **24** (1997) 316–319.

LEÓN, A., et al., Novel mixed ligand technetium complexes as 5-HT$_{1A}$ receptor imaging agents, Nucl. Med. Biol. **29** (2002) 217–226.

MALLO, L., et al., "Preliminary evaluation of a novel ^{99m}Tc complex for imaging 5-HT$_{1A}$ serotonin receptors", Technetium, Rhenium and other Metals in Chemistry and Nuclear Medicine (NICOLINI, M., MAZZI, U., Eds), SG Editoriali, Padua (1999) 503–506.

PAPAGIANOPOULOU, D., et al., Development of novel mixed ligand oxotechnetium [SNS/S] complexes as potential 5-HT$_{1A}$ receptor imaging agents, J. Biol. Inorg. Chem. **6** (2001) 256–265.

PAPAGIANOPOULOU, D., et al., Oxotechnetium ^{99m}TcO[SN(R)S/S] Complexes as Potential 5-HT$_{1A}$ Receptor Imaging Agents (in preparation).

PIETZSCH, H.-J., et al., Synthesis and autoradiographical evaluation of a novel high-affinity Tc-99m ligand for the 5-HT$_{2A}$ receptor, Nucl. Med. Biol. **26** (1999) 865–875.

PIRMETTIS, I., et al., Synthesis, labelling with Tc-99m and biological study of a novel 5-HT$_{1A}$ receptor ligand, J. Lab. Comput. Radiopharm. **44** (2001) S550–S552.

PIRMETTIS, I., et al., Synthesis of oxorhenium(V) and oxotechnetium(V) [SN(R)S/S] mixed ligand complexes containing a phenothiazine moiety on the tridentate SN(R)S ligand, Bioorg. Med. Chem. Lett. **11** (2001) 1859–1862.

REY, A., et al., Synthesis and characterization of novel '2 + 1 + 1' rhenium complexes, Technetium, Rhenium and other Metals in Chemistry and Nuclear Medicine (NICOLINI, M., MAZZI, U., Eds), SG Editoriali, Padua (1999) 213–216.

REY, I., et al., Synthesis and characterization of mixed ligand oxorhenium complexes with the SNN type of ligand: Isolation of a novel ReO[SN][S][S] complex, Inorg. Chem. **39** (2000) 4211–4218.

SCHEUNEMANN, M., JOHANNSEN, B., A simple and efficient synthesis of a derivatized pseudotripeptide containing a methylene thioether isoster and its use for the design of bifunctional rhenium and technetium chelating agents, Tetrahedron Lett. **38** (1997) 1371–1372.

SIVAPRASAD, N., KARMALKAR, C.P., GEETHA, R., GHODKE, A.S., RAMAMOORTHY, N., "Development of an in vitro receptor assay for the evaluation of CNS receptor imaging agents", paper presented at Int. Conf. on Probing in Biological Systems, Mumbai, 2000.

SIVAPRASAD, N., et al., "Preparation and evaluation of serotonin labelled with ^{125}I", paper presented at Nuclear Chem. Radiochem. Symp. (NUCAR-99), Mumbai, 1999.

SPIES, H., et al., Synthesis and molecular structure of a rhenium complex derived from 8-alpha-amino-6-methyl-ergoline, Chem. Ber. **130** (1997) 839–841.

PART II

REPORTS BY PARTICIPANTS IN THE
CO-ORDINATED RESEARCH PROJECT

Chapter 2

RATIONAL PLANNING OF ANTAGONIST ANALOGUES FOR IMAGING SEROTONIN 5-HT$_{1A}$ RECEPTOR SUBTYPES BASED ON ^{99m}Tc

O.G. CARVALHO, M.M. GONÇALVES, A.B. ZERAIB,
E. MURAMOTO, M.A.T.M. ALMEIDA
Departamento de Produção de Radioisótopos,
Instituto de Pesquisas Energéticas e Nucleares,
São Paulo, Brazil

Abstract

Rational planning follows some logical steps in order to reduce the probability of synthesizing chemical compounds that possess low performance. The first step of this kind of procedure is to collect the maximum amount of information available in databases and the literature. Data are normally collected about quantitative structure activity and quantitative structure property studies. The goal is achieved when the main molecular descriptor is discovered in terms of biological activity. This descriptor is then quantified, allowing the choice of the most promising molecular candidates. In this paper, the aim is to convert molecules with high 5-HT$_{1A}$ affinity to ^{99m}Tc derivatives. Once such derivatives have to retain receptor affinity, it is very important to find drug–receptor interactions due to: chemical groups with common drug structures, the existence of intra-atomic distances between chemical ligands and physico-chemical properties that drive drug–receptor complexation.

2.1. MATERIALS

The main data used in this kind of rational planning are structure activity data of high affinity 5-HT$_{1A}$ drugs, such as partition coefficient values (log P), the inhibition constant (K_i), and structure property data such as X ray crystallography data and molecular volumes.

2.2. METHODS

2.2.1. Comparative studies

In order to optimize the insight in terms of drug–receptor interactions and methodological determination of molecular volumes of terminal amide (or imide) groups of high 5-HT$_{1A}$ affinity drugs by optimization of their geometries, the semi-empirical AM1 method (MOPAC-SYBYL version 6.5) has been used.

2.2.2. Exploration of drug–receptor interactions using SAR studies

By analysing the structure–activity relation (SAR) of different drugs possessing high 5-HT$_{1A}$ biological receptor affinity, it is noticed that at least two different workable drug binding states seem to exist.

2.2.2.1. Binding state 1

The first binding state (Fig. 2.1) is characterized by a drug structure including a lipoidal moiety and an N1-arylpiperazine group.

The lipoidal moiety plays an important role in the 5-HT$_{1A}$ receptor affinity. The lipophilic character of the substituent exerts a relevant function once the 5-HT$_{1A}$ affinity is influenced by its partition coefficient. Comparing cyclohexylethyl with phenylethyl piperazine derivatives (Fig. 2.2), the most lipophilic derivative (cyclohexylethyl) has a lower K_i value [2.1].

If the alkyl chain is lengthened, the 5-HT$_{1A}$ affinity is also increased (compounds 1–4) [2.1–2.3] as shown in Fig. 2.3 and Table 2.1.

Further elongation of the alkyl chain provokes an inversion in the K values. This is a typical phenomenon that occurs with partition coefficients. The additive constitutive property of the partition coefficients no longer holds, because the structure conformation has become folded [2.4, 2.5]. Thus, the

Lipoidal moiety ⎯ N ⎯ N ⎯

R = heteroatom
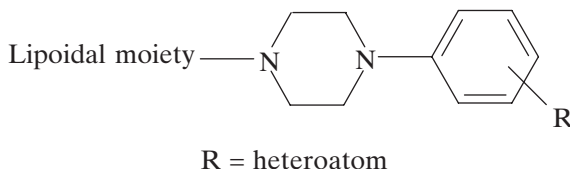
FIG. 2.1. General structure fulfilling binding state 1.

(a)

(b)
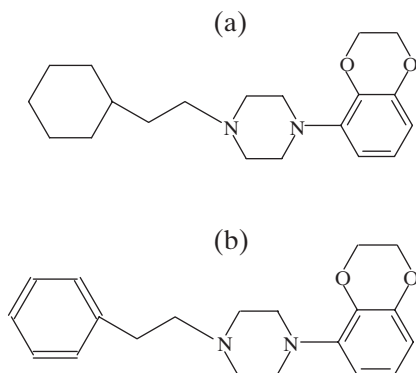
FIG. 2.2. Values of $K_i \pm (SEM)$ (nM), 5-HT_{1A}: (a) $K_i = 0.25 \pm 0.07$, (b) $K_i = 0.47 \pm 0.07$. The structures present a 180° turn.

(a)

$H_3C-(CH_2)_n$

(b)

$H_3C-(CH_2)_n$
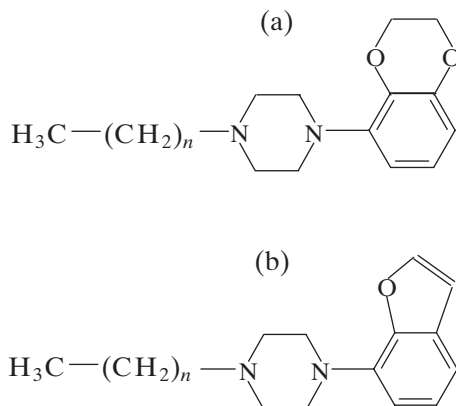
FIG. 2.3. Increase of 5-HT_{1A} affinity with alkyl chain length: (a) compounds 1a–6a, (b) compounds 1b–6b.

predicted partition coefficients tend to assume higher values than the real ones. As a result, one can realize higher K_i values for these derivatives (compounds 5 and 6).

2.2.2.2.   Binding state 2

The second binding state (Fig. 2.4) consists of an N1-arylpiperazine group, an alkyl chain (spacer) and an imide (or amide) group.

TABLE 2.1. INFLUENCE OF THE ARYL CHAIN ON K_i VALUES (5-HT$_{1A}$)

Compound	n	$K_i \pm$ SEM (nM) 5-HT$_{1A}$	Compound	n	$K_i \pm$ SEM (nM) 5-HT$_{1A}$
1a	2	80 ± 11	1b	2	29 ± 2
2a	3	12 ± 2	2b	3	5.9 ± 2
3a	4	2.2 ± 0.4	3b	4	0.81 ± 0.06
4a	5	0.5 ± 0.09	4b	5	0.54 ± 0.13
5a	7	0.61± 0.07	5b	7	1.7 ± 0.4
6a	9	1.0 ± 0.3	6b	9	8.0 ± 2.5

2.2.3.   N1-arylpiperazine group

Compounds having 5-HT$_{1A}$ affinity that play the role of binding state 2 can present different N1-arylpiperazine groups with heteroatoms (Fig. 2.5).

2.2.4.   Spacer alkyl group

The spacer alkyl group possessing four methylene groups (Table 2.2) is generally most suitable for binding state 2, mainly when associated with the N1-(2-methoxyphenyl)-piperazine [2.9] shown in Fig. 2.6.

Even when other types of arylpiperazines are used, the spacer possessing four carbon atoms (Tables 2.3 and 2.4) is the best choice [2.9], see Figs 2.7 and 2.8.
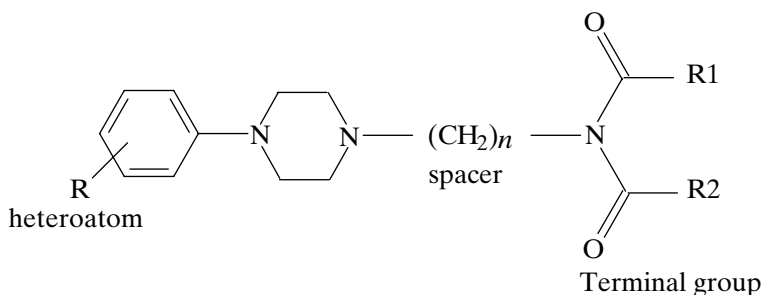
FIG. 2.4. General structure fulfilling binding state 2.

(a)

(b)

(c)

(d)

(e)
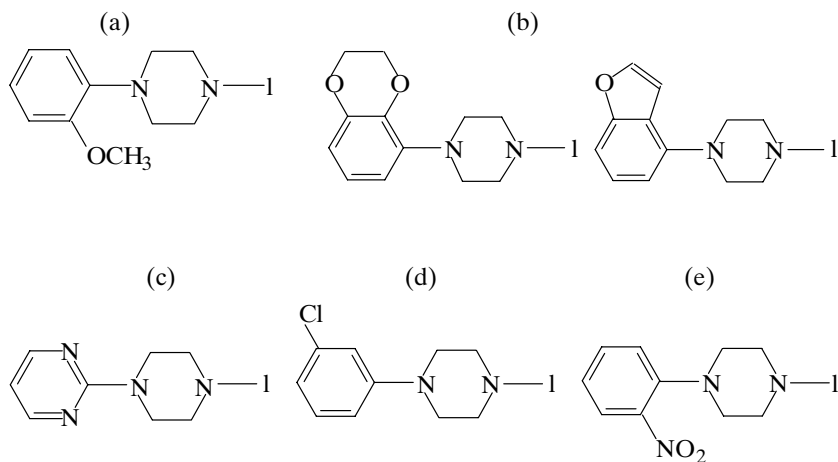
FIG. 2.5. *N1-arylpiperazine groups suitable for binding state 2. The structures present a 180° turn. For more details, see (a) Ref. [2.6], (b) Ref. [2.1], (d) Ref. [2.7] and (e) Ref. [2.8].*
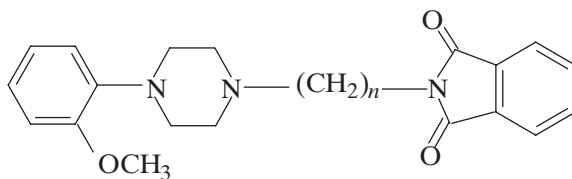
FIG. 2.6. *The N1-(2-methoxyphenyl)-piperazine group.*

TABLE 2.2. DATA FOR COMPLEX SHOWN IN FIG. 2.6

Compound	n	$K_i \pm$ SEM (nM) 5-HT$_{1A}$
7	4	0.6
8	5	5.0 ± 0.8

TABLE 2.3. DATA FOR COMPLEX SHOWN IN FIG. 2.7

Compound	n	$K_i \pm$ SEM (nM) 5-HT$_{1A}$
9	2	250 ± 25
10	3	48 ± 6
11	4	11 ± 1

TABLE 2.4. DATA FOR COMPLEX SHOWN IN FIG. 2.8

Compound	n	$K_i \pm$ SEM (nM) 5-HT$_{1A}$
12	2	1330 ± 270
13	3	45 ± 7
14	4	25 ± 8
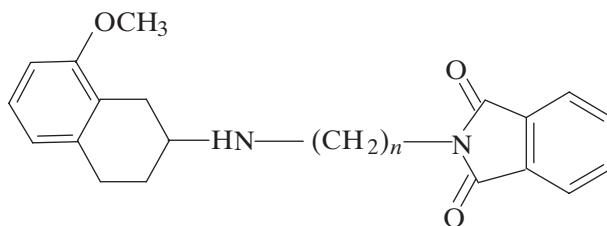
FIG. 2.7.
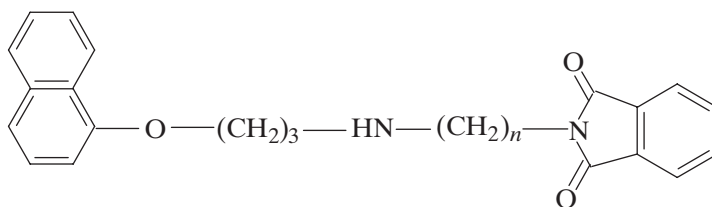
FIG. 2.8.

2.2.5. Bulky annelated imide groups or amide moities associated with annelated groups

Terminal annelated imide group moieties (or amide groups associated with annelated structures) (Fig. 2.9) present in 5-HT$_{1A}$ antagonists that complex in the biological receptor with binding state 2.

Binding state 2 can be successfully achieved when the derivatives include bulky alkyl annelated groups near the amide group. Compound RK-153 (Fig. 2.10) fulfils the structural requirements for binding state 2 and may be considered as a template.

Buspirone   Ipsapirone

Flesinoxan   Befiperide
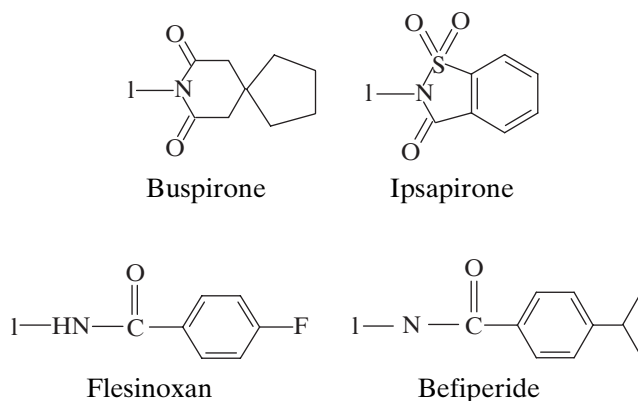
FIG. 2.9. *Imide and amide terminal groups suitable for binding state 2. The structures present a 180° turn.*
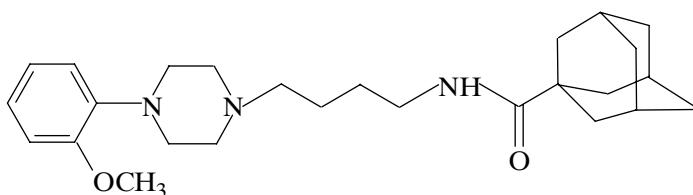
FIG. 2.10. *Compound RK-153.*

2.2.6. Analogues of RK-153 with high 5-HT$_{1A}$ affinity

The influence of different terminal groups on 5-HT$_{1A}$ affinity [2.10] is shown below. Note that the structures present a 180° turn.
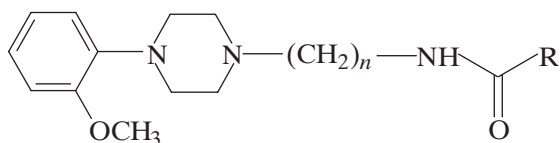
R group	n	$K_i \pm$ SEM (nM) 5-HT$_{1A}$
	2	0.24 ± 0.07
	4	0.63 ± 0.05
	2	0.12 ± 0.03
	4	0.23 ± 0.09
	2	0.21 ± 0.02
	4	0.40 ± 0.02

It is possible to obtain some derivatives that can possess alkyl chains with two carbon atoms retaining very high 5-HT$_{1A}$ affinity, even higher than those of the derivatives with four methylene groups. However, if one desires to build 5-HT$_{1A}$ antagonists based on ^{99m}Tc derivatives, the alkyl chain must not be one with two carbon atoms, because the amide groups are very sensitive to the molecular modifications caused by ^{99m}Tc complexes. Interestingly, N1-(2-methoxyphenyl)-piperazine derivatives, possessing chains with four carbon atoms, are very insensitive to modifications near the amide group.

2.3.   MOLECULAR DESCRIPTOR OF BINDING STATE 2

2.3.1.   Molecular volume of terminal group

The general structure is shown in Fig. 2.11.

Quantitative structure property relationship and comparative molecular field analysis (CMFA) studies have demonstrated that the molecular descriptor of binding state 2, in terms of 5-HT$_{1A}$ affinity, is the molecular volume of the terminal group. Mokrosz et al. [2.11], working with 1, 2, 3 and 4 tetrahydroiso-quinolines (THIQ), have shown that the volumes of the imide terminal fragments of some derivatives strongly affect (Table 2.5) their 5-HT$_{1A}$ affinities (Fig. 2.12).

In order to better elucidate the influence of the molecular volume, ten terminal groups (Fig. 2.13) present in high 5-HT$_{1A}$ drugs have been taken from the literature and the volumes of eight of these have been calculated (Table 2.6) using the MOPAC (SYBYL version 6.5) code.

Van Steen et al. [2.1], in CMFA studies, have proved that: "the affinity of the amide derivatives can be fully explained by their steric field properties". They have also concluded that the steric and electrostatic field properties contribute in a 98:2 ratio.

However, the presence of a probable hydrophobic pocket in the 5-HT$_{1A}$ receptor gives rise to limitations: a derivative with a too large terminal group
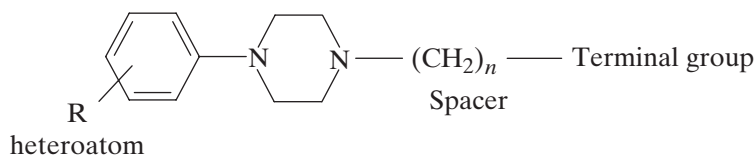
FIG. 2.11.   General structure suitable for binding state 2.
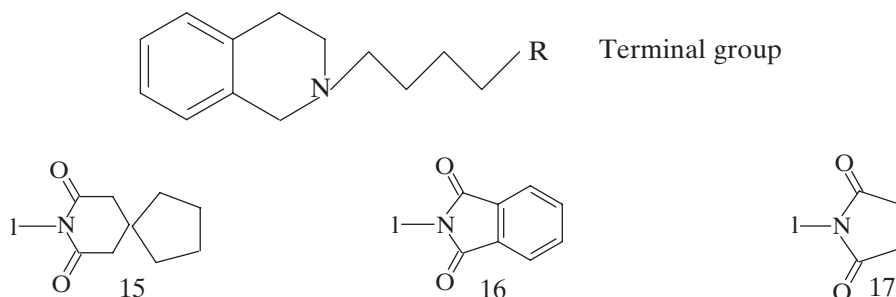
FIG. 2.12.   Imide terminal fragments. The structures present a 180° turn.

TABLE 2.5. INFLUENCE OF VAN DER WAALS VOLUME ON 5-HT$_{1A}$ AFFINITY [2.11]

Compound	Van der Waals volume[a] (Å^3)	$K_i \pm$ SEM (nM) 5-HT$_{1A}$	Volume[b] (Å^3)
15	126.8	5 ± 2	169.56
16	104.1	140 ± 10	128.8403
17	68.1	2920 ± 90	87.84

[a] The Van der Waals volumes versus volumes calculated by minimization of fragments 21, 22 and 23 showed parallelism.
[b] Volumes (Å^3) calculated by the semi-empirical AM1 method (MOPAC SYBYL version 6.5). Minimizations have been made at Instituto de Química – Universidade de São Paulo.

TABLE 2.6. INFLUENCE OF TERMINAL FRAGMENT VOLUME ON 5-HT$_{1A}$ AFFINITY

Terminal group	Volume [a] (Å)^3	$K_i \pm$ SEM (nM) 5-HT$_{1A}$
18	116.56	1.00 ± 0.02
19	122.22	1.88 ± 0.22
20	141.77	0.6 ± 0.1
21	148.55	0.23 ± 0.09
22	167.48	0.63 ± 0.05
23	190.35	0.40 ± 0.03
24[b]	169.56	0.23
fac-[^{99m}Tc(CO)$_3$] complex[c]	196.35	

[a] Volumes (Å^3) calculated by the semi-empirical AM1 method (MOPAC SYBYL version 6.5). Minimizations have been made at Instituto de Química – Universidade de São Paulo.
[b] Compound WY-48,723 [2.12]
[c] See Ref. [2.13].

volume can lead to a reduction in 5-HT$_{1A}$ affinity. The crucial question is how large the terminal group can be.

In order to explore the creation of serotonergic derivatives based on ^{99m}Tc, it is very important to optimize the volume of the terminal group. So,
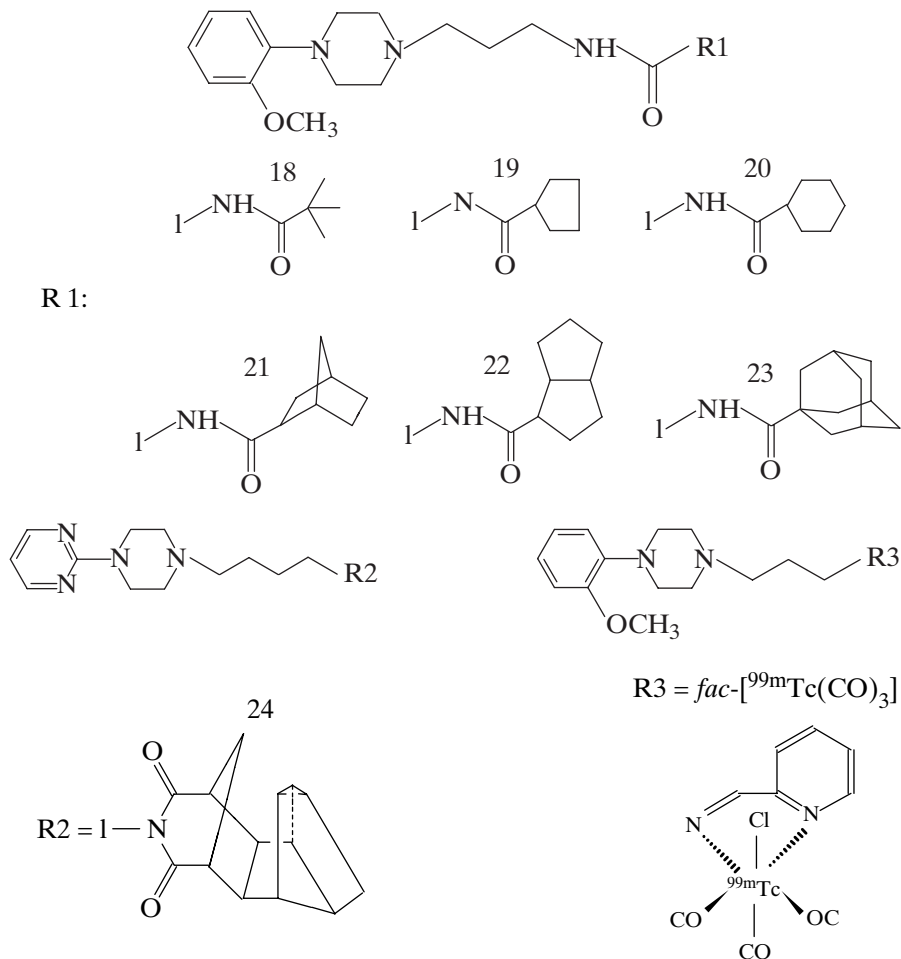
FIG. 2.13. *Ten terminal groups present in high 5-HT$_{1A}$ drugs.*

some bulky high 5-HT$_{1A}$ affinity derivatives have been taken from the literature (Table 2.6).

Strikingly, compounds possessing bulk terminal amide or imide groups and alkyl chains of four methylene groups are very insensitive to volume alterations. Compounds possessing terminal fragments with volumes ranging from 116.53 to 190.35 Å^3 showed almost equal K_i values, and one may conclude that the best terminal volume lies near 148.55 Å^3.

The 5-HT$_{1A}$ *fac*-[^{99m}Tc(CO)$_3$] derivative created by Alberto and co-workers [2.13] showed a very good 5-HT$_{1A}$ affinity and a low 50% inhibitory concentration (IC$_{50}$) value of 5 ± 2 nM (competitor [^{3}H]8-OH-DPAT). Its terminal volume lies near the range of those of compounds 18–24 and, in order

to verify the molecular volume of the *fac*-[^{99m}Tc(CO)$_3$] terminal fragment, an additional calculation has been made using X ray crystal co-ordinates given in Ref. [2.13]. The volume was 241.7 Å^3 when the *fac*-[^{99m}Tc(CO)$_3$] fragment was docked onto an orthorhombic solid. The 5-HT$_{1A}$ *fac*-[^{99m}Tc(CO)$_3$] derivative may be considered as binding state 1 due to the absence of an amide or imide group.

Some 5-HT$_{1A}$ candidates based on ^{99m}Tc fulfilling binding state 2 are shown in Fig. 2.14.

All the K_i values presented here refer to competitive experiments using 8-OH-DPAT. The shapes of the fragments found are shown in Fig. 2.15.

(a)

(b)
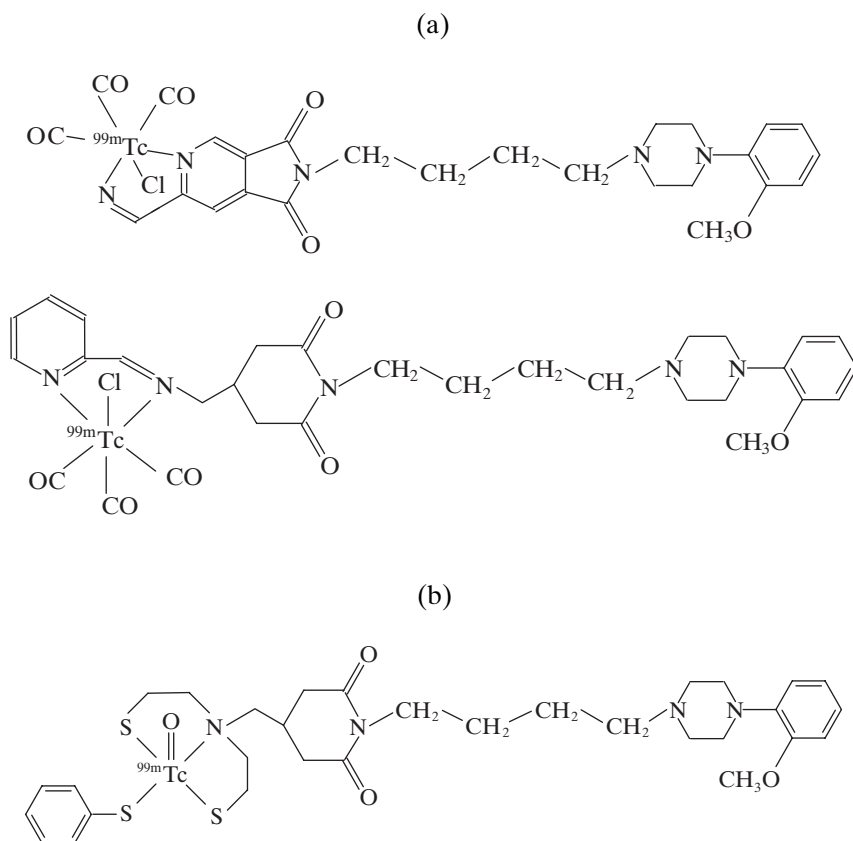
FIG. 2.14. *New 5-HT$_{1A}$ candidates based on ^{99m}Tc: (a) fac-[^{99m}Tc(CO)$_3$] derivatives, (b) the 3 + 1 ^{99m}Tc complex.*
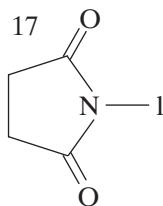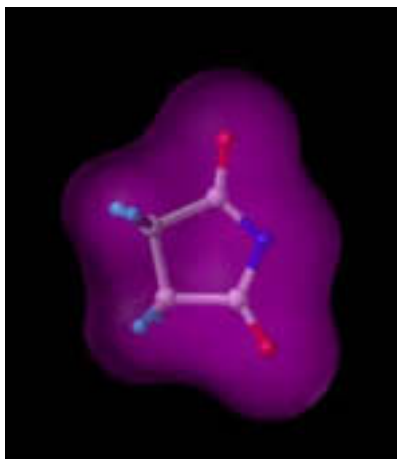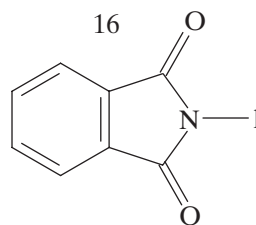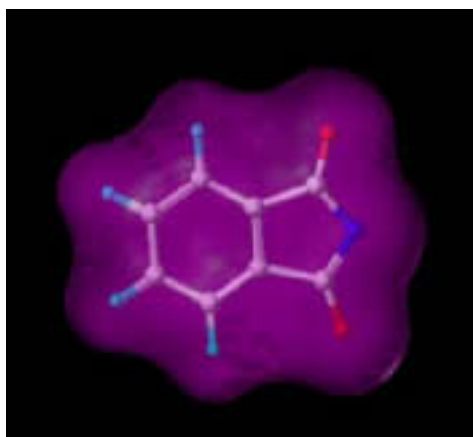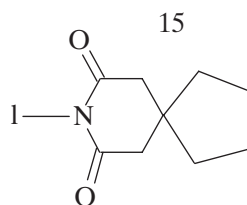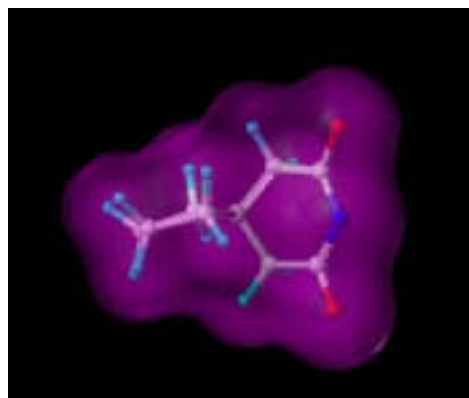
FIG. 2.15. Fragments of 5-HT$_{1A}$ drugs found.
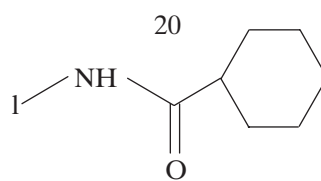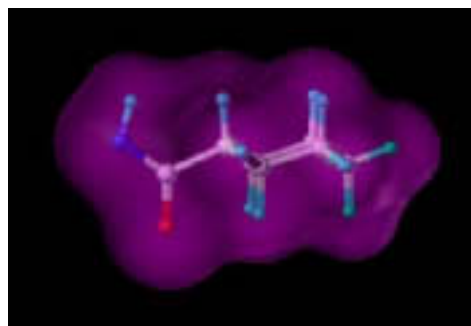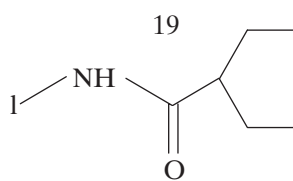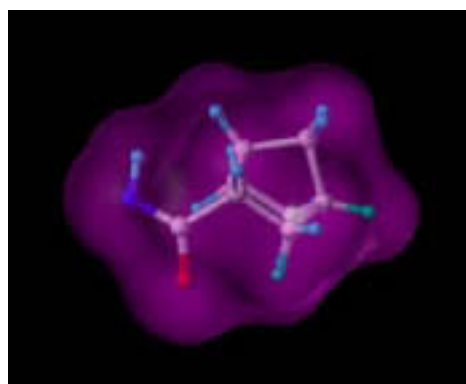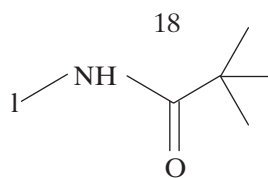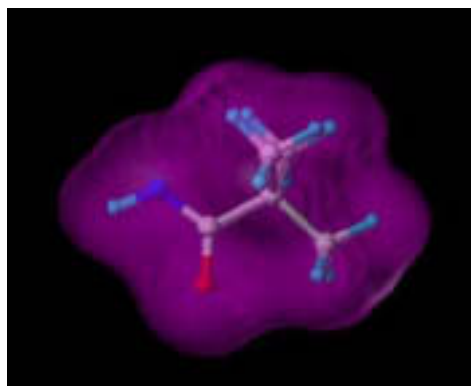
FIG. 2.15. (cont.)

FIG. 2.15. (cont.)

24
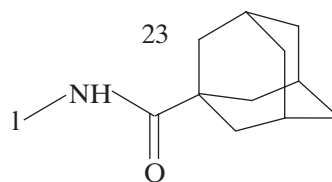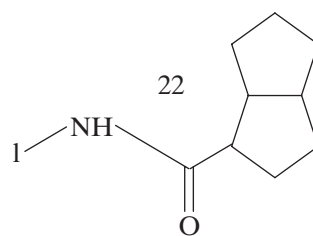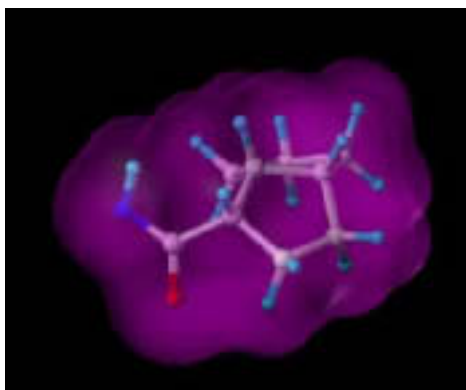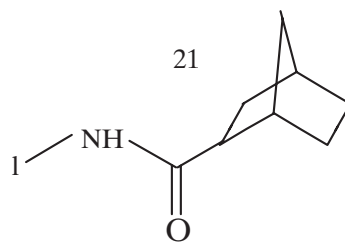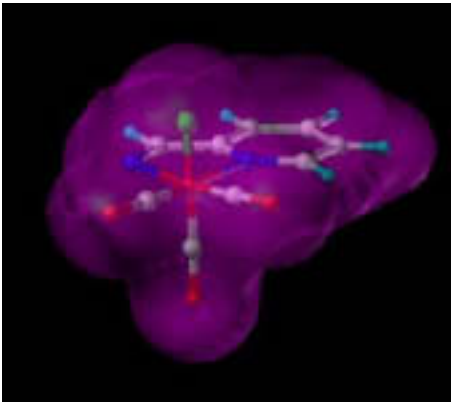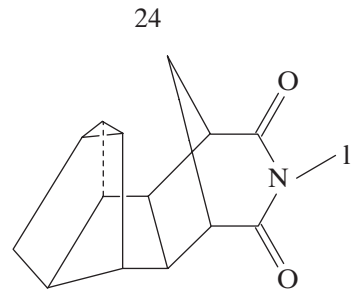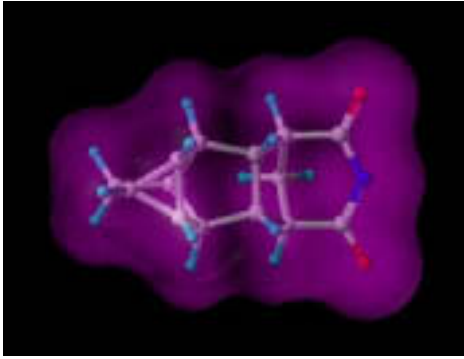
$fac - [^{99m}Tc(Co_3)]$ complex

FIG. 2.15. (cont.)

ACKNOWLEDGEMENTS

REFERENCES TO CHAPTER 2

[2.1] VAN STEEN, B.J., VAN WIJNGAARDEN, I., TULP, M.T.M., SOUDIJN, W., Structure-affinity relationship studies on 5-HT$_{1A}$ receptor ligands, 1. Heterocyclic phenylpiperazines with N4-aralkyl substituents, J. Med. Chem. **36** (1993) 2751–2760.

[2.2] MOKROSZ, J.L., et al., Quantitative analysis of the alkyl chain effects on the 5-HT$_{1A}$ and 5-HT$_{2A}$ receptor affinities of 4-alkyl-1-arylpiperazines and their analogs, Arch. Pharm. (Weinheim) **328** (1995) 143–148.

[2.3] YASUNAGA, T., et al., Synthesis and pharmacological characterization of novel 6-fluorochroman derivatives as potential 5-HT$_{1A}$ receptor antagonists, J. Med. Chem. **41** 15 (1998) 2765–2778.

[2.4] GLENNON, R.A., NAIMAN, N.A., LYON, R.A., TITELER, M., Arylpiperazine derivatives as high-affinity 5-HT$_{1A}$ serotonin ligands, J. Med. Chem. **31** 10 (1988) 1968–1971.

[2.5] LEO, A., HANSCH, C., ELKIN, D., Partition coefficients and their uses, Chem. Rev. **71** 6 (1971) 525–616.

[2.6] KUIPERS, W., et al., 5-HT$_{1A}$ – versus D$_2$-receptor selectivity of flesinoxan and analogous N^4-substituted N^1-arylpiperazines, J. Med. Chem. **40** 3 (1997) 300–312.

[2.7] MOKROSZ, M.J., et al., 5-HT$_{1A}$ and 5-HT$_{2A}$ receptor affinity and functional profile of some N-[3-(4-arylpiperazinyl)propyl] derivatives of indolin-2(1H)-one, quinolin-2(1H)-one and isoquinolin-1(2H)-one, Pharmazie **52** 6 (1997) 423–428.

[2.8] RAGHUPATHI, R.K., RYDELEK-FITZGERALD, L., TEITLER, M., GLENNON, R.A., Analogues of the 5-HT$_{1A}$ serotonin antagonist 1-(2-methoxyphenyl)-4-[4-(2-phthalimido)butyl]piperazine with reduced α1-adrenergic affinity, J. Med. Chem. **34** (1991) 2633–2638.

[2.9] GLENNON, R.A., et al., N-(phthalimidoalkyl) derivatives of serotonergic agents: A common interaction at 5-HT$_{1A}$ serotonin binding sites?, J. Med. Chem. **32** 8 (1989) 1921–1926.

[2.10] MOKROSZ, J.L., et al., 4-[2-Cycloalkanecarbamido)ethyl-1-(2-methoxyphenyl)-piperazines: High-affinity agonists, Arch. Pharm. (Weinheim) **328** (1995) 770–774.

[2.11] MOKROSZ, J.L., et al., 8-[4-[2(1, 2, 3, 4-Tetrahydroisoquinolinyl)butyl]-8-azaspiro[4.5]decane-7, 9-dione: A new 5-HT$_{1A}$ receptor ligand with the same activity profile as buspirone, J. Med. Chem. **39** 5 (1996) 1125–1129.

[2.12] CHILMONCZYK, Z., et al., Conformational flexibility of serotonin$_{1A}$ receptor ligands from crystallographic data. Updated model of the receptor pharmacophore, Arch. Pharm. Med. Chem. **330** (1997) 146–160.

[2.13] ALBERTO, R., et al., First application of *fac*-[^{99m}Tc(OH$_2$)$_3$(CO)$_3$]$^+$ in bioorganometallic chemistry: design, structure, and in vitro affinity of a 5-HT$_{1A}$ receptor ligand labelled with ^{99m}Tc, J. Am. Chem. Soc. **121** 25 (1999) 6076–6077.

[2.14] LANG, L., et al., Development of fluorine-18-labelled 5-HT$_{1A}$ antagonists, J. Med. Chem. **42** 9 (1999) 1576–1586.

Chapter 3

STUDY OF ^{99m}Tc LABELLED WAY ANALOGUES FOR 5-HT$_{1A}$ RECEPTOR IMAGING

Liu FEI, Youfeng HE, Luo ZHIFU
Department of Isotopes, China Institute of Atomic Energy,
Beijing, China

Abstract

This work focuses on the ^{99m}Tc labelled analogue of WAY 100635 as a potential serotonin 5-HT$_{1A}$ receptor imaging agent. 1-(2-methoxyphenyl)-(4-mercaptoethyl)-piperazine (MPMEP) as monodentate; N,N-bis(2-mercaptoethyl)-N′,N′diethylethylene-diamine (BMPDEEDA) and N,N-bis(2-mercaptoethyl)benzylamine (BMPBA) as tridentate have been synthesized and characterized by infrared analysis (IR), ^{1}H nuclear magnetic resonance (NMR) and element analysis. Two complexes ^{99m}TcO(MPMEP)(BMPDEEDA) (^{99m}Tc-1) and ^{99m}TcO(MPMEP)(BMPBA) (^{99m}Tc-2) have been prepared by the 3 + 1 mixed ligand approach. The labelling conditions were optimized and the complexes were purified by extraction with CH$_2$Cl$_2$ and high performance liquid chromatography. Two complexes were lipophilic and stable for at least 5–7 h at room temperature. The biodistributions of the two ^{99m}Tc complexes were evaluated in mice. The brain uptakes were 1.63 and 1.77% ID/g (percentage of the injected dose per gram), and the retention was 0.87 and 0.46% ID/g for ^{99m}Tc-1 and ^{99m}Tc-2, respectively. The ratios of hippocampus to cerebellum increased with time, reaching a maximum value of 1.24 at 180 min in Wistar rats. The analogous Re complexes were synthesized and characterized by IR, ^{1}H NMR and elemental analysis as a surrogate for the ^{99m}Tc complexes for use in receptor binding assays. During in vitro binding assays, the Re complexes were tested with the competition against [^{3}H]-8-OH-DPAT. Values of 98.7 and 23.2nM were found for the 50% inhibitory concentration (IC$_{50}$) for Re-1 and Re-2, respectively. The hippocampus homogenate from Wistar rats was prepared as a source of 5-HT$_{1A}$ receptor. A scintigraphic investigation in monkeys was carried out after administration with 410 MBq/1.2 mL of ^{99m}Tc-1 and 321 MBq/1.0 mL of ^{99m}Tc-2 for single photon emission computerized tomography imaging. The main area that contains a 5-HT$_{1A}$ receptor-rich region, for example the raphe, septum, cingulatum and hypothalamus, can be seen.

3.1. INTRODUCTION

Serotonin (5-HT) is a major brain neurotransmitter that elicits a multitude of physiological functions by interactions with seven major families of receptors (5-HT$_1$–5-HT$_7$) and their various subtypes. There is substantial evidence from studies of post-mortem tissue of a link between abnormal levels of brain 5-HT$_{1A}$ receptors and neuropsychiatric diseases, including depression [3.1], schizophrenia [3.2, 3.3], dementia of the Alzheimer type, insomnia and anxiety.

WAY 100635 is widely recognized as the first highly selective antagonist (silent antagonist) for the study of 5-HT$_{1A}$ receptors [3.4]. Important research has been focused on the radiolabelling of WAY 100635 with ^{11}C, providing the first effective radiopharmaceuticals to study the 5-HT$_{1A}$ receptors in human brains with positron emission tomography (PET) [3.5–3.8]. The radiolabelling of p-MPPF, a fluoro-analogue of WAY 100635, with ^{18}F has obtained very encouraging results in vivo by autoradiography in cats [3.9], monkeys [3.10] and human beings [3.11]. Despite the success of these tracers as PET imaging agents, a WAY 100635 analogue incorporating the radionuclide ^{99m}Tc would be more desirable for several reasons.

3.2. MATERIALS

A high performance liquid chromatography (HPLC) analysis was performed on a Waters 600 multisolvent delivery system coupled to both a UV absorbance detector set at 254 nm and a Berthold LB506C-1 HPLC gamma detector, as well as a reverse phase C18 column (Waters Spherisorb BDS 5 μm, Φ 4.6 mm × 250 mm).

All laboratory chemicals were reagent grade and used without further purification. Solvents for chromatographic analysis were HPLC grade.

[^{99m}Tc]NaTcO$_4$ was obtained from a commercial [99]Mo/^{99m}Tc generator produced by the China Institute of Atomic Energy (CIAE), Beijing.

[^{3}H]-8-OH-DPAT (specific activity of 135 Ci/mmol (4995 GBq/mmol)) was purchased from NEN[TM] Life Sciences Products, Inc., Boston, MA, USA.

3.3.   METHODS

3.3.1.   Synthesis of the pharmacophore moiety as a monodentate ligand

In previous reports, we have described the synthesis and characterization of the monodentate ligand 1-(2-methoxyphenyl)-4-(2-mercaptoethyl)-piperazine according to the literature [3.12].

3.3.2.   Synthesis of SNS ligands

The SNS ligands, N,N-bis(2-mercaptoethyl)-N′,N′-diethylethylene-diamine (BMPDEEDA) and N,N-bis(2-mercaptoethyl)benzylamine were synthesized by the reaction of N,N-diethylethylenediamine and benzylamine with ethylene sulphide in an autoclave at 110ºC and were purified by fractional distillation under high vacuum.

Each product was characterized by infrared (IR) spectrometry, ^{1}H nuclear magnetic resonance (NMR) and element analysis.

The yield of BMPDEEDA was 41.7%. ^{1}H NMR (300 MHz, CDCl$_3$) gave the following results: δ (ppm): 1.1 (t, 6H CH$_3$), 1.9 (s, 2H, SH), 2.8 (m, 16H (CH$_2$)$_2$ + CH$_2$(ethyl)). Element analysis found the following elements: C: 51.21, H: 9.78, N: 12.24, S: 27.30. The calculated values for C$_{10}$H$_{24}$N$_2$S$_2$ were: C: 51.24, H: 9.46, N: 11.95, S: 27.35.

The yield of N,N-bis(2-mercaptoethyl)benzylamine (BMPBA) was 38.4%. ^{1}H NMR (200 MHz, CDCl$_3$) gave the following results: δ (ppm): 1.7 (s, 2H, SH), 2.5–2.8 (m, 8H, ethyl), 3.6 (s, 2H, phenyl-CH$_2$), 7.3 (m, 5H, phenyl). Element analysis found the following elements: C: 58.43, H: 7.28, N: 6.43, S: 28.75. The calculated values for C$_{11}$H$_{17}$NS$_2$ were: C: 58.11, H: 7.54, N: 6.16, S: 28.20.

3.3.3.   Preparation of ^{99m}Tc-1 and ^{99m}Tc-2 complexes

The ^{99m}Tc complex formations (scheme 1) are shown in Fig. 3.1.

First, 125 mg of glucoheptonate was dissolved in 50 mL water, then 1N HCl solution of 50 mg SnCl$_2$·2H$_2$O was added to the solution and the pH was adjusted to 7.5. After filtration through a 0.22 μm millipore filter, the solution was divided into 50 vials and lyophilized. An eluate of 1 mL Na^{99m}TcO$_4$ (1850–3700 MBq) was added to a lyophilized kit. The labelling efficiency was 98%.

To an equal molar (1×10^{-6}–1×10^{-8} mol) mixture of monodentate ligand and tridentate ligand in ethanol solution, 5–50 mCi (185–1850 MBq) of the ^{99m}Tc glucoheptonate precursor (radiochemical purity >95%) was added. The monodentate and tridentate ligand concentrations, reaction time, pH and
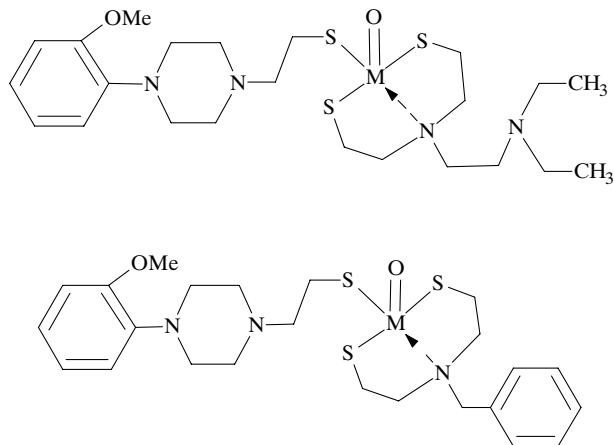
FIG. 3.1. ^{99m}Tc complex formations (M = ^{99m}Tc, Re).

temperature of the reaction system were optimized to achieve a high labelling yield (Fig. 3.2).

The radiochemical purity of the ^{99m}Tc complexes was determined by thin layer chromatography and HPLC. The thin layer chromatography was performed on a Whatman No. 1 strip and eluted with a 0.9% saline solution and CHCl$_3$:CH$_3$OH = 9:1 (vol./vol.), respectively. An HPLC analysis and purification (Fig. 3.3) was performed with a reverse phase C18 column. The isocratic solvent methanol:water ratio was 70:30 for ^{99m}Tc-1 and 75:25 for ^{99m}Tc-2, with a flow of 1 mL/min.

The characterization of ^{99m}Tc complexes was accomplished by comparative studies after co-injection of the Re complexes and corresponding ^{99m}Tc complexes at tracer level with HPLC analysis and simultaneous UV–vis and gamma detection.

The stability of the ^{99m}Tc complexes was determined at room temperature (Table 3.1) by measuring radiochemical purity values at different times (1, 3, 5, 7 h) after preparation.

3.3.4. Determination of the partition coefficient for ^{99m}Tc complexes

The partition coefficient was determined by mixing the complex with equal volumes of 1-octanol and phosphate buffer (0.025M, pH7.0 and pH7.4,
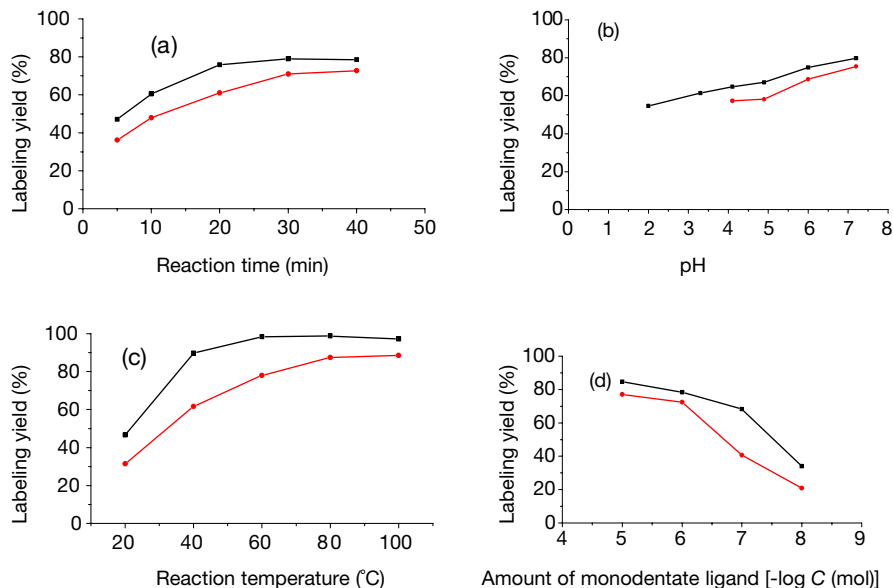
FIG. 3.2. *Influence of different reaction parameters on labelling yield: (a) reaction time, (b) pH, (c) reaction temperature, (d) amount of monodentate ligand. Black lines, ^{99m}Tc-1; red lines, ^{99m}Tc-2.*
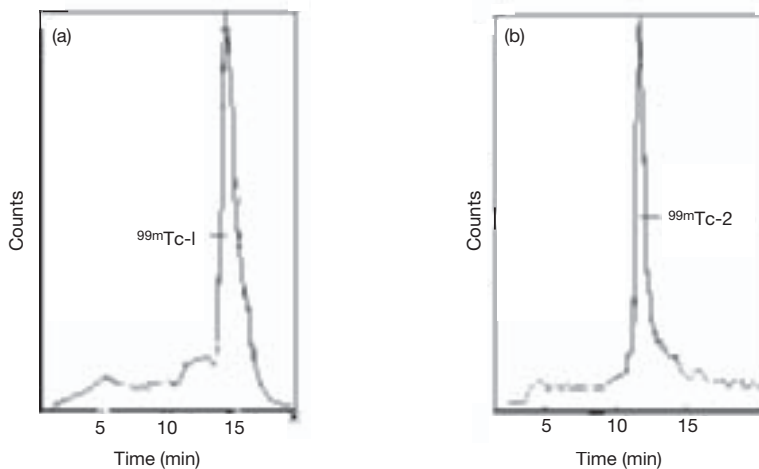
FIG. 3.3. *The HPLC radiochromatogram of ^{99m}Tc complexes (Waters Spherisorb BDS2, 5 µm, Φ 4.6 mm $\times$ 250 mm; isocratic). Solvent: (a) ^{99m}Tc-1, methanol:water ratio of 70:30; (b) ^{99m}Tc-2, methanol:water ratio of 75:25. The flow was 1 mL/min.*

TABLE 3.1.   STABILITY OF ^{99m}Tc COMPLEXES AT ROOM TEMPERATURE

Radiochemical purity (%)	Time after preparation (h)			
	1	3	5	7
^{99m}Tc-1	96.4	95.1	96.1	95.0
^{99m}Tc-2	94.7	94.3	92.1	93.2

respectively) in a centrifuge tube. The mixture was vortexed at room temperature for 1 min and then centrifuged at 5000 rev./min for 5 min. Subsequently 100 μL samples from the 1-octanol and aqueous layers were pipetted into other test tubes and counted in a well gamma counter. The measurement was repeated three times. The partition coefficient value was expressed as log *P*.

3.3.5.   Biodistribution study of ^{99m}Tc complexes

Twelve Kunming mice (weighing 18–20 g) were divided into four groups. Each mouse was injected with ^{99m}Tc-1 or ^{99m}Tc-2 (0.55–0.74 MBq/100 μL H$_2$O, maximum of 25% MeOH purification by HPLC) in the lateral tail vein. Mice were sacrificed at 2, 15, 30 and 60 min post-injection. The organs and tissues of interest were removed. The wet organs were weighed and the radioactivity was determined in a gamma counter. Suitable standards, representing 1/100 of the injected dose, were prepared from the injection material. The results were expressed as % dose/organ and % dose/g. The brain/blood ratio was calculated from the corresponding percentage of the injected dose per gram (% ID/g) values.

Studies of brain region uptake were performed in normal Wistar rats (150–200 g, four animals per group) by injection of ^{99m}Tc-1 or ^{99m}Tc-2 (200–300 μCi (7.4–11.1 MBq)/200 μL H$_2$O, maximum of 25% MeOH) purified by concentrated organic extraction, then HPLC separation. The rats were sacrificed by exsanguination at 30, 60, 120 and 180 min post-injection. Their whole brains were removed and frozen for an hour. The hippocampus, striatum, cortex and cerebellum were dissected, weighed and measured for radioactivity. The radioactivity in each region was expressed in units of % ID/g. Tissue/cerebellum (T/CB) ratios were calculated (Tables 3.2–3.5, SD stands for standard deviation).

TABLE 3.2. BIODISTRIBUTION OF ^{99m}Tc-1 IN MICE ($X \pm$ SD; $n = 3$)

Tissue	% ID				% ID·g^{-1}			
	2 min	15 min	30 min	60 min	2 min	15 min	30 min	60 min
Blood	19.38 ± 4.22	4.10 ± 0.26	2.99 ± 0.10	1.18 ± 0.54	51.45 ± 10.64	10.00 ± 0.81	7.50 ± 0.34	4.45 ± 1.01
Brain	0.63 ± 0.07	0.56 ± 0.04	0.55 ± 0.05	0.37 ± 0.04	1.63 ± 0.27	1.33 ± 0.13	1.26 ± 0.15	0.87 ± 0.05
Heart	3.62 ± 0.18	1.27 ± 0.19	1.17 ± 0.38	0.65 ± 0.09	31.52 ± 1.53	12.40 ± 2.38	10.03 ± 2.15	6.19 ± 0.31
Liver	10.21 ± 1.37	41.44 ± 11.73	26.83 ± 6.59	30.09 ± 14.52	24.44 ± 4.23	50.67 ± 7.35	36.07 ± 14.56	32.98 ± 2.78
Kidneys	10.12 ± 2.62	10.24 ± 2.37	8.75 ± 2.15	4.97 ± 0.32	41.19 ± 9.72	34.96 ± 7.28	32.56 ± 6.18	17.67 ± 1.13
Lungs	15.62 ± 2.12	12.87 ± 3.99	13.54 ± 4.94	9.89 ± 2.06	95.22 ± 36.29	72.25 ± 17.27	78.38 ± 18.95	55.27 ± 10.05
Brain/blood					0.03	0.13	0.17	0.19

TABLE 3.3. BIODISTRIBUTION OF ^{99m}Tc-2 IN MICE ($X \pm$ SD; $n = 3$)

Tissue	% ID				% ID·g^{-1}			
	2 min	15 min	30 min	60 min	2 min	15 min	30 min	60 min
Blood	1.84 ± 0.24	0.92 ± 0.25	0.88 ± 0.29	0.62 ± 0.20	5.04 ± 1.03	2.22 ± 0.19	2.40 ± 0.86	1.42 ± 0.14
Brain	0.69 ± 0.07	0.41 ± 0.02	0.34 ± 0.02	0.19 ± 0.04	1.77 ± 0.16	1.02 ± 0.04	0.80 ± 0.06	0.46 ± 0.15
Heart	1.07 ± 0.09	0.28 ± 0.02	0.23 ± 0.04	0.14 ± 0.03	12.30 ± 3.04	3.16 ± 0.12	2.48 ± 0.39	1.56 ± 0.25
Liver	16.26 ± 3.82	15.01 ± 2.50	18.76 ± 1.46	18.65 ± 3.33	26.87 ± 4.99	22.00 ± 3.25	26.11 ± 2.81	24.10 ± 5.11
Kidneys	5.02 ± 0.42	3.50 ± 0.40	3.59 ± 0.87	2.11 ± 0.42	18.57 ± 2.32	11.02 ± 2.05	12.20 ± 2.81	7.64 ± 1.77
Lungs	3.95 ± 0.53	1.28 ± 0.35	1.19 ± 0.28	0.73 ± 0.18	46.04 ± 13.27	11.39 ± 2.41	8.14 ± 1.28	4.91 ± 1.33
Brain/blood					0.31	0.46	0.33	0.32

TABLE 3.4. BRAIN REGIONAL UPTAKE OF ^{99m}Tc-1 IN FEMALE WISTAR RATS
(percentage dose/g) (means ± SD, n = 4)

Tissue	Time post-injection (min)			
	30	60	120	180
Oblongatal	0.082 ± 0.015	0.071 ± 0.026	0.088 ± 0.018	0.040 ± 0.032
Hippocampus (HP)	0.077 ± 0.073	0.068 ± 0.008	0.084 ± 0.018	0.067 ± 0.022
Frontal	0.081 ± 0.001	0.086 ± 0.022	0.100 ± 0.009	0.052 ± 0.029
Occipital	0.086 ± 0.018	0.093 ± 0.028	0.108 ± 0.021	0.052 ± 0.029
Thalamus	0.091 ± 0.026	0.100 ± 0.014	0.154 ± 0.078	0.090 ± 0.072
Striatum	0.065 ± 0.012	0.088 ± 0.022	0.104 ± 0.027	0.061 ± 0.030
Parietal	0.089 ± 0.012	0.082 ± 0.028	0.103 ± 0.016	0.060 ± 0.018
Temporal	0.081 ± 0.012	0.058 ± 0.019	0.096 ± 0.030	0.058 ± 0.018
Remainder	0.080 ± 0.001	0.076 ± 0.026	0.099 ± 0.012	0.050 ± 0.022
Cerebellum (CB)	0.086 ± 0.017	0.074 ± 0.015	0.095 ± 0.003	0.054 ± 0.031
HP/CB	0.847	0.880	0.921	1.244

TABLE 3.5. BRAIN REGIONAL UPTAKE/CB RATIOS OF ^{99m}Tc-1 IN FEMALE WISTAR RATS
(percentage dose/g, means ± SD, n = 4)

Ratio	Time post-injection (min)			
	30	60	120	180
Oblongatal/CB	0.951	0.924	0.962	0.740
Hippocampus/CB	0.847	0.880	0.921	1.244
Frontal/CB	0.941	1.049	1.158	0.973
Occipital/CB	0.996	1.128	1.259	0.968
Thalamus/CB	1.053	1.617	1.356	1.684
Striatum/CB	0.752	1.092	1.185	1.132
Parietal/CB	1.026	1.077	1.106	1.113
Temporal/CB	0.933	1.006	0.780	1.079
Remainder/CB	0.928	1.034	1.026	0.924

3.3.6.   Synthesis of oxorhenium complexes Re-1 and Re-2

To a mixture of 166 mg (0.2 mmol) trichloro-bis(triphenylphosphine) rhenium (V) oxide in 10 mL methanol and 164 mg (2 mmol) anhydrous sodium acetate in 2 mL methanol was added a solution under stirring of 65 mg (0.2 mmoL) monodentate ligand 1-(2-methoxyphenyl)-(4-mercaptoethyl)-piperazine (MPMEP) and 47 mg (0.2 mmol) tridentate BMPDEEDA in 1 mL methanol. The reaction mixture was refluxed for 3 h until the green yellow colour of the precursor turned to dark green and the solution became dark green. After cooling to room temperature, the reaction mixture was diluted with dichloromethane (20 mL) and then washed with water. The organic layer was separated from the mixture. The volume of the solution was reduced to 5 mL. Re-1 was purified using a chromatography column (silica gel $GF_{254}(60)$; the retention fraction R_f of Re-1 was 0.5 with the eluting system being dichloromethane:acetone = 2/1; the R_f of the others was 1).

With the same method, to a mixture of 340 mg (0.4 mmoL) trichloro-bis(triphenylphosphine) rhenium (V) oxide in 20 mL methanol and 350 mg (4 mmoL) anhydrous sodium acetate in 5 mL methanol were added a solution under stirring of 130 mg (0.4 mmol) monodentate ligand MPMEP and 100 mg (0.4 mmol) tridentate ligand BMPBA in 5 mL methanol. The reaction mixture was refluxed for 3 h until the green yellow colour of the precursor turned to dark green and the solution became dark green. The mixture was stirred overnight at room temperature, then the reaction mixture was diluted with dichloromethane (30 mL) and washed with water. The organic layer was separated from the mixture. The volume of the solution was reduced to 5 mL. Re-2 was purified using a chromatography column (silica gel $GF_{254}(60)$ and R_f = 0.4 with the eluting system being acetonitrile:dichloromethane:benzene = 6:1:1; the R_f of the others was 1).

3.3.7.   Preparation of a membrane receptor for binding assays

Wistar rats were decapitated, and their brains were rapidly chilled and dissected to obtain the hippocampus on an ice cold plate. The tissue was homogenized in 40 volumes of ice cold tris-HCl buffer (50mM, pH7.4 at 22℃) with FS-2 Polytron. The homogenate was centrifuged at 20 000g for 20 min at 4℃. The resulting pellet was then resuspended in the same buffer, and the centrifugation and resuspension process was repeated three times to wash the membranes. Between the second and third repetitions the resuspended membranes were incubated for 10 min at 37℃ to facilitate the removal of endogenous 5-HT. The final pellet was resuspended in the buffer to a final concentration and stored at –60℃ in 1 mL aliquots. The protein content was

determined according to Lowry's method, with bovine serum albumin used as a standard.

3.3.8. In vitro receptor binding assay

Competition binding experiments were performed in a final volume of 250 µL duplicate by using [^{3}H]-8-OH-DPAT as radioligand (Fig. 3.4). Aliquots of volume 50 µL (which corresponded to 50 µg of protein) of rat hippocampal homogenates were mixed with 50 µL [^{3}H]-8-OH-DPAT (0.185nM) tris-HCl buffer (50mM tris-HCl, 0.1% ascorbic acid, 2mM CaCl$_2$, pH7.5) and 50 µL of increasing concentrations (10^{-5}–10^{-10}M) of competing Re-1 or Re-2. Non-specific binding was defined with 10µM 8-OH-DPAT. Incubation was carried out for 20 min at 37°C and then by separation of bound from free radioligand by filtration through GF/B glass fibre filters, presoaked with 1% bovine serum albumin (BSA). The filters were then washed three times with 3 mL of ice cold tris-HCl buffer (50mM tris-HCl, 154mM NaCl) and dried in an oven for 10 min, then placed in a 2 mL scintillation cocktail. Radioactivity was measured by liquid scintillation spectrometry. The results of competitive experiments were analysed with the computer software Origin (version 6.0) to obtain the IC$_{50}$ values:

IC$_{50}$ = 5.61 × 10^{-9} (±1.12 × 10^{-11}) mol/L (n = 2)   IC$_{50}$ = 2.63 × 10^{-8} (±5.42 × 10^{-9}) mol/L (n = 2)

IC$_{50}$ = 9.87 × 10^{-8} (±1.51 × 10^{-9}) mol/L (n = 3)   IC$_{50}$ = 2.32 × 10^{-8} (±3.11 × 10^{-8}) mol/L (n = 3).

3.3.9. In vivo SPECT imaging in monkeys

A normal male monkey (4–5 kg), three years old, was put into 400 mg KClO$_4$ for blocking of the choroid plexus. After 60 min, the monkey was anaesthetized with 5% ketamine by intramuscular administration, then 321 MBq/1.0 mL ^{99m}Tc-1 was administered through a vein. Single photon emission computerized tomography (SPECT) imaging was performed for 70 min, and whole body imaging for 150 min.

410 MBq/1.2 mL ^{99m}Tc-2 was administered via a vein. SPECT imaging was performed with the same procedure.

The results are shown in Fig. 3.5.
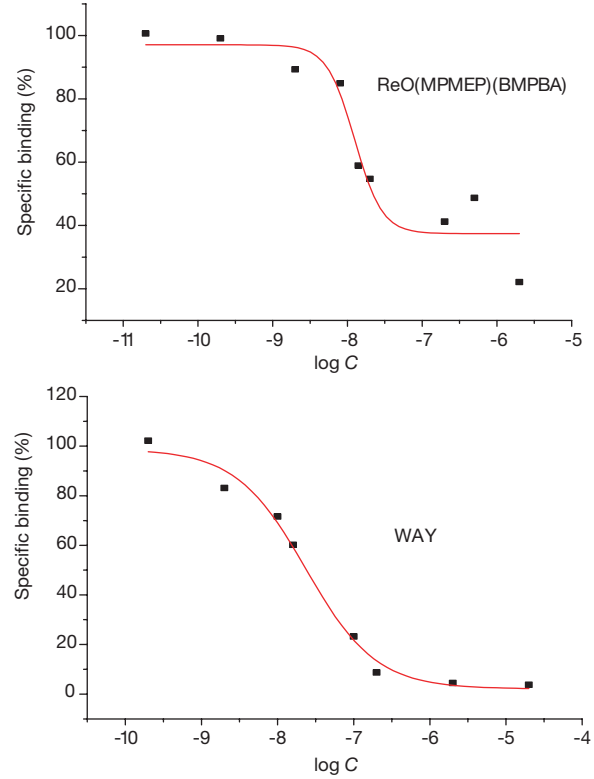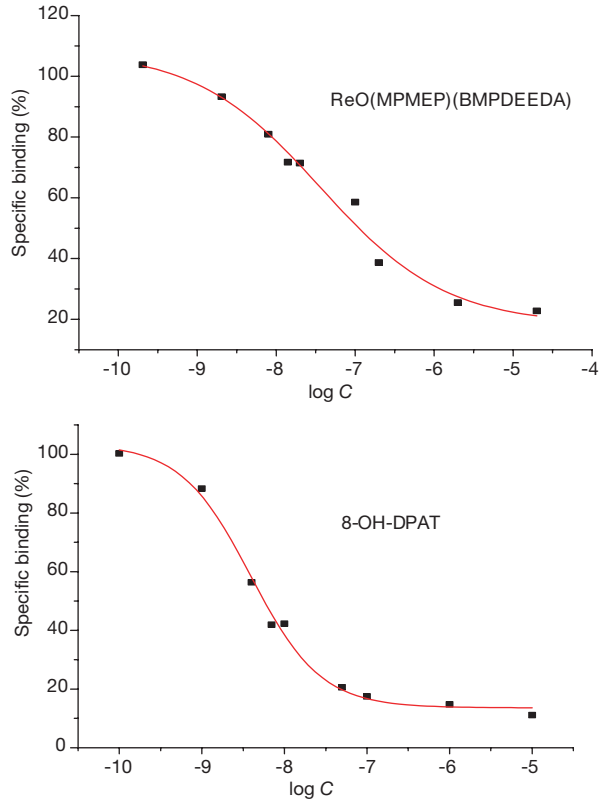
FIG. 3.4. Competition curves (C is the ligand concentration) of the Re complexes and co-ligand MPMEP for specific [³H]-8-OH-DPAT binding sites in rat hippocampal homgenate. 8-OH-DPAT was used as control.
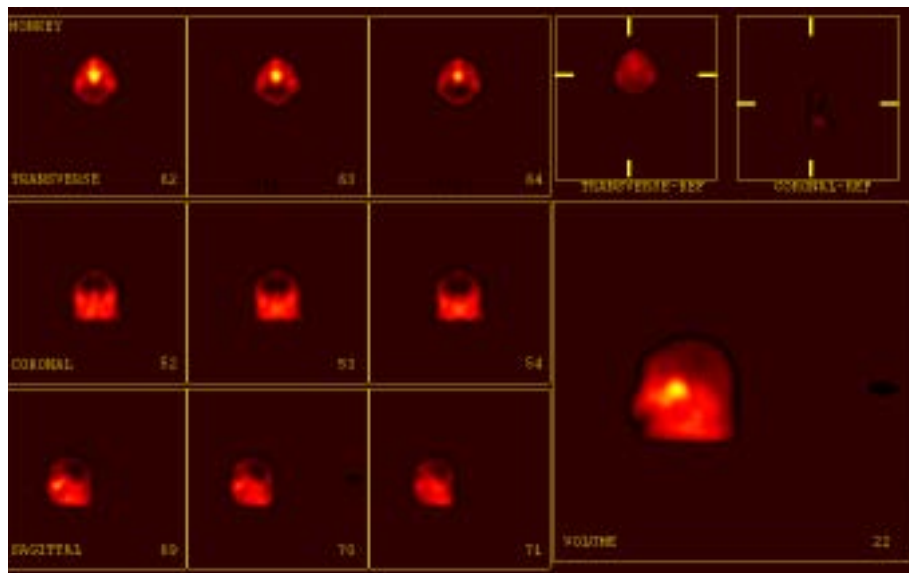
FIG. 3.5. SPECT images of ^{99m}Tc-2 in monkeys.

3.4. RESULTS AND DISCUSSION

Tracer level preparation was achieved using ^{99m}Tc glucoheptonate as precursor. Effects of reaction time, pH, reaction temperature and quantity of the monodentate ligand for labelling yield were investigated, and the results are shown respectively in Figs 3.2(a)–(d). If the pH is raised to 7–8, the precipitate occurred in solution.

^{99m}Tc-1 and ^{99m}Tc-2 were obtained in high labelling yield and high radio-chemical purity (>95%) by dichloromethane extraction and HPLC purification, by heating at 60–70°C for 30 min; concentrations ranged from 1×10^{-7} to 1×10^{-6} mol.

HPLC analysis indicates the formation of a major complex with radio-chemical purity above 80% for complex ^{99m}Tc-1 and above 70% for complex ^{99m}Tc-2. The radiochemical purity of the organic extract was above 95% by HPLC for both complexes. Major peaks with retention times of 14.5 min for ^{99m}Tc-1 and 12.3 min for ^{99m}Tc-2 were obtained. The retention times of the non-labelling monodentate ligand were 18.5 and 15.0 min for the ^{99m}Tc-1 and ^{99m}Tc-2 labelling systems, respectively.

Both complexes were stable (radiochemical purity >90%) after being purified by HPLC at room temperature. The partition coefficients (log P) were

calculated as 1.30 and 1.57 for ^{99m}Tc-1 and ^{99m}Tc-2, respectively, showing that the two complexes are good lipophilics and possibly cross the intact blood–brain barrier (BBB).

Biodistribution studies have demonstrated that both complexes can penetrate the BBB. Higher brain uptake (1.63 and 1.77% ID/g for ^{99m}Tc-1 and ^{99m}Tc-2, respectively, at 2 min) and good retention (0.87 and 0.46% ID/g for ^{99m}Tc-1 and ^{99m}Tc-2 at 60 min) were observed in mice. The ratio (brain/blood) was 0.19 and 0.32 after administration for 60 min for ^{99m}Tc-1 and ^{99m}Tc-2, respectively. The clearance of radioactivity from blood of ^{99m}Tc-1 is more rapid than that of ^{99m}Tc-2. But both radioactivity levels in blood are high. Two complexes showed high lung and liver uptakes and excretion, mainly through the hepatobiliary system and urinary elimination.

Further evaluation for ^{99m}Tc-1 — studies of the brain region biodistribution — showed a slight accumulation of activity in the hippocampus area, where 5-HT$_{1A}$ is abundant, in comparison with regions with no serotonin (i.e. the cerebellar region). Ratios of HP/CB increased as time passed; the maximum value was 1.244 at 180 min. The regional brain distribution indicated that the complex was concentrated in the thalamus area. Experiments for ^{99m}Tc-2 are in progress.

The affinities of the two Re complexes and monodentate ligand MPMEP for the 5-HT$_{1A}$ receptor subtypes were assessed in vitro on the basis of their ability to compete with the [^{3}H]-8-OH-DPAT binding to rat hippocampal tissue homogenate. The competition curves are shown in Fig. 3.4. Displacements of the specific binding of [^{3}H]-8-OH-DPAT to 5-HT$_{1A}$ binding sites on addition of increasing doses of both Re complexes and the monodentate ligand MPMEP were seen. The binding affinity of the monodentate ligand MPMEP displayed a moderate affinity for the 5-HT$_{1A}$ receptor (IC$_{50}$ = 26.3nM) in a competition assay against [^{3}H]-8-OH-DPAT. No significant effect after introduction of a Re metal group into MPMEP was observed during in vitro receptor binding assays (IC$_{50}$ = 98.7nM for Re-1 and IC$_{50}$ = 23.2nM for Re-2). The value of IC$_{50}$ of 8-OH-DPAT was 5; 61nM (IC$_{50}$ < 10nM in the literature) was used as control.

A scintigraphic investigation showed a lower brain uptake in monkeys in SPECT imaging, but the radioactivity was observed in the areas that are rich in 5-HT$_{1A}$ receptor and moderately high septum, cingulate and hypothalamus, for example. The scintigraphic imaging showed that activity uptake was significant in the area that contains raphe and high 5-HT$_{1A}$ receptor density but was absent in cerebellum.

3.5. CONCLUSIONS

A monodentate ligand 1-(2-methoxyphenyl)-(4-mercaptoethyl)-piperazine and both SNS BMPDEEDA and N,N-bis(2-mercaptoethyl) benzylamine have been synthesized and characterized by IR, ^{1}H NMR and element analysis. Two 3 + 1 mixed ligand complexes were prepared by a ligand exchange reaction with ^{99m}Tc glucoheptonate as a potential 5-HT$_{1A}$ receptor imaging agent. Ligand concentration, reaction time and temperature were optimized to achieve high substitution yield and radiochemical purity. Both complexes were good lipophilics and stable for at least 5–7 h at room temperature in vitro. Biodistribution studies for both ^{99m}Tc complexes showed selective brain uptake and retention in mice. The brain uptake in mice was higher than the data reported in the literature, but the brain/blood ratio was low due to the high blood activities. No significant uptake in 5-HT$_{1A}$ receptor-rich regions (hippocampus) was observed at 30, 60 and 120 min, but there was a slight retention at 180 min for ^{99m}Tc-1 in the brain region distribution of Wistar rats. The analogous Re compounds were synthesized as a surrogate for the ^{99m}Tc complexes for use in receptor binding assays. During in vitro binding assays, the Re analogues were tested with a competition assay against [^{3}H]-8-OH-DPAT. A scintigraphic investigation of monkeys was carried out after administration of ^{99m}Tc-1 and ^{99m}Tc-2 for SPECT imaging. The main area that contains a 5-HT$_{1A}$ receptor-rich region can be seen.

ACKNOWLEDGEMENTS

REFERENCES TO CHAPTER 3

[3.1] MATSUBARA, S., ARORA, R.C., MELTZER, H.Y., Serotonergic measures in suicide brain 5-HT$_{1A}$ binding-sites in frontal cortex of suicide victims, J. Neural Transm. **85** (1991) 181–194.

[3.2] BURNETT, P.W.J., EASTWOOD, S.L., HARRISON, P., [^{3}H] WAY 100635 for 5-HT$_{1A}$ receptor autoradiography in human brain: A comparison with [^{3}H]8-OH-DPAT and demonstration of increased binding in the frontal cortex in schizophrenia, Neurochem. Int. **30** (1997) 565–574.

[3.3] HASHIMOTO, T., NISHINO, N., NAKAI, H., TANAKE, C., Increase of serotonin 5-HT$_{1A}$ receptors in prefrontal and temporal cortices of brain with chronic schizophrenia, Life Sci. **48** (1991) 355–365.

[3.4] FLETCHER, A., et al., A pharmacological profile of WAY-100635, a potent and selective 5-HT$_{1A}$ receptor antagonist, Br. J. Pharmacol. **112** (1994) 91.

[3.5] FARDE, L., ITO, H., SWAHN, C.G., PIKE, V.W., HALLDIN, C., Quantitative analyses of carbonyl-carbon-11-WAY-100635 binding to central 5-hydroxytryptamine-1A receptors in man, J. Nucl. Med. **39** (1998) 1965–1971.

[3.6] GUNN, R.N., et al., Tracer kinetic modeling of the 5-HT$_{1A}$ receptor ligand [carbonyl-^{11}C]WAY-100635 for PET, Neuroimage **8** (1998) 426–440.

[3.7] ITO, H., HALLDIN, C., FARDE, L., Localization of 5-HT$_{1A}$ receptors in the living human brain using [carbonyl-^{11}C]WAY-100635: PET with anatomic standardization technique, J. Nucl. Med. **40** (1999) 102–109.

[3.8] PIKE, V.W., et al., [Carbonyl-^{11}C]desmethyl-WAY-100635 (DWAY) is a potent and selective radioligand for central 5-HT$_{1A}$ receptors in vitro and in vivo, Eur. J. Nucl. Med. **25** (1998) 338–346.

[3.9] LE BARS, D., et al., High-yield radiosynthesis and preliminary in vivo evaluation of *p*-[^{18}F]MPPF, a fluoro analog of WAY-100635, Nucl. Med. Biol. **25** (1998) 343–350.

[3.10] SHIUE, C.Y., et al., p-[F-18]-MPPF: A potential radioligand for PET studies of 5-HT$_{1A}$ receptors in humans, Synapse **25** (1997) 147–154.

[3.11] PLENEVAUX, A., et al., 5-HT$_{1A}$ receptors visualization with *p*-[^{18}F]MPPF in healthy volunteers, J. Labelled Compd. Radiopharm. **42** Suppl. 1 (1999) S60–S61.

[3.12] INTERNATIONAL ATOMIC ENERGY AGENCY, Report on 3rd Research Co-ordination Meeting of the Co-ordinated Research Project on Development of Agents for Imaging Central Neural System Receptors based on ^{99m}Tc held in Montevideo, 2000, internal report, IAEA, Vienna.

Chapter 4

PREPARATION AND EVALUATION OF MIXED LIGAND TECHNETIUM COMPLEXES FOR IMAGING CENTRAL NEURAL SYSTEM RECEPTORS

J.C. ARENCIBIA, A.A. RAMÍREZ,
L.H. FERNÁNDEZ
Centro de Isótopos,
Havana, Cuba

Abstract

Oxo-Tc (V) complexes with functionalized thiol ligands, so called 3 + 1 complexes of the general formula $[MOL_1K_1]$ (where L is a tridentate di- or tri-thiol ligand and K is a monothiol ligand), play an important role in the development of receptor binding Tc complexes. A few five co-ordinated oxorhenium and oxotechnetium mixed ligand complexes containing a SNS/S or SSS/S atom set were synthesized and characterized. In almost all the complexes obtained, one of the ligands carries a piperazino-N-Ph-OCH$_3$ moiety, a group which has been investigated for its affinity and specificity for the serotonin 5-HT$_{1A}$ brain receptors. Reproduction of the analogous Tc complexes at tracer level was undertaken and the corroboration of their structure with their chemically characterized analogues at carrier level was investigated by chromatographic methods. Preliminary results show that Tc (V) complexes at non-carrier level can be obtained in suitable yields using different procedures adding first the monodentate co-ligand and with precise control of the quantity of both ligands. Biodistribution data indicate that synthesized complexes cross the blood–brain barrier but they do not show significant uptake and retention for receptor imaging.

4.1. INTRODUCTION

Radiopharmaceuticals that bind to CNS receptors in vivo are potentially useful for understanding the pathophysiology of a number of neurological and psychiatric disorders, their diagnosis and treatment. Labelled compounds with ultrashort lived isotopes for positron emission tomography (PET) imaging have played a vital role in establishing the usefulness of imaging of CNS receptors and relating the receptor density to disease status [4.1]. Owing to the high cost of PET studies, there is considerable interest in the design and development of new technetium radiopharmaceuticals for imaging CNS receptors [4.2].

The major CNS receptor types include the opioid, adrenergic, benzodi-azepine, cholinergic, serotonin and dopamine receptors. Great efforts have been focused on the study of serotonin-1A (5-HT$_{1A}$) receptors of the CNS. The serotonin system is an important neurotransmission network which is involved in the modulation of various physiological functions and behaviour, such as thermoregulation, cardiovascular function, aggressive and sexual behaviour, mood, appetite and the sleep–wake cycle. These receptors are implicated in the pathogenesis of anxiety, depression, hallucinogenic behaviour, travel sickness and eating disorders. For the visualization of these receptors several ligands have been evaluated, starting from the lead structure of WAY 100635 [4.2–4.4], a selective antagonist whose residue, 1-(2-methoxyphenyl)piperazine, is known to bind with high affinity to the serotonin receptors.

At the second and third meetings of the Co-ordinated Research Programme, held in Athens (1998) and Montevideo (2000), arose a recommen-dation to pursue the study of ^{99m}Tc serotonin receptors based on the WAY 100635 template molecule using different labelling approaches. The purpose of this work was to explore the 3 + 1 and 2 + 1 + 1 concepts for the preparation of ^{99m}Tc compounds bearing the 1-(2-methoxyphenyl)piperazine moiety in the structure. This report covers the investigations on Tc labelled complexes carried out at the Centro de Isótopos, Havana, during the past four years.

4.2. MATERIALS

ReOCl$_3$(PPh$_3$)$_2$, N,N-bis(mercaptoethyl)-N,N-diethylethylenediamine and (4-methylthio-phenolato)-[N′, N′-diethylethylenediamine-(N,N-bis(2-mercapto-ethyl)]-oxorhenium (V) were provided by M. Papadopoulos from the Demokritos National Centre for Scientific Research, Athens.

The compound 1-(2-methoxyphenyl)-4-(2-mercaptoethyl)-piperazine was synthesized from the 1-(2-methoxyphenyl)piperazine following the known procedure [4.5]: A solution of 1-(2-methoxyphenyl)piperazine in dry toluene was mixed with ethylene sulphide and placed in an autoclave and heated to 120ºC. After cooling the solvent was removed and the desired product was collected by fractional distillation under reduced pressure.[4.1]

[4.1] This compound was obtained from the Demokritos National Centre for Scien-tific Research, Athens, during the fellowship of a Cuban specialist sponsored by Centro de Isótopos, Havana**.**

The compound chloro-(3-thiapentan-1,5-dithiolato)-oxorhenium (V) was also synthesized, as follows.[4.2] A chloroform solution of 2.55 g of $[(C_4H_9)N][ReOCl_4]$ was mixed with 620 mg of 3-thiopentan-1,5-dithiol at 0–5ºC. The reaction mixture was left overnight at –18ºC. Then $CHCl_3$ was removed by vacuum filtration and the product was recrystallized from chloroform. The yield was 70%.

All other chemicals were purchased from Sigma (United States of America) or Merck (Germany) and were used without further purification.

Technetium-99 in the form of NH_4TcO_4 was purchased from Amersham Biosciences (United Kingdom) and [99mTc] was obtained from a commercial [99Mo]–[99mTc] generator (Cis Bio International, Gif-sur-Yvette). The [[99mTc]Tc] (V)-gluconate intermediate was produced using a home-made kit containing 20 mg of sodium gluconate and 0.1 mg of $SnCl_2$.

4.3. METHODS

4.3.1. General

Complexes prepared at carrier level were characterized by infrared (IR), ultraviolet to visible (UV–vis), thin layer chromatography (TLC) and high performance liquid chromatography (HPLC) analysis. Infrared spectra were obtained from KBr pellets on a Pye Unicam FT-IR spectrophotometer. UV–vis spectra were obtained in chloroform using a Spectromic Genesys 5 spectrophotometer.

Aluminium sheets of silica gel G-60 plates were used for TLC analysis. Three different systems were used as mobile phase: $CHCl_3$:MeOH (9:1), MeOH:HCl (9:1) and ethanol:dichloromethane:acetonitrile (1:1:1). Detection of the compounds of interest was made by UV at 254 nm and by autoradiography.

HPLC analyses were performed on a Shimadzu chromatograph equipped with an RPC-18 column using different mixtures as mobile phase at 1 mL/min flow rate. Detection of compounds of interest was accomplished with a photodiode array detector for recording the UV–vis spectrum. For the radio-activity measurements, fractions of 0.5 mL were collected and measured.

[4.2] This compound was synthesized at the Institute of Bioinorganic and Radio-pharmaceutical Chemistry of Forschungszentrum Rossendorf, Germany, during the fellowship of a Cuban specialist sponsored by the IAEA.

The radioactivity was measured in a well type automatic gamma counter (a Wallac Wizard instrument).

4.3.2. Preparation of Tc (V) gluconate precursor

The preparation of Tc (V) gluconate precursor at carrier and non-carrier level was undertaken following a known procedure [4.6]. The yield was over 90% at carrier level and more than 99% at non carrier level.

4.3.3. Preparation of complex Re-1

The synthesis of [1-(2-methoxyphenyl)-4-(2-mercaptoethyl)-piperazine]-[3-thiapentan-1, 5-dithiolato]-oxorhenium (V) (complex Re-1) was carried out according to the general procedure for this kind of Re (V) complex described in Refs [4.7–4.9]. To a solution of 156 mg (0.4 mmol) of chloro-(3-thiapentan-1,5-dithiolato)-oxorhenium (V) in 20 mL acetonitrile were added under stirring 201.6 mg (0.8 mmol) of the co-ligand (1-(2-methoxyphenyl)-4-(2-mercap-toethyl))piperazine in acetonitrile. The reaction mixture was heated and stirred for 2 h at 55–60ºC in a water bath until the solution became dark red and a solid appeared. After cooling to room temperature the solid was collected by Buchner filtration, dried, and characterized by UV and IR spectroscopy, TLC and HPLC.

4.3.4. Preparation of Tc complexes at carrier level (^{99}Tc)

A fresh solution of ^{99}Tc (V) gluconate (Section 4.3.2) was added under stirring to a mixture of 0.2 mmol of the tridentate and monodentate ligands. The solution was stirred for 20 min and then extracted twice with dichloromethane (20 mL each). The organic phase was separated, dried over $MgSO_4$ and filtered. The volume of the solution was reduced to 5 mL, and then 5 mL of ethanol were added. Slow evaporation of solvents under N_2 flow at room temperature afforded the product as crystals.

4.3.5. Preparation of Tc complexes at tracer level (^{99m}Tc)

Different procedures were used: in the first, ^{99m}Tc (V) gluconate solution was added to a vial containing equimolar quantities (0.02 mmol) of ligand and co-ligand, while in the second the co-ligand was added first and after the pH adjustment the ligand was added. After that the mixture was agitated, extracted twice with 2 mL of dichloromethane, dried over $MgSO_4$ and filtered.

When it was possible, the identity of the ^{99m}Tc complexes was established by comparative HPLC and TLC studies of the corresponding Re complexes.

4.3.6. Biodistribution studies

Complexes prepared at tracer level were evaluated in male Wistar rats. 100–200 µL of solution of the desired ^{99m}Tc complex was injected into the tail vein. The rats were sacrificed at different times after injection and the main organs were weighed and counted. The percentage dose per gram was calculated.

4.4. RESULTS AND DISCUSSION

A few five co-ordinated oxorhenium and oxotechnetium mixed ligand complexes containing the SNS/S or SSS/S atom set were synthesized and characterized. Most of the complexes carried a piperazino-N-Ph-OCH$_3$ moiety, a group which has been investigated for its affinity and specificity for the serotonin 5-HT$_{1A}$ brain receptors. Given that the tridentate ligand and monodentate co-ligand were deprotonated upon co-ordination to the MO^{3+} core, neutral complexes are generated in both the oxo-Re and oxo-Tc complexes.

Table 4.1 summarizes the results obtained in the synthesis of Re and Tc mixed complexes.

4.4.1. Synthesis of Re mixed complexes

Substitution of SNS/SSS ligands and co-ligands on the $[Re(V)O]^{3+}$ precursor in a molar ratio of 1:1 yielded mainly one complex according to chromatographic analysis. The complexes Re-1 and Re-2 were obtained with yields of 65 and 22%, respectively.

ReO stretching vibration frequencies of 945 and 948 cm^{-1} are consistent with other frequencies reported for oxo-Re (V) complexes and demonstrated the presence of the $[Re(V)O]^{3+}$ core. The absence of bands associated with –SH stretching ($\approx$2540 cm^{-1}) is a sign of the deprotonation of this group upon compl-exation with oxo-Re (V). UV–vis spectra showed an absorption band at 376–380 nm, probably related to the S–Re charge transfer transition. Additional absorption at shorter wavelengths (230–270 nm) should correspond to the ligands (tridentate and monodentate).

TABLE 4.1. MIXED RHENIUM AND TECHNETIUM COMPLEXES

Complex	Ligand	Coligand
Re-1	SH-(CH$_2$)$_2$-S-(CH$_2$)$_2$-SH	SH$_2$CH$_2$-piperazino-N-C$_6$H$_4$-o-OCH$_3$
Re-2	(C$_2$H$_5$)$_2$N-(CH$_2$)$_2$-N-(CH$_2$CH$_2$SH)$_2$	SH$_2$CH$_2$-piperazino-N-C$_6$H$_4$-o-OCH$_3$
Re-3	(C$_2$H$_5$)$_2$N-(CH$_2$)$_2$-N-(CH$_2$CH$_2$SH)$_2$	CH$_3$-C$_6$H$_4$-SH
Tc-1 non-carrier level only	SH-(CH$_2$)$_2$-S-(CH$_2$)$_2$-SH	SH$_2$CH$_2$-piperazino-N-C$_6$H$_4$-o-OCH$_3$
Tc-2 carrier and non-carrier level (3 + 1)	(C$_2$H$_5$)$_2$N-(CH$_2$)$_2$-N-(CH$_2$CH$_2$SH)$_2$	SH$_2$CH$_2$-piperazino-N-C$_6$H$_4$-OCH$_3$
Tc-3 carrier and non-carrier level (3 + 1)	(C$_2$H$_5$)$_2$N-(CH$_2$)$_2$-N-(CH$_2$CH$_2$SH)$_2$	CH$_3$-C$_6$H$_4$-SH
Tc-4 non-carrier level only (2 + 1 + 1)	SH$_2$CH$_2$-piperazino-N-C$_6$H$_4$-o-OCH$_3$	p-CH$_3$O-C$_6$H$_4$-SH
Tc-5 non-carrier level only (2 + 1 + 1)	SH$_2$CH$_2$-piperazino-N-C$_6$H$_4$-o-OCH$_3$	CH$_3$-C$_6$H$_4$-SH

4.4.2. Synthesis of Tc mixed complexes

The corresponding Tc(V)O complexes at carrier level were obtained using ^{99}Tc(V) gluconate as a precursor. The desired complexes were then purified by organic extraction in dichloromethane. Two complexes with ^{99}Tc were obtained:

Complex Tc-1: TcO[(CH$_3$-CH$_2$)$_2$-N-CH$_2$-CH$_2$-N-(CH$_2$-CH$_2$S)$_2$][CH$_3$-C$_6$H$_4$-S] (4-methoxy thiophenolato)-[N′,N′-diethylethylenediamine-(N,N-bis(2-mercaptoethyl))]-oxotechnetium (V).

Complex Tc-2: TcO[(CH$_3$-CH$_2$)$_2$-N-CH$_2$-CH$_2$-N-(CH$_2$-CH$_2$S)$_2$][SCH$_2$CH$_2$-piperazino-N-Ph-o-OCH$_3$] (3-thiapentan-1,5-dithiolato)[1-(2-methoxyphenyl)-4-(2-mercaptoethyl)-piperazine].

The UV–vis spectra showed maxima in the region 495–525 nm, characteristic of the Tc(V)O S charge transfer band, as reported for other Tc(V)O-thiolato complexes [4.7, 4.10, 4.11]. The identity of these Tc complexes was
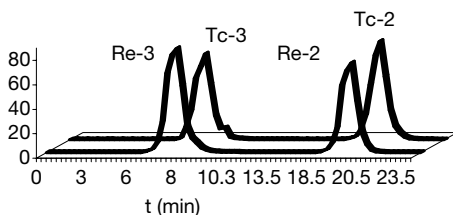
FIG. 4.1. HPLC chromatograms of ^{99}Tc and Re complexes. Re-2 = ReO[(CH$_3$CH$_2$)$_2$-N-CH$_2$CH$_2$-N-(CH$_2$CH$_2$S)$_2$][SH$_2$CH$_2$-piperazino-N-Ph-o-OCH$_3$], Tc-2 = TcO[(CH$_3$CH$_2$)$_2$-N-CH$_2$CH$_2$-N-(CH$_2$CH$_2$S)$_2$][SH$_2$CH$_2$-piperazino-N-Ph-o-OCH$_3$], Re-3 = ReO[(CH$_3$CH$_2$)$_2$-N-CH$_2$CH$_2$-N-(CH$_2$CH$_2$S)$_2$][CH$_3$C$_6$H$_4$S], Tc-3 = TcO[(CH$_3$CH$_2$)$_2$-N-CH$_2$CH$_2$-N-(CH$_2$CH$_2$S)$_2$][CH$_3$C$_6$H$_4$S].

established by comparative HPLC studies using samples of the corresponding Re complexes as references (Fig. 4.1). The retention times (R_t) found are similar to those reported for these compounds [4.8].

4.4.3. Synthesis of Tc mixed complexes at tracer level

It is widely accepted that the results for Re and ^{99}Tc compounds at carrier level show a good agreement and that there is a similarity of the structure of the corresponding compounds, so it is possible to carry out the preparation of Tc mixed complexes by stoichiometric ligand exchange reaction. However, some discrepancies could appear at tracer level. It has been found [4.10] that competition between the ligand (L) and co-ligand (K) may give rise to the formation of by-products, the content of which can sometimes exceed the main expected complex (Me:L:K). We evaluated two different ways for the preparation of ^{99m}Tc mixed ligand complexes. Two different tridentate ligands and three co-ligands were used in these experiments.

In our case the results showed that, when using equimolar quantities of ligand and co-ligand (procedure A), the labelling yield was poor and the purity of the expected ^{99m}Tc OLK complex was less than 60% (after extraction). TLC analysis showed the presence of several complexes in the extraction mixture (Fig. 4.2). On the other hand, it was possible to improve the yield and the purity of the desired complex when the labelling was done in two steps (procedure B). In this case it is very important to control the concentration of the ligands, since it is likely to play an important role in the course and the kinetics of the reaction (Fig. 4.2). The presence of different complexes was found in the extraction mixture (extraction yields were always more than 90% with reference to the total activity of the sample) when adding 1 or 2 mg of the
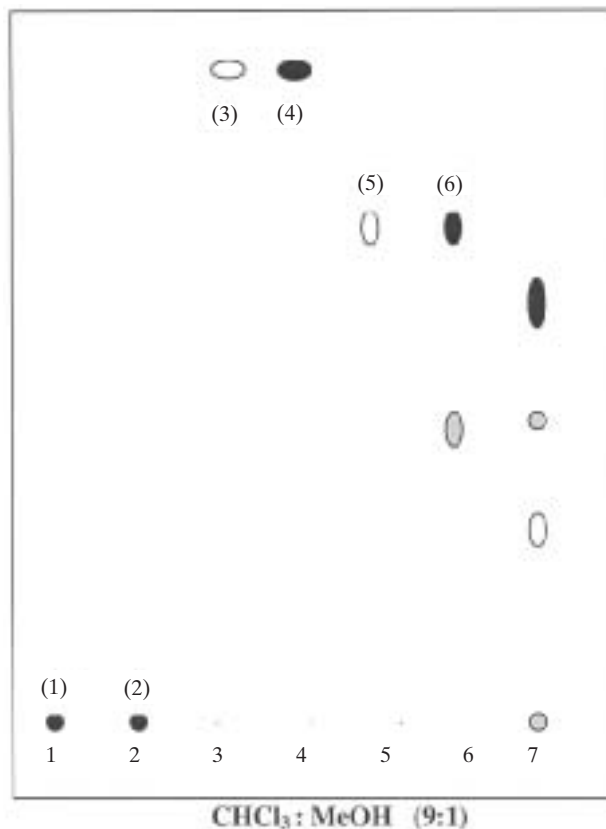
FIG. 4.2. TLC profile of obtained ^{99m}Tc complexes: (1) TcO$_4^-$, (2) Tc gluconate, (3) Re-1, (4) Tc-1, (5) Re-2, (6) Tc-2, (7) Tc-4. Detection by UV and autoradiography.

ligand and/or the co-ligand. The exact composition of the by-products was not investigated but the TLC profiles showed the presence of Tc complexes containing only ligands or only co-ligands (Fig. 4.2).

For the biodistribution studies, complexes with the desired composition (M:L:K (3 + 1) (Tc-2) or M:L:K$_2$ (2 + 1 + 1) (Tc-3 and Tc-4)) (Table 4.1) were purified by HPLC and then redissolved in ethanol:saline solution (20:80). All three complexes were stable for at least 1.5 h at room temperature after purification. Biodistribution studies demonstrated that the complexes Tc-2, Tc-3 and Tc-4 present low brain uptake and retention (Table 4.2) and, because of the high activity in blood, the brain to blood ratio was very low too. All complexes showed high liver and lung accumulations.

TABLE 4.2. BRAIN UPTAKE OF TECHNETIUM COMPLEXES IN RATS
(% ID, per cent of injected dose per gram (n = 3))

Time post-injection (min)	Tc-2	Tc-3	Tc-4
5	0.12 ± 0.01	0.130 ± 0.012	0.105 ± 0.009
20	0.110 ± 0.009	0.115 ± 0.014	0.092 ± 0.010
60	0.108 ± 0.009	0.109 ± 0.009	0.095 ± 0.009

4.5. CONCLUSIONS

In the present study, different complexes of oxo-Tc (V) and oxo-Re (V) were obtained on the basis of the 3 + 1 and 2 + 1 + 1 mixed ligand approach. The complexes were obtained at both carrier and tracer levels. As a co-ligand was used a compound bearing the 1-(2-methoxyphenyl)piperazine moiety, a group which has been investigated for its affinity and specificity for the serotonin 5-HT$_{1A}$ brain receptors.

REFERENCES TO CHAPTER 4

[4.1] McCARTHY, T.J., et al., Nuclear medicine and PET: An overview, J. Chem. Ed. **71** (1994) 830–836.

[4.2] HORN, R.K., KATZENELLENBERG, J.A., Tc-99m labelled receptor-specific small-molecule radiopharmaceuticals: Recent developments and encouraging results, Nucl. Med. Biol. **24** (1997) 485–498.

[4.3] FLETCHER, A., CLIFFE, I.A., DORISH, C.T., Silent 5-HT$_{1A}$ receptor antagonist: Utility as research tools and therapeutic agents, TiPS **14** (1995) 441–448.

[4.4] PASSCHIER, J., VAN WAARDE, A., Visualization of serotonin-1A(5-HT$_{1A}$) receptors in the central nervous system, Eur. J. Nucl. Med. **28** (2001) 113–129.

[4.5] CORBIN, J.L., et al., Preparation and properties of tripodal and linear tetradentate NS-donor ligands and their complexes containing the MoO_2^{2+} core, Inorg. Chim. Acta **90** (1984) 41–51.

[4.6] JOHANNSEN, B., SPIES, H., Chemie und Radiopharmakologie von Technetium-Komplexen, Akademie der Wissenschaften, Dresden (1981).

[4.7] PAPADOPOULOS, M., et al., Synthesis and characterization of five-coordinated rhenium (V) and technetium (V) mixed ligand bifunctional complexes carrying the SNS/S or the SNN/S donor atom set, Inorg. Chim. Acta **285** (1999) 97–106.

[4.8] PAPADOPOULOS, M., et al., Syn-anti-isomerism in a mixed-ligand oxorhenium complex, Inorg. Chem. **35** (1996) 7377–7383.

[4.9] INTERNATIONAL ATOMIC ENERGY AGENCY, Report on the Second Research Co-ordination Meeting of the CRP on Developments of Agents for Imaging CNS Receptors based on ^{99m}Tc held in Athens, internal report, IAEA, Vienna, 1998.

[4.10] SEIFERT, S., et al., No carrier added preparation of '3 + 1' mixed-ligand Tc-99m complexes, Appl. Radiat. Isot. **49** (1998) 5–11.

[4.11] PIRMETTIS, I.C., et al., Synthesis and characterization of oxotechnetium (V) mixed-ligand complexes containing a tridentate N-substituted bis(2-mercapto-ethyl)amine and a monodentate thiol, Inorg. Chem. **35** (1996) 1685–1691.

Chapter 5

DESIGN AND BIOLOGICAL EVALUATION OF ^{99m}Tc LIGANDS DERIVED FROM WAY 100635 AND DESMETHYL WAY 100635 FOR SEROTONIN 5-HT$_{1A}$ AND α1-ADRENERGIC RECEPTOR BINDING

A. DREWS, I. HEIMBOLD, M. KRETZSCHMAR, H.-J. PIETZSCH, S. SEIFERT, R. SYHRE, B. JOHANNSEN
Forschungszentrum Rossendorf,
Institut für Bioanorganische und Radiopharmazeutische Chemie,
Dresden, Germany

K. VARNÄS, H. HALL, C. HALLDIN, P. KARLSSON, C. JOHNSSON
Department of Clinical Neuroscience, Karolinska Institute,
Karolinska Hospital,
Stockholm, Sweden

W. KRAUS
Bundesanstalt für Materialforschung,
Berlin, Germany

Abstract

Investigations on Tc labelled ligands for the 5-HT$_{1A}$ receptor carried out at Forschungszentrum Rossendorf from 1999 to 2001 in collaboration with the Karolinska Institute, Stockholm, are reported. The novel Tc labelled receptor ligands basically consist of a Tc chelate unit with the metal in the oxidation state +5 or +3 and 1-(2-methoxyphenyl)piperazine as the receptor targeting domain. Both moieties are linked by alkyl spacers of various chain lengths. Rhenium was used as Tc surrogate for complete chemical characterization and in vitro receptor binding studies. All complexes display in competition experiments not only subnanomolar affinities for the 5-HT$_{1A}$ receptor but also high affinities for the α1-adrenergic receptor. Biodistribution studies in rats show brain uptakes between 0.2 and 0.6% of the injected dose five minutes post-injection. In vitro autoradiographic studies in rat brains and post-mortem human brains indicate the accumulation of the ^{99m}Tc complexes in areas which are rich in 5-HT$_{1A}$ receptors and additionally in areas rich in α1-adrenergic receptors. This in vitro enrichment can be blocked respectively by the 5-HT$_{1A}$ receptor agonist 8-OH-DPAT or by prazosin hydrochloride, an α1-adrenergic receptor antagonist.

5.1. INTRODUCTION

Since 5-HT$_{1A}$ receptors are implicated in a number of neuropsychiatric disorders [5.1], their visualization in the human brain using positron emission tomography (PET) or single photon emission computer tomography (SPECT) is of great interest, which stimulates the development of ^{11}C, ^{18}F, ^{123}I and ^{99m}Tc radioligands. Several approaches have been pursued for the design of such PET and SPECT imaging agents [5.2]. WAY 100635 [N-(2-(1-(4-(2-methoxyphenyl)-piperazinyl)ethyl))-N-(2-pyridinyl) cyclohexanecarboxamide], a potent and selective 5-HT$_{1A}$ receptor antagonist [5.3], has proved to be a very useful lead structure for the design of 5-HT$_{1A}$ radioligands. Outstandingly, [carbonyl-^{11}C]WAY 100635 has been shown with PET to be suitable for exquisite delineation of 5-HT$_{1A}$ receptors in the human brain [5.4]. This considerable advance also provided an impetus for the development of ^{99m}Tc complexes by making use of structural features of WAY 100635 in the design of ^{99m}Tc containing molecules. Potential receptor ligands with different linkers between the 1-(2-methoxyphenyl)piperazine moiety derived from WAY 100635 and N$_2$S$_2$ chelates have been described [5.5], among them a diamine dithiol (DADT) complex linked via a three carbon alkyl linker to 1-(2-methoxy-phenyl)piperazine. Little progress had been made in developing ^{99m}Tc agents for 5-HT$_{1A}$ receptor imaging by other structural arrangements, mainly because of failure in brain uptake [5.6].

Here we describe novel ^{99m}Tc ligands with subnanomolar affinities for the 5-HT$_{1A}$ receptor. Additionally, some compounds show a remarkably high affinity for the α1-adrenergic receptor. The complexes were characterized by several in vitro receptor binding assays, by biodistribution studies and by in vitro autoradiography in rat brains. Some representatives were evaluated by in vitro autoradiography on post-mortem human brain slices and by SPECT studies on non-human primates.

The present paper covers the investigations on Tc labelled ligands for the 5-HT$_{1A}$ receptor carried out in collaboration with the Karolinska Institute, Stockholm, at Forschungszentrum Rossendorf from 1999 to 2001 as published in Refs [5.7–5.9].

5.2. MATERIALS

Technetium-99 as NH$_4$TcO$_4$ was obtained from Amersham Biosciences as 0.3M aqueous solution. ^{99m}TcO$_4^-$ was eluted from a Mallinckrodt generator. All chemicals and solvents were obtained from commercial sources and were of analytical grade. For preparations of ^{99m}Tc compounds with no carrier added as

well as for synthesis and characterization of analogous Re complexes, refer to Refs [5.7–5.9].

5.3. METHODS

Receptor binding assays, in vitro autoradiography on rat brains and post-mortem human brain slices, biodistribution studies in rats and SPECT image acquisition and processing in cynomolgus monkeys have been described elsewhere [5.7–5.11].

5.4. RESULTS AND DISCUSSION

Encouraged by our recent results in developing high affinity ^{99m}Tc ligands for the 5-HT$_{2A}$ receptor derived from ketanserin [5.10, 5.11], we directed our efforts towards developing analogous compounds for the 5-HT$_{1A}$ receptor. All the complexes described in the following consist of a Tc chelate with the metal in the oxidation state +5 or +3 and with 1-(2-methoxyphenyl)piperazine as the receptor targeting domain. Both moieties are linked by alkyl spacers of various chain lengths. Rhenium was used as a Tc surrogate for complete chemical characterization and in vitro receptor binding studies.

5.4.1. Technetium receptor ligands with 3 + 1-SNS/S co-ordination

The complexes [^{99m}Tc]Tc-1 and Re-1 (Figs 5.1 and 5.2) combine a neutral Tc/Re chelate prepared according to the 3 + 1 mixed ligand approach and 1-(2-methoxyphenyl)piperazine linked by a hexyl spacer. Similar retention times resulting from high performance liquid chromatography (HPLC) runs after co-injection of [^{99m}Tc]Tc-1 and Re-1 under various elution conditions confirm the structural similarity of these two substances. In experiments with glutathione we found about 70% of the parent compound [^{99m}Tc]Tc-1 after an incubation time of 120 min, suggesting a sufficiently high stability in vivo.

5.4.1.1. In vitro receptor binding

For both reference compounds [^{99}Tc]Tc-1 and Re-1, a subnanomolar affinity for the 5-HT$_{1A}$ receptor was found (Table 5.1). The affinity for the 5-HT$_{2A}$ receptor is considerably lower; the Tc complex shows more than a thousandfold selectivity for 5-HT$_{1A}$ compared with 5-HT$_{2A}$ receptors. The compounds [^{99}Tc]Tc-1 and Re-1 also display a relatively high affinity for the rat
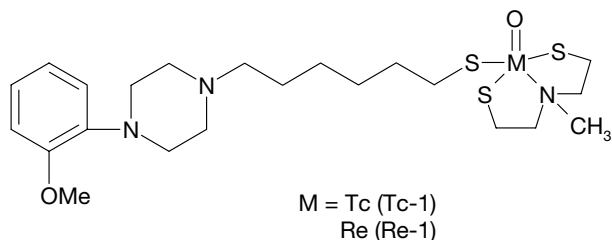
FIG. 5.1. 3 + 1 complexes with a subnanomolar affinity for the 5-HT$_{1A}$ receptor.
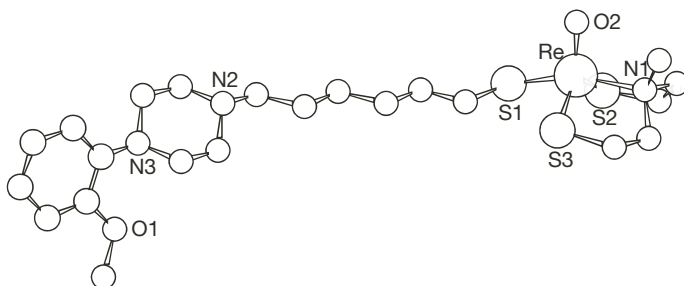
FIG. 5.2. Molecular structure of Re-1 as obtained by X ray diffraction.

D$_2$ receptor. A better selectivity was found for Re-1 towards cloned human D$_2$ receptors (a 50% inhibitory concentration (IC$_{50}$) value of 162nM), indicating a better selectivity in humans. This observation suggests a species dependence. The high degree of homology between the 5-HT$_{1A}$ receptor subtype and the α1-adrenergic receptor (approximately 45%) causes for a great number of 5-HT$_{1A}$ receptor ligands a poor selectivity against the α1-adrenergic receptor. This problem was also observed for many arylpiperazine compounds. The [^{99}Tc]Tc-1 and Re-1 complexes investigated here show an even better affinity for the α1-adrenergic receptor than for the 5-HT$_{1A}$ receptor and thus have no selectivity with regard to this type of receptor.

5.4.1.2. *In vitro autoradiography in rat brains*

The regional in vitro distribution and accumulation of [^{99m}Tc]Tc-1 was measured in several sections of rat brains. Intense labelling was observed in regions known for 5-HT$_{1A}$ sites such as the hippocampus, especially the gyrus dentatus, entorhinal cortex and septal nucleus. Additionally, ^{99m}Tc binding was observed in brain regions such as the thalamus, frontal cortex, external plexiform layer and internal granular layer of the olfactory bulb. This distribution pattern is characteristic of the α1-adrenergic receptor. The respective proportions for the several binding sites were determined by competition

TABLE 5.1. INHIBITION CONSTANTS (IC_{50} (nM)) OF [^{99}Tc]Tc-1 AND Re-1 FOR VARIOUS RECEPTORS AND 5-HT AND DOPAMINE TRANSPORTERS (5-HTT, DAT)

Complex	5-HT$_{1A}$	5-HT$_{2A}$	D$_2$	α1	5-HTT	DAT
[^{99}Tc]Tc-1	0.13 ± 0.01	154 ± 1	3.3 ± 0.1	0.03 ± 0.01	ND[a]	ND[a]
Re-1	0.24 ± 0.09	103 ± 1	47 ± 1 162 ± 2[b]	0.05 ± 0.02	900 ± 7	0.03 ± 0.01 1280 ± 32

[a] ND, not determined.
[b] Tested in cloned human D$_2$ receptors.

studies. (R)-(+)-8-OH-DPAT, a selective 5-HT$_{1A}$ receptor agonist, displaced the binding in regions rich in 5-HT$_{1A}$ receptors between 49 and 56%. Prazosin hydrochloride, an α1-adrenergic receptor antagonist, blocked the α1-adrenergic receptor-rich regions between 71 and 82%.

5.4.1.3. *In vitro autoradiography in post-mortem human brain*

In post-mortem human brains [^{99m}Tc]Tc-1 showed an accumulation in 5-HT$_{1A}$ receptor-rich regions such as the hippocampus and cerebral cortex, and a weaker accumulation in the basal ganglia and the α1-adrenergic thalamus receptor-rich region. The accumulation of [^{99m}Tc]Tc-1 in the hippocampus and the cerebral cortex of the post-mortem human brain sections was relatively homogeneous. The addition of 8-OH-DPAT, a selective 5-HT$_{1A}$ agonist, clearly blocked part of the binding of [^{99m}Tc]Tc-1 to the hippocampus and cerebral cortex, whereas other regions known to have lower densities of 5-HT$_{1A}$ receptors were not affected. Displacement studies with the α1-adrenergic selective antagonist prazosin have not been performed yet. This autoradiographic investigation was a first overview of this receptor binding ^{99m}Tc tracer in sections of post-mortem human brains, and further investigations should deal with quantitative measurements.

5.4.1.4. *Biodistribution studies in rats*

Table 5.2 summarizes the distribution and elimination of [^{99m}Tc]Tc-1 in blood, brain and selected peripheral organs 5 and 120 min post-injection. [^{99m}Tc]Tc-1 was rapidly extracted by the lungs (up to 9% ID/2 min post-injection), followed by a fast elimination of the radioactivity from the lungs. The initial liver extraction of the compound was high and increased drastically

TABLE 5.2. DISTRIBUTION DATA (% ID) AFTER INJECTION OF [^{99m}Tc]Tc-1 IN 5–6 WEEK OLD MALE WISTAR RATS
(mean ± SD; n = 6)

Post-injection time (min)	Brain	Heart	Lungs	Liver	Kidneys
5	0.22 ± 0.03	0.9 ± 0.3	5.4 ± 1.0	28.5 ± 6.6	4.8 ± 0.8
120	<0.05	0.1 ± 0.05	0.5 ± 0.2	42.5 ± 2.1	3.0 ± 0.5

with time. A considerable amount of the complex accumulated in the kidneys. It was ascertained that [^{99m}Tc]Tc-1 is capable of penetrating the blood–brain barrier of rats.

A log $P_{O/W}$ value of 1.4 ± 0.2 ($n = 9$) was determined at pH7.4. Corresponding to this value the complex shows an initial brain uptake of up to 0.33 ± 0.03% ID/2 min post-injection. Furthermore, it was observed that the moderate brain uptake is followed by a rapid brain washout. The brain washout of [^{99m}Tc]Tc-1 is associated with a fast elimination from the blood.

5.4.2. Technetium receptor ligand with tetradendate N_2S_2 co-ordination

The high affinity of [^{99m}Tc]Tc-1 to the α1-adrenoceptor indicated that the conformation of this radioligand has to be modified in terms of sufficient selectivity. For this reason and for better brain uptake, we took advantage of the recent development of a new analogue of WAY 100635, namely desmethyl WAY 100635 (DWAY) [5.7].

The new ^{99m}Tc receptor ligand [^{99m}Tc]Tc-2 (Fig. 5.3) combines an N_2S_2 diamino dithiol ligand as complexing moiety for oxotechnetium (V) and 2-(1-piperazino)phenol via a C_6 alkyl chain derived from DWAY. HPLC analyses indicate the presence of two isomers (*syn* and *anti*), configurationally based on the relationship between the Tc=O core and the substituent at the tertiary amine. For the investigations described here we used the mixture of both isomers.

5.4.2.1. *In vitro receptor binding*

With an IC$_{50}$ value of 1.3nM, [^{99}Tc]Tc-2 displays a good affinity for the 5-HT$_{1A}$ receptor (Table 5.3), whereas the crucial affinity to α1-adrenergic receptors is reduced to an IC$_{50}$ of 8.1nM.
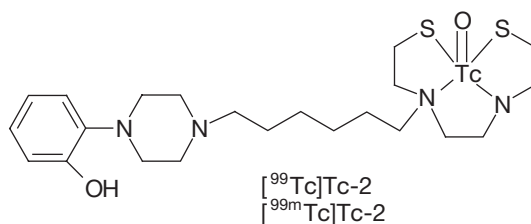
FIG. 5.3. *Tetradendate Tc ligand with a subnanomolar affinity for the the* 5-HT$_{1A}$ *receptor.*

The affinities for the 5-HT$_{2A}$ and D$_2$ receptors are considerably lower; the Tc complex shows more than a 700-fold selectivity for 5-HT$_{1A}$ compared with 5-HT$_{2A}$ receptors and about a 150-fold selectivity for 5-HT$_{1A}$ compared with D$_2$ receptors. These results could be confirmed by in vitro autoradiography.

5.4.2.2. In vitro autoradiography in rat brains

Intense enrichment of radioactivity was observed in the hippocampus, in frontal cortical areas and in the lateral septal nucleus. These regions are known for high densities of 5-HT$_{1A}$ sites. The accumulation in these areas could be displaced by (R)-(+)-8-OH-DPAT, a selective 5-HT$_{1A}$ receptor agonist. Besides a strong accumulation of the radioactivity in 5-HT$_{1A}$ receptor-rich brain areas, primarily in the hippocampus, a low level of radioactivity was observed in the thalamus, known for high densities of α1-adrenoceptors. Addition of the selective α1-adrenergic receptor antagonist prazosin hydrochloride reduced the accumulated radioactivity in this region.

TABLE 5.3. INHIBITION CONSTANTS (IC$_{50}$ (nM)) OF [^{99}Tc]Tc-2 FOR VARIOUS RECEPTORS, THE 5-HT$_{2A}$/5-HT$_{1A}$ RATIO AND THE α1/5-HT$_{1A}$ RATIO

Complex	5-HT$_{1A}$ [^{3}H]8-OH-DPAT	5-HT$_{2A}$ [^{3}H]ketanserine	D$_2$ [^{3}H]spiperone	α-1 [^{3}H]prazosin	5-HT$_{2A}$/ 5-HT$_{1A}$	α-1/ 5-HT$_{1A}$
[^{99}Tc]Tc-2	1.29 ± 0.02	931 ± 11	192 ± 5	8.12 ± 0.02	722	6.3

5.4.2.3.   *Biodistribution studies in rats*

[^{99m}Tc]Tc-2 was taken up in rat brains up to $0.56 \pm 0.07\%$ ID, 2.5 min post-injection. This value is comparable with that of [^{99m}Tc]TRODAT-1 (0.43% ID, 2 min post-injection). The relatively slow brain washout accompanied with a fast blood clearance led to good brain to blood ratios in the time interval of 2.5–120 min post-injection. The radioactivity in heart and kidneys was also cleared, whereas the high liver activity remained nearly constant. Representative amounts of the injected dose were accumulated in the pancreas, spleen and adrenal glands (Table 5.4).

5.4.3.   Technetium receptor ligands with tetradentate/monodentate NS$_3$/isonitrile co-ordination

Previous studies have shown that Tc (III) mixed ligand complexes with tetradentate/monodentate NS$_3$/isonitrile co-ordination, [Tc(NS$_3$)(CN-R)], are lipophilic and stable against exchange reactions in vivo [5.12]. This type of 4 + 1 Tc complex appears suitable to wrap the metal well in a molecule with receptor binding functionality and hopefully sufficient brain uptake. The compounds [^{99m}Tc]Tc-3–[^{99m}Tc]Tc-5 introduced here contain the methoxy-phenyl piperazine (MPP) moiety linked to the neutral and oxo-free Tc chelate unit via

TABLE 5.4.   BIODISTRIBUTION OF [^{99m}Tc]Tc-2 IN WISTAR RATS
(male; 5–6 weeks old; mean of % ID/organ ± SD; n = 7)

Time post-injection (min)	5	120
Brain	0.52 ± 0.08	0.11 ± 0.02
Heart	0.56 ± 0.08	0.09 ± 0.02
Lungs	4.94 ± 0.81	0.89 ± 0.10
Pancreas	1.06 ± 0.19	0.75 ± 0.15
Spleen	0.79 ± 0.22	0.48 ± 0.13
Adrenal glands	0.36 ± 0.06	0.12 ± 0.03
Kidneys	6.54 ± 0.83	1.93 ± 0.45
Liver	20.2 ± 3.0	16.5 ± 3.2

	R
[^{99m}Tc]Tc-3, Re-3	(CH$_2$)$_4$-MPP
[^{99m}Tc]Tc-4, Re-4	(CH$_2$)$_5$-MPP
[^{99m}Tc]Tc-5, Re-5	(CH$_2$)$_6$-MPP
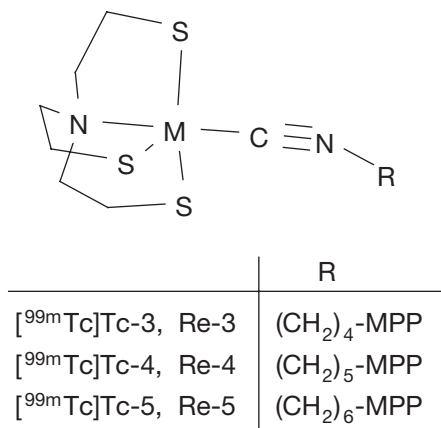
FIG. 5.4. 4 + 1 complexes with subnanomolar affinity for the 5-HT$_{1A}$ receptor.

a longer alkyl chain (Fig. 5.4). The molecular structure of the technetium surrogate Re-4 obtained by X ray structure analysis is presented in Fig. 5.5.

5.4.3.1. In vitro receptor binding

IC$_{50}$ values are compiled in Table 5.5. Subnanomolar affinities for the 5-HT$_{1A}$ receptor were obtained for Re-3 (IC$_{50}$ = 0.29nM) and Re-4 (IC$_{50}$ = 0.62nM), whereas Re-5 showed a lower affinity for the 5-HT$_{1A}$ receptor (IC$_{50}$ = 4.5nM). The selectivity against the 5-HT$_{2A}$ receptor is sufficient for all three compounds and decreases with increasing alkyl chain length (C4 > C5 > C6). The selectivity against the D$_2$ receptor is less pronounced, ranging from ratios of 4 to 112, again with the best selectivity for the complex with the shortest spacer length. Re-3 showed a slightly increased selectivity against the D$_2$ receptors (IC$_{50}$ = 33nM).
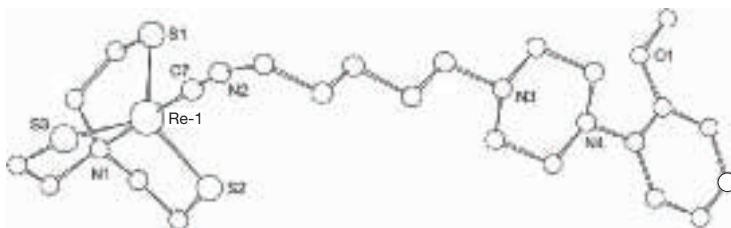
FIG. 5.5. Molecular structure of Re-4 as obtained by X ray diffraction.

TABLE 5.5. INHIBITION CONSTANTS ((IC$_{50}$ (nM)) OF Re-3, Re-4 AND Re-5 FOR VARIOUS RECEPTORS, AND THE 5-HT$_{2A}$/5-HT$_{1A}$ RATIO

Complex	5-HT$_{1A}$ [^{3}H]8-OH-DPAT rat hippocampus homogenate	5-HT$_{2A}$ [^{3}H]ketanserin rat cortex homogenate	D$_2$ [^{3}H]spiperone rat striatum homogenate	α-1 [^{3}H]prazosin rat cortex homogenate	α-2 [^{3}H]MK-912 rat cortex homogenate	5-HT$_{2A}$/ 5-HT$_{1A}$
Re-3	0.29 ± 0.01	156 ± 1	32.7 ± 0.6	<1	18.3 ± 0.2	538
Re-4	0.62 ± 0.17	114 ± 2	18.6 ± 0.2	<1	20.5 ± 0.1	182
Re-5	4.5 ± 0.1	94 ± 2	18.4 ± 0.4	1.1 ± 0.01	21.3 ± 0.1	21

The Re complexes were also investigated for their affinity for the α1-adrenergic receptors, because some arylpiperazine bearing 5-HT$_{2A}$ receptor ligands are known for such a cross-reactivity. All the compounds show high affinities for the α1-adrenoceptor and therefore insufficient selectivity. Nanomolar affinities were obtained also for the α2-adrenoceptor, indicating moderate selectivity only for the 5-HT$_{1A}$ receptor.

5.4.3.2. *Autoradiography of post-mortem human brains*

[^{99m}Tc]Tc-4 was investigated in autoradiographical studies in sections of post-mortem human brains and showed a dense labelling of the hippocampus, i.e. part of the CA3 region, and of the cerebral cortex.

The binding in the neocortex was relatively homogeneous, although a slightly higher density could be seen in the superficial layers. Considering the high affinities of the candidate molecules to 5-HT$_{1A}$ and α1 receptors, the contrast in the autoradiographical images might result from these affinities and the location patterns of the receptors. Since addition of high concentrations of prazosin hydrochloride as a specific antagonist for α1-adrenergic receptors or 8-OH-DPAT as specific agonist for 5-HT$_{1A}$ receptors did not significantly affect the binding of [^{99m}Tc]Tc-4 in the hippocampus region or elsewhere, non-specific accumulation seems to prevail. Previous studies in the laboratory of the Karolinska Institute, as well as in other laboratories, have shown that α1-adrenoceptors are present in the hippocampus to a high extent. The reasons for labelling the hippocampus despite the lack of specific binding is not clear.

5.4.4. Biodistribution in rats

The distribution data are listed in Table 5.6. All complexes were able to cross the blood–brain barrier. Furthermore, the complexes showed a fast clearance from the brain as well as from the circulating blood. The radioactivity accumulation in the lungs increases slightly with the number of C atoms in the spacer and parallels the lipophilicity (log $P_{O/W}$) of the complexes.

5.4.4.1. SPECT study on non-human primates

The SPECT study in cynomolgus monkeys with [99mTc]Tc-4 showed hardly any brain uptake. This indicates a strong species dependence, since in rats the complex showed a brain uptake of $0.41 \pm 0.08\%$ ID, 5 min post-injection, which should be sufficient for imaging. Metabolism can be ruled out as the factor responsible for the failure because in cynomolgus monkeys approximately 90% intact [99mTc]Tc-4 could be observed by HPLC 120 min after injection.

TABLE 5.6.   BIODISTRIBUTION OF [99mTc]Tc-3, [99mTc]Tc-4 AND [99mTc]Tc-5 IN WISTAR RATS
(mean of % ID/g tissue ± SD; n = 5)

Time post-injection (min)	Blood	Brain	Lungs	Kidneys	Liver
99mTc-3					
5	0.23 ± 0.04	0.32 ± 0.05	3.73 ± 0.47	4.63 ± 0.65	4.07 ± 0.64
120	0.19 ± 0.04	< 0.05	0.34 ± 0.07	1.55 ± 0.27	4.01 ± 0.84
99mTc-4					
5	0.32 ± 0.05	0.29 ± 0.03	4.1 ± 0.06	3.6 ± 0.14	6.3 ± 2.01
120	0.16 ± 0.03	< 0.05	0.4 ± 0.06	1.3 ± 0.24	6.0 ± 1.55
99mTc-5					
5	0.18 ± 0.03	0.18 ± 0.06	4.42 ± 1.69	4.47 ± 1.20	4.28 ± 1.12
120	0.10 ± 0.01	< 0.05	0.37 ± 0.13	1.13 ± 0.19	4.90 ± 0.88

5.5. CONCLUSIONS

It has been possible to synthesize ^{99m}Tc based ligands with subnanomolar affinity for the 5-HT$_{1A}$ receptor, as evident both in receptor binding displacement assays and in autoradiographic studies. These results could be obtained by exploiting the lead structures developed in our previous studies on technetium complexes containing neutral Tc (V) or Tc (III) chelate units and a moiety derived from WAY 100635 and DWAY. Both substructures are connected by an alkyl spacer of variable chain length.

A neutral oxotechnetium (V) chelate in the form of a mixed ligand 3 + 1 unit bearing 4-(6-mercaptohexyl)-1-(2-methoxyphenyl)piperazine exhibited significant accumulation in 5-HT$_{1A}$ receptor-rich areas of the brain and in such brain regions which are rich in α1-adrenergic receptors. The in vitro enrichment can be blocked by the 5-HT$_{1A}$ receptor agonist 8-OH-DPAT and by prazosin hydrochloride, an α1-adrenergic receptor antagonist, respectively.

A novel tetradendate co-ordinated ^{99m}Tc radioligand derived from DWAY showed a nanomolar affinity for the 5-HT$_{1A}$ receptor, whereas the crucial affinity to α1-adrenoceptors was reduced. Besides reduction of the affinity for α1-adrenoceptors, optimization of the radioligand structure led to an increased initial brain uptake in rats, which gives good expectations for further in vivo studies.

The new type of 4 + 1 ^{99m}Tc mixed ligand complexes has the potential to provide high affinity ligands for the brain 5-HT$_{1A}$ receptor. Functionalization with the (2-methoxy-phenyl)piperazinyl moiety linked via a butylene or pentylene spacer to the chelate unit resulted in subnanomolar affinities for the 5-HT$_{1A}$ brain receptor, associated with substantial selectivities against the 5-HT$_{2A}$ brain receptor and low selectivity against the α1-adrenoceptors. A prototypic representative species dependence of brain uptake occurred and disqualified the compound for SPECT imaging in non-human primates. Additionally, distribution patterns in autoradiographic images of post-mortem human brain slices could not be appropriately altered in displacement experiments with specific ligands. The attainment of ^{99m}Tc based 5-HT$_{1A}$ brain receptor ligands will require further ligand modification.

REFERENCES TO CHAPTER 5

[5.1] OLIVIER, B., SOUDIJN, W., VAN WIJNGAARDEN, I., The 5-HT$_{1A}$ receptor and its ligands: Structure and function, Prog. Drug Res. **52** (1999) 103–165.

[5.2] PASSCHIER, J., VAN WARDE, A., Visualization of serotonin-1A (5-HT$_{1A}$) receptors in the central nervous system, Eur. J. Nucl. Med. **28** (2001) 113–129.

[5.3] FLETCHER, A., et al., A pharmacological profile of WAY-100635, a potent and selective 5-HT$_{1A}$ receptor antagonist, Br. J. Pharmacol. **112** (1994) 91.

[5.4] PIKE, V.W., et al., Exquisite delineation of 5-HT$_{1A}$ receptors in human brain with PET and [carbonyl-^{11}C]WAY-100635, Eur. J. Pharmacol. **301** (1996) R5–R7.

[5.5] MAHMOOD, J.F., et al., "Technetium(V) and rhenium(V) analogues of Way 100635; 5-HT$_{1A}$ receptor-binding complexes", Technetium, Rhenium and Other Metals in Chemistry and Nuclear Medicine (NICOLINI, M., MAZZI, U., Eds), Vol. 5, SGE Editoriali, Padua (1999) 393–399.

[5.6] JOHANNSEN, B., PIETZSCH, H.-J., Development of technetium-99m-based CNS receptor ligands: Have there been any advances?, Eur. J. Nucl. Med. **29** (2002) 263–275.

[5.7] HEIMBOLD, I., et al., A novel Tc-99m radioligand for the 5-HT$_{1A}$ receptor derived from Desmethyl-WAY-100635 (DWAY), Eur. J. Nucl. Med. **29** (2002) 82–87.

[5.8] DREWS, H.-J., et al., Synthesis and biological evaluation of Technetium (III) mixed-ligand complexes with high affinity for the cerebral 5-HT$_{1A}$ receptor and the alpha1-adrenergic receptor, Nucl. Med. Biol. **29** (2002) 389–398.

[5.9] HEIMBOLD, I., et al., Synthesis, biological and autoradiographic evaluation of a novel Tc-99m radioligand derived from WAY 100635 with high affinity for the 5-HT$_{1A}$ receptor and the alpha1-adrenergic receptor, Nucl. Med. Biol. **29** (2002) 375–387.

[5.10] JOHANNSEN, B., et al., Technetium (V) and rhenium (V) complexes for 5-HT$_{2A}$ serotonin receptor binding: Structure-affinity considerations", Nucl. Med. Biol. **23** (1996) 429–438.

[5.11] PIETZSCH, H.-J., et al., Synthesis and autoradiographical evaluation of a novel high-affinity Tc-99m ligand for the 5-HT$_{2A}$ receptor, Nucl. Med. Biol. **26** (1999) 865–875.

[5.12] PIETZSCH, H.-J., GUPTA, A., SYHRE, R., LEIBNITZ, P., SPIES, H., Mixed-ligand technetium (III) complexes with tetradendate/monodendate NS3/isocyanide co-ordination: A new non-polar technetium chelate system for the design of neutral and lipophilic complexes stable in vivo, Bioconjug. Chem. **12** (2001) 538–544.

Chapter 6

DEVELOPMENT OF NOVEL MIXED LIGAND TECHNETIUM COMPLEXES (3 + 1 COMBINATION) FOR IMAGING CENTRAL NEURAL SYSTEM RECEPTORS

I. PIRMETTIS, D. PAPAGIANNOPOULOU, M. PAPADOPOULOS,
E. CHIOTELLIS
Demokritos National Centre for Scientific Research,
Radiopharmaceuticals Laboratory of the Institute of Radioisotopes
    and Radiodiagnostic Products,
Athens, Greece

Abstract

A series of mixed ligand oxotechnetium-99m complexes carrying the 1-(2-methoxyphenyl)piperazine moiety has been synthesized. For structural characterization, and for in vitro binding assays, the analogous oxorhenium or oxotechnetium-99 complexes were prepared. As demonstrated by appropriate competition binding tests in rat hippocampal preparations, all oxorhenium analogues showed affinity for the 5-HT$_{1A}$ receptor binding sites with 50% inhibitory concentration values in the nanomolar range (IC$_{50}$ = 6–106nM). All ^{99m}TcO[SN(R)S]/[S] complexes showed a significant brain uptake in rats at 2 min post-injection (0.24–1.31 dose/organ). The regional distribution is inhomogeneous but the ratio between areas rich and poor in 5-HT$_{1A}$ receptor was not high. Structural modifications to this system may further improve the biological profile of these compounds and eventually provide efficient ^{99m}Tc receptor imaging agents.

6.1. INTRODUCTION

During the last decade, the evaluation of the receptor function of the central nervous system (CNS) has become a very interesting field in radiopharmaceutical research. The method usually involves the use of ^{11}C and ^{18}F labelled agents for positron emission tomography (PET) imaging and ^{123}I agents for single photon emission computed tomography (SPECT) imaging in order to study the location and density of brain receptors. Owing to the fact that ^{99m}Tc is inexpensive, readily available, easy to image and has decay energies that minimize the dose burden to patients, many efforts have been focused on developing brain receptor imaging agents based on ^{99m}Tc [6.1].

Despite its advantages, it is very difficult to incorporate technetium into a receptor specific molecule without drastically changing the molecule's chemical and physical properties, and thereby its interaction with the receptor. However, considerable progress has been made in the last few years in the labelling with ^{99m}Tc receptor ligands of various receptor systems [6.1]. Recently, the successful development of ^{99m}Tc-TRODAT as a radioligand for the dopamine transporter has shown the feasibility of imaging specific transporters in the brain with radiotracers based on [99m]Tc [6.2].

The development of radiopharmaceuticals specific for serotonergic receptors is of particular interest, since alterations in the concentration or function of these receptors are implicated in neurological disorders such as anxiety, depression, schizophrenia and Alzheimer's disease. Starting from derivatives of arylpiperazines, WAY 100635, a 5-HT_{1A} receptor antagonist that displays antagonistic properties at both pre- and post-synaptic receptor sites [6.3], has been developed. Carbon-11 and ^{18}F derivatives of WAY 100635 have been synthesized and evaluated for use in PET [6.4, 6.5], while its iodinated analogues have been reported for use in SPECT imaging of serotonin 5-HT_{1A} subtype neuroreceptors [6.6]. In order to imitate this prototypic organic compound, several neutral and lipophilic oxotechnetium complexes have been synthesized and evaluated as potential imaging agents for 5-HT_{1A} receptors [6.7–6.9]. Fragments of WAY 100635 were combined with different tetradentate N_2S_2 chelates (the conjugate approach), such as amine-amide dithiols or diaminedithiols, with different linkers between the receptor binding moiety, 1-(2-methoxyphenyl)piperazine, and the metal chelate. The major disadvantage of these compounds is their poor brain uptake in experimental animals, which precludes their usefulness as brain receptor imaging agents. This has been attributed mainly to their high molecular size.

In this work our attempts to synthesize ^{99m}Tc as potential agents for imaging 5-HT_{1A} receptors have been focused on three basic tasks: synthesis, characterization and evaluation.

6.2. SYNTHESIS, CHARACTERIZATION AND EVALUATION (IN VIVO AND IN VITRO) OF THE 3 + 1 MIXED LIGAND COMPLEXES OF THE GENERAL FORMULA MO[SNS/S]

The 3 + 1 concept for the preparation of neutral, lipophilic, small size oxotechnetium or oxorhenium complexes $M^VOL^1L^2$ has been applied in the development of novel diagnostic or therapeutic radiopharmaceuticals [6.10]. In general, the preparation of 3 + 1 complexes requires the simultaneous action of a dianionic tridentate ligand L^1H_2, containing the SSS, SOS or SN(R)S donor

atom set and a monodentate thiol, L^2H co-ligand, on a suitable oxotechnetium (V) or oxorhenium precursor. When the tridentate ligand contains the SN(R)S donor atom set, two stereoisomers are expected, *syn* and *anti*, depending on the orientation of the R functionality with respect to the TcO or ReO group. Our findings have demonstrated that the major product of the reaction is the *syn* isomer (yield >98%). A series of $^{99m}TcO[L^1L^2]$ complexes have been synthesized and evaluated in experimental animals as potential brain radio-pharmaceuticals [6.11, 6.12] or as specific radiopharmaceuticals for the mapping of brain receptors [6.13–6.16]. We report here the synthesis, character-ization and biological evaluation of novel mixed ligand complexes of the general formula MO(SNS)(S): structure A, $MO[CH_3CH_2N(CH_2CH_2S)_2]$ $[SCH_2CH_2N(CH_2CH_2)_2NC_6H_4OCH_3\text{-}o)$, where M = Re, Tc and ^{99m}Tc, complexes 1 (Fig. 6.1), and structure B, $MO[o\text{-}CH_3OC_6H_4N$ $(CH_2CH_2)_2N(CH_2)_3N(CH_2CH_2S)_2][SR]$, where M = Re, Tc and ^{99m}Tc, complexes 2–13, respectively (Fig. 6.1). In these complexes, the receptor specific 1-(2-methoxyphenyl)piperazine moiety has been introduced either on the monodentate ligand [S] (complexes 1) or on the tridentate ligand [SN(R)S] (complexes 2–13).

6.2.1. Experimental results

6.2.1.1. Materials and methods

Technetium-99 is a weak beta emitter (0.292 MeV) with a half-life of 2.12 $\times 10^5$ years. All manipulations of solutions and solids containing this radionu-clide were carried out in a laboratory approved for the handling of low energy particle emitting radionuclides. To prevent contamination, normal safety procedures were followed at all times.

Infrared spectra were recorded for KBr pellets in the range 4000–500 cm^{-1} on a Perkin–Elmer 1600 FT-IR spectrophotometer. The NMR spectra were recorded in deuterochloroform on a Bruker AC 250E spectrometer with TMS as internal standard. Elemental analysis was performed on a Perkin–Elmer 2400/II automated analyser. Technitium-99g was purchased as ammonium pertechnetate from the Oak Ridge National Laboratory, United States of America. The impure black solid was purified prior to its use by treatment overnight with hydrogen peroxide and ammonium hydroxide in methanol. Evaporation of the solvent afforded ammonium pertechnetate as a white powder. $Na^{99m}TcO_4$ was obtained in physiological saline as a commercial $^{99}Mo/$ ^{99m}Tc generator eluate (Cis International). All laboratory chemicals were reagent grade. The precursors $ReOCl_3(PPh_3)_2$ [6.17] and $^{99g}Tc(V)$ gluconate [6.18] were synthesized according to methods described in the literature. The

No.	n	R	M
		Structure A	

Structure A

| 1 | — | — | Re, ^{99m}Tc, ^{99}Tc |

| | | Structure B | |

Structure B

2	2	$C_6H_5^-$	Re, ^{99m}Tc
3	2	$4\text{-}CH_3OC_6H_4^-$	Re, ^{99m}Tc
4	3	$C_6H_5^-$	Re, ^{99m}Tc, ^{99}Tc
5	3	$4\text{-}CH_3OC_6H_4^-$	Re, ^{99m}Tc
6	3	$4\text{-}CH_3C_6H_4^-$	Re, ^{99m}Tc, ^{99}Tc
7	3	$4\text{-}C_2H_5C_6H_4^-$	Re, ^{99m}Tc
8	3	$4\text{-}n\text{-}C_4H_9C_6H_4^-$	Re
9	3	$4\text{-}ClC_6H_4^-$	Re, ^{99m}Tc
10	3	$3\text{-}BrC_6H_4^-$	Re, ^{99m}Tc
11	3	$C_6H_5CH_2CH_2^-$	Re, ^{99m}Tc, ^{99}Tc
12	3	$4\text{-}CH_3OC_6H_5CH_2^-$	Re
13	3	$4\text{-}t\text{-}C_4H_9C_6H_4CH_2^-$	Re
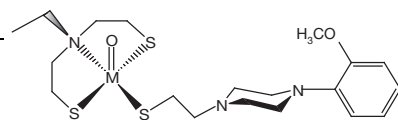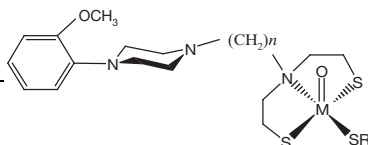
FIG. 6.1. Structures of the 3 + 1 mixed ligand complexes.

tridentate ligand $CH_3CH_2N(CH_2CH_2SH)_2$ was synthesized as described previously [6.12]. The tridentate ligand $o\text{-}CH_3OC_6H_4N(CH_2CH_2)_2N(CH_2)_2$ $N(CH_2CH_2SH)_2$ or $o\text{-}CH_3OC_6H_4N(CH_2CH_2)_2N(CH_2)_3N(CH_2CH_2SH)_2$ was synthesized by reaction of the secondary amine $o\text{-}CH_3OC_6H_4N(CH_2CH_2)_2NH$ with $BrCH_2CN$ or $BrCH_2CH_2CN$ followed by reduction of the nitrile with $LiAlH_4$. Treatment of the resulting primary amine with ethylene sulphide in an autoclave at 110ºC afforded the final products. Both compounds were purified by flash chromatography. The monodentate ligand $o\text{-}CH_3OC_6H_4N$ $(CH_2CH_2)_2NCH_2CH_2SH$ was synthesized by reaction of the secondary amine $o\text{-}CH_3OC_6H_4N(CH_2CH_2)_2NH$ with ethylene sulphide in an autoclave at 110ºC. The compound was purified by vacuum distillation. All compounds were characterized by IR and NMR spectroscopy.

A high performance liquid chromatography (HPLC) analysis was performed on a Waters 600E chromatography system coupled to both a Waters

991 photodiode array detector (UV trace for ^{99g}Tc, Re and ligands) and a GABI gamma detector from Raytest (Straubenhardt, Germany) (gamma trace for ^{99m}Tc). Separations were achieved on a Techsil C18 (10 μm, 250 mm × 4 mm) column eluted with a binary gradient system at a flow rate of 1.0 mL/min. Mobile phase A is 0.1% TFA in methanol, while mobile phase B is 0.1% TFA in water. The elution profile consists initially of 50% phase A, followed by a linear gradient to 70% A over 10 min; this composition was held for another 20 min. After a column wash with 95% A for 5 min, the column was re-equilibrated applying the initial conditions (50% phase A) for 15 min prior to the next injection.

The radioactivity content of biological samples was counted in an automatic gamma counter (NaI(Tl) crystal, Camberra Packard Auto-Gamma 5000 series instrument). Liquid scintillation measurements were conducted in a TRI-CARB 2100 TR beta counter with a 60% efficiency for ^{3}H.

[^{3}H]-8-hydroxy-2-(di-N-propylamino)tetralin, [^{3}H]-8-OH-DPAT, of specific activity 124.9 Ci/mmol, was purchased from NEN Life Sciences Products, Inc. (Boston, USA); 5-hydroxytryptamine (5-HT) hydrochloride was obtained from RBI Signaling Innovation; tris-(hydroxymethyl)aminomethane and CaCl$_2$ were obtained from Riedel-de-Haën (Seelze, Germany); ascorbic acid and bovine serum albumin (BSA, fraction V) were purchased from Merck (Darmstadt, Germany); a protein determination kit from Sigma Diagnostics (St. Louis, USA) was utilized.

6.2.1.2. *General synthesis of ReO complexes*

A typical synthetic procedure is given for complex 1. Trichlorobis(triphenylphosphine)rhenium (V) oxide (166 mg, 0.2 mmol) was added to a solution of CH_3COONa (164 mg, 2 mmol) in methanol (12 mL). To this suspension, $CH_3CH_2N(CH_2CH_2SH)_2$ (33 mg, 0.2 mmol) and o-$CH_3OC_6H_4N(CH_2CH_2)_2NCH_2CH_2SH$ (51 mg, 0.2 mmol) were added simultaneously under stirring. The mixture was refluxed until the green yellow suspension turned to a dark green solution. After cooling to room temperature, the reaction mixture was diluted with dichloromethane (30 mL) and then washed with water. The organic layer was separated from the mixture and dried over $MgSO_4$. The volume of the solution was reduced to 5 mL, and then 5 mL of methanol were added. Analysis of the solution by HPLC (conditions are given in the previous section) demonstrated the formation of one complex. Slow evaporation of the solvents at room temperature afforded the product as green crystals (50% yield). Crystals of Re-1, Re-4 and Re-11 suitable for X ray crystallography were obtained by recrystallization from CH_2Cl_2/CH_3OH.

Complex Re-1: retention fraction R_f = 0.7 (silica gel, CH$_2$Cl$_2$/CH$_3$OH 9/1). FT-IR (cm^{-1}, KBr pellet): 952 (Re=O). Analytical calculation for C$_{19}$H$_{32}$N$_3$O$_2$S$_3$Re: C, 36.96; H, 5.23; N, 6.81; S, 15.59. Found: C, 36.49; H, 5.28; N, 6.65; S, 15.26. UV–vis (nm): 217, 280sh, 379. ^{1}H NMR (ppm, CDCl$_3$): 7.03–6.87 (4H, N-o-OCH$_3$phenyl), 3.93 (2H, SC$\underline{H}_2$CH$_2$Npiperazine), 3.90 (2H, CH$_3$C$\underline{H}_2$N), 3.87 (3H, OC$\underline{H}_3$), 3.58, 2.98 (4H, EtNCH$_2$C$\underline{H}_2$S), 3.28, 2.60 (4H, EtNC$\underline{H}_2$CH$_2$S), 3.15, 2.83 (8H, piperazine), 2.91, (2H, SCH$_2$C$\underline{H}_2$Npiperazine), 1.38 (3H, C$\underline{H}_3$CH$_2$N). ^{13}C NMR (ppm, CDCl$_3$): 152.30, 141.41, 122.82, 120.98, 118.29, 111.18 (N-o-OCH$_3$phenyl), 61.81 (EtN$\underline{C}$H$_2$CH$_2$S), 60.78 (SCH$_2$$\underline{C}H_2$Npiperazine), 57.91 (CH$_3$$\underline{C}H_2$N), 55.35 (O$\underline{C}H_3$), 53.31, 50.50 (piperazine), 41.68 (EtNCH$_2$$\underline{C}H_2$S), 41.17 (S$\underline{C}H_2CH_2$Npiperazine), 8.75 ($\underline{C}H_3CH_2$N).

Complex Re-4: R_f = 0.5 (silica gel, CH$_2$Cl$_2$/CH$_3$OH 9/1). FT-IR (cm^{-1}, KBr pellet): 946 (Re=O). Analytical calculation for C$_{24}$H$_{34}$N$_3$O$_2$S$_3$Re 0.5 C$_2$H$_5$OH: C, 42.78; H, 5.31; N, 5.99; S, 13.70. Found: C, 42.66; H, 5.19; N, 6.35; S, 14.09. UV–vis (nm): 208, 280, 412. ^{1}H NMR (ppm, CDCl$_3$): 7.65–7.21 (5H, S-phenyl), 7.02–6.87 (4H, N-o-OCH$_3$phenyl), 3.92 (2H, NC$\underline{H}_2$CH$_2$CH$_2$Npiperazine), 3.87 (3H, OC$\underline{H}_3$), 3.59, 2.84 (4H, NCH$_2$C$\underline{H}_2$S), 3.30, 2.73 (4H, NC$\underline{H}_2$CH$_2$S), 3.13, 2.72 (8H, piperazine), 2.52 (2H, NCH$_2$CH$_2$C$\underline{H}_2$Npiperazine), 2.08 (2H, NCH$_2$C$\underline{H}_2$CH$_2$Npiperazine). ^{13}C NMR (ppm, CDCl$_3$): 153.36, 133.51, 127.96, 126.55 (S-phenyl), 152.25, 140.97, 123.18, 121.04, 118.28, 111.26 (N-o-OCH$_3$phenyl), 62.67 (N$\underline{C}$H$_2$CH$_2$S), 62.41 (N$\underline{C}$H$_2$CH$_2$CH$_2$Npiperazine), 55.52 (NCH$_2$CH$_2$$\underline{C}H_2$Npiperazine), 55.38 (OCH$_3$), 53.55, 50.45 (piperazine), 41.69 (NCH$_2$$\underline{C}H_2$S), 20.69 (NCH$_2$$\underline{C}H_2CH_2$Npiperazine).

Complex Re-11: R_f = 0.6 (silica gel, CH$_2$Cl$_2$/CH$_3$OH 9/1). FT-IR (cm^{-1}, KBr pellet): 946 (Re=O). Analytical calculation for C$_{26}$H$_{38}$N$_3$O$_2$S$_3$Re: C, 44.17; H, 5.42; N, 5.94; S, 13.60. Found: C, 44.46; H, 5.12; N, 6.28; S, 13.90. UV–vis (nm): 217, 280sh, 388. ^{1}H NMR (ppm, CDCl$_3$): 7.28–7.20 (5H, SCH$_2$CH$_2$phenyl), 7.01–6.87 (4H, N-o-OCH$_3$phenyl), 3.99 (2H, SC$\underline{H}_2$CH$_2$Ph), 3.91 (2H, NC$\underline{H}_2$CH$_2$CH$_2$Npiperazine), 3.87 (3H, OC$\underline{H}_3$), 3.62, 3.03 (4H, NCH$_2$C$\underline{H}_2$S), 3.32, 2.62 (4H, NC$\underline{H}_2$CH$_2$S), 3.12, 2.69 (8H, piperazine), 3.11 (2H, SCH$_2$C$\underline{H}_2$Ph), 2.51 (2H, NCH$_2$CH$_2$C$\underline{H}_2$Npiperazine), 2.07 (2H, NCH$_2$C$\underline{H}_2$CH$_2$Npiperazine). ^{13}C NMR (ppm, CDCl$_3$): 152.24, 141.02, 123.12, 121.03, 118.25, 111.24 (N-o-OCH$_3$phenyl), 141.77, 128.68, 128.30, 125.95 (SCH$_2$CH$_2$phenyl), 62.78 (N$\underline{C}$H$_2$CH$_2$S), 61.54 (N$\underline{C}$H$_2$CH$_2$CH$_2$Npiperazine), 55.55 (NCH$_2$CH$_2$$\underline{C}H_2$Npiperazine), 55.37 (O$\underline{C}H_3$), 53.56, 50.53 (piperazine), 46.27 (S$\underline{C}$H$_2$CH$_2$phenyl), 41.91 (NCH$_2$$\underline{C}H_2$S), 39.34 (SCH$_2$$\underline{C}H_2$phenyl), 21.00 (NCH$_2$$\underline{C}H_2CH_2$Npiperazine).

6.2.1.3. General synthesis of ^{99g}TcO complexes (^{99}Tc-1, ^{99}Tc-4 and ^{99}Tc-11)

A typical synthetic procedure is given for complex ^{99}Tc-1. A solution of stannous chloride (45 mg, 0.24 mmol) in HCl (1N, 1.0 mL) was added to an aqueous solution of NH$_4$^{99g}TcO$_4$ (36.2 mg, 0.2 mmol) containing ^{99m}TcO$_4^-$ (0.1 mL, 0.5 mCi) and sodium gluconate (200 mg) to obtain $^{99g/99m}$TcO gluconate. The pH of the solution was adjusted to 7.5 with NaOH (1N). This solution was added while stirring to a mixture of CH$_3$CH$_2$N(CH$_2$CH$_2$SH)$_2$ (33 mg, 0.2 mmol) and *o*-CH$_3$OC$_6$H$_4$N(CH$_2$CH$_2$)$_2$NCH$_2$CH$_2$SH (51 mg, 0.2 mmol). The solution was stirred for 15 min and then extracted twice with dichloromethane (20 mL). The organic phase was separated, dried over MgSO$_4$ and filtered. The volume of the solution was reduced to 5 mL, and then 5 mL of methanol was added. Slow evaporation of the solvents at room temperature afforded the product as red brown crystals.

Complex ^{99}Tc-1: R_f = 0.7 (silica gel, CH$_2$Cl$_2$/CH$_3$OH 9/1). FT-IR (cm^{-1}, KBr pellet): 930 (Tc=O). Analytical calculation for C$_{19}$H$_{32}$N$_3$O$_2$S$_3$Tc: C, 43.17; H, 6.10; N, 7.95; S, 18.19. Found: C, 42.96; H, 5.85; N, 7.59; S, 18.61. UV–vis (nm): 205, 280sh, 466. ^{1}H NMR (ppm, CDCl$_3$): 7.01–6.85 (4H, N-*o*-OC<u>H</u>$_3$<u>phenyl</u>), 3.91 (2H, SC<u>H</u>$_2$CH$_2$Npiperazine), 3.92 (2H, CH$_3$C<u>H</u>$_2$N), 3.87 (3H, OC<u>H</u>$_3$), 3.60, 3.05 (4H, EtNCH$_2$C<u>H</u>$_2$S), 3.48, 2.61 (4H, EtNC<u>H</u>$_2$CH$_2$S), 3.15, 2.89 (8H, piperazine), 2.92 (2H, SCH$_2$C<u>H</u>$_2$Npiperazine), 1.38 (3H, C<u>H</u>$_3$CH$_2$N). ^{13}C NMR (ppm, CDCl$_3$): 152.20, 141.20, 122.79, 120.95, 118.29, 111.15 (N-*o*-OCH$_3$<u>phenyl</u>), 60.72 (EtN<u>C</u>H$_2$CH$_2$S), 59.81 (SCH$_2$<u>C</u>H$_2$Npiperazine), 56.20 (CH$_3$<u>C</u>H$_2$N), 55.36 (O<u>C</u>H$_3$), 53.25, 50.62 (piperazine), 36.48 (EtNCH$_2$<u>C</u>H$_2$S), 35.20 (S<u>C</u>H$_2$CH$_2$Npiperazine), 8.80 (<u>C</u>H$_3$CH$_2$N).

Complex ^{99}Tc-4: R_f = 0.5 (silica gel, CH$_2$Cl$_2$/CH$_3$OH 9/1). FT-IR (cm^{-1}, KBr pellet): 924 (Tc=O). Analytical calculation for C$_{24}$H$_{34}$N$_3$O$_2$S$_3$Tc: C, 48.80; H, 5.80; N, 7.11; S, 16.28. Found: C, 48.51; H, 5.48; N, 6.94; S, 16.06. UV–vis (nm): 217, 370, 499. ^{1}H NMR (ppm, CDCl$_3$): 7.65–7.24 (5H, S-<u>phenyl</u>), 7.04–6.88 (4H, N-*o*-OC<u>H</u>$_3$<u>phenyl</u>), 3.97 (2H, NC<u>H</u>$_2$CH$_2$CH$_2$Npiperazine), 3.87 (3H, OC<u>H</u>$_3$), 3.60, 2.96 (4H, NCH$_2$C<u>H</u>$_2$S), 3.52, 2.73 (4H, NC<u>H</u>$_2$CH$_2$S), 3.15, 2.76 (8H, piperazine), 2.57 (2H, NCH$_2$CH$_2$C<u>H</u>$_2$Npiperazine), 2.12 (2H, NCH$_2$C<u>H</u>$_2$CH$_2$Npiperazine). ^{13}C NMR (ppm, CDCl$_3$): 152.27, 141.97, 123.21, 121.07, 118.32, 111.31 (N-*o*-OCH$_3$<u>phenyl</u>), 146.72, 134.00, 127.83, 126.91 (S-<u>phenyl</u>), 61.03 (N<u>C</u>H$_2$CH$_2$S), 61.03 (N<u>C</u>H$_2$CH$_2$CH$_2$Npiperazine), 55.69 (NCH$_2$CH$_2$<u>C</u>H$_2$Npiperazine), 55.39 (O<u>C</u>H$_3$), 53.55, 50.36 (piperazine), 36.70 (NCH$_2$<u>C</u>H$_2$S), 20.75 (NCH$_2$<u>C</u>H$_2$CH$_2$Npiperazine).

Complex ^{99}Tc-11: R_f = 0.6 (silica gel, CH$_2$Cl$_2$/CH$_3$OH 9/1). FT-IR (cm^{-1}, KBr pellet): 928 (Tc=O). Analytical calculation for C$_{26}$H$_{38}$N$_3$O$_2$S$_3$Tc: C, 50.47; H, 6.19; N, 6.79; S, 15.54. Found: C, 50.24; H, 5.88; N, 6.52; S, 15.14. UV–vis (nm): 208, 280sh, 370, 454. ^{1}H NMR (ppm, CDCl$_3$): 7.30–7.20 (5H, SCH$_2$CH$_2$<u>phenyl</u>),

7.05–6.86 (4H, N-o-OCH$_3$phenyl), 3.98 (2H, SC$\underline{H}_2$CH$_2$Ph), 3.94 (2H, NC$\underline{H}_2$CH$_2$CH$_2$Npiperazine), 3.86 (3H, OC$\underline{H}_3$), 3.65, 3.08 (4H, NCH$_2$C$\underline{H}_2$S), 3.52, 2.62 (4H, NC$\underline{H}_2$CH$_2$S), 3.13, 2.72 (8H, piperazine), 2.91 (2H, SCH$_2$C$\underline{H}_2$Ph), 2.62 (2H, NCH$_2$CH$_2$C$\underline{H}_2$N piperazine), 2.09 (2H, NCH$_2$C$\underline{H}_2$CH$_2$Npiperazine). ^{13}C NMR (ppm, CDCl$_3$): 152.24, 141.08, 122.92, 120.99, 118.22, 111.20 (N-o-OCH$_3$$\underline{phenyl}$), 141.21, 128.58, 128.53, 126.43 (SCH$_2$CH$_2$$\underline{phenyl}$), 61.12 (N$\underline{C}H_2CH_2$S), 59.99 (N$\underline{C}H_2CH_2CH_2$Npiperazine), 55.70 (NCH$_2CH_2$$\underline{C}H_2$Npiperazine), 55.36 (O$\underline{C}H_3$), 53.45, 50.60 (piperazine), 40.29 (S$\underline{C}$H$_2$CH$_2$phenyl), 38.67 (SCH$_2$$\underline{C}H_2$phenyl), 36.56 (NCH$_2$$\underline{C}H_2$S), 20.94 (NCH$_2$$\underline{C}H_2CH_2$Npiperazine).

6.2.1.4. Synthesis at tracer ^{99m}Tc level – general method

A typical synthetic procedure is given for complex ^{99m}Tc-1. A Gluco/ Demoscan kit was reconstituted with 10 mL water, and then a 1.0 mL aliquot was mixed with 0.5–1.0 mL of ^{99m}Tc pertechnetate solution (5–10 mCi). The ^{99m}Tc(V)O-glucoheptonate solution was added to a centrifuge tube containing equimolar quantities (0.02 mmol) of the tridentate ligand CH$_3$CH$_2$N(CH$_2$CH$_2$SH)$_2$ and the monodentate ligand o-CH$_3$OC$_6$H$_4$N (CH$_2$CH$_2$)$_2$NCH$_2$CH$_2$SH. The mixture was agitated in a vortex mixer and left to react at room temperature for 10 min. The complexes were extracted with dichloromethane (3 × 1.5 mL), and the combined organic extracts were dried over MgSO$_4$ and filtered. The extracts were nearly quantitative. The identity of the ^{99m}Tc complex (50 μL, 50–100 μCi) was established by comparative HPLC studies using as references the well characterized analogous oxorhenium Re-1 and oxotechnetium ^{99}Tc-1 complexes.

6.2.1.5. 5-HT$_{1A}$ receptor binding assay

Male Wistar rats (9 weeks old) were decapitated and the brains were rapidly removed, chilled and dissected to obtain the hippocampi. The hippocampi were then homogenized in 50mM tris-HCl buffer with pH7.6 (1/9, original wet weight/volume) using an Ultra Turrax T-25 homogenizer (30 s, 20 000 rev./min). The tissue suspension was centrifuged at 18 000g for 40 min at 4°C. The resulting pellet was then resuspended in the same buffer and the centrifugation–resuspension process was repeated twice to wash the homogenate. The final pellet was resuspended in 5 mL and stored at –80°C in 200 μL aliquots. The protein content was determined according to Lowry's method [6.19] using a protein determination kit containing BSA as a standard.

Competition binding experiments were performed in triplicates, using [^{3}H]-8-OH-DPAT as the radioligand, in a final volume of 2.5 mL. Briefly, in

each assay, tube aliquots (250 μL, corresponding to 50 μg protein) of rat hippocampal homogenates were mixed with tris-HCl buffer (50mM tris-HCl, 0.1% ascorbic acid, 2mM $CaCl_2$, pH7.5), which contained 250 μL [^{3}H]-8-OH-DPAT (0.14nM final concentration) and 250 μL of increasing concentrations (10^{-11}–10^{-6}M) of the competing oxorhenium complexes. Non-specific binding was defined as the amount of activity bound in the presence of 10μM native 5-HT. Incubations were carried out for 20 min at 37°C and then terminated by separation of bound from free radioligand by rapid filtration through glass fibre filters on a Brandel cell harvester; filters were presoaked with 1% BSA. After filtration, filters were rinsed four times with 3 mL of ice-cold tris-HCl buffer (50mM tris-HCl, 154mM NaCl) and placed in a 10 mL scintillation cocktail. Radioactivity was measured by liquid scintillation spectrometry using a beta counter. The results of competition experiments were subjected to a non-linear regression analysis using the GraphPad computer software (Version 2.0) to calculate the 50% inhibitory concentration (IC_{50}) values.

6.2.1.6. *Regional distribution in rat brains*

Three groups of male Wistar rats (200 g, four animals per group) were injected through the femoral vein with 0.2 mL 15–30 μCi of HPLC purified and 30% methanol reconstituted ^{99m}Tc complex under ether anaesthesia. The animals were sacrificed by cardiectomy under a slight ether anaesthesia at predetermined time intervals (2, 30 and 60 min) and blood samples were collected. The brains were rapidly removed, chilled and dissected. Samples from different brain regions (cortex, striatum, hippocampus, hypothalamus and cerebellum) were collected, weighed and counted. The percentage dose/g of each sample was calculated by comparison of sample counts with the counts of diluted initial dose (1/100).

6.2.1.7. *X ray crystal structure determination*

Diffraction measurements for Re-1 were made on a P2_1 Nicolet diffractometer upgraded by Crystal Logic (Los Angeles) using monochromated Cu Kα radiation, while data collection for Re-4 and Re-11 was performed on a Crystal Logic dual goniometer–diffractometer using graphite monochromated Mo Kα radiation. The unit cell dimensions were determined and refined by using the angular settings of 25 automatically centred reflections in the range $24 < 2\theta < 54°$ (where θ is the angle of incidence) (for Re-1) and $11 < 2\theta < 23°$ (for Re-4 and Re-11). Intensity data were recorded using a θ–2θ scan. Three standard reflections monitored every 97 reflections, showing less than 3% variation and no decay. Lorentz, polarization and psi scan absorption corrections were

applied using Crystal Logic software. The structures were solved by direct methods using SHELXS-86 [6.20] and refined by full-matrix least-squares techniques on F^2 with SHELXL-93 [6.21].

6.2.2. Results and discussion

6.2.2.1. Synthesis

The MO[SN(R)S][S] complexes synthesized fall into two classes (Fig. 6.1):

(1) Those with the 1-(2-methoxyphenyl)piperazine moiety on the monodentate ligand (complexes 1),
(2) Those with the 1-(2-methoxyphenyl)piperazine moiety on the tridentate ligand (complexes 2–13).

The oxorhenium complexes were prepared by reacting the respective tridentate and monodentate ligands with the $ReOCl_3(PPh_3)_2$ precursor in the ratio rhenium:tridentate:monodentate ligand of 1:1:1. The corresponding oxotechnetium complexes were produced by ligand exchange reaction in a similar manner but using ^{99g}TcO gluconate as precursor. All complexes are lipophilic. They were extracted in dichloromethane and isolated as crystalline products by slow evaporation from a solution of dichloromethane and methanol. The compounds were characterized by elemental analysis, IR, UV–vis and ^1H and ^{13}C NMR spectroscopies. Complexes are soluble in $CHCl_3$ and CH_2Cl_2, slightly soluble in CH_3OH and C_2H_5OH, and insoluble in n-C_5H_{12} and water. They are stable in the solid state as well as in organic solutions (for a period of months), as shown by HPLC and NMR. Their stability is not affected by the presence of air or moisture.

It is known that during the ligand exchange reaction the amine substituent of the tridentate ligand [SN(R)S] may be locked in either a *syn-* or an *anti*-position with respect to the oxygen of the oxometal core [6.22]. Therefore, the formation of two stereoisomers is theoretically possible. However, HPLC analysis of the crude reaction mixture of all the complexes showed the formation of only one species that was identified as the *syn*-isomer by detailed spectroscopic and X ray crystallographic data. The existence of the *anti*-isomer (expected to have shorter retention times and a different UV–vis spectrum) could not be established by HPLC studies.

The IR spectra of the complexes show characteristic peaks at 952–946 cm^{-1} for rhenium complexes and 930–924 cm^{-1} for technetium complexes, which can be attributed to stretching of the metal–oxygen bond. The stretch of Re=O in

oxorhenium complexes is approximately 20 cm^{-1} higher than the stretch of Tc=O in oxotechnetium complexes. This shift to higher frequencies from Tc=O to Re=O complexes has been also reported for other ligand systems, such as BAT and monoamide monoamine (MAMA), and is attributed to the greater overlap of the 5d orbitals of rhenium than that of the 4d orbitals of technetium. The absence of bands associated with SH stretching modes is an indication of deprotonation of this group upon complexation with oxorhenium and oxotechnetium. The electronic absorption spectra of the complexes at the oxorhenium and oxotechnetium levels were determined during HPLC analysis by employing the photodiode array detector. The UV–vis spectra of the oxorhenium complexes are characterized by intense bands at 379, 412 and 388 nm for Re-1, Re-4 and Re-11, respectively, while the UV–vis spectra of the oxotechnetium complexes are characterized by intense bands at 466, 499 and 454 nm for ^{99}Tc-1, ^{99}Tc-4 and ^{99}Tc-11, respectively. The NMR spectra of the complexes are typical for the 3 + 1 oxorhenium and oxotechnetium complexes of the *syn*-configuration of the side chain on nitrogen [6.22, 6.23].

6.2.2.2.   *Description of the structures*

ORTEP (Oak Ridge thermal ellipsoid plot) diagrams of compounds Re-1, Re-4 and Re-11 are shown in Fig. 6.2. The co-ordination sphere about oxorhenium in the complexes studied is defined by the SNS donor atom set of the tridentate ligand and the sulphur atom of the monodentate co-ligand. The trigonality index, τ [6.24], calculated for Re-1, is 0.36 ($\tau = 0$ for a perfect square pyramid and $\tau = 1$ for a perfect trigonal bipyramid). Thus, the co-ordination geometry can be described as trigonally distorted square pyramidal. Rhenium lies 0.65 Å out of the basal plane of the square pyramid towards the oxo group. The two five-membered rings in the co-ordination sphere adopt the stable envelope configuration, with C2 and C4 being out of the mean plane of the remaining atoms (displacement ≈0.57 Å for both atoms). The torsion angles of the tridentate ligand, S1–C1–C2–N1 and N1–C3–C4–S2, are ≈55.6 and 44.7º, respectively. The ethyl substituent on N1 is directed *cis* to the oxo group (O1 … C5 = 3.15 Å).

The trigonality index calculated in Re-4 and Re-11 is 0.66 and 0.61, respectively. Thus, the co-ordination geometry about rhenium can be described as distorted trigonal bipyramidal. Rhenium lies ~0.1 Å out of the O1–S1–S2 mean plane towards the monodentate thiol. The two five-membered rings in the co-ordination sphere exist in the envelope configuration with C2 and C3, adjacent to the nitrogen, displaced out of the best mean plane of the remaining four atoms (C2/C3 = –0.65/0.58 Å in 8 and 0.66/–0.57 Å in 7). The torsion angles
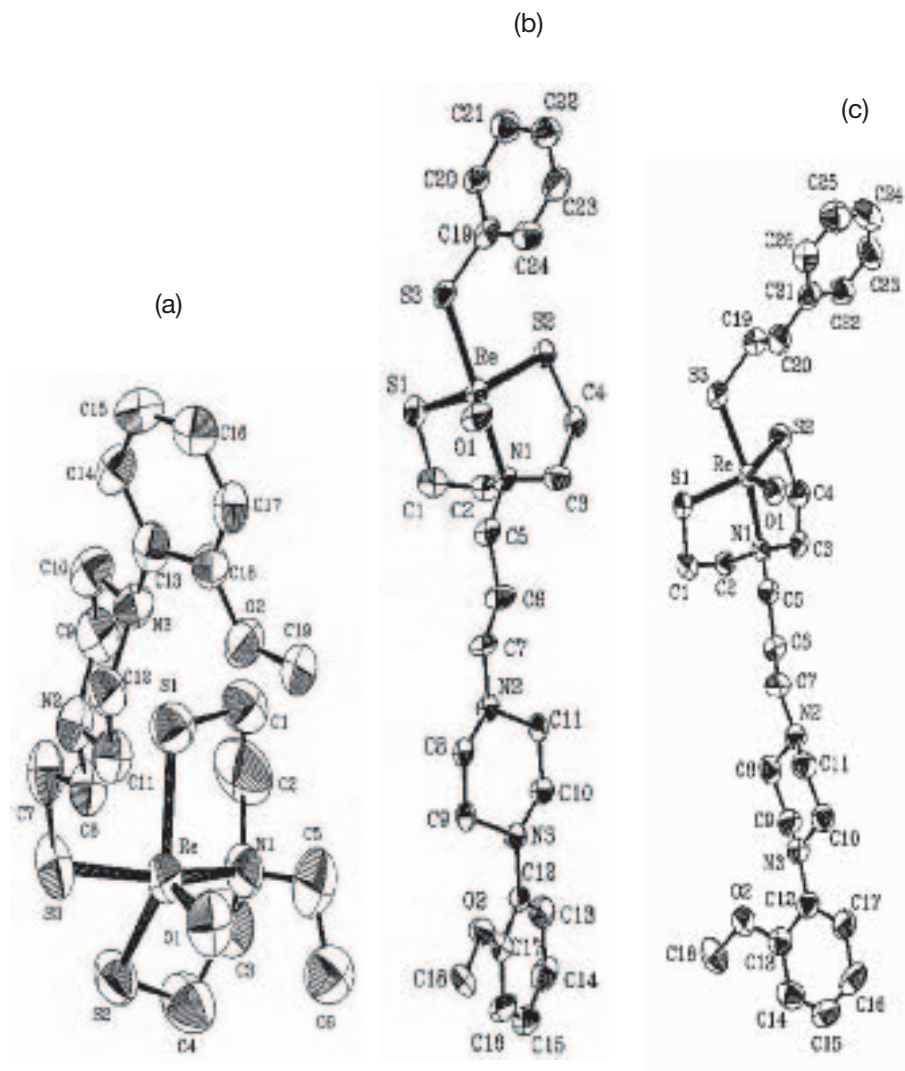
FIG. 6.2. ORTEP diagrams of complexes (a) Re-1, (b) Re-4 and (c) Re-11.

defined by the atoms of the tridentate ligand, i.e. S1–C1–C2–N1 and N1–C3–C4–S2, are 52.1 and 46.4° in Re-4 and 51.8 and 43.5° in Re-11.

The 1-(2-methoxyphenyl)piperazine group attached to the tridentate ligand is in the *cis* configuration with respect to the oxo group (O1 … C5 = 2.96 and 2.93 Å in complexes 4 and 11, respectively). The piperazino moiety in all

three compounds adopts the chair configuration, where the two nitrogen atoms are displaced from the best mean plane of the remaining four carbon atoms (N2/N3 = 0.63/-0.70 Å in Re-1, –0.71/0.65 Å in Re-4 and –0.65/0.63 Å in Re-11).

6.2.2.3. *Synthesis at ^{99m}Tc level*

The ^{99m}Tc complexes (Fig. 6.1) were prepared by ligand exchange reaction using ^{99m}TcO-glucoheptonate as the precursor in the ratio tridentate:monodentate ligand of 1:1. Owing to the co-ordinating power of the SNS/S system, the reaction was fast and nearly quantitative as determined by organic solvent extraction of the aqueous reaction mixture. Aliquots of the organic extracts were analysed by HPLC. In order to establish the structural analogy between the ^{99m}Tc complexes prepared at tracer level with the respective oxorhenium and oxotechnetium-99g complexes prepared in macroscopic amounts, comparison by HPLC adopting parallel radiometric and photometric detection was pursued. Thus, by co-injection of the respective ReO and ^{99m}TcO complexes, identical retention times were exhibited, revealing their structural analogy. The radioactivity recovery from the column after injection of ^{99m}TcO complexes was monitored and found to be quantitative.

Prior to further evaluation, the ^{99m}Tc complexes were purified by HPLC and used thereafter as a 30% aqueous methanolic solution. The stability and purity of the final solution was tested throughout the time of biological studies by HPLC analysis. The HPLC purified ^{99m}Tc complexes were found to be stable in dichloromethane and in a 30% aqueous methanolic solution for more than 6 h.

6.2.2.4. *In vitro evaluation*

The oxorhenium complexes synthesized (Re-1–Re-13) were tested for their ability to displace [^{3}H]8-OH-DPAT, a potent and specific 5-HT$_{1A}$ receptor agonist, from 5-HT$_{1A}$ binding sites in rat hippocampal homogenates. The IC$_{50}$ values, indicating the concentration of the compound which inhibits 50% of the [^{3}H]8-OH-DPAT specific binding, are summarized in Table 6.1. The IC$_{50}$ values of the compounds tested were between 5.8 and 103nM, indicating their capability in binding to 5-HT$_{1A}$ receptors. Among them, complexes 4 and 5 displayed a higher affinity (6.0 and 5.8nM respectively). These values are in the same range as reported values for other radioligands such as WAY 100635 (2.2, 6.0nM) and its analogues, *p*-MPPF (5.6nM) and 8-OH-DPAT (5.0nM), indicating that the attachment of the ReO(SN(R)S)(S) backbone on the *o*-methoxy-phenylpiperazine moiety does not modify the in vitro affinity for 5-HT$_{1A}$ receptors. The substitution of the aromatic ring of the monodentate ligand with

TABLE 6.1. BRAIN UPTAKE IN RATS OF ^{99m}Tc COMPLEXES POST-INJECTION (% ID/ORGAN ± SD) AND POTENCIES OF THE CORRE-SPONDING OXORHENIUM COMPLEXES TO INHIBIT THE SPECIFIC BINDING OF [^{3}H]8-OH-DPAT IN RAT HIPPOCAMPAL HOMOGENATE

Complex	IC_{50} (nM) Re complexes	Brain uptake of ^{99m}Tc complexes post-injection		
		2 min	30 min	60 min
1	31.0	0.413 ± 0.097	0.066 ± 0.018	0.045 ± 0.000
2	22.0	1.311 ± 0.095	0.583 ± 0.037	0.424 ± 0.061
3	20.0	0.780 ± 0.070	0.335 ± 0.079	0.264 ± 0.025
4	6.0	0.468 ± 0.101	0.319 ± 0.075	0.202 ± 0.024
5	5.8	0.410 ± 0.093	0.247 ± 0.036	0.233 ± 0.040
6	12.0	0.420 ± 0.021	0.290 ± 0.021	0.227 ± 0.033
7	26.6[a]	0.363 ± 0.108	0.197 ± 0.005	0.198 ± 0.041
8	103	—	—	—
9	—	0.529 ± 0.070	0.319 ± 0.010	0.324 ± 0.017
10	26.0	0.619 ± 0.053	0.332 ± 0.016	0.319 ± 0.024
11	12	0.242 ± 0.059	0.179 ± 0.037	0.119 ± 0.024
12	17	—	—	—
13	80	—	—	—

[a] IC_{50} for 5-HT$_{2A}$ and D$_2$, 540 and 480nM, respectively.

bulky groups results in a drop of the affinity to the 5-HT$_{1A}$ receptor. The length of the alkyl group connecting the nitrogen of the piperazine and the nitrogen co-ordinated to the metal was also crucial. A decrease of the affinity was measured for complexes with an ethylene chain (IC_{50} of 22 and 20nM for complexes 2 and 3, respectively) compared with those with a propylene chain (IC_{50} of 6.0 and 5.8nM for complexes 4 and 5, respectively). Thus, the increase of the chain length to four or five carbon atoms may further improve the in vitro affinity of the complexes, as reported for the analogous oxorhenium complexes, having the *o*-MPP moiety on the monodentate ligand.

6.2.2.5. *In vivo evaluation*

The in vivo distributions of the most potent ^{99m}Tc mixed ligand complexes ^{99m}Tc-1–^{99}Tc-7 and ^{99m}Tc-9–^{99}Tc-11 were examined in male Wistar rats. All complexes, after an intravenous injection, were able to cross the blood–brain

barrier, resulting in a significant initial brain uptake (0.242–1.311% dose/organ at 2 min post-injection). The brain uptakes of complexes 2 and 3, having an ethylene chain between the nitrogen of the piperazine and the nitrogen co-ordinated to the metal, were about double those of the analogous complexes with three carbon chains, complexes 4 and 5. The brain uptakes for most of the compounds are higher than the reported values of other ^{99m}Tc complexes designed for imaging 5-HT$_{1A}$ or other CNS receptors. In addition, in similar complexes designed for imaging dopamine transporters, complexes of SNS/S [6.16] exhibit good in vivo and in vitro binding properties, but with the major disadvantage of low brain uptake. The washout of activity from the brain was quite fast during the first 30 min for all the complexes, 40–60% of the initial activity being retained in the brain, while the washout from 30–60 min post-injection was much slower. Especially for complexes 5, 7, 9 and 10 the brain uptake values at 30 and 60 min post-injection were not varied.

The initial distribution of the complexes in various brain regions is inhomogeneous. The concentration of radioactivity was higher in the cortex, followed by the cerebellum (CB) and hypothalamus, indicating a distribution according to the cerebral blood flow. On the other hand, the concentration of radioactivity in the hippocampus (HIPP), which is an area rich in 5-HT$_{1A}$ receptors, was the lowest. The faster washout from the cerebellum than that from the hippocampus resulted in an increase of the HIPP/CB ratio. The highest ratio was calculated for complex 4, 1.19 at 60 min post-injection compared with 0.74 at 2 min post-injection (Table 6.2).

The failure of the complexes studied to bind to 5-HT$_{1A}$ receptors to any appreciable extent in vivo is puzzling, given their high in vitro affinities and their high brain uptakes. An explanation may be the affinity of the complexes for other types of receptor. Complex 7 was tested for its affinity for 5-HT$_{2A}$ and D$_2$ receptors, and the IC$_{50}$ values indicate that its affinities are not negligible (540 and 480nM, respectively). The low selectivity can be attributed to the lack of a pyridine ring from the molecule, as has been reported for other derivatives of WAY 100635. Moreover, the lack of pyridine may give an agonist action to the molecule, resulting in a fast washout from the receptors, as reported for other derivatives of WAY 100635.

6.2.3.   Conclusions

Receptor specific oxorhenium and oxotechnetium complexes based on the SN(R)S/S mixed ligand system were synthesized and characterized at macroscopic level. An affinity for the serotonin 5-HT$_{1A}$ brain receptor subtype is imparted by the 1-(2-methoxyphenyl)piperazine moiety, which has been located on the tridentate ligand. As demonstrated by appropriate competition

TABLE 6.2. REGIONAL DISTRIBUTION OF ^{99m}Tc COMPLEXES 1–7 IN RAT BRAINS AT 2, 30 AND 60 min POST-INJECTION (% ID/g ± SD)

	Time	Hippocampus	Cortex	Striatum	Hypo-thalamus	Cerebellum	HIPP/CB[a]
1	2 min	0.248 ± 0.093	0.279 ± 0.025	0.239 ± 0.029	0.314 ± 0.042	0.271 ± 0.062	0.92
	30 min	0.051 ± 0.015	0.048 ± 0.006	0.041 ± 0.001	0.053 ± 0.009	0.039 ± 0.011	1.31
	60 min	0.031 ± 0.004	0.050 ± 0.011	0.024 ± 0.002	0.041 ± 0.010	0.024 ± 0.002	1.27
2	2 min	0.671 ± 0.059	0.973 ± 0.051	0.804 ± 0.152	0.838 ± 0.165	0.843 ± 0.165	0.80
	30 min	0.360 ± 0.003	0.380 ± 0.013	0.342 ± 0.015	0.376 ± 0.029	0.368 ± 0.011	0.98
	60 min	0.250 ± 0.051	0.223 ± 0.032	0.226 ± 0.017	0.268 ± 0.031	0.295 ± 0.027	0.85
3	2 min	0.406 ± 0.066	0.500 ± 0.068	0.443 ± 0.052	0.451 ± 0.002	0.497 ± 0.031	0.82
	30 min	0.211 ± 0.052	0.219 ± 0.059	0.202 ± 0.037	0.240 ± 0.063	0.212 ± 0.043	0.99
	60 min	0.170 ± 0.037	0.166 ± 0.031	0.169 ± 0.021	0.209 ± 0.067	0.184 ± 0.035	0.92
4	2 min	0.249 ± 0.068	0.315 ± 0.078	0.276 ± 0.091	0.292 ± 0.117	0.339 ± 0.101	0.74
	30 min	0.250 ± 0.094	0.223 ± 0.105	0.186 ± 0.081	0.219 ± 0.085	0.208 ± 0.029	1.20
	60 min	0.130 ± 0.018	0.137 ± 0.021	0.123 ± 0.023	0.129 ± 0.016	0.109 ± 0.012	1.19
5	2 min	0.271 ± 0.003	0.422 ± 0.144	0.257 ± 0.018	0.299 ± 0.027	0.262 ± 0.020	1.03
	30 min	0.154 ± 0.039	0.256 ± 0.026	0.148 ± 0.037	0.208 ± 0.060	0.148 ± 0.040	1.04
	60 min	0.147 ± 0.024	0.169 ± 0.036	0.144 ± 0.021	0.165 ± 0.019	0.143 ± 0.029	1.03
6	2 min	0.255 ± 0.085	0.263 ± 0.035	0.212 ± 0.032	0.189 ± 0.071	0.199 ± 0.013	1.28
	30 min	0.189 ± 0.025	0.226 ± 0.042	0.176 ± 0.010	0.200 ± 0.017	0.182 ± 0.014	1.04
	60 min	0.141 ± 0.021	0.163 ± 0.029	0.142 ± 0.029	0.165 ± 0.045	0.127 ± 0.001	1.11
7	2 min	0.189 ± 0.057	0.275 ± 0.101	0.190 ± 0.057	0.217 ± 0.063	0.247 ± 0.076	0.76
	30 min	0.117 ± 0.001	0.151 ± 0.001	0.113 ± 0.005	0.131 ± 0.010	0.126 ± 0.003	0.93
	60 min	0.122 ± 0.025	0.153 ± 0.030	0.117 ± 0.018	0.126 ± 0.024	0.122 ± 0.028	1.00

[a] Hippothalmus/cerebellum.

TABLE 6.2. REGIONAL DISTRIBUTION OF ^{99m}Tc COMPLEXES 1–7 IN RAT BRAINS AT 2, 30 AND 60 min POST-INJECTION (% ID/g ± SD) (cont.)

	Time	Hippocampus	Cortex	Striatum	Hypo-thalamus	Cerebellum	HIPP/CB[a]
9	2 min	0.306 ± 0.048	0.377 ± 0.020	0.273 ± 0.013	0.342 ± 0.062	0.360 ± 0.084	0.85
	30 min	0.198 ± 0.023	0.271 ± 0.007	0.204 ± 0.020	0.251 ± 0.033	0.194 ± 0.013	1.02
	60 min	0.191 ± 0.006	0.229 ± 0.017	0.201 ± 0.018	0.253 ± 0.006	0.195 ± 0.005	0.98
10	2 min	0.335 ± 0.027	0.434 ± 0.004	0.389 ± 0.015	0.422 ± 0.053	0.451 ± 0.029	0.74
	30 min	0.187 ± 0.001	0.282 ± 0.040	0.193 ± 0.041	0.190 ± 0.008	0.219 ± 0.028	0.86
	60 min	0.189 ± 0.009	0.238 ± 0.021	0.190 ± 0.011	0.244 ± 0.012	0.201 ± 0.007	0.94
11	2 min	0.123 ± 0.041	0.160 ± 0.057	0.142 ± 0.067	0.150 ± 0.049	0.170 ± 0.056	0.72
	30 min	0.116 ± 0.039	0.127 ± 0.041	0.122 ± 0.033	0.139 ± 0.032	0.110 ± 0.028	1.06
	60 min	0.074 ± 0.021	0.081 ± 0.016	0.067 ± 0.019	0.074 ± 0.021	0.067 ± 0.011	1.08

[a] Hippothalmus/cerebellum.

binding tests in rat hippocampal preparations, all oxorhenium analogues showed an affinity for the 5-HT$_{1A}$ receptor binding sites with IC$_{50}$ values in the nanomolar range. In particular, complexes 4 and 5 exhibited a significantly higher affinity for the 5-HT$_{1A}$ receptor subtype in vitro, with IC$_{50}$ values in the lower nanomolar range (5.8 and 6.0nM, respectively).

Complexes were also successfully prepared at tracer level using ^{99m}Tc-glucoheptonate as precursor. Tissue distribution studies in healthy rats demonstrated that all ^{99m}Tc complexes were able to cross the blood–brain barrier, showing a significantly high initial uptake in the brain (0.24–1.31% ID/organ at 2 min post-injection). Moreover, a significant percentage of radioactivity was retained in the brain at 30 and 60 min post-injection. However, a clear correlation between the distribution of radioactivity and the distribution of 5-HT$_{1A}$ could not be established. Structural modifications to this system may further improve the biological profile of these compounds and eventually provide efficient ^{99m}Tc receptor imaging agents.

6.3. SYNTHESIS, CHARACTERIZATION AND EVALUATION
(IN VIVO AND IN VITRO) OF THE 2 + 1 + 1 MIXED LIGAND
COMPLEX OF THE GENERAL FORMULA: MO[o-CH$_3$O-PH-N-
PIPERAZINO-N-CH$_2$CH$_2$S] [SR]$_2$, WHERE M = Re, ^{99}Tc, ^{99m}Tc

We report here the synthesis of a novel ^{99m}Tc-[NS][S][S], ^{99m}TcO[o-CH$_3$OC$_6$H$_4$N(CH$_2$CH$_2$)$_2$NCH$_2$CH$_2$S][4-CH$_3$-C$_6$H$_4$S] mixed ligand complex that carries the 1-(2-methoxyphenyl)piperazine moiety, a fragment of the prototypic compound WAY 100635, on the bidentate ligand [NS]. The aim of the investigation reported here was to generate, for the fist time, a specific mixed ligand complex, as a potential radiopharmaceutical for 5-HT$_{1A}$ receptors, based on the 2 + 1 + 1 mixed ligand concept [6.25].

The synthesis of the bidentate ligand was performed by reacting equimolar amounts of the amine o-CH$_3$OC$_6$H$_4$N(CH$_2$CH$_2$)$_2$NH and ethylene sulphide in an autoclave at 110ºC. The compound was purified by vacuum distillation. The oxorhenium complex Re-14 was prepared by reacting the bidentate and the monodentate ligands with the ReOCl$_3$(PPh$_3$)$_2$ precursor in the ratio rhenium:bidentate:monodentate ligand of 1:1:1, as previously described (Fig. 6.3). The corresponding oxotechnetium complex Tc-14 was produced by ligand exchange reaction in a similar manner but using the technetium(V)gluconate as precursor. Both complexes are lipophilic. They were extracted in dichloromethane and isolated as crystalline products by slow evaporation from a solution of dichloromethane and methanol. The compounds were characterized by elemental analyses: IR, UV–vis and ^{1}H NMR spectroscopies. The complexes are soluble in CHCl$_3$ and CH$_2$Cl$_2$, slightly
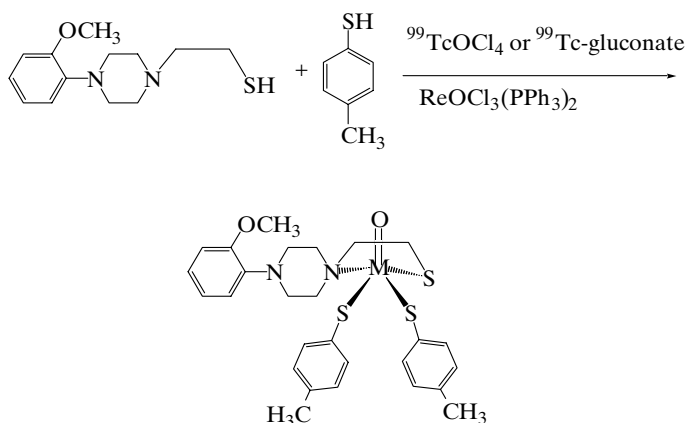
FIG. 6.3. *Structures of the mixed ligand complexes MO[SN][S]$_2$, where M = Re, complex Re-14, M = ^{99}Tc, complex ^{99}Tc-14 and M = ^{99m}Tc, complex ^{99m}Tc-14.*

soluble in MeOH and EtOH, and insoluble in pentane and water. They are stable in the solid state as well as in organic solutions (for a period of months), as shown by HPLC and NMR. Their stability is not affected by the presence of air or moisture.

The IR spectra of the complexes show characteristic peaks at 944 cm^{-1} for the oxorhenium complex and 930 cm^{-1} for the oxotechnetium complex, which can be attributed to stretching of the metal–oxygen bond. The Re=O stretch in complex Re-14 is higher than the Tc=O stretch in complex Tc-14. The absence of bands associated with SH stretching modes is an indication of deprotonation of this group upon complexation with oxorhenium and oxotechnetium. The electronic absorption spectra of the complexes at the oxorhenium and oxotech-netium levels were determined during HPLC analysis by employing the photodiode array detector. The UV–vis spectrum of complex Re-14 is charac-terized by an intense band at 403 nm, while the UV–vis spectrum of the oxotechnetium complex Tc-14 is characterized by an intense band at 487 nm. The NMR spectrum of the complexes displayed the basic characteristics of the aminothiol complexes observed in our previous studies [6.25]. An ORTEP diagram is given in Fig. 6.4.
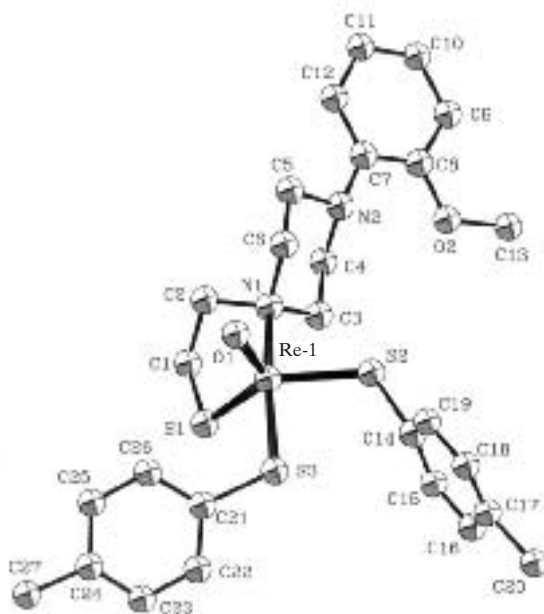
FIG. 6.4. ORTEP diagram of the Re-14 complex.

6.3.1. Synthesis at ^{99m}Tc level

The ^{99m}Tc-14 complex was prepared by ligand exchange reactions using ^{99m}TcO-glucoheptonate as precursor in the ratio bidentate:monodentate ligand of 1:1. Since the complex [^{99m}TcMO(NS)(S)$_2$] is preferentially formed at a low concentration of ligands, we performed the synthesis of the complex ^{99m}Tc-14 by reacting 100 nmol of each ligand [6.25]. The reaction was fast and the complex was extracted from the reaction mixture with dichloromethane. The labelling yield was more than 70% as calculated by organic solvent extraction of the aqueous reaction mixture. Aliquots of the organic extracts were analysed with HPLC. In order to establish the structural analogy between the ^{99m}Tc complex prepared at tracer level with the respective oxorhenium and oxotechnetium-99 complexes prepared in macroscopic amounts, comparison by HPLC adopting parallel radiometric and photometric detection was pursued. Thus, by co-injection of the oxorhenium Re-14, oxotechnetium-99 Tc-14 and oxotechnetium-99m ^{99m}Tc-14 complexes, identical retention times were exhibited, revealing their structural analogy. The radioactivity recovery from the column was monitored and found to be quantitative.

Complex ^{99m}Tc-14 was purified with HPLC and used thereafter as a 30% aqueous methanolic solution. The biodistribution of the ^{99m}Tc complex was studied in male rats, 2, 30 and 60 min post-injection. The results are presented in Table 6.3. The complex demonstrates a low brain uptake, which declined further at 30 min post-injection. The accumulation of the radioactivity was not homogeneous in the brain. Areas rich in 5-HT$_{1A}$ receptors, such as the hippocampus, showed low concentrations of radioactivity resulting in HIPP/CB ratios of 0.55, 0.68 and 0.65 at 2, 30 and 60 min post-injection, respectively. In conclusion, this complex displays low brain uptake and does not bind specifically to 5-HT$_{1A}$ receptors in vivo.

6.4. A NOVEL 5-HT$_{1A}$ RECEPTOR LIGAND USING TECHNETIUM CARBONYLS

In this work a novel compound, HYNIC-o-MPP, has been synthesized. HYNIC-o-MPP contains 1-(2-methoxyphenyl)piperazine (o-MPP), a fragment of the WAY 100635 complex, which has been incorporated into the HYNIC moiety. Its complexation to the tricarbonylmetal(I) centre of technetium as well as the biological evaluation of the resulting complex as a potential 5-HT$_{1A}$ receptor imaging agent are presented here.

The synthesis of HYNIC-o-MPP is depicted in Fig. 6.5. The compound was purified by flash chromatography and characterized by IR and NMR

TABLE 6.3. REGIONAL DISTRIBUTION OF ^{99m}Tc COMPLEX IN RAT BRAINS AT 2, 30 AND 60 min POST-INJECTION (% ID/g)

Region	2 min	30 min	60 min
Brain	0.153 ± 0.001	0.061 ± 0.001	0.054 ± 0.006
Hippocampus	0.126 ± 0.005	0.058 ± 0.003	0.051 ± 0.001
Cerebellum	0.228 ± 0.014	0.085 ± 0.000	0.079 ± 0.007
Hypothalamus	0.0173 ± 0.005	0.054 ± 0.001	0.053 ± 0.001
Striatum	0.106 ± 0.003	0.060 ± 0.008	0.035 ± 0.002
Cortex	0.175 ± 0.007	0.061 ± 0.008	0.055 ± 0.006
HIPP/CB	0.55	0.68	0.65

spectroscopy. Labelling was achieved by incubation of the precursor $[^{99m}Tc(CO)_3(H_2O)_3]^+$ (7, 8) for 10 min at 45ºC with 1 mg of HYNIC-*o*-MPP. HPLC studies demonstrate that the reaction results in a single complex with yield >95%, which is stable for more than 6 h [6.26]. Typical HPLC profiles are presented in Fig. 6.6.

The biodistribution of the ^{99m}Tc complex was studied in male rats, 2 and 60 min post-injection. The results are presented in Tables 6.4 and 6.5. Briefly, the bulk of the radioactivity was directed mainly to the hepatobiliary system. The complex demonstrates a low brain uptake, which declined further at 60 min post-injection. The accumulation of the radioactivity was homogeneous in
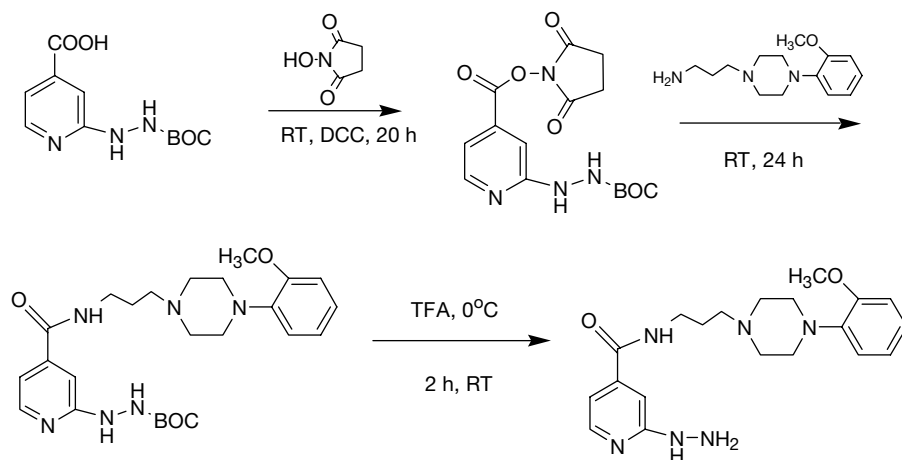
FIG. 6.5. Synthesis of HYNIC-o-MPP.

97
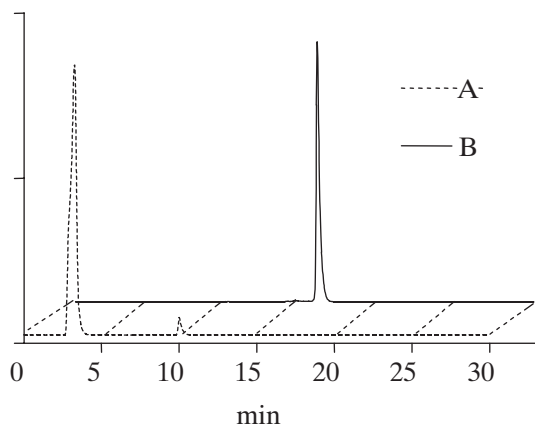
FIG. 6.6. Chromatographic analysis by reversed-phase high performance liquid chromatography (RP-HPLC): A, [$^{99m}Tc(CO)_3(H_2O)_3$]$^+$; B, $^{99m}Tc(CO)_3(HYNIC-o-MPP)(X)$.

all brain regions at 2 and 60 min post-injection except for the cerebellum, where the highest concentration was measured. Areas rich in 5-HT$_{1A}$ receptors, such as the hippocampus, showed a low concentration of radioactivity, resulting in HIPP/CB ratios of 0.48 and 0.45 at 2 and 60 min post-injection, respectively.

In conclusion, HYNIC-o-MPP reacts with [$^{99m}Tc(CO)_3(H_2O)_3$]$^+$ resulting in a single stable complex, $^{99m}Tc(CO)_3(HYNIC-L)(X)$. This complex displays low brain uptake and does not bind specifically to 5-HT$_{1A}$ receptors in vivo.

TABLE 6.4. BIODISTRIBUTION DATA OF $^{99m}Tc(CO)_3(HYNIC-o-MPP)(X)$ IN RATS AT 2 AND 60 min POST-INJECTION (% ID/g)

Region	2 min	60 min
Blood	3.68 ± 0.20	1.33 ± 0.15
Heart	0.90 ± 0.07	0.50 ± 0.05
Liver	3.88 ± 0.28	6.23 ± 0.55
Stomach	0.12 ± 0.02	0.29 ± 0.09
Lungs	1.30 ± 0.01	0.58 ± 0.05
Brain	0.11 ± 0.01	0.04 ± 0.01

TABLE 6.5. REGIONAL DISTRIBUTION OF ^{99m}Tc(CO)$_3$(HYNIC-o-MPP)(X) IN RAT BRAINS AT 2 AND 60 min POST-INJECTION (% ID/g)

Brain region	2 min	60 min
Hippocampus	0.089 ± 0.02	0.034 ± 0.00
Cerebellum	0.186 ± 0.04	0.074 ± 0.02
Hypothalamus	0.119 ± 0.03	0.037 ± 0.01
Striatum	0.062 ± 0.01	0.029 ± 0.01
Cortex	0.099 ± 0.01	0.037 ± 0.01
HIPP/CB	0.48	0.45

REFERENCES TO CHAPTER 6

[6.1] HOM, R.K., KATZENELLENBOGEN, J.A., Technetium-99m-labelled receptor-specific small-molecule radiopharmaceuticals: Recent developments and encouraging results, Nucl. Med. Biol. **24** (1997) 485–489 and references therein.

[6.2] KUNG, H.F., et al., Imaging of dopamine transporters in humans with technetium-99m TRODAT-1, Eur. J. Nucl. Med. **23** (1996) 1527–1537.

[6.3] FORSTER, E.A., et al., A pharmacological profile of the selective silent 5-HT$_{1A}$ receptor antagonist, WAY-100635, Eur. J. Pharmacol. **25** (1995) 81–88.

[6.4] WILSON, A.A., et al., Derivatives of WAY 100635 as potential imaging agents for 5-HT$_{1A}$ receptors: Syntheses, radiosyntheses, and in vitro and in vivo evaluation, Nucl. Med. Biol. **25** (1998) 769–776.

[6.5] MENSONIDES-HARSEMA, M.M., et al., Synthesis and in vitro and in vivo functional studies of ortho-substituted phenylpiperazine and N-substituted 4-N-(o-methoxyphenyl)aminopiperidine analogues of WAY 100635, J. Med. Chem. **43** (2000) 432–439.

[6.6] ZHUANG, Z.-P., KUNG, M.-P., KUNG, H.F., Synthesis and evaluation of 4-(2′-methoxyphenyl)-1-[2′-[N-(2″-pyridinyl)-p-iodobenzamido]ethyl]piperazine (p-MPPI): A new iodinated 5-HT$_{1A}$ ligand, J. Med. Chem. **37** (1994) 1406–1407.

[6.7] KUNG, H.F., et al., "New TcO(III) and ReO(III) N$_2$S$_2$ complexes as potential CNS 5-HT$_{1A}$ receptor imaging agents", Technetium and Rhenium in Chemistry and Nuclear Medicine (NICOLINI, M., BANDOLI, G., MAZZI, U., Eds), SGE Editoriali, Padua (1995) 293–298.

[6.8] MAHMOOD, A., et al., "Technetium(V) and rhenium(V) analogues of WAY 100635 5-HT$_{1A}$ receptor-binding complexes", Technetium, Rhenium and Other Metals in Chemistry and Nuclear Medicine (NICOLINI, M., MAZZI, U., Eds), SGE Editoriali, Padua (1999) 393–399.

[6.9] VANBILLOEN, H., et al., "Synthesis and biological evaluation of a conjugate of ^{99m}Tc-ECC with 1-(2-methoxyphenyl)-4-(2-(2-pyridylamino) ethylpiperazine (Way-100634)", ibid., pp. 479–484.

[6.10] SPIES, H., PIETZSCH, J.H., JOHANNSEN, B., "The n + 1" mixed-ligand approach in the design of specific technetium radiopharmaceuticals: Potentials and problems", ibid., pp. 101–108.

[6.11] PIRMETTIS, I.C., et al., Synthesis and characterization of oxotechnetium(V) mixed ligand complexes containing a tridentate N-substituted bis-(2-mercapto-ethyl)-amine and a monodentate thiol, Inorg. Chem. **34** (1996) 1685–1691.

[6.12] PIRMETTIS, I.C., PAPADOPOULOS, M.S., CHIOTELLIS, E., Novel ^{99m}Tc aminobis-thiolato/monothiolato "3 + 1" mixed ligand complexes: Structure–activity relationships and preliminary in vivo validation as brain blood flow imaging agents, J. Med. Chem. **40** (1997) 2539–2546.

[6.13] JOHANNSEN, B., et al., Technetium(V) and rhenium(V) complexes for 5-HT$_{2A}$ serotonin receptor binding: Structure–affinity considerations, Nucl. Med. Biol. **23** (1996) 429–438.

[6.14] PIETZSCH, H.-J., et al., Synthesis and autoradiographic evaluation of a novel high-affinity Tc-99m ligand for the 5-HT$_{2A}$ receptor, Nucl. Med. Biol. **26** (1999) 865–875.

[6.15] MEEGALLA, S.K., et al., First example of a ^{99m}Tc complex as transporter imaging agent, J. Am. Chem. Soc. **117** (1995) 11037–11038.

[6.16] MEEGALLA, S.K., et al., Tc-99m-labelled tropanes as dopamine transporter imaging agents, Bioconjug. Chem. **7** (1996) 421–429.

[6.17] CHATT, J., ROWE, G.A., Complex compounds of tertiary arsine with rhenium (V), rhenium (III), J. Chem. Soc. (1962) 4019–4033.

[6.18] JOHANNSEN, B., SPIES, H., Chemie und Radiopharmakologie von Technetium-Komplexen, Akademie der Wissenschaften der DDR, Dresden (1981) 213 pp.

[6.19] LOWRY, O.H., ROSEBOUGH, N.J., FARR, A.L., RANDALL, R.J., Protein measurement with Folin phenol reagent, J. Biol. Chem. **193** (1951) 265–275.

[6.20] SHELDRIC, G.M., SHELXS-86: Structure Solving Program, University of Göttingen (1986).

[6.21] SHELDRIC, G.M., SHELXL-93: Crystal Structure Refinement, University of Göttingen (1993).

[6.22] PAPADOPOULOS, M.S., et al., Syn–anti isomerism in a mixed-ligand oxorhenium complex, ReO[SN(R)S][S], Inorg. Chem. **35** (1996) 7377–7383.

[6.23] PELECANOU, M., CHRYSSOU, K., STASSINOPOULOU, C.I., Trends in NMR chemical shifts and ligand mobility of TcO(V) and ReO(V) complexes with aminothiols, J. Inorg. Biochem. **79** (2000) 347–351.

[6.24] ADDISON, A.W., et al., Synthesis, structure and spectroscopic properties of copper(II) compounds containing nitrogen–sulfur donor ligands: The crystal and molecular structure of aqua[1, 7-bis(N-methylbenzimidazol-2-yl)-2′, 6-dithiahep-tane] copper(II) perchlorate, J. Chem. Soc., Dalton Trans. (1984) 1349–1356.

[6.25] BOUZIOTIS, P., et al. Novel oxorhenium and oxotechnetium complexes from an aminothiol[NS]/thiol[S] mixed-ligand system, Chem. J. Eur. **7** (2001) 3671–3680.

[6.26] ALBERTO, R., et al., A novel organometallic aqua-complex of technetium for the labelling of biomolecules: Synthesis of $[^{99m}Tc(OH_2)_3(CO)_3]^+$ from $[^{99m}TcO_4]^-$ in aqueous solution and its reaction with a bifunctional ligand, J. Am. Chem. Soc. **120** (1998) 7987–7988.

Chapter 7

RADIOCHEMICAL AND BIOLOGICAL EVALUATION OF A NEW BRAIN SEROTONIN$_{1A}$ RECEPTOR IMAGING AGENT

K. BODÓ, G.A. JÁNOKI, L. BALOGH, D. MÁTHÉ, R. KIRÁLY,
G. ANDÓCS, L. KÖRÖSI
Frédéric Joliot-Curie National Research Institute for
    Radiobiology and Radiohygiene,
Budapest, Hungary

Abstract

Radiochemical and biological evaluations are made of a new bidentate radio-ligand as a potential brain serotonin$_{1A}$ (5-HT$_{1A}$) receptor imaging agent. The bidentate part of the complex was a derivative of the well known serotonin$_{1A}$ receptor antagonist molecule, namely WAY 100635; the monodentate parts were thiocresol, thiosalicylic acid and thio-2-naphthol. The labelling procedure was performed through the ^{99m}Tc(V)-glucoheptonate precursor. The bidentate + monodentate complex formed during the reaction in the case of thiocresol was identified as ^{99}TcO(o-CH$_3$-C$_6$H$_4$-N(CH$_2$-CH$_2$)$_2$N-CH$_2$CH$_2$S)(p-C$_6$H$_4$CH$_3$)$_2$ (^{99m}Tc-1). Its labelling efficiency and stability were determined by thin layer chromatography, the organic solvent extraction method and high performance liquid chromagraphy. The biodistribution of the labelled compound was found by using male Wistar rats. On the basis of these data, kinetic curves were constructed for different organs and the dosimetry for humans was calculated. The brain uptake and pharmacokinetics were followed by planar and single photon emission computed tomography (SPECT) imaging in rats. Average brain count density was calculated and different regional count densities (counts/gram tissue) were obtained for the hippocampus and other receptor-rich regions. A detailed SPECT study was carried out after administration of ^{99m}Tc-1 to a cynomolgus monkey (*Macaca cynomolgus*). The results found show that, of three investigated aromatic thiol compounds, the labelling efficiency was the highest in the case of thiocresol as the monodentate part. Therefore all further studies were carried out using thiocresol. The labelling efficiency of this bidentate complex was about 80%, and the molecule was stable for up to one hour. The biodistribution data show that more than 0.1% of the injected dose is present in the rat brains a few minutes after administration, and the metabolic pathway is through the hepatobiliary system. From the results obtained with the study of the distribution among various parts of the brain, the conclusion was drawn that the highest activity could be found in the hippocampus and hypothalamus, which contain a high concentration of 5-HT$_{1A}$ receptors. The same results were obtained from SPECT studies of monkeys.

7.1. INTRODUCTION

It is well known that non-invasive radioligand imaging studies for brain receptors are useful in human neuropsychopharmacology and in the development of novel drugs for use in the therapy of neurological and psychiatric disorders.

It is also well known that serotonin is a major brain neurotransmitter with a multitude of physiological functions through its interactions with seven major families of receptors (5-HT_1–5-HT_7) and their various subtypes [7.1]. Among all of these receptors, the G protein coupled 5-HT_{1A} receptor is structurally, pharmacologically and functionally the best characterized. It was the first of all the 5-HT receptors to be cloned and sequenced [7.2–7.4], and a specific polyclonal antibody was developed for it [7.3, 7.5].

The development of a large series of selective ligands is also connected to the present extensive knowledge of 5-HT_{1A} receptors. Among these molecules, which are pharmacologically agonist or antagonist, a selective 5-HT_{1A} receptor antagonist molecule, namely WAY 100635 [7.6, 7.7], proved to have very good binding characteristics. Some derivatives of it were developed for ^{99m}Tc labelling based on the 3 + 1 complex concept to obtain a neutral, lipophylic, small sized oxotechnetium complex [7.8–7.10].

In our earlier work we studied the radiochemical and biological properties of a tridentate + monodentate complex received through the IAEA from M. Papadopoulos of the Democritos National Centre for Scientific Research, Athens. In the present study we present the radiochemical and biological results obtained with the new bidentate + monodentate complex, namely ^{99m}Tc-1, which also came from M. Papadopoulos.

7.2. MATERIALS AND METHODS

7.2.1. Preparation of ^{99m}Tc-1

The chemical 1-(2-methoxyphenyl)-(4-mercaptoethyl)-piperazine was obtained from M. Papadopoulos.

Bidentate ligand (L_1H_2), derivative of WAY 100635:

1-(2-methoxyphenyl)-(4-mercaptoethyl)-piperazine with molecular weight 256 daltons has the form shown in Fig. 7.1.

The following aromatic thiol compounds are used as monodentate ligands:
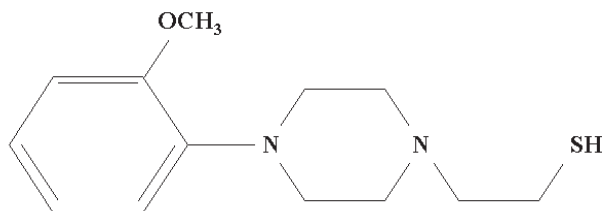
FIG. 7.1. *The form of the bidentate ligand L_1H_2.*

(1)   *p*-thiocresol (^{99m}Tc-1),
(2)   Thiosalicylic acid (^{99m}Tc-2),
(3)   Thio-2-naphthol (^{99m}Tc-3).

Labelling of compounds at the tracer level was carried out as follows: The glucoheptonate kit containing 200 mg calcium glucoheptonate and 3 mg tin chloride was dissolved in 10 mL water. To 1 mL in an aliquot was added 0.5–1.0 mL of ^{99m}Tc-pertechnetate solution (up to 15 GBq). The ^{99m}Tc(V)O-glucoheptonate solution was added to the vial containing an equimolar amount (0.02 mmol) of bidentate ligand (WAY 100635 derivative) and monodentate ligands.

The mixture was agitated in a vortex mixer and left to react at room temperature for 10 min. The labelled complexes were extracted three times with dichloromethane, the organic layer was evaporated under N_2 gas and the remaining layer was dissolved in 96% alcohol.

The chemical structure of the labelled bidentate ligand using the WAY 100635 derivative compound and thiocresol is shown in Fig. 7.2.

7.2.2.   Radiochemical investigation of ^{99m}Tc-1

7.2.2.1. *Determination of radiochemical labelling efficiency of bidentate complexes by thin layer chromatography*

The labelling efficiency was determined by instant thin layer chromatography (ITLC). The derivative of WAY 100635 and three aromatic thiols were labelled with ^{99m}Tc through glucoheptonate. The aromatic thiol parts of the bidentate complex used in experiments were thiocresol, thiosalicylic acid (Koch Laboratory, Pasadena, California) and thio-2-naphthol (Ferak, Berlin). During this procedure, various running systems were used as follows:
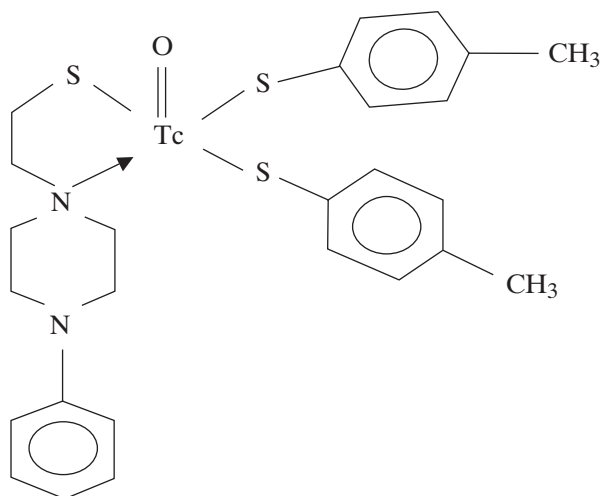
FIG. 7.2. Chemical structure of the labelled bidentate ligand using WAY 100635 and thiocresol.

(1) Physiological saline
Retention fraction R_f value of ^{99m}Tc-1 = 0–0.1,
R_f value of ^{99m}TcO$_4^-$ = 0.9–1;
(2) Chloroform:methanol:NH$_4$OH = 9:1:0.002
R_f value of ^{99m}Tc-1 = 0.8–1,
R_f value of ^{99m}TcO$_4^-$ = 0.2–0.4;
(3) Methanol:0.1N HCl = 9:1
R_f value of ^{99m}Tc-1 = 0.6–0.9,
R_f value of ^{99m}TcO$_4^-$ = 0.2–0.4;
(4) Ethanol:dichloromethane:acetonitril = 1:1:1
R_f value of ^{99m}Tc-1 = 0.9–1,
R_f value of ^{99m}TcO$_4^-$ = 0.9–1;
(5) Butanol:methanol:NH$_4$OH = 1:1:0.002
R_f value of ^{99m}Tc-1 = 0.6–1,
R_f value of ^{99m}TcO$_4^-$ = 0.9–1.

The R_f values of various aromatic thiols and WAY 100635 derivative bidentate complexes were the same in different running systems (Figs 7.3 and 7.4).
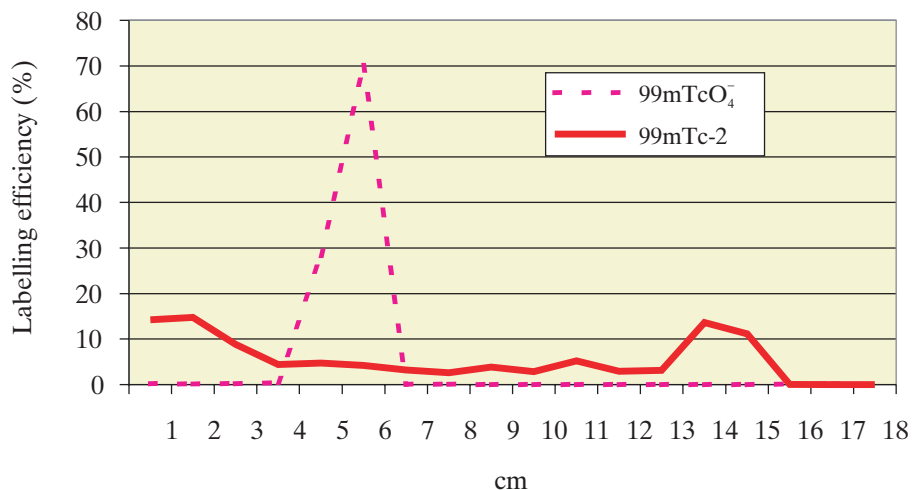
FIG. 7.3.   Radiochromatogram of ^{99m}Tc-2 using ITLC-SG in chloroform:methanol: NH$_4$OH (9:1:0.002) at room temperature (22°C). The aromatic thiol part was thiosalycilic acid.
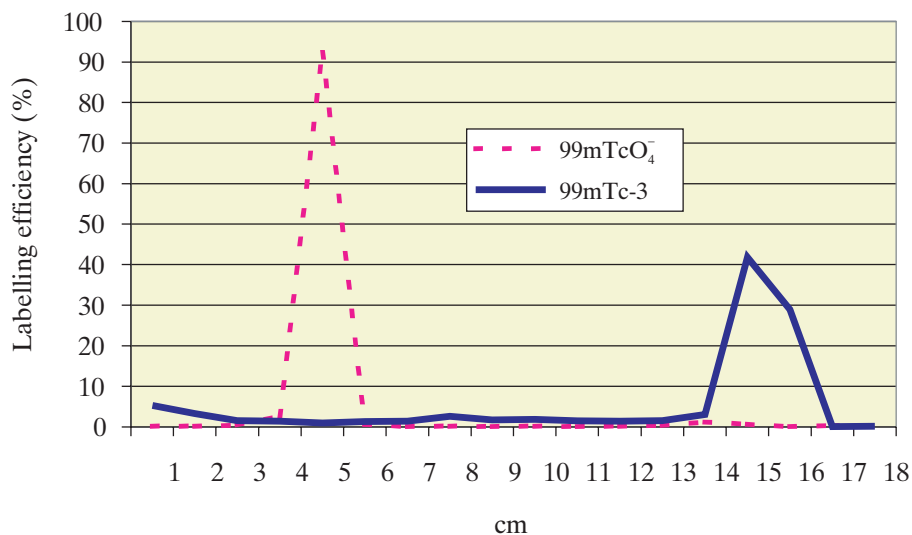
FIG. 7.4.   Radiochromatogram of ^{99m}Tc-3 using ITLC-SG in chloroform:methanol:NH$_4$OH (9:1:0.002) at room temperature (22°C). The aromatic thiol part was thio-2-naphthol.

7.2.2.2. *Determination of radiochemical stability using thin layer chromatography and the solvent extraction method*

The stability of the labelled compound was followed by radiochromatography and the solvent extraction method up to 24 h at room temperature (22°C) and in a refrigerator (4°C). Owing to the lipophilicity of the ^{99m}Tc-1 the radiochemical stability was determined by the solvent extraction method. The organic phase was chloroform, and the anorganic phase was 0.9% physiological saline in the same volume (Figs 7.5–7.8, Tables 7.1 and 7.2).

TABLE 7.1. DETERMINATION OF STABILITY OF ^{99m}Tc-1 BY RADIO-CHROMATOGRAPHY USING ITLC-SG DEVELOPED IN 0.9% PHYSIOLOGICAL SALINE AND CHLOROFORM:METHANOL:NH$_4$OH (9:1:0.002)
(stability values in per cent)

Elution time	22°C		4°C	
	Saline	Chloroform: methanol:NH$_4$OH	Saline	Chloroform: methanol:NH$_4$OH
0 min	83.87	88.7	89.76	87.5
30 min	86.56	81.79	88.69	85.84
1 h	85.44	76.69	86.31	74.85
4 h	81.61	54.55	83.92	71.98
24 h	56.92	16.75	76.62	63.19

TABLE 7.2. DETERMINATION OF STABILITY OF ^{99m}Tc-1 USING THE SOLVENT EXTRACTION METHOD
(stability values in per cent)

Elution time	22°C	4°C
0 min	94.3	—
30 min	86.5	86.8
1 h	87.0	86.12
4 h	82.4	83.5
24 h	80.2	84

Note: Chloroform:physiological saline = 1:1.
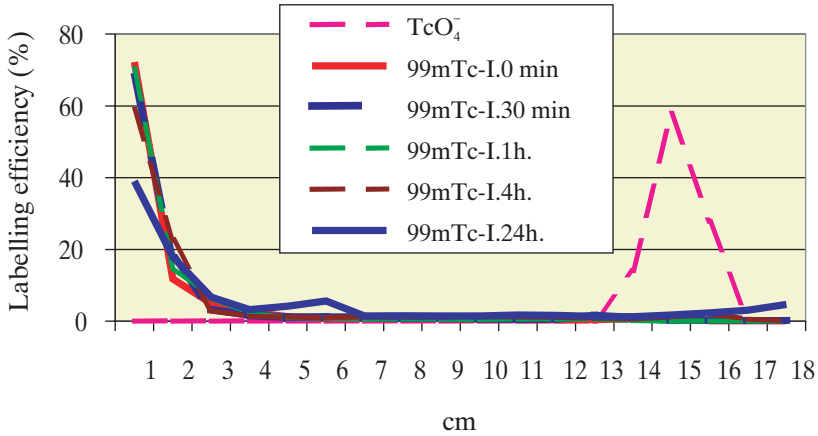
FIG. 7.5. Stability study of ^{99m}Tc-1 using ITLC-SG in saline at room temperature (22^oC).
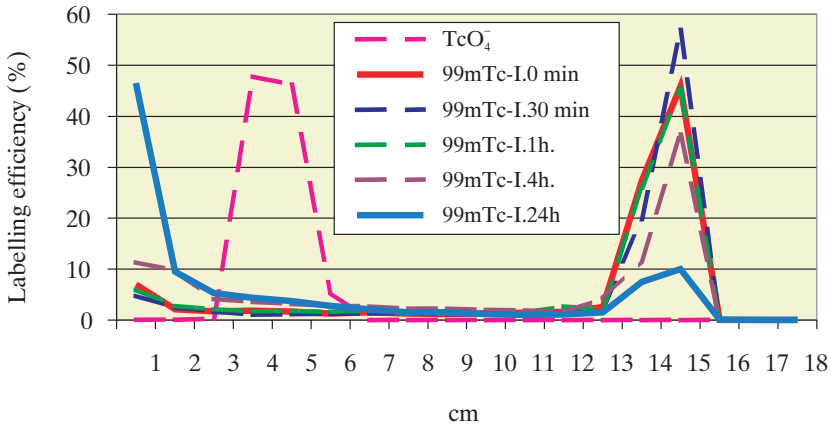
FIG. 7.6. Stability study of ^{99m}Tc-1 using ITLC-SG in chloroform:methanol:NH_4OH (9:1:0.002) at room temperature (22^oC).

7.2.2.3. Analysis of ^{99m}Tc-1 using high performance liquid chromatography

An analysis of ^{99m}Tc-1 in 96% ethanol and also diluted with physiological saline was made by the high performance liquid chromatography (HPLC) method using a BIO_RAD 800 HPLC system (computer controlled pump, UV–vis variable detector and integrator) based on a suggestion of M. Papadopoulos. A CHROMPACK RP-C18, 250 m × 4.6 mm, column was used and the solvents were:
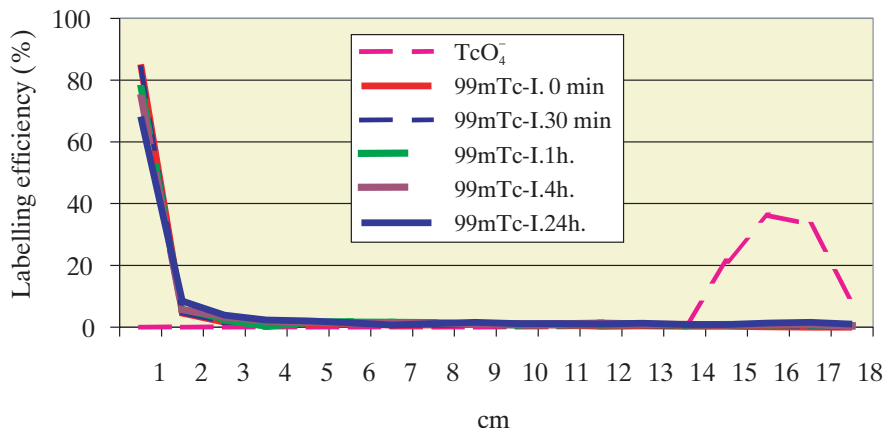
FIG. 7.7. Stability study of ^{99m}Tc-1 using ITLC-SG in saline in a refrigerator (4ºC).
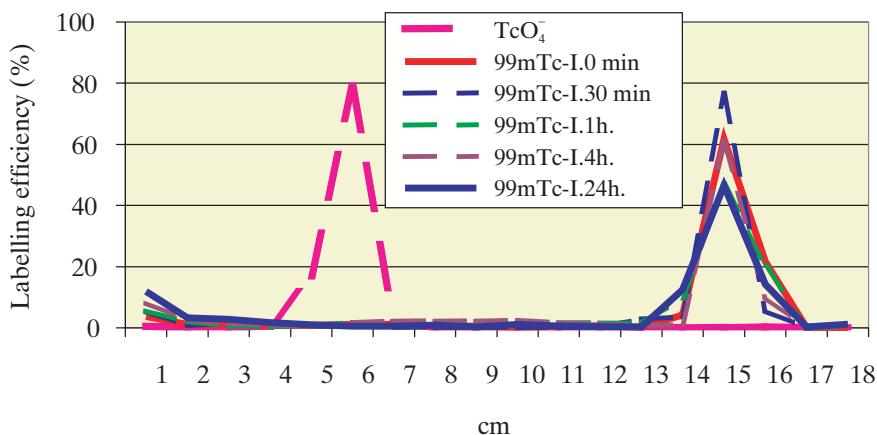
FIG. 7.8. Stability study of ^{99m}Tc-1 using ITLC-SG in chloroform:methanol:NH$_4$OH (9:1:0.002) in a refrigerator (4ºC).

A = methanol,
B = H$_2$O + 0.1% TFA.

The elution profile was as follows:

0–5 min, 50% A–50% B;
5–10 min, 80% A–20% B (linear);

10–30 min,   80% A–20% B;
30–35 min,   100% A–0% B;
35–45 min,   50% A–50% B.

The flow rate was 10 mL/min. The absorbance was monitored at 254 nm. An ISCO 568-9001 fraction collector was used to collect 0.4 mL per 0.5 min fractions and the activity of samples was measured by an automatic gamma counter (Figs 7.9–7.14). Here, AUSF stands for absorbance unit full scale.

7.2.3. Biological investigation of ^{99m}Tc-1

7.2.3.1. Biodistribution study of ^{99m}Tc-1 in rats after intravenous injection

Male Wistar rats (150–200 g) received 15–20 MBq of high specific activity radiotracer (≥40 GBq/mM) in 0.5 mL 96% ethanol diluted with saline (the ethanol concentration of the injected solution was not more than 20%) via a tail vein vasodilated under an infrared lamp. The rats were decapitated at various points of time after treatment, the various organs were quickly removed and the radioactivity was measured by an automatic sample sorter.

Experiments were conducted on groups of three rats per time point with results expressed (mean ± SD) as the percentage injected dose per whole organ
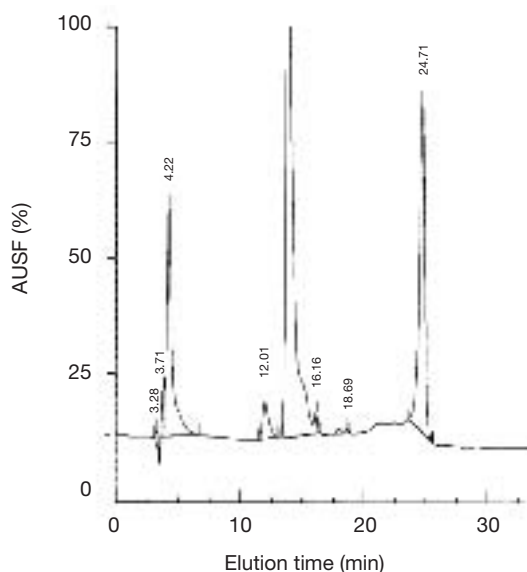
FIG. 7.9. Representative HPLC profile of ^{99m}Tc-1 in ethanol 10 min after labelling. (Details about the HPLC method are given in the text.)
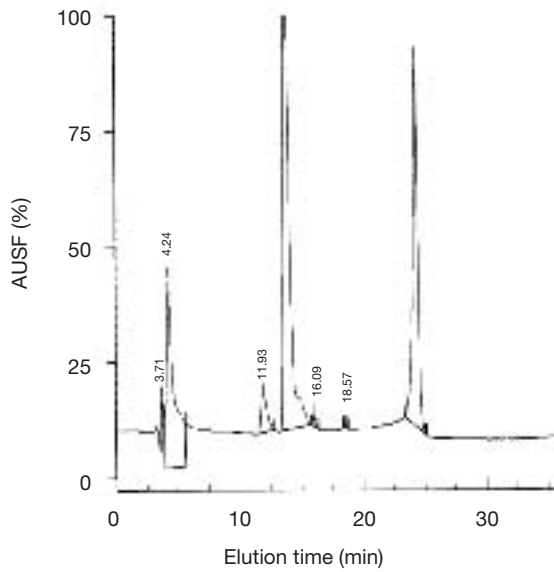
FIG. 7.10. Representative HPLC profile of ^{99m}Tc-1 in ethanol 1 h after labelling.
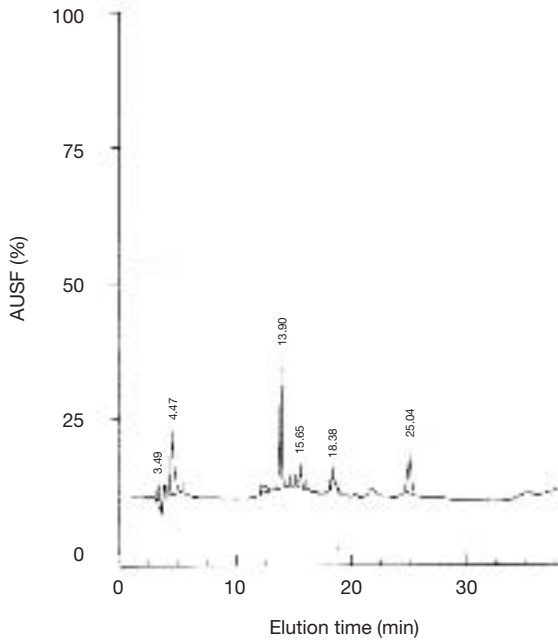
FIG. 7.11. Representative HPLC profile of ^{99m}Tc-1 in physiological saline 10 min after labelling.
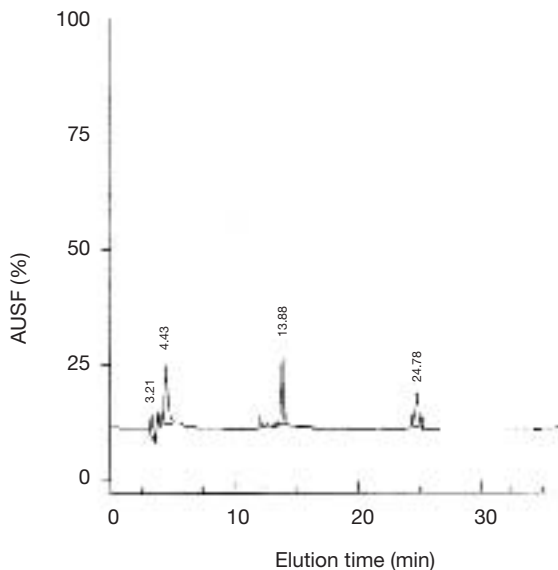
FIG. 7.12. Representative HPLC profile of ^{99m}Tc-1 in physiological saline 1 h after labelling.
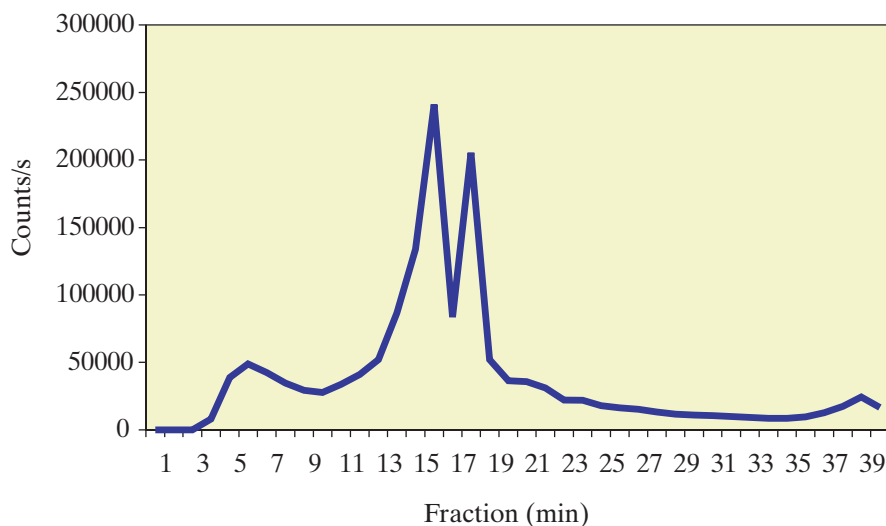
FIG. 7.13. Radioactivity curve after HPLC separation of ^{99m}Tc-1 in physiological saline 10 min after labelling. (Details about the method are given in the text.)
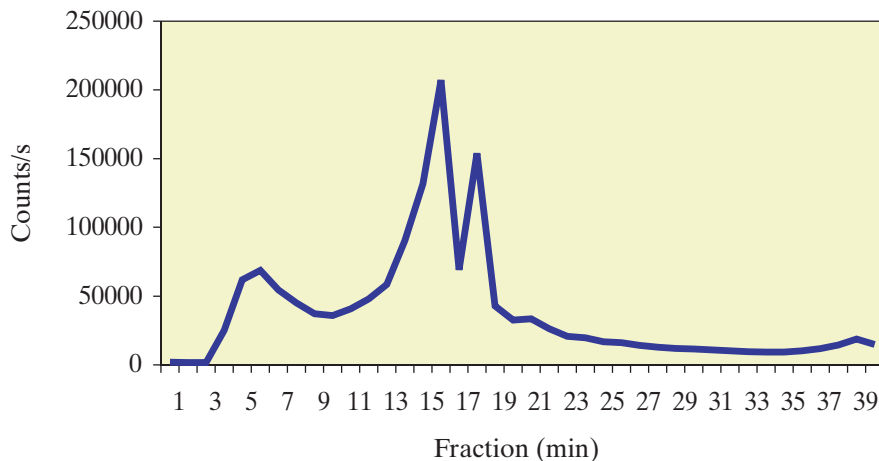
FIG. 7.14. Radioactivity curve after HPLC separation of ⁹⁹ᵐTc-1 in physiological saline 1 h after labelling.

(ID %/whole organ) and as the percentage injected dose per gram of wet tissue (ID %/g) (Tables 7.3 and 7.4).

7.2.3.2. Kinetic studies

From the biodistribution data at various points of time after treatment of ⁹⁹ᵐTc-1, kinetic curves were constructed for different organs using the Microcal Origin 5.0 software. The kinetics of the labelled compound were followed by a scintigraphy investigation of rats and a SPECT study of cynomolgus monkeys.

7.2.3.3. Extrapolation to humans and dose calculation

Data for kinetic studies are generally derived from those for animal studies. In an animal study, the radiopharmaceutical is administered to a number of animals which are then sacrificed at different times, and the organs are harvested and counted for activity. The extrapolation of animal data to humans is not an exact science. We used the %kg/g method for extrapolation. In this method, the animal organ data need to be reported as a percentage of the injected activity per gram of tissue, and the whole body weight of the animal must be known (Fig. 7.15, Table 7.5). The extrapolation to humans then uses the human organ and total body (TB) weight, as follows:

$$[(\%/g \text{ organ})_{animal}(kg \text{ TB weight})_{animal}](g \text{ organ}/kg \text{ TB weight})_{human} = (\%/\text{organ})_{human}.$$

TABLE 7.3.   BIODISTRIBUTION OF ^{99m}Tc-1 IN RATS AFTER INTRA-VENOUS INJECTION

(results are presented as a percentage of injected dose/whole organ and the mean of three rats per point of time)

Region	Time after intravenous injection						
	5 min	15 min	30 min	60 min	2 h	4 h	24 h
Muscle	11.82	7.59	10.64	9.8	7.55	6.71	4.46
Bone and bone marrow	5.92	4.16	5.68	7.01	3.48	2.79	1.75
Heart	0.76	0.4	0.41	0.35	0.31	0.22	0.09
Thyroid	0.09	0.07	0.08	0.06	0.05	0.04	0.02
Lungs	2.13	2.46	2.3	1.75	1.5	0.89	0.41
Liver	31.59	34.93	35.85	36.06	33.95	30.57	22.3
Spleen	0.89	1.05	1.87	1.83	1.52	1.36	1.06
Kidneys	3.25	2.8	4.15	4.17	4.16	4.07	3.85
Stomach	0.6	0.96	1.94	1.61	0.56	0.33	2.56
Small intestine	10.13	20.55	26.39	31.14	32.31	8.58	4.64
Large intestine	0.73	0.7	0.9	0.83	1.13	29.08	25.34
Blood	28.68	20.17	15.01	11.2	8.15	6.74	3.37
Brain	0.14	0.11	0.09	0.07	0.08	0.05	0.04

7.2.3.4.   Scintigraphic investigations of Wistar rats after treatment with ^{99m}Tc-1

Scintigraphic investigations were carried out using a MEDISO Nucline X-ring digital whole body gamma camera after treatment of rats with 100 MBq/0.1 mL ^{99m}Tc-1 at various times (Figs 7.16(a)–(d), 7.17(a) and (b)).

A dynamic scintigraphy was performed in the first part of the rat study. The dynamic scintigraphy consisted of two sections: the first short perfusion part, and the longer post-perfusion part. A MEDISO Nucline X-Ring digital gamma camera was used for imaging with a LEHR collimator. The detector gantry was rotated down and the experimental animal was placed in the collimator directly. The rats were anaesthetized with Nembutal. Data acquisition started sometime after injection.

TABLE 7.4.   BIODISTRIBUTION DATA OF ^{99m}Tc-1 FOR HUMANS
EXTRAPOLATED FROM DATA FOR ANIMALS
(results are presented as a percentage of injected dose/whole organ)

Region	Time after intravenous injection						
	5 min	15 min	30 min	60 min	2 h	4 h	24 h
Muscle	10.64	7.72	9.02	9.50	7.16	6.17	3.98
Bone and bone marrow	5.21	4.19	4.8	6.17	3.19	2.37	1.50
Heart	1.78	1.08	1.07	0.89	0.74	0.59	0.28
Thyroid	0.036	0.041	0.02	0.02	0.017	0.013	0.009
Lungs	5.45	5.92	5.53	4.83	3.92	2.39	0.88
Liver	27.55	30.91	30.93	32.78	31.0	27.0	27.32
Spleen	0.88	0.97	1.85	1.8	1.82	1.50	1.26
Kidneys	1.59	1.36	1.98	2.03	2.16	2.02	2.20
Stomach	0.40	0.55	1.43	1.08	0.42	0.21	1.68
Small intestine	5.83	13.10	17.64	21.28	23.78	6.39	3.96
Large intestine	0.29	0.24	0.31	0.34	0.41	11.75	10.67
Blood	36.87	28.35	19.05	15.09	10.78	8.79	4.53
Brain	0.31	0.23	0.19	0.16	0.16	0.12	0.08

The set-up of the camera was as follows:

I. Perfusion part:
   Number of frames: 120
   Time/frame: 2 s
   Detector mask: 18 cm
   Resolution: 128 × 128 × 16;

II. Post-perfusion part:
   Number of frames: 60
   Time/frame: 60 s
   Detector mask: 18 cm
   Resolution: 128 × 128 × 16.

Static images were taken of the animals 5 min, 15 min, 30 min, 1 h and 4 h after the intravenous injection.

Set-up of the camera:
    Detector mask: 18 cm
    Time: 180 s
    Resolution: $256 \times 256 \times 16$.

(a)

(b)
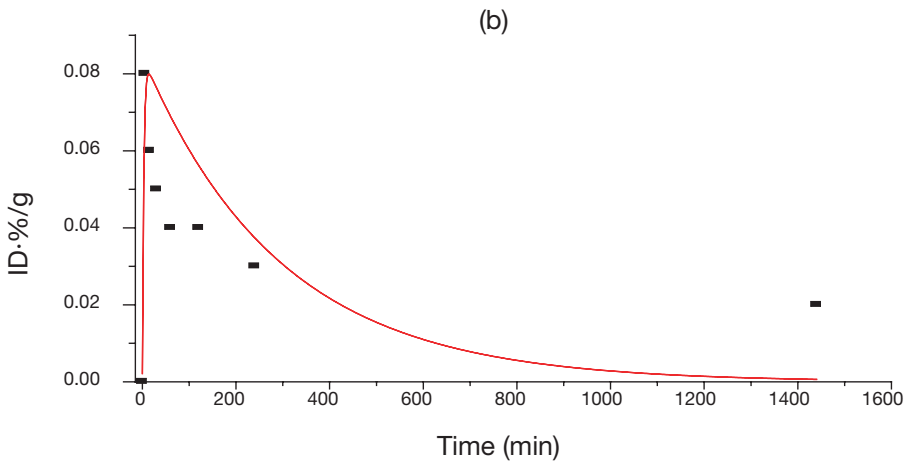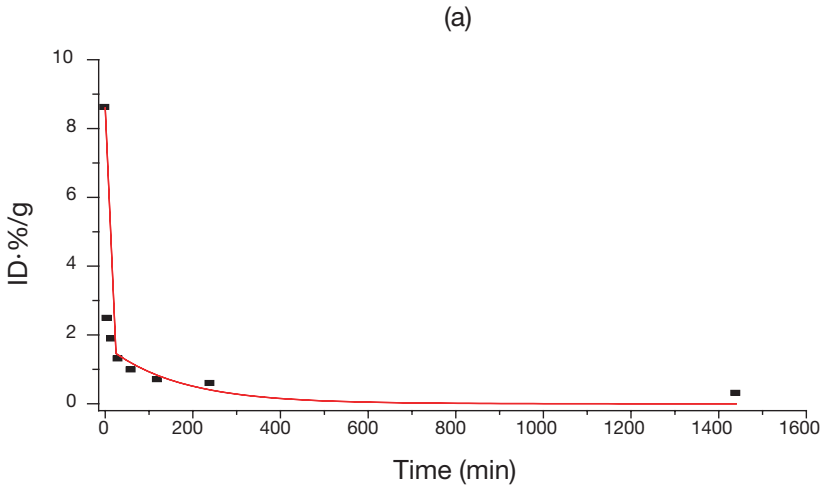
FIG. 7.15. Kinetic curves based on biodistribution study data for (a) brain and (b) blood in rats. In (a) $r^2 = 0.995$ and the curve is given by $y(t) = 6.9exp(-ln\ 2/1.65t) + 1.69exp(-ln\ 2/115.5t)$.

TABLE 7.5. DOSIMETRY OF ^{99m}Tc-1 COMPARED WITH ^{99m}Tc-HM-PAO

Target organ	^{99m}Tc-1 (mGy/MBq)	^{99m}Tc-HM-PAO (mGy/MBq)
Adrenal glands	1.46E–2	5.12E–3
Brain	1.17E–3	7.51E–3
Breasts	3.53E–3	1.04E–3
Gall bladder wall	2.81E–2	2.10E–2
LLI wall	4.44E–2	2.18E–2
Small intestine	4.15E–2	2.11E–2
Stomach	1.63E–2	4.90E–3
ULI wall	6.49E–2	2.60E–2
Heart wall	1.15E–2	2.64E–3
Kidneys	3.57E–2	3.77E–2
Liver	6.91E–2	1.75E–2
Lungs	1.26E–2	1.08E–2
Muscle	5.50E–3	1.84E–3
Ovaries	1.71E–2	1.33E–2
Pancreas	1.58E–2	4.90E–3
Red marrow	6.97E–3	2.63E–3
Bone surfaces	1.16E–2	3.13E–3
Skin	2.77E–3	7.10E–4
Spleen	3.47E–2	3.03E–3
Testes	2.62E–3	1.81E–3
Thymus	4.11E–3	1.10E–3
Thyroid	3.52E–3	5.11E–4
Urinary bladder wall	6.36E–3	1.06E–2
Uterus	1.23E–2	5.93E–3
Total body	8.27E–3	3.01E–3
Effective dose equivalent (mSv/MBq)	2.30E–2	1.29E–2
Effective dose (mSv/MBq)	1.96E–2	1.08E–2

7.2.3.5. Brain biodistribution experiments

Five adult male Wistar rats weighing between 250 and 300 g (mean 280 g, standard deviation 9.8 g) were used in the experimental procedure. 0.5 mL of
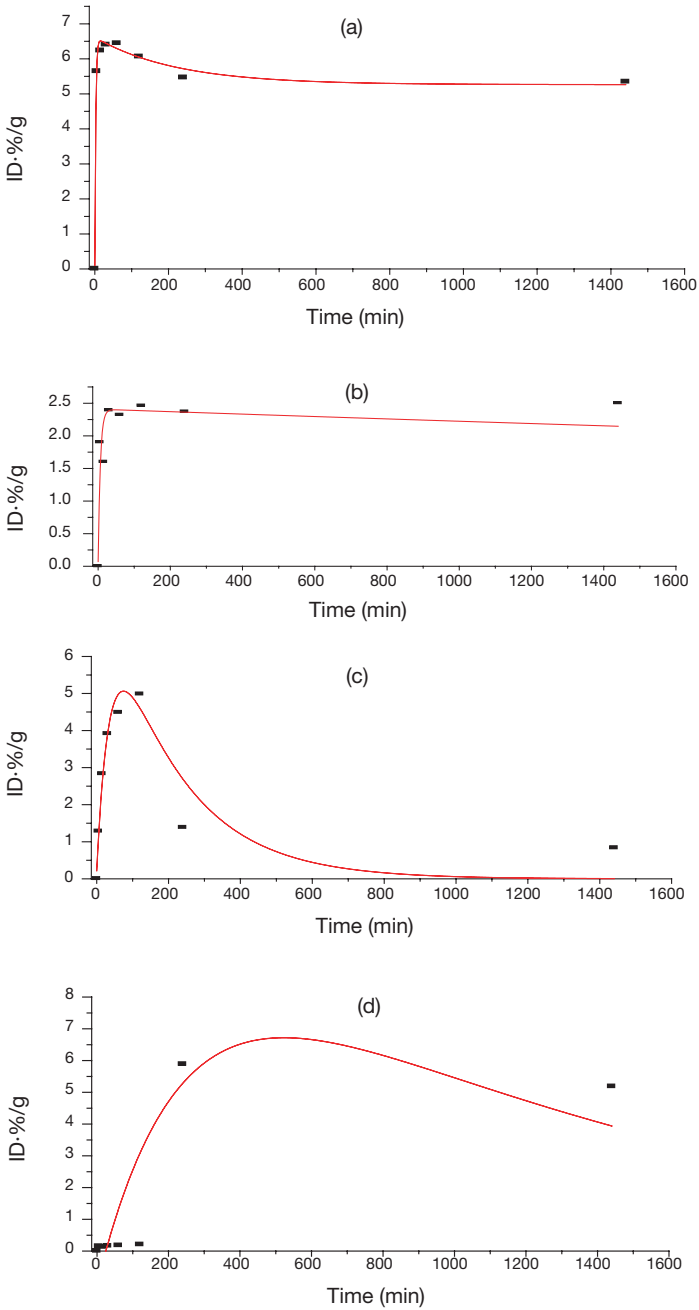
FIG. 7.16. Kinetic curves of the ^{99m}Tc-1 compound in important organs in rats: (a) liver, (b) kidneys, (c) small intestine, (d) large intestine.
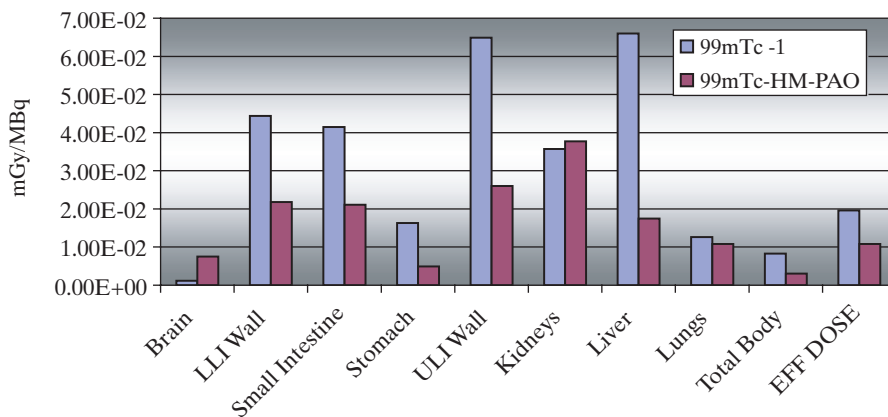
FIG. 7.17. Dose comparison between ^{99m}Tc-1 and ^{99m}Tc-HM-PAO.

labelled ^{99m}Tc-1 solution in 96% ethanol with an activity of 400 MBq was administered via the tail vein to each rat. A standard was set for the calculation of the activity retained in tissues.

After 15 min, the rats were euthanized with pentobarbital intraperitoneally, their chests opened and their circulation perfused by 50 mL of physiological saline. The brains were removed and placed in ice, washed with physiological saline, their weight measured on an analytical balance and their activity counted in a well counter (Gamma-NK 350). The brains were then dissected, and the following regions removed:

(a)   The pons as a whole, containing the dorsal and the medial rhaphe nuclei, where a dense network of cells expressing 5-HT$_{1A}$ autoreceptors is present;
(b)   Hippocampal formations, together with mixed samples from both of the parietal and temporal cortices as receptor-rich regions;
(c)   The hypothalami, known to contain many subtypes of 5-HT receptors, also rich in the 5-HT$_1$ and 5-HT$_3$ types;
(d)   The cerebellum;
(e)   The basal ganglia, the latter two serving as controls, being free from 5-HT$_{1A}$ receptors.

However, the cerebellum, as recently observed by others, also contains a high binding, which might be due to tissue heterogeneity. That is the reason why basal ganglia, also known to be free of 5-HT$_{1A}$ receptors, were chosen as the control.

7.2.3.6. Whole body scintigraphy and SPECT investigation with ^{99m}Tc-1 in cynomolgus monkeys

Dynamic and SPECT studies were performed in the case of cynomolgus monkeys (*Macaca cynomolgus*) with 1000 MBq/1.5 mL ^{99m}Tc-1 (Figs 7.18 and 7.19). An 11 year old cynomolgus monkey was anaesthetized with 2 mg/kg Ketamin. The monkey was placed on the examining bed in the prone position. Data acquisition started at the time of injection.

7.2.3.7. Evaluation of SPECT pictures

An 11 year old male cynomolgus monkey was injected with 2.2 GBq of 1 mL ^{99m}Tc-1 product dissolved in 96% ethanol; the specific activity was 2.2 GBq/mM. The images were taken 15 min after injection with a Mediso X Ring
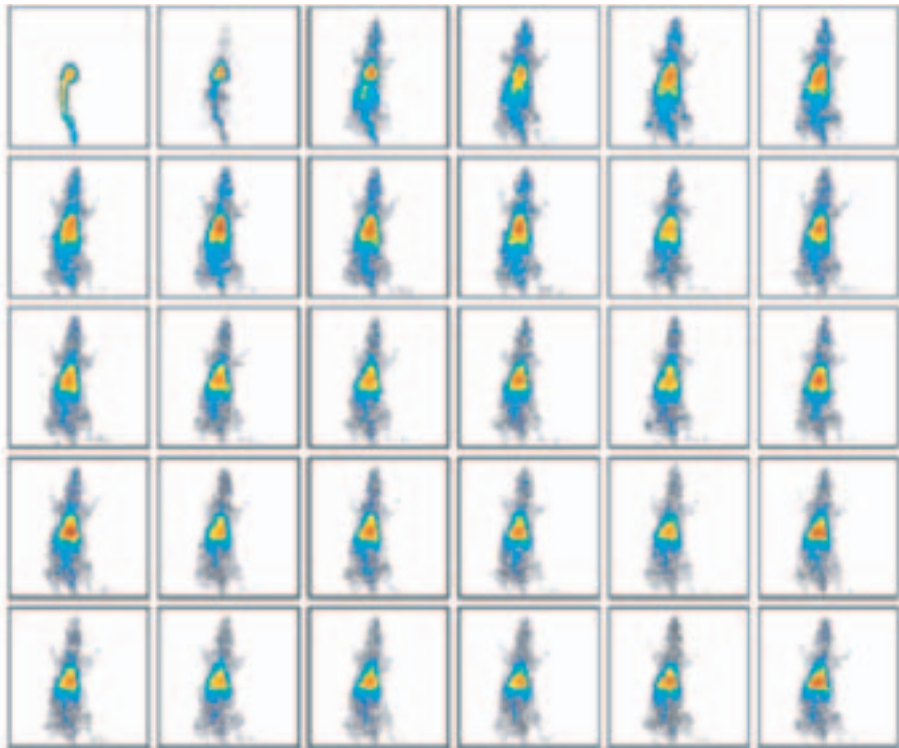
FIG. 7.18. Dynamic scintigraphy examination with ^{99m}Tc-1 in Wistar rats: perfusion phase.
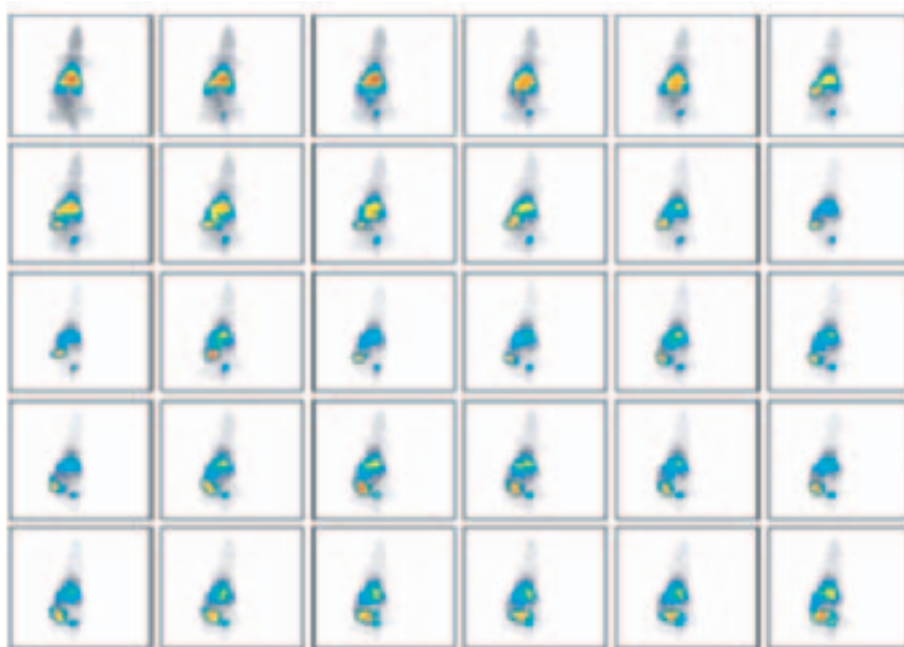
FIG. 7.19. Dynamic scintigraphy examination with ^{99m}Tc-1 in Wistar rats: post-perfusion.

single head rotating SPECT camera (Mediso, Hungary). The head-in-prone position was used, while a total of 64 frames were taken counter-clockwise.

The images were reconstructed using filtered backprojection with a Butterworth prefilter (cut-off 0.16 cycles/pixel, order 20). Plane sections in three directions were co-registered to help identification, and a magnetic resonance image (MRI) atlas of Japanese macaque heads and the University of Washington's Primate Center's Template Atlas of the Primate Brain were used to identify the regions where binding was found (Figs 7.20–7.22).

7.3. RESULTS AND DISCUSSION

7.3.1. Results of radiochemical investigation

The labelling efficiency and stability determined by thin layer chromatography using ITLC-SG and the solvent extraction method were higher than 80% at room temperature (22°C) or in a refrigerator (4°C) for up to 24 h (Figs 7.5 and 7.6, Tables 7.1 and 7.2).
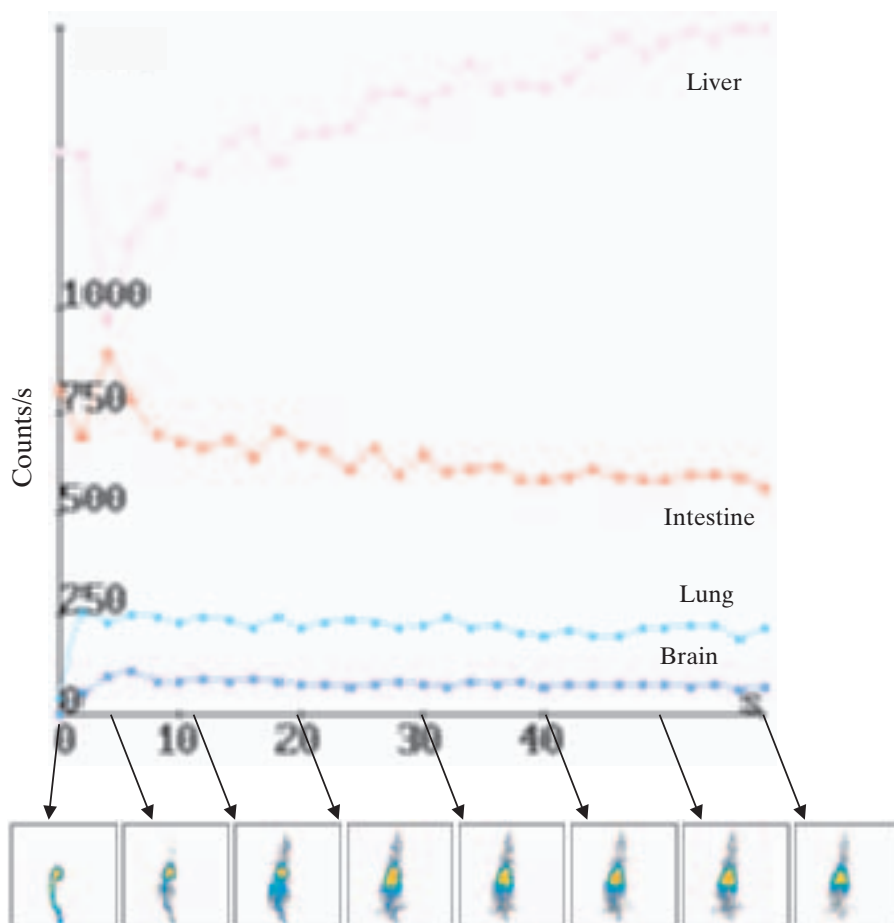
FIG. 7.20. Time–activity curve of ^{99m}Tc-1 in Wistar rats: perfusion phase.

On the basis of the results of radiochromatography studies, it was established that the labelling efficiency in the case of ^{99m}Tc-2 and ^{99m}Tc-3 was very low; therefore in further experiments we used only ^{99m}Tc-1.

On the basis of the solvent extraction method, the labelling efficiency was about 80% for up to 24 h, but the results of detailed radiochromatography show that the molecule is stable for only one hour.
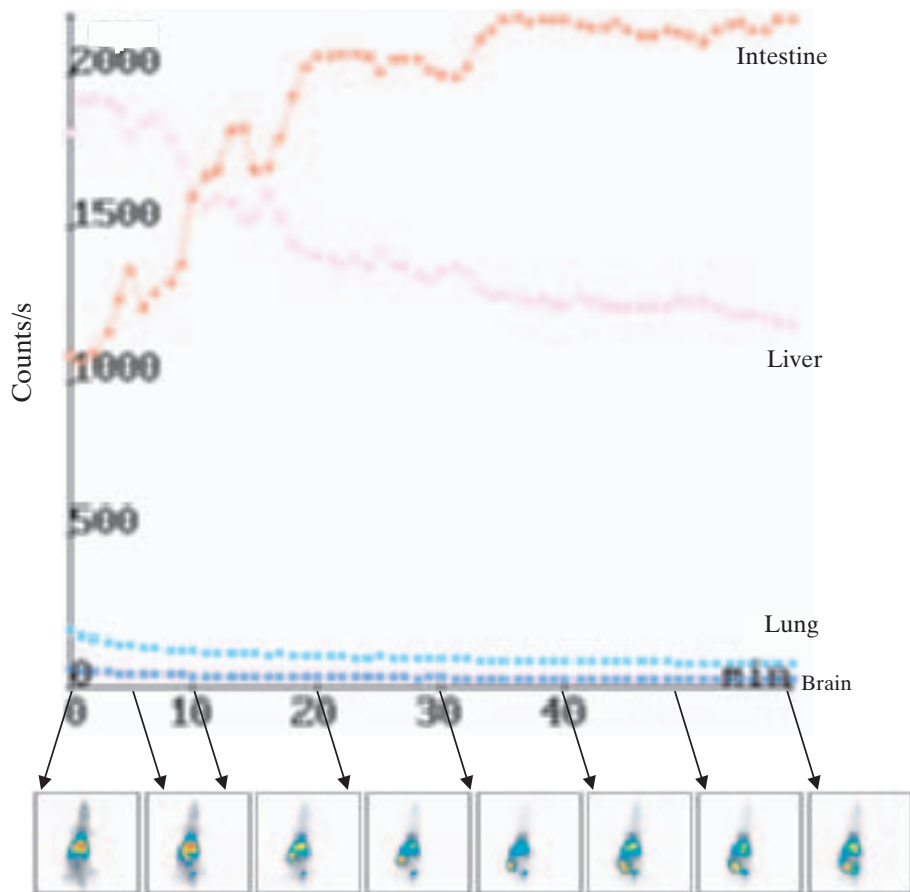
FIG. 7.21. Time–activity curve of ^{99m}Tc-1 in Wistar rats: post-perfusion phase.

There are two main peaks in the HPLC profile, one at 13 min and the other at 24 min. The radioactivity curves show good agreement with the HPLC profile.

7.3.2. Results of biological investigations

7.3.2.1. Biodistribution studies

The results of biodistribution studies of ^{99m}Tc-1, a specific 5-HT$_{1A}$ receptor imaging agent, are summarized in Tables 7.3 and 7.4.
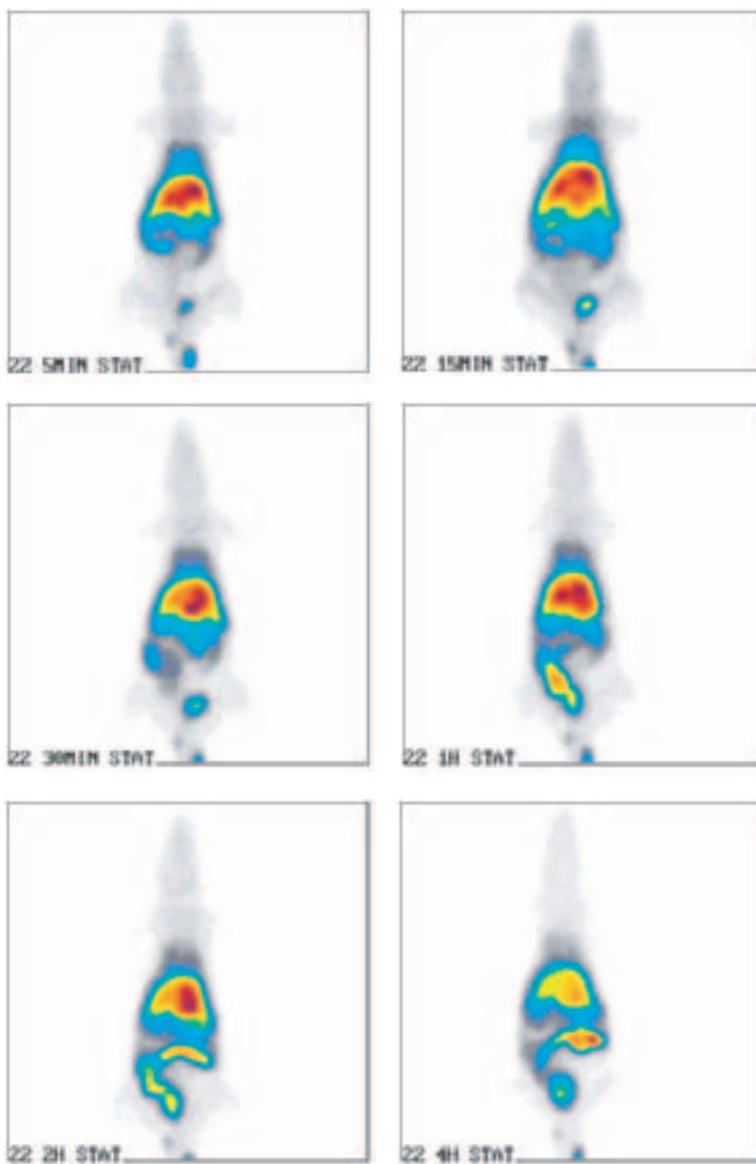
FIG. 7.22. Biodistribution of ^{99m}Tc-1 in Wistar rats as a function of time.

7.3.2.2. Kinetic studies

On the basis of data for biodistribution studies, kinetic curves were constructed for the most important organs.

The regression curve for rat brains has $r^2 = 0.998$ and the rat brain dose is $D_{brain} = 0.34$ µGy when the administrated activity was 18 MBq in 0.2 µL for a brain of weight 2.00 g.

The curves in Fig. 7.16 were constructed with the Microcal Origin 5.0 software.

7.3.2.3. Extrapolation to humans and dose calculation

Results are presented as a percentage of the injected dose/whole organ in humans. From Table 7.4 we calculate for each organ the residence time and the organ doses for adults with the method recommended by the Medical Internal Radiation Dose (MIRD) Committee and Mirdose3.1 software.

The MIRD assumptions are the following:

(a)   The internal organs are not spheres. They are more like ellipsoids, cylindroids, conical cylindroids and prolate cylindroids.
(b)   The uptake of organs is not instantaneous. It is more like an exponential function of time.
(c)   Organ retention times are variable. The concentration is homogeneous.
(d)   Removal from the organ can be represented by a single or composite exponential function of time.
(e)   The area under the curve represents the cumulative activity or residence time.

The MIRD equation is

$$D = A_0 \tau S$$

where A_0 is administered activity (MBq), τ is residence time (s) and S is absorbed dose per unit of cumulative activity (mGy·MBq^{-1}·s^{-1}).

With knowledge of the administered activity and from the bioassay data that have been extrapolated to humans we calculated the residence times. With the S values for adults, which can be taken from the Mirdose software, we calculated the doses shown in Fig. 7.17.

7.3.2.4. Scintigraphic investigation after intravenous injection of 100 MBq/0.1 mL of ^{99m}Tc-1 in Wistar rats

From the scintigraphs in Fig. 7.18 it can be seen that most of the activity is in the liver. (During perfusion, ^{99m}Tc-1 stays in the blood.)

Figure 7.19 shows that the metabolic pathway of ^{99m}Tc-1 goes through the hepatobiliary system. (In the post-perfusion phase, ^{99m}Tc-1 is distributed throughout the tissue of the various organs.)

In Fig. 7.20 a rapid uptake of ^{99m}Tc-1 by the brain and the liver, as well as the lungs, is apparent. In Fig. 7.21 the slow clearance of ^{99m}Tc-1 from the brain and its metabolic path from the liver through the bile and to the intestines is seen. Figure 7.23 shows a small activity uptake in centrobasal parts of the brain which can be localized in the hypothalamic or hippocampal regions. The highest activity uptake is shown by the salivary glands.

7.3.2.5. Brain biodistribution in rats

An average brain binding index was calculated by dividing the brain total counts by the total brain weight. This index, taken as the average brain binding index, was valued as 100%. Regional binding indices were calculated in the same way, thus dividing the counts of the different regions by their respective weights. A proportion between average brain binding index and specific regional binding index could be set. In our experiments, the hippocampus showed a 1.521-fold higher binding index than the average brain level, while
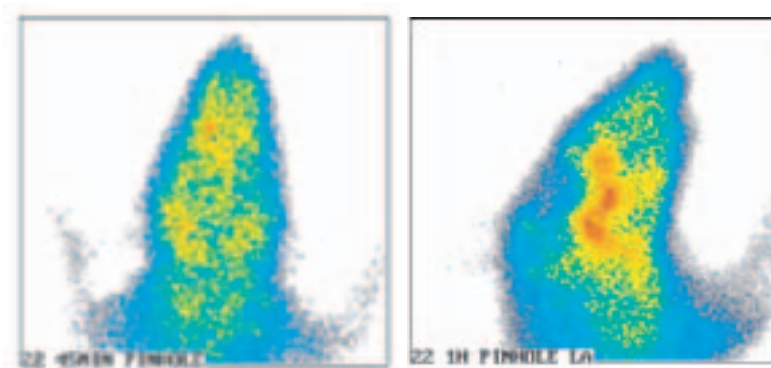
FIG. 7.23. Biodistribution of ^{99m}Tc-1 in Wistar rats as a function of time (pinhole pictures).

the control basal ganglia showed a lower average binding index than the average brain level (Fig. 7.24).

It seems that the 5-HT receptor-rich regions have a significantly higher binding index than the control basal ganglia. High non-specific cerebellar binding is present.

7.3.2.6. Whole body scintigraphy and SPECT investigation after intravenous injection of 1000 MBq/1.5 mL with ^{99m}Tc-1 in cynomolgus monkeys

In the series of scintographs shown in Fig. 7.25, a rapid uptake can be seen by the liver and the olfactory laminae, also at the olfactory bulbs. A small signal appears in the brain. Olfactorious uptake is due to the dense anastomoses of the ethmoidal veins at the olfactory laminae creating a 'hole' in the blood–brain barrier.

Figure 7.26 shows the rapid elimination of ^{99m}Tc-1 with circulation, after which it remained at a stable level in the brain.

The sensitivity of imaging in Fig. 7.27 was enhanced by zoom optics and a pinhole collimator. In the pinhole pictures (Fig. 7.27(c)) a slight regional uptake is present in the brain.

7.3.2.7. Evaluation of SPECT pictures

The regions shown in Figs 7.28–7.31 were found to bind the ligand.
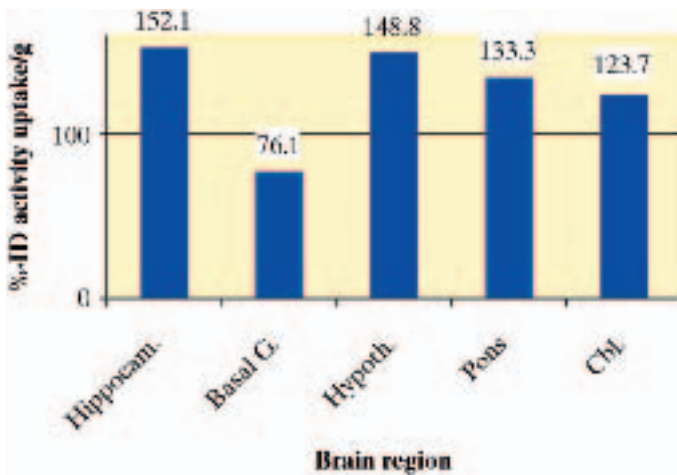
FIG. 7.24. *Mean activity uptake in relation to total mean activity uptake in brain tissue (100%).*

FIG. 7.25. *Dynamic scintigraphy examination with* ^{99m}*Tc-1 in cynomolgus monkeys (Macaca cynomolgus): perfusion phase.*

The hippocampus, amygdala and pons show ligand binding, but as a result of poor penetration to the brain the signal-to-noise ratio is very low. In images 43–53 (Fig. 7.32) hippocampal binding is apparent and, because of the oblique sectioning plane, becomes unilateral. The olfactory bulbs show the highest uptake due to the poor penetration of the ligand at the brain–blood barrier. As the veins of the olfactory bulbs anastomose directly to the ethmoidal vein, penetration is possible to the brain, leaving out the barrier.

7.4.   CONCLUSIONS

In conclusion, WAY 100635 is useful in the development of new ^{99m}Tc radioligands for the imaging of 5-HT$_{1A}$ receptors. Further effort is needed to obtain a much more lypophilic and stable complex, and a specific binding capacity to 5-HT$_{1A}$ brain receptors is required to enhance brain uptake.
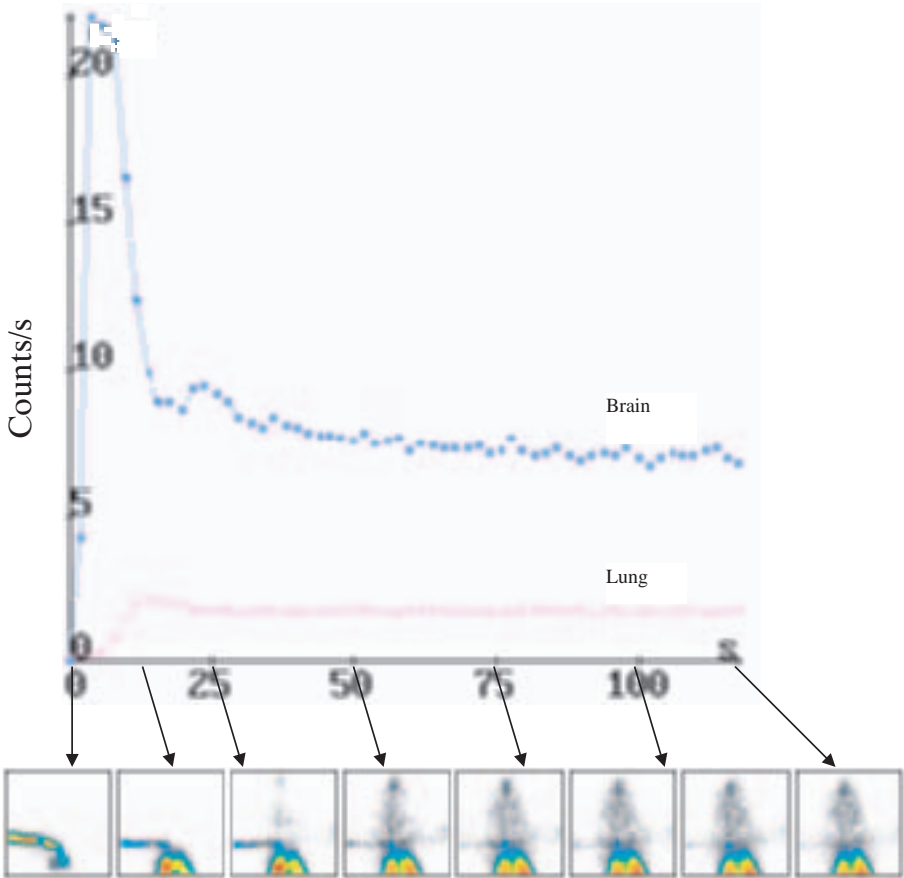
FIG. 7.26. Time–activity curve of ^{99m}Tc-1 in cynomolgus monkeys (Macaca cynomolgus): perfusion phase.

(a)

(b)

(c)
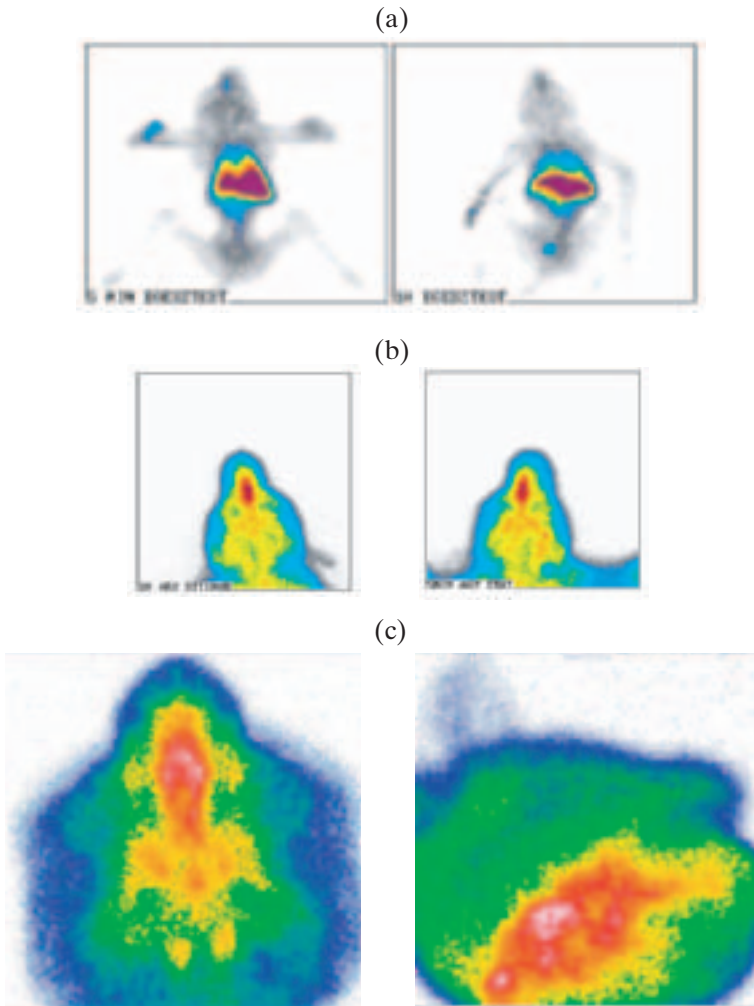
FIG. 7.27. Static scintigraphs with ^{99m}Tc-1 of a cynomolgus monkey (Macaca cynomolgus): (a) whole body, (b) brain (zoom), (c) pinhole pictures.
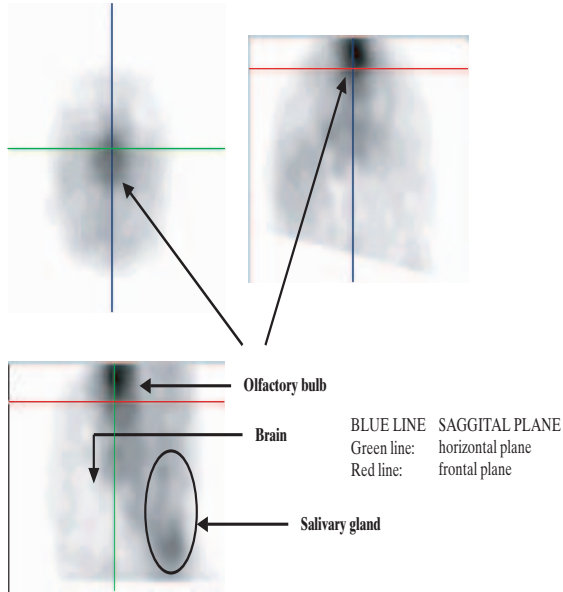
FIG. 7.28. Three plane SPECT images of the olfactory bulb region of a monkey: left upper image, frontal section; right upper image, horizontal section; left lower image, sagittal section.
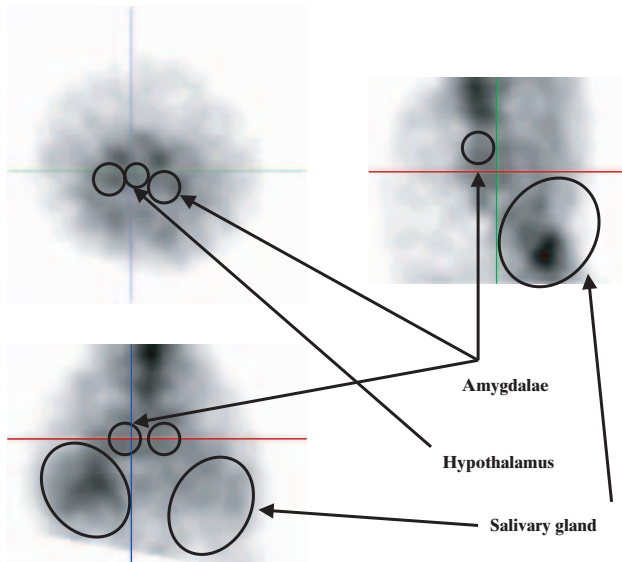
FIG. 7.29. Three plane SPECT images of the amygdalae and hypothalamus region of a monkey: left upper image, frontal section; right upper image, horizontal section; left lower image, sagittal section.
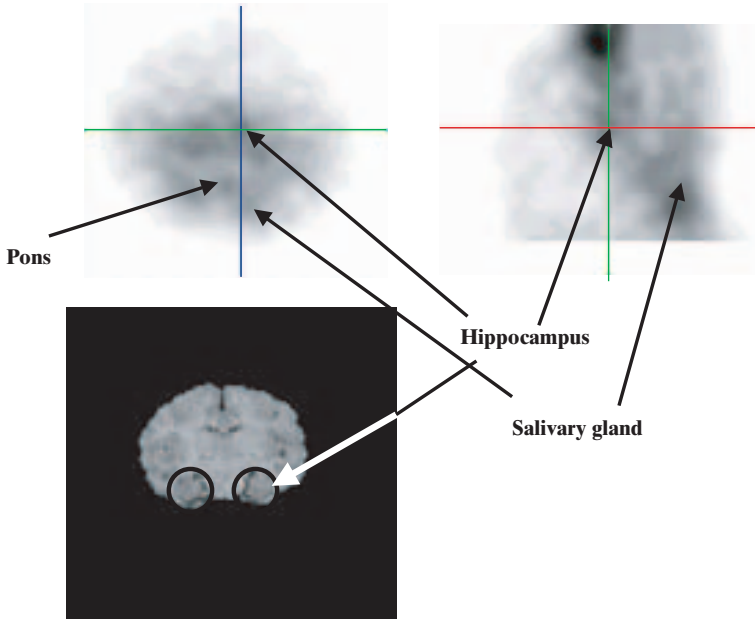
FIG. 7.30. SPECT images of the head of a monkey: left upper image, frontal section; right upper image, sagittal section; left lower image, MRI image of the macaque head at the level of the hippocampus, frontal section. The arrows indicate binding in the hippocampus and the pons (the section plane of the SPECT also contains the pons).

Brain stem and pons

Hippocampal formation
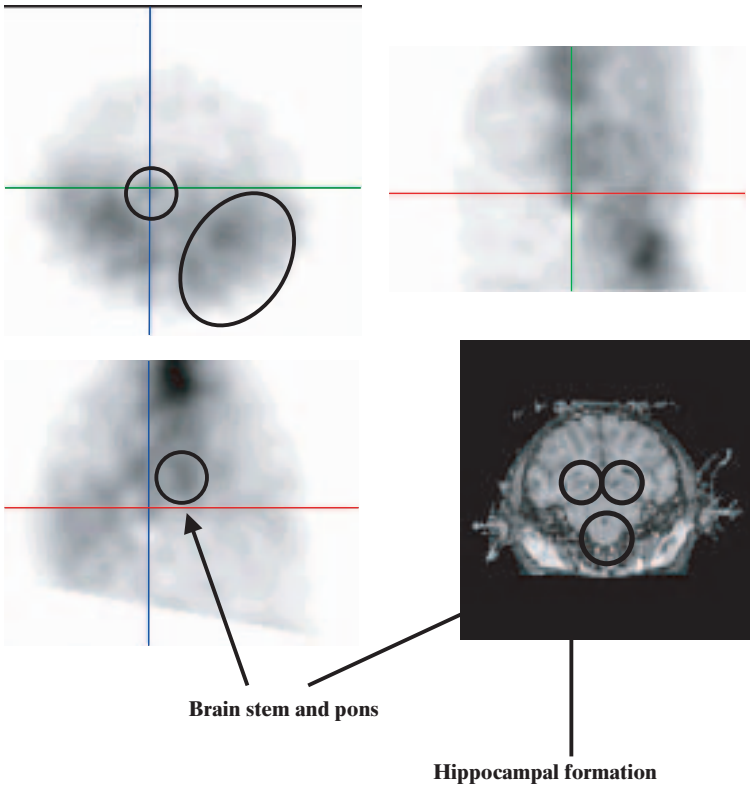
FIG. 7.31. Three plane SPECT images of the hippocampus and piriform cortex region of a monkey: left upper image, frontal section; right upper image, horizontal section; left lower image, sagittal section of the head; right lower image, MRI image of the macaque brain at the level of the hippocampal formation and pons.

FIG. 7.32. Overview of SPECT pictures.

ACKNOWLEDGEMENTS

REFERENCES TO CHAPTER 7

[7.1] BAUMGARTEN, H.G., GÖTHERT, M., "Serotoninergic neurons and 5-HT receptors in the CNS", Handbook of Experimental Pharmacology, Springer-Verlag, Berlin (1997).

[7.2] KOBILKO, B., Adrenergic receptors as models for G protein-coupled receptors, Ann. Rev. Neurosci. **15** (1992) 87.

[7.3] FARGIN, A., et al., The genomic clone G-21 which resembles a β-adrenergic receptor sequence encodes the 5-HT$_{1A}$ receptor, Nature **335** (1988) 388.

[7.4] ALBERT, P.R., CHAN, Q.Y., VAN TOL, H.H., BUNZON, J.R., CIVELLI, O., Cloning, functional expression and mRNA tissue distribution of the rat 5-HT$_{1A}$ receptor gene, J. Biol. Chem. **265** (1990) 5825.

[7.5] El MESTIKAWY, S., et al., Production of specific anti-rat 5-HT$_{1A}$ receptor antibodies in rabbits injected with a synthetic peptide, Neurosci. Lett. **118** (1990) 183.

[7.6] FLETCHER A., et al., WAY 100635: A novel selective antagonist at presympatic and postsympatic 5-HT$_{1A}$ receptors, Eur. J. Pharmacol. **237** (1993) 283.

[7.7] GURLING, J., ASHWORTH-PREECE, M.A., DOURISH, C.T., ROUTLEDGE, C., Effects of acute and chronic treatment with the selective 5-HT$_{1A}$ receptor antagonist WAY 100635 on hippocampus 5-HT release in vivo, Br. J. Pharmacol. **112** (Proc. Suppl.) (1994) 299.

[7.8] PAPADOPOULOS, M.S., et al., A new donor atom system [(SNN)(S)] for the synthesis of neutral oxotechnetium(V) mixed-ligand, Complexes Inorg. Chem. **35** 15 (1996) 4478–4483.

[7.9] PAPADOPOULOS, M.S., et al., Syn–anti isomerism in a mixed-ligand oxorhenium complex ReO[SN(R)S][S], Inorg. Chem. **35** 25 (1996) 7377–7383.

[7.10] PIRMETTIS, I.C., et al., Synthesis and characterization of oxotechnetium(V) mixed-ligand complexes containing a tridentate N-substituted bis(2-mercaptoethyl)amine and a monodentate thiol, Inorg. Chem. **35** 5 (1996) 1685–1691.

Chapter 8

STUDIES ON THE DEVELOPMENT OF 99mTc LABELLED SEROTONIN RECEPTOR AVID MOLECULES

N. SIVAPRASAD, R. GEETHA, A.S. GHODKE, S.S. SACHDAV,
P. KUMAR, N.M. PARKAR, C. AURJUN, G. SHANMUGAM,
D.V. RANGANATHA
Board of Radiation and Isotope Technology,
Department of Atomic Energy,
Navi Mumbai, India

Abstract

Among the central nervous system (CNS) receptors, serotonin is reported to be very important with respect to the study of brain disorders. Hence this work focuses on serotonin. A summary of the studies that were carried out is given. These include: (a) standardization of the method of serotonin receptor preparation from rat brains and development of a radioreceptor assay using radio-iodinated serotonin, (b) standardization of the method of radio-iodination of serotonin using a tyrosylmethyl ester derivative of serotonin and the preparation of ^{14}C labelled serotonin, (c) synthesis of the SNS tridentate ligand (following the procedure developed by the Democritos National Centre of Scientific Research (NCSR), Athens) and evaluation of a ^{99m}Tc complex formed with the tridentate SNS ligand and thiocresol for use as a CNS receptor imaging agent and (d) evaluation of the ^{99m}Tc complex formed with a SNS piperazine based tridentate ligand and a monodentate co-ligand (thiophenol obtained from NCSR). This limited study on brain uptake of the complex in rats showed that more structural modification of the ligand is required for preparation of a complex suitable for CNS receptor imaging. Also included is a design for synthesis of a novel complex based on the reported information on the 5-iodo-2-[(2-dimethyl)aminomethylphynoxy]benzyl alcohol compound, which is reported to have a binding affinity for serotonin re-uptake sites.

8.1. INTRODUCTION

The 5-HT (serotonin) receptors play an important role as the mediator of the peripheral and central effects of the neuro-hormonal substance serotonin (5-HT). The distribution and the density of these receptors have direct links with some central nervous system (CNS) disorders such as anxiety, depression

and Alzheimer's disease. Scintigraphy is expected to provide valuable diagnostic information about these CNS receptors. Although a few positron emission tomography (PET) radiopharmaceuticals are available for imaging these receptors, they are too expensive for small nuclear medicine centres in developing countries. On the other hand, ^{99m}Tc is the first choice in nuclear medicine due to its ready availability, its ideal nuclear characteristics and its cost effectiveness. Radioligands labelled with ^{99m}Tc will be, therefore, the ideal alternative to PET radiopharmaceuticals. Hence many investigators are now focusing their efforts towards the development of ^{99m}Tc based CNS receptor imaging agents, in spite of the various difficulties encountered with respect to structural integrity, binding affinity and permeability through the blood–brain barrier (BBB). The studies we carried out in our laboratory as participants of the Co-ordinated Research Project (CRP) are presented here. Participation in this CRP provided us with expertise in:

(a) Preparation of a serotonin receptor from rat brains and its characterization,
(b) Development of radio receptor assays,
(c) Synthesis and evaluation of the ligand aryl piperazine based on the procedures developed by Papadopoulos et al.

Apart from this, preliminary evaluation of ligands provided by M. Papadopoulos (Democritos National Centre of Scientific Research (NCSR), Athens) is also presented here. Work has also been initiated in the synthesis of 5-amino-2-[2-[(dimethylamino)methylphenyl]oxy]benzyl alcohol for labelling with ^{99m}Tc through a S_2N_2 complex as a possible agent for serotonin receptor imaging.

8.2. STANDARDIZATION OF A PROTOCOL FOR PREPARATION OF THE SEROTONIN RECEPTOR

The serotonin receptor is present in high density in the stem and hippocampus of the brain. The receptor was extracted from the brains of adult Wister rats. The protocol of the preparation is given in Appendix 8.1. The receptor preparations were diluted and the protein content was determined by Lowry's method. The preparations were then stored at –20°C. The protein concentrations of the receptor preparations were found to be in the range 7.4–9.8 mg/mL.

8.3. RECEPTOR ASSAY

Initially we characterized the receptor using an ^{125}I labelled serotonin prepared in-house, due to the non-availability of ^{3}H labelled serotonin analogues. An increasing quantity of receptors ranging from 5 to 18 mg (total protein concentration) was incubated for 3 h with radio-iodinated serotonin in a reaction volume of 500 μL. At the end of the incubation, the receptor–radioserotonin complex was separated using a glass fibre filter. The radio-activity trapped was assayed in a gamma scintillation counter set for [125]I. An average binding of about 11% was observed. An increase in binding was observed with an increase in quantity of the receptor. A displacement assay using 50 pmol of cold serotonin gave an inhibition of the order of 19–31%. The variation between assays was about 16–20%.

8.3.1. Preparation of labelled serotonin

Owing to high cost and to other strategic reasons, we could procure neither ^{3}H ketanserine (or any other serotonin analogue), which is known to be the ideal tracer for serotonin receptor assays, nor tritium for radiolabelling of serotonin (or its analogue). As our laboratory has the facility for protein radio-iodination we prepared radio-iodinated serotonin by conjugating thyrosyl-methylester (TME). The radio-iodination procedure is given in Appendix 8.2. Though initially direct radio-iodination was carried out on serotonin, the radio-iodinated serotonin was found to be unstable. Hence radio-iodination was attempted through TME conjugation. In addition, preparation of ^{14}C labelled serotonin was attempted. This involved three steps:

(1) 5-hydroxyinole was condensed with formaldehyde and dimethylamine in ethanol to obtain 5-hydroxygrammine. This reaction was almost quanti-tative. Purification was carried out on TLC (solvent system benzene: acetic acid:water in the ratio 4:1:5).

(2) 5-hydroxygrammine in ethanol was condensed with $K^{14}CN$ to obtain the product ^{14}C-5-hydroxyinole-acetoisonitrile. Ethanol was evaporated by the rotary method.

(3) 5-hydroxyinole-acetoisonitrile was reduced to serotonin by $LiAlH_4$ in dry ether prior to taking up labelling. An inactive compound was prepared and characterized by thin layer chromotography (TLC) (serotonin retention fraction R_f in TLC is 0.5) and spectrophotometry (absorption peaks at 278.7 and 303 nm).

The data were comparable with those of authentic serotonin.

8.4. SYNTHESIS AND EVALUATION OF SNS TRIDENTATE LIGAND

A synthesis of the SNS tridentate ligand, $(CH_2CH_2)NCH_2CH_2N$ $(CH_2CH_2SH)_2$ L^1H_2, has been carried out following the procedure developed by NCSR, Athens, with minor modification. The IR characteristics of the ligand were compared with those of the authentic ligand obtained from NCSR. A mixed ligand complex of ^{99m}Tc using L^1H_2 as tridentate ligand and SCH_2CH-piperazino-N-Ph-CH_3-o, L_2H, as the co-ligand obtained from NCRS was prepared by the transchelation method with in-house prepared glucohep-tonate. The co-ligand carries the 1-(2-methoxy)piperazine moiety, which forms part of the most promising antagonist compound, WAY 100635, and this moiety is responsible for the binding with the 5-HT receptor. Radiochemical studies of the complex were carried out using instant thin layer chromatography (ITLC) in saline and ethyl acetate. The same mixed ligand complex was prepared by the ligand obtained from NCSR and the radiochemical properties were studied.

8.4.1. Synthesis of SNS tridentate ligand

The ligand was prepared by reaction of N,N-diethylene diamine with ethylene sulphide in an autoclave at 110°C and purified by vacuum distillation following the NCSR procedure with minor modification. The fractional distillation under reduced pressure further yielded the SNS ligand $[(CH_2CH_2)NCH_2CH_2N(CH_2CH_2SH)_2]$ (distilled at 160°C/2 mm) as well as the NNS ligand $[(CH_2CH_2)NCH_2CH_2NHCH_2CH_2SH]$ (distilled at 125°C). The IR spectra of the synthesized and authentic compounds were comparable.

8.4.2. Preparation of a mixed ligand ^{99m}Tc complex

Two complexes were prepared, complex A (SNS tridentate ligand and thiocresol monodentate co-ligand complex) and complex B (SNS tridentate ligand and piperazine monodentate co-ligand).

A vial containing a lyophilized mixture of 0.5 mg $SnCl_2$ and 200 mg gluco-hetonate (prepared in-house) was reconstituted with 10 mL of water for injection. Of this solution, 1.0 mL was mixed with 0.5–1.0 mL of pertechnatate solution from a solvent extraction generator (made in-house). Two such vials were processed. The resultant ^{99m}Tc-glucoheptonate complex in the first vial was added to the complex containing equimolar quantities of SNS ligand (L^1H_2) and thiocresol for the preparation of complex A. The other complex was added to equimolar quantities of SNS ligand and piperazine co-ligand for the preparation of complex B. The mixtures were agitated in vortex mixtures

and the reactions were carried out for 10 min to enable exchange between the ^{99m}Tc-glucoheptonate complex and the ligands. Radiochemical studies of the complexes were then carried out.

The radiochemical studies were carried out by ITLC in saline. ITLC was also carried out for complex A in ethyl acetate and for complex B in a mixture of acetonitrile:benzene:dichloromethane (3:1:1). The percentage labelling and R_f were measured for aqueous media and a complex extracted with dichloromethane. The mixed ligand complex was extracted with dichloromethane (3 × 1.5 mL), dried over MgSO$_4$ and filtered using Whatman filter paper.

The R_f value for the complex in both physiological saline and in solvents was found to be 0.1. The labelling efficiency as measured by ITLC in saline for complex A was observed to be 88 and 78% before and after extraction, respectively. In the case of ITLC in ethyl acetate, the corresponding values of complex A were 93 and 68% respectively. The labelling measured by ITLC for complex B was greater than 97%, irrespective of the extraction and solvent used for ITLC. Table 8.1 gives the results of a comparative study of R_f in ITLC and percentage labelling as observed in different solvent systems for complex A. Table 8.2 gives the results of a similar study for complex B using the ascending paper chromatography technique. The complexes were observed to be stable for more than about 6 h.

TABLE 8.1. ITLC RESULTS FOR COMPLEX A

Solvent	First band		Second band	
	R_f	RCP[a] (%)	R_f	RCP[a] (%)
Chloroform	0.05	99.9		
Acetone	0.1	98.0		
Methanol	0.1	94.4	0.6–0.8	5.5
CCl$_4$	0.05	99.8		
Acetonitrile	0.1	98.2		
Methylethyl ketone	0.1	73.2	0.6–0.8	26.7
Saline	0.2	99.8	0.6–0.8	0.13
Benzene	0.05	99.9		
Ethyl acetate	0.1	92.0	0.6–0.8	7.9

[a] RCP, radiochemical purity.

TABLE 8.2. ITLC RESULTS FOR COMPLEX B

Solvent	First band		Second band	
	R_f	RCP (%)	R_f	RCP (%)
Chloroform	0.05	99.9		
Acetone	0.1	68.9	0.8	10.5
Methanol	0.1	82.5	0.6–0.8	17.5
CCl_4	0.05	99.5		
Acetonitrile	0.1	87.7	0.6–0.8	16.7
Methylethyl ketone	0.1	81.2	0.6–0.8	18.7
Saline	0.1–0.2	95.5	0.6–0.8	4.1
Benzene	0.05	99.9		
Ethyl acetate	0.1	96.6	0.6–0.8	3.3

8.4.3. Biological studies

The experiments were conducted in conformity with national regulations. The complexes were evaluated for their biological efficacy by biodistribution studies carried out in adult Wister rats. Rats were injected intravenously with 0.1 mL of the complex into their tail vains. The animals were decapitated at different times ranging from 15 min to 2 h post-injection. Their major organs were removed and assayed. The percentage dose per organ was calculated. The biodistribution in rats showed that brain uptake is about 0.17% after 15 min. The percentage decreased with time; Table 8.3 gives the data.

8.5. DESIGN OF A RADIOLIGAND FOR SEROTONIN RECEPTOR BINDING

Zhuang et al. [8.1] reported the synthesis of a novel iodine containing ligand 5-iodo-2-[2-[(dimethylamino)methylphenyl]oxybenzyl alcohol and termed this compound ODAM. Zhuang et al. further reported the preparation of ^{125}I labelled ODAM (^{125}I ODAM) and investigated the bindability of this with rat brain cortex membrane homogenate and its biodistribution in rats. This radioligand displayed a good binding affinity in in-vitro receptor binding displacement assays (reported value 1.49 at 30 min post-injection, intravenous). In the biodistribution studies of this radioligand in rats, it is reported to have

TABLE 8.3. STABILITY OF COMPLEXES C
AND D IN AQUEOUS MEDIA

Time of contact	RCP (%)	
	Complex C	Complex D
0 min	99.8	95.5
30 min	97.1	98.5
60 min	98.0	93.8
4 h	98.5	94.2
24 h	99.7	98.0

rapid brain uptake and washout. This compound was designed by this group based on the fact that antidepression drugs such as fluoxetine, sertaaline and paroxetin inhibit the primary binding sites for serotonin re-uptake. The imaging of these sites (serotonin re-uptake sites (SERT)) may thus provide useful information on depressive illnesses. The finding shows that this ligand displays desirable properties for developing it into an agent for imaging SERT sites. On the basis of the report of Zhuang et al. [8.1] on ODAM, it has been planned to synthesize 5-amino-2-[2-(dimethylamino)methylphenyl]oxybenzyl alcohol, which is the precursor of ODAM and couples an S_2N_2 complex of ^{99m}Tc to it at the amino group.

8.6. EVALUATION OF A PIPERAZINE BASED TRIDENTATE LIGAND

Another set of novel piperazine based tridentate ligands, o-MeOC$_6$H$_4$N(CH$_2$CH$_2$)N(CH$_2$)$_3$N(CH$_2$CH$_2$SH)$_2$ (L^{3}H$_2$), and monodentate ligands, o-MeC$_6$H$_4$N(CH$_2$CH$_2$)$_2$NCH$_2$CH$_2$SH (L^{4}H), developed and synthesized by M. Papadopoulos and his team at NCSR, was received, as well as thiophenol.

8.6.1. Preparation of the complex

The procedure followed is similar to that described in Section 8.4.2. Complex C was prepared from the tridentate ligand L^{3}H$_2$ and thiophenol, while complex D was prepared from the monodentate ligand L^{4}H and thiophenol.

8.6.2. Radiochemical studies

The mixed ligand complex was extracted with chloroform and its extract-ability studied. Both complexes could be extracted instantaneously to the extent of 98 to almost 100%. The extractability did not change even after a 24 h contact.

8.6.3. Radiochemical purity

The mixed ligand complex was subjected to ITLC in several solvents — physiological saline, ethyl acetate, chloroform, carbon tetrachloride, acetonitrile, acetone, methylethyl ketone, methanol and benzene. Both ligands produced two complexes, which were observed in ITLC in some of the solvent systems (Tables 8.1 and 8.2).

8.6.4. Stability studies

The stability of complexes C and D was studied. The complexes were found to be stable in aqueous media and serum (Tables 8.3 and 8.4). The complexes were kept in chloroform for different intervals of time and later extracted; the percentage radiochemical purity (RCP) was determined by ITLC in saline. The result shows that in organic solvents the complexes were stable and that more than 98% could be extracted, indicating that the complexes are lyphophilic (Table 8.5).

TABLE 8.4. STABILITY OF COMPLEXES C AND D IN HUMAN SERUM

Time of contact	RCP (%)	
	Complex C	Complex D
0 min	99.9	98.7
30 min	99.1	98.0
120 min	96.0	97.2
18 h	97.5	96.7

TABLE 8.5. EXTRACTABILITY WITH
CHLOROFORM

Time of contact before extraction	ITLC in saline, RCP (%)	
	Complex C	Complex D
0 min	99.8	99.7
30 min	98.1	99.2
60 min	98.5	98.5
4 h	98.4	99.0
24 h	97.8	99.7

8.6.5. Biological study

Rats were injected intravenously with 1 mL of complex D. The animals were sacrificed and a biodistribution study was carried out from 1 to 45 min. The brain uptake was not adequate (0.2%) and retention was not sufficient to use for receptor imaging (Table 8.6).

TABLE 8.6. BIODISTRIBUTION OF COMPLEX D AT
VARIOUS TIMES POST-INJECTION
(percentage uptake/organ)

Region	1 min	10 min	45 min
Brain	0.13	0.02	0.01
Blood	20.28	0.68	0.29
Blood[a]	2.07	0.58	0.17
Lungs	10.98	1.71	0.24
Stomach	0.87	0.394	0.25
Liver	70.28	29.18	14.52
Spleen	0.67	0.71	0.31
Kidneys	1.46	0.28	0.17
Small intestine	1.18	2.81	2.10
Large intestine	2.54	1.13	2.267

[a] Percentage uptake/g.

8.6.6.   Conclusion

The ligand studied provides efficient labelling, in vitro stability is good and stability in serum indicates in vivo structural integrity. However, inadequate brain uptake and insufficient retention were observed. The complex has good clearance through the digestive system.

Appendix 8.1

RECEPTOR PREPARATION

The receptor is prepared using the following procedure:

(1)   Carry out the work in a biohazard hood. Use a three month old rat.
(2)   Dissect out cortex and hippocampal regions of rat brain in ice.
(3)   Homogenize the tissue in 2 mL tris-sucrose buffer (pH7.6) for 5 min and cool on ice for 5 min.
(4)   Homogenize the tissue again and reconstitute to 200 mL with tris-sucrose buffer in an iced centrifuge tube.
(5)   Centrifuge at 1000g at 4ºC for 10 min.
(6)   Discard the pellet and centrifuge the supernatant at 33 000g at 4ºC for 25 min.
(7)   Discard the supernatant and vortex the pallet in tris buffer; incubate at 37ºC for 15 min.
(8)   Centrifuge at 33 000g at 4ºC for 25 min.
(9)   Reconstitute in paragylin buffer and use for receptor assay.

Appendix 8.2

RADIO-IODINATION OF SEROTONIN

Radio-iodination was carried out in two steps:

First step: Radio-iodination of TME

(1)   Take 0.3 µg of TME in 0.05M phosphate buffer, pH7.5.
(2)   Add 500 µCi Na ^{125}I and 0.3 µg of chloramines T.
(3)   Maintain the reaction volume at 40 µL.
(4)   Allow the reaction to proceed for about 1 min.

(5)   After 1 min, arrest the reaction by adding 100 µg of sodium metabisul-
      phate in 100 µL of phosphate buffer.
(6)   Purify the reaction mixture over Sephadex G25 and elute with 0.05M
      phosphate buffer, pH7.5 (for separation of free iodide).
(7)   Collect and pool the second peak of radioactivity containing the radio-
      iodinated TME.

Second step: Conjugation of radio-iodinated TME to serotonin

(1)   Dissolve 0.3 µg of serotonin in 0.05M phosphate buffer, pH7.5.
(2)   Add equimolar quantity of ^{125}I TME.
(3)   Add 0.6 µg of 1-(3-dimethylaminopropyl)carbodiimide HCl, followed by
      tributyl amine.
(4)   Allow the reaction to continue for 24 h under stirring.
(5)   Purify the reaction mixture over Sephadex G25 (1 cm × 15 cm column)
      and elute with phosphate buffer, pH7.5.
(6)   Identify the fraction by TLC on silica gel (solvent system:
      chloroform:ethanol, 3:1), R_f(^{125}I TME) = 0.9 and R_f(^{125}I TME-serotonin)
      = 0.05.

ACKNOWLEDGEMENTS

REFERENCE TO CHAPTER 8

[8.1]   ZHUANG, Z.-P., et al., Synthesis of ^{125}I ODAM as a serotonin transporter
        imaging agent, J. Labelled Compd. Radiopharm. **42** (1999) S357–S359.

Chapter 9

DESIGN OF A NEW SEROTONIN RECEPTOR 5-HT$_{1A}$ IMAGING AGENT BASED ON ^{99m}Tc

Sunju CHOI, Young Don HONG, Sang Mu CHOI,
Kyung Bae PARK
Hanaro Application Centre, Korea Atomic Energy Research Institute,
Taejon, Republic of Korea

Abstract

Serotonin is one of the neurotransmitters found in the brain and mediates brain functions. It is very well known that serotonin related brain abnormalities are exerted mainly via serotonin receptors in a similar manner to other neurotransmitters found in the brain. Recently, it has also been found that serotonin is involved in Alzheimer's disease either directly or indirectly by its actions on serotonergic neurons. To understand and treat the diseases caused by abnormalities in the serotonergic system in the brain, it is certain that its mechanism of function has to be well investigated. So far several 5-HT receptors and receptor subtypes have been well characterized. Moreover, serotonin agonists and antagonists acting on specific receptors are chemically synthesized and are now available for the prevention or treatment of serotonergic related diseases. In recent years, a great demand for developing neuroimaging agents has emerged for the diagnosis of abnormal brain functions in the area of nuclear medicine. Since arylpiperazine, WAY 100635, in the present investigation, has been recognized as a highly selective ligand for the 5-HT$_{1A}$ receptor, it has been used for the development of brain imaging agents based on serotonin receptors. First, S,S′-bis(trityl) monoamide monoamine (MAMA-Tr$_2$) was synthesized, followed by synthesis of an arylpiperazine ligand. The synthesis of the analogue of WAY 100635 was completed and it lead to successful labelling with ^{99m}Tc without a by-product. Deprotection of the S,S-Tr$_2$ group of MAMA-Tr$_2$ was efficiently conducted by incubation at 100°C for 1 h under acidic conditions (pH2–3), followed by labelling with ^{99m}Tc. Its radiochemical purity was checked by high performance liquid chromatography, and a labelled compound of >99% radiochemical purity was used for an in vivo bioavailability study using a gamma ray camera. An animal biodistribution study was also conducted to ascertain the serotonergic neuronal imaging effect of ^{99m}Tc labelled arylpiperazine derivative. It was concluded that derivatives of arylpiperazine labelled with ^{99m}Tc would be the most successful radioligands available for visualization and quantification of this important neuroreceptor in the human brain, especially as an imaging agent in the serotonergic receptor enriched area.

9.1. INTRODUCTION

In nuclear medicine, very small amounts of radioactive materials are introduced into the body for the diagnosis of diseases using imaging techniques. Owing to their attraction to specific organs, bones or tissues, they can be crucial for the provision of information about particular types of disease. Information gathered from the nuclear imaging technique is much more comprehensive than that from other techniques because it describes not only the structure but also the function of the organs. Most diseases can be diagnosed by using imaging techniques much earlier than by other techniques and before treatment is too late.

Recently, there has been great interest and effort made in the area of the central nervous system, due to increasing incidence of brain diseases. Neurotransmitters play important roles in brain functions. Among the neurotransmitters involved in brain functions, serotonin is the one that is mainly implicated in the aetiology and treatment of various disorders such as anxiety, depression, obsessive–compulsive disorder and schizophrenia. The serotonin (5-hydroxytryptamine, 5-HT) system is an important neurotransmission network which is involved in the modulation of various physiological functions and behaviour, such as thermoregulation, cardiovascular function, aggressive and sexual behaviour, mood, appetite, the sleep–wake cycle and even memory and learning [9.1–9.3]. Neurotransmitters produce their effects as a consequence of interactions with appropriate receptors. Therefore, a major factor in our understanding of the role of 5-HT in disorders related to the serotonergic system would be understanding the physiological roles in various serotonin receptors and their subtypes. It was also known that agonists, as well as antagonists, for a specific receptor type have to be well correlated with brain function. The highest densities of 5-HT_{1A} receptors are found in the limbic forebrain (hippocampus, entorhinal cortex and septum), whereas the lowest densities are observed in the extrapyramidal areas (basal ganglia and substantia nigra) and in the adult cerebellum [9.4, 9.5]. The localization of 5-HT_{1A} receptors in the limbic system suggests that this subtype is involved in the modulation of emotion, as well as the function of the hypothalamus [9.3]. The 5-HT_{1A} subtype of serotonin receptors is implicated in the pathogenesis of anxiety, depression, hallucinogenic behaviour, motion sickness and eating disorders, and is therefore an important target for drug therapy [9.6–9.11].

Partial agonists with high affinity to 5-HT_{1A} receptors are being used as anxiolytics and antidepressants [9.12–9.14]. These compounds decrease central 5-HT neurotransmission via antagonism of post-synaptic 5-HT_{1A} receptors in the hippocampus and the cerebral cortex, and through inhibition of neuronal firing by an agonist action at the somatodendritic 5-HT_{1A} autoreceptors [9.15,

9.16]. The arylpiperazine, WAY 100635, has been found to be a highly selective ligand for imaging the 5-HT$_{1A}$ receptor, distinguishing it from other serotonergic receptors. Thus, many researchers have tried to develop a radioligand capable of assessing in vivo changes in 5-HT$_{1A}$ receptors in patients with depression, anxiety disorders, Alzheimer's disease and schizophrenia, using positron emission tomography (PET). Recently the para-fluorobenzyl analogue of WAY 100635 (P-MPPF), labelled with ^{18}F, has been reported. DWAY also appears to exhibit all the favourable features of WAY as a selective radioligand for 5-HT$_{1A}$ receptors in the human brain.

Owing to its nuclear properties, its availability from [99]Mo/^{99m}Tc generators and its relatively low cost, technetium is a transition metal of major importance for the design of suitable ligands for use in single photon emission computed tomography. It is well known that when sodium pertechnetate is reduced in the presence of a suitable reducing agent and a chelating ligand, such as N_2S_2, a $[TcO]^{3+}N_2S_2$ centre core is formed [9.17]. It has been demonstrated in several recent reports that it is possible to incorporate the N_2S_2 ligand into potential receptor-selective imaging agents for cholinergic receptors [9.18, 9.19], steroid hormone receptors [9.20] and dopamine transporters [9.21]. In general, arylpiperazine derivatives display higher 5-HT$_{1A}$ affinity and selectivity than other derivatives. Among them, WAY 100635 (N-(2-(1-(4-(2-methoxyphenyl)piperazinyl)ethyl))-N-(2-pyridinyl)-cyclohexane carboxamide), has been recognized as a highly selective and potent antagonist at the central 5-HT$_{1A}$ receptor. In order to obtain a more useful ligand for evaluation of the 5-HT$_{1A}$ receptor, WAY 100635 derivatives were synthesized in which the chelating ligand group was designed and N_2S_2 was attached to the molecule via the pendant approach.

At the beginning of the study, it was hypothesized that an arylpiperazine derivative would be a potential ligand for imaging the 5-HT$_{1A}$ receptor. Therefore, the synthesis of arylpiperazine derivatives as potential ligands for imaging the 5-HT$_{1A}$ receptor has been attempted, a ^{99m}Tc labelling method has been developed and the biological activity of the candidate for the imaging agent has been investigated.

9.2. MATERIALS

Unless otherwise stated, all solvents, materials and chemicals were of reagent grade and were used as received from the Aldrich Company. Organic compounds were characterized by their melting point, ^{1}H NMR spectra, IR spectra and HPLC–UV spectra. [99m]TcO$_4^-$ was obtained from [99]Mo by the solvent extraction method. The labelling yield was checked by the instant thin

layer chromatography (ITLC) method and the high performance liquid chromatography (HPLC) method. The ITLC system consists of an ITLC scanner (an EG&G Berthold linear analyser) and a Berthold Chroma program in a control computer for a one dimensional analysis. The reversed phase HPLC system was equipped with two Waters 501 pumps, a μBondapak C-18 column (3.9 mm × 300 mm, 10 μm, Waters), a Waters automated gradient controller, an ultraviolet detector, a gamma ray detector, an autochro-data module and an autochro-WIN analysis program in the control computer.

9.3. METHODS

9.3.1. Synthesis of S,S′-bis(trityl)-MAMA ligand

The synthesis of S,S′-bis(trityl) monoamide monoamine (MAMA-Tr$_2$) (4) is shown in Fig. 9.1. Cysteamine hydrochloride was protected by S-trityl by allowing it to react with triphenylmethanol in trifluoroacetic acid, to provide the crystalline-free amine 2 upon basic workup. N-acylation of the amine 2 with bromoacetyl bromide in the presence of triethylamine provided the primary bromide 3, which was then treated with an additional equivalent of amine 2 under more vigorous conditions, to give S,S′-bis(trityl) MAMA, 4.
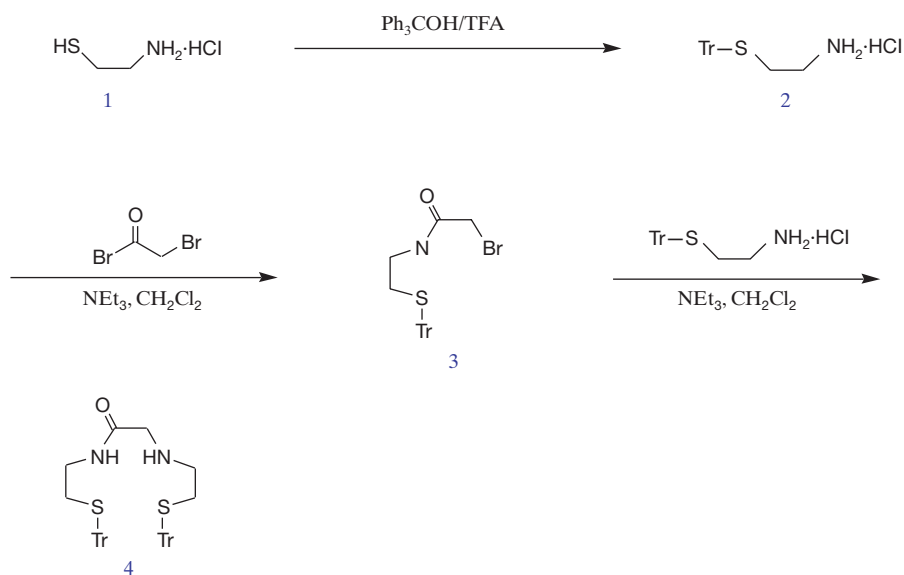
FIG. 9.1. Stages in the synthesis of S,S-bis(trityl)-MAMA (I).

9.3.2. Synthesis of arylpiperazine ligand (II)

Arylpiperazine ligand (II) was prepared by a similar procedure to that described for the preparation of arylpiperazine ligand (I) and is shown in Fig. 9.2. But the final arylpiperazine ligand (II) was obtained using a different N_2S_2 moiety: ^1H NMR (300 MHz; CDCl$_3$) δ = 8.11 (d, 1H, pyridine-H), 7.40 (t,
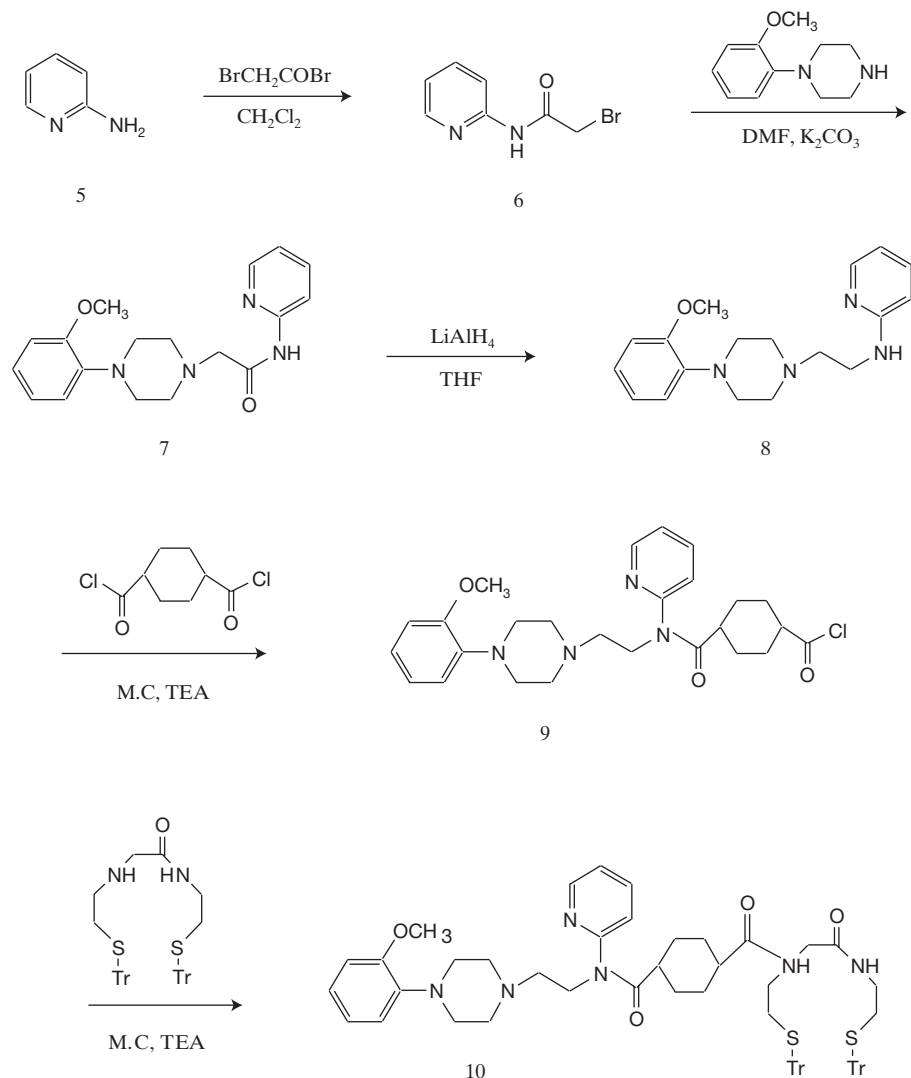
FIG. 9.2. *Stages in the synthesis of arylpiperazine ligand (II).*

1H, pyridine-H), 7.39 < 7.44 (m, 12H, Ar), 7.18 < 7.30 (m, 18H, Ar), 7.05 < 6.85 (m, 4H, Ar), 6.5 (t, 1H, Ar), 6.4 (d, 1H, Ar), 3.87 (s, 3H, OCH$_3$), 3.65 (m, 4H), 3.33 < 3.29 (bs, 10H), 2.78 < 2.59 (bs, 6H), 2.38 < 2.19 (bs, 8H), 1.78 < 1.36 (bs, 8H).

9.3.3. Deprotection method

As indicated by Dezutter et al. [9.22], the standard deprotection method for S-trityl groups involved treatment of the compound in tartaric acid with SnCl$_2$ under acidic conditions (pH2–3), followed by incubation at 100°C. Its radiochemical purity was checked by HPLC.

9.3.4. Biodistribution studies

Biodistribution studies were carried out using SPF graded 6 week old Sprague–Dawly male rats, which were injected via their tail veins with 0.01 mCi per rat. The rats were then sacrificed with ethyl ether 5, 30 and 60 min post-injection. Specific organs were excised, weighed and their radioactivity counted, along with the same dose of injected standard radiopharmaceuticals using a gamma well counter.

9.3.5. Dynamic acquisition and analysis

A week-old New Zealand white male rabbit anaesthetized with ketamine and xylazine was used for imaging studies. The rabbit was injected with ^{99m}Tc-arylpiperazine complex via the left ear vein with 37 MBq/0.5 mL (1.0 mCi/0.5 mL). The rabbit was placed in the posterior position and whole body dynamic images were taken for 30 min. For the accumulated images, the static images were collected at predetermined time intervals by a gamma ray camera. For this purpose, a gamma ray camera was fitted with a low energy all-purpose collimator whose 20% window was centred around 81 keV. Image data were analysed under the dynamic procedure of the Microdelta system. Regions of interest were set and the time–radioactivity curves for brain uptake were also obtained.

9.4. RESULTS

9.4.1. Radiolabelling of arylpiperazine ligand (II) with ^{99m}Tc

Twenty-three micrograms of arylpiperazine ligand (0.07µM), 125 µg of SnCl$_2$ (0.056µM) and 1 mg of tartaric acid were dissolved in 0.05N of

hydrochloric acid in a 10 mL vial under an N_2 gas atmosphere. Sodium pertechnetate (370–740 MBq) was added to the vial, followed by a 1 min sonication in a water bath. The additional incubation was applied for 1 h using a heating block adjusted to 100°C. After the incubation, the vial was stood for 20 min at room temperature to cool down.

The reaction solution was subjected to an HPLC analysis for definition of the radiochemical purity. The ^{99m}Tc-arylpiperazine complex solution (Fig. 9.3) was filtered and analysed by reversed phase HPLC using a gradient system of H_2O and acetonitrile with a flow rate of 1 mL/min. The retention time of the main peak of the ^{99m}Tc-arylpiperazine complex was 16 min (Fig. 9.4) with a labelling yield of 100%; ^{99m}Tc is shown at the retention time of 3 min. Degradation of arylpiperazine or reactant by-products was also noted using UV absorbance at 254 nm. The stability of the ^{99m}Tc-arylpiperazine complex was further checked and it was found to be stable for up to 5 h (Fig. 9.5).

9.4.2. Dynamic acquisition and analysis of ^{99m}Tc-arylpiperazine (WAY) complex

Images of ^{99m}Tc-arylpiperazine (WAY) complex in rabbits were obtained from the time immediately after injection of the rabbit. The whole body was
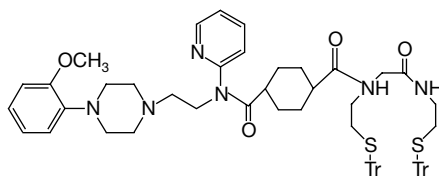
Arylpiperazine (WAY) ligand
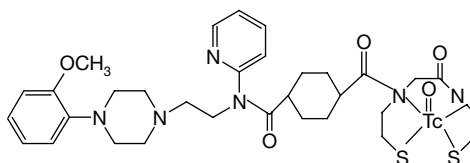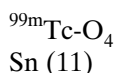
[99m]Tc-O$_4$
Sn (11)

[99m]Tc – Arylpiperazine (WAY) complex

FIG. 9.3. Presumed structure of the ^{99m}Tc-arylpiperazine (WAY) complex.
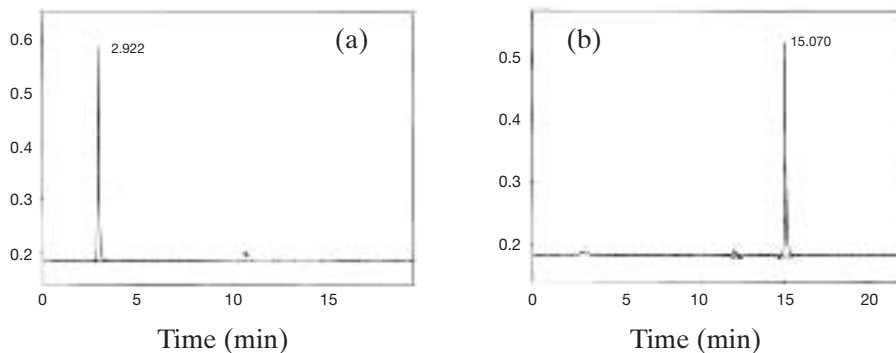
FIG. 9.4. HPLC analysis data of (a) free $^{99m}TcO_4$ and (b) ^{99m}Tc-arylpiperazine complex: the reaction complex was filtered and its radiochemical purity was checked by use of a gradient system with water and acetonitrile for 40 min with a flow rate of 1 mL/min.

scanned for 60 min using a low energy all-purpose collimator according to the dynamic procedure of Microdelta Systems. In addition, a brain image was obtained by use of a pinhole collimator for 80 min after injection. This form of complex was thought to be taken up in the liver very quickly and excreted through the urinary pathway (Fig. 9.6) with minimal uptake by any other tissues or organs. Images from the pinhole collimator showed persistent brain uptake for 80 min as indicated in Fig. 9.7, as well as a time–activity curve (Fig. 9.8).
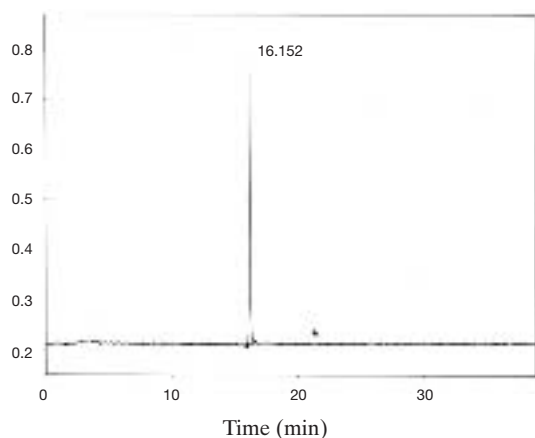
FIG. 9.5. Stability of the ^{99m}Tc-arylpiperazine complex: the reaction complex was mixed with phosphate buffer (0.05M, pH7.2) and its stability was checked for 5 h by HPLC.
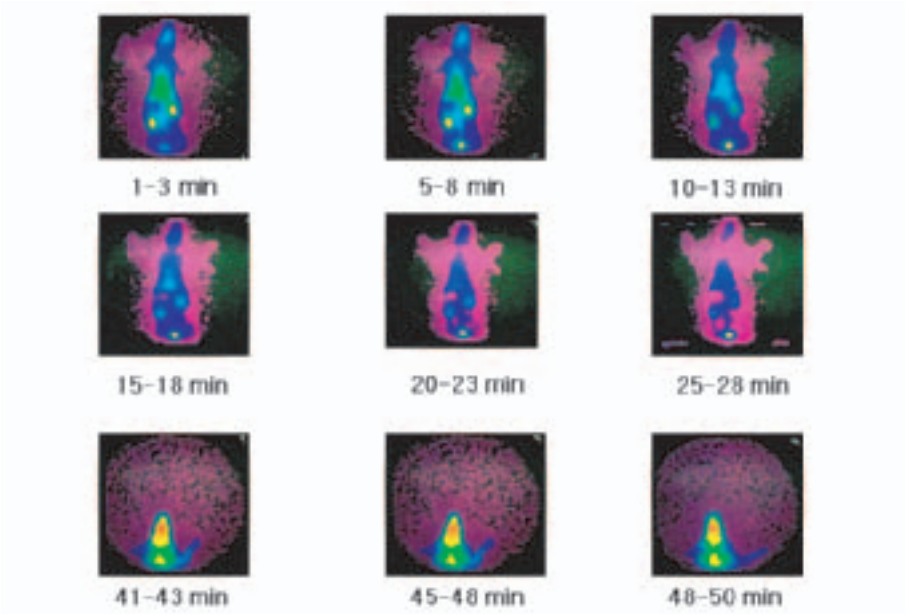
FIG. 9.6. Whole body scans of ^{99m}Tc-arylpiperazine (WAY) complex by a gamma ray camera for 60 min post-injection. Static images were recorded for 2 min at predetermined times.
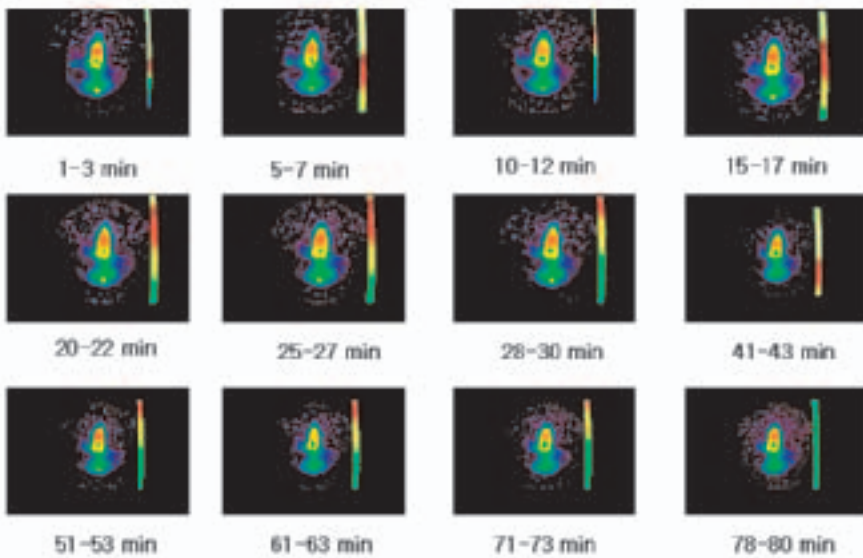
FIG. 9.7. Images of ^{99m}Tc-arylpiperazine (WAY) complex taken by use of a pinhole collimator for 80 min. Static images were recorded for 2 min at predetermined times.

(a)
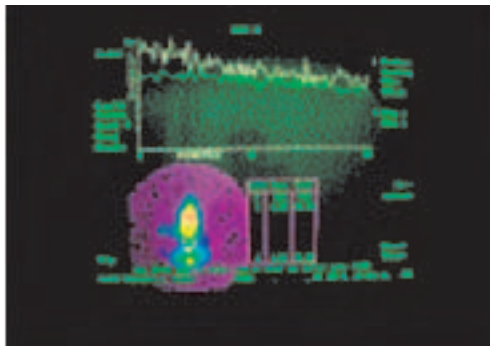
(b)
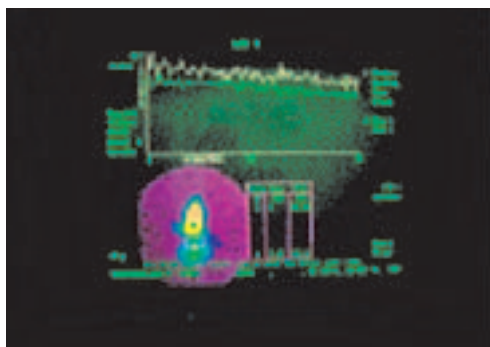
FIG. 9.8. Time–activity curves obtained for the regions of interest in the brain after injection of a normal rabbit with ^{99m}Tc-arylpiperazine (WAY) complex: (a) 0–30 min post-injection, (b) 40–80 min post-injection.

9.4.3. Biodistribution study of ^{99m}Tc-arylpiperazine (WAY) complex

The biodistribution data of the ^{99m}Tc-arylpiperazine (WAY) complex in normal Sprague–Dawly rats are listed in Tables 9.1 and 9.2 and Figs 9.9 and 9.10. A quantitive analysis of the gamma ray camera images of ^{99m}Tc-arylpiperazine during one hour post-injection are indicated in Tables 9.1 and 9.2. The results show that most of the ^{99m}Tc complex was found in the kidney and bladder 60 min after injection, which proved that the complex was readily excreted through the urinary track. Of the labelled complex, 0.04% was taken up into the whole brain region. In the brain tissues dissected, a rather high

TABLE 9.1. BIODISTRIBUTION (ID %/g) OF ^{99m}Tc-ARYLPIPERAZINE (WAY) IN SPRAGUE–DAWLEY RATS

	Blood	Kidneys	Spleen	Liver	Heart	Lungs	Brain
5 min	3.03	7.17	2.70	1.80	2.85	2.31	0.17
30 min	2.00	5.18	2.60	1.64	1.41	1.24	0.08
60 min	1.10	3.72	2.62	1.47	0.69	0.76	0.04

radioactivity was found in the hippocampus and cortex region 60 min after injection.

9.5.   DISCUSSION AND CONCLUSIONS

On the basis of their structure–activity relationship, many compounds have been studied that mimic agonists and antagonists for the 5-HT$_{1A}$ receptor in the development of potential 5-HT$_{1A}$ receptor imaging agents. In the present research, WAY 100635 derivatives were synthesized as a labelling ligand because they are very well known as antagonists for the 5-HT$_{1A}$ receptor, with a selective high affinity to the 5-HT$_{1A}$ receptor. WAY 100635 is also believed to be metabolized by different metabolic pathways without metabolism by the human liver. According to our results, a successful synthesis of arylpiperazine derivative as a ligand for ^{99m}Tc labelling has been achieved and its labelling condition with ^{99m}Tc has also been established. According to our data from dynamic acquisition and analysis, it is easy to show that the arylpiperazine ligand can be a good candidate for a serotonin receptor imaging agent. Although a receptor affinity study for it has not been conducted, reasonable, possibly even promising, data have been obtained from the present study, especially for the uptake of ^{99m}Tc-arylpiperazine derivative into certain brain regions. For further study, as indicated by other work, receptor affinity studies

TABLE 9.2. BIODISTRIBUTION (ID %/g) OF ^{99m}Tc-ARYLPIPERAZINE (WAY) IN SPRAGUE–DAWLEY RAT BRAIN TISSUES

	Hypothalamus	Cerebellum	Frontal cortex	Striatum	Hippocampus
5 min	4.0	2.6	4.3	1.7	1.7
30 min	1.9	1.5	1.1	1.0	1.0
60 min	1.0	1.1	1.1	0.8	1.2
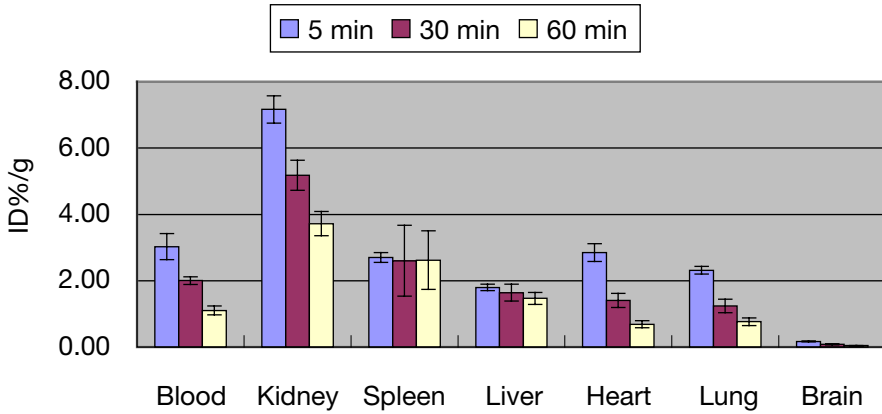
FIG. 9.9. Radioactivities (ID%/g) in blood, major organs and tissues at 5, 30 and 60 min after intravenous administration (30–40 µCi/0.2 mL) of ^{99m}Tc-arylpiperazine derivative (WAY) complex. The data represent mean ± SD (n = 3).

of disorders such as neurodegenerative diseases, which can be expected to result in a loss of 5-HT$_{1A}$ receptors in well defined brain regions, should be undertaken, although it is well known that the high affinity antagonists of WAY derivatives produce images of the 5-HT$_{1A}$ receptor distribution in the human brain with superior contrast [9.23].
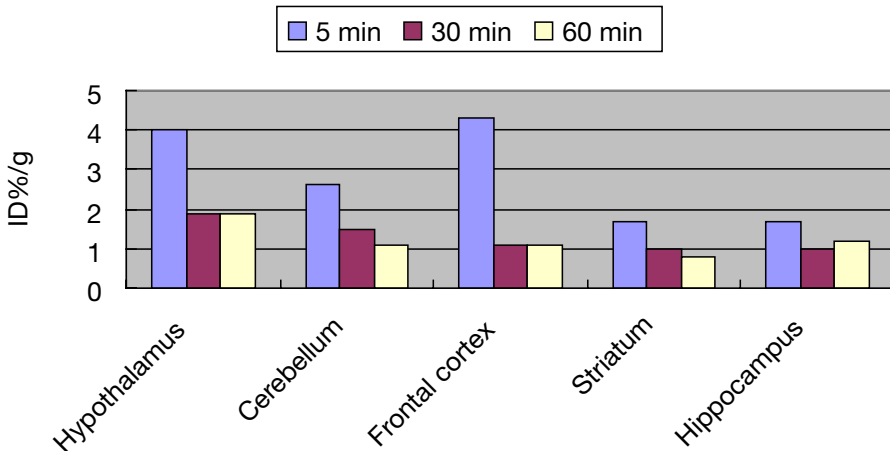
FIG. 9.10. Radioactivities (ID %/g) in brain tissues at 5, 30 and 60 min after intravenous administration (30–40 µCi/0.2 mL) of ^{99m}Tc-arylpiperazine derivative (WAY) complex. The brains were dissected into five regions and each region was pooled from three brains.

REFERENCES TO CHAPTER 9

[9.1]   FRAZER, A., MAAYANI, S., WOLFE, B.B., Subtypes of receptors for serotonin, Annu. Rev. Pharmacol. Toxicol. **30** (1990) 307–348.

[9.2]   HARTIG, P.R.L., BRANCHEK, T., WEINSHANK, R., Serotonin receptor subtypes, Psycho-pharmacol. Ser. **10** (1993) 15–25.

[9.3]   HOYER, D., et al., International Union of Pharmacology classification of receptors for 5-hydroxytryptamine(serotonin), Pharmacol. Rev. **46** (1994) 157–203.

[9.4]   PAZOS, A., PROBST, A., PALACIOS, J.M., Serotonin receptors in the human brain, III. Autoradiographic mapping of serotonin-1 receptors, Neuroscience **21** (1987) 97–122.

[9.5]   DEL OLMO, E., et al., Transient localization of 5-HT$_{1A}$ receptors in human cerebellum during development, Neurosci. Lett. **166** (1994) 149–152.

[9.6]   SCHREIBER, R., DE VRY, J., 5-HT$_{1A}$ receptor ligands in animal models of anxiety, impulsivity and depression: Multiple mechanisms of action?, Prog. Neuropsycho. Pharmacol. Biol. Psychiatry **17** (1993) 87–104.

[9.7]   GLENNON, R.A., Serotonin receptors: Clinical implications, Neurosci. Biobehav. Rev. **14** (1990) 35–47.

[9.8]   FRAZER, A., HENSLER, J.G., 5-HT$_{1A}$ receptors and 5-HT$_{1A}$-mediated responses: Effect of treatments that modify serotonergic neuro-transmission, Ann. N.Y. Acad. Sci. **600** (1990) 460–474.

[9.9]   BALDWIN, D., RUDGE, S., The role of serotonin in depression and anxiety, Int. Clin. Psychopharmacol. **9** Suppl 4 (1995) 41–45.

[9.10] BEREDSEN, H.H., Interactions between 5-hydroxytryptamine receptor subtypes: Is disturbed receptor balance contributing to the symptomatology of depression in humans?, Pharmacol. Ther. **66** (1995) 17–37.

[9.11] SAXENA, P.R., Serotonin receptors: Subtypes, functional responses and therapeutic relevance, Pharmacol. Ther. **66** (1995) 339–368.

[9.12] EISON, A.S., AZAPIRONES: History of development, J. Clin. Psychopharmacol. **10** (1990) 2S–5S.

[9.13] FLETCHER, A., CLIFFE, I.A., DOURISH, C.T., Silent 5-HT$_{1A}$ receptor antagonists: Utility as research tools and therapeutic agents, Trends Pharmacol. Sci. **14** (1993) 41–48.

[9.14] CHARNEY, D.S., KRYSTAL, J.H., DELGADO, P.L., HENINGER, G.R., Serotonin-specific drugs for anxiety and depressive disorders, Annu. Rev. Med. **41** (1990) 437–446.

[9.15] ANDRADE, R., NICOLL, R.A., Novel anxiolytics discriminate between postsynaptic serotonin receptors mediating different physiological responses on single neurons of the rat hippocampus, Naunyn-Schmiedeberg's Arch. Pharmacol. **336** (1987) 5–10.

[9.16] SRPOUSE, J.S., AGHAJANIAN, G.K., Responses of hippocampal pyramidal cells to putative serotonin 5-HT$_{1A}$ and 5-HT$_{1B}$ agonist: A comparative study with dorsal raphe neurons, Neuropharmacology **27** (1988) 707–715.

[9.17] OYA, S., PLOSSL, K., KUNG, M.P., STEVENSON, D.A., KUNG, H.F., Small and neutral Tc^VO BAT, bisaminoethanethiol (N_2S_2) complexes for developing new brain imaging agents, Nucl. Med. Biol. **25** (1998) 135–140.

[9.18] LEVER, S.Z., et al., Novel technetium ligands with affinity for the muscarinic cholinergic receptor, Nucl. Med. Biol. **21** (1994) 157–164.

[9.19] DEL ROSARIO, R.B., JUNG, Y.W., BAIDOO, K.E., LEVER, S.Z., WIELAND, D.M., Synthesis and in vivo evaluation of a $^{99m}/^{99}$Tc-DADT-benzovesamicol: A potential marker for cholinergic neurons, Nucl. Med. Biol. **21** **(**1994) 197–203.

[9.20] DIZIO, J.P., FIASCHI, R., DAVISON, A., JONES, A.G., KATZENELLEN-BOGEN, J.A., Progestin–rhenium complexes: Metal-labelled steroids with high receptor binding affinity, potential receptor-directed agents for diagnostic imaging or therapy, Bioconjug. Chem. **2** (1991) 353–366.

[9.21] KUNG, H.F., et al., Imaging of dopamine transporters in humans with technetium-99m TRODAT-1, Eur. J. Nucl. Med. **23** (1996) 1527–1530.

[9.22] DEZUTTER, N.A., DE GROOT, T.J., BUSSON, R.H., JANSSEN, G.A., VERBRUGGEN, A.M., Preparation of ^{99m}Tc-N_2S_2 conjugates of chrysamine G, potential probes for the beta-amyloid protein of Alzheimer's disease, J. Labelled Compd. Radiopharm. **42** (1999) 309–324.

[9.23] JAN, P., AREN, V.W., Visualization of serotonin-1A (5-HT$_{1A}$) receptors in the central nervous system, Eur. J. Nucl. Med. **28** 1 (2001) 113–129.

Chapter 10

LABELLING OF CENTRAL NEURAL SYSTEM RECEPTOR LIGANDS WITH THE *fac*-[Tc(CO)₃]⁺ MOIETY

R. ALBERTO, J. BERNHARD, J. WALD
Institute of Inorganic Chemistry, University of Zürich,
Zürich, Switzerland

Abstract

During the period of the IAEA Co-ordinated Research Project on Development of Agents for the Imaging of CNS Receptors based on ^{99m}Tc, many efforts were made to find an improved system or alternative methods for the labelling of various central nervous system (CNS) receptor binding agents based on the *fac*-[Tc(CO)₃]⁺ fragment. Within the same period the chemistry of the *fac*-[Tc(CO)₃]⁺ fragment has been developed as a useful label more and more not only for the labelling of CNS receptor ligands but also for peptides, antibodies and other biologically active molecules such as B12. Especially the latter molecule is known to be taken up as well through the blood–brain barrier but is obviously not an CNS receptor ligand. One of the most important achievements over the whole period of the project has been the final formulation of a kit useful for the preparation of [^{99m}Tc(OH₂)₃(CO)₃]⁺ without the requirement for using free CO. Much time was invested in that particular topic, since it will allow this relevant moiety to be applied not only on a routine basis but also for research into CNS ligands. A major achievement has thus been the commercial availability of these kits by the beginning of 2002.

During the period of the project, a number of new systems were introduced, some of which were specially designed not only for CNS receptor ligands but also for other biomolecules. Among these is that for the syntheses of highly lipophilic ligands, the complex formation of which is based on classical co-ordination chemistry. In addition, the feasibility of the mixed ligand concept from a chemical point of view has been proved in principle. A number of complexes have been prepared where the CNS receptor ligand is attached to the monodentate ligand system. In principle it can also be attached to the bidentate moiety, allowing a screening of the biological behaviour as a function of the co-ligand.

A major breakthrough could be achieved with the aqueous synthesis of cymantren-like technetium complexes [(R-C₅H₄)^{99m}Tc(CO)₃], where R represents basically any type of organic substituent, in particular the serotonergic receptor ligand WAY. A way of derivatizing this receptor ligand could be found with a cyclopentadienyl moiety, being reasonably stable in water and which can be labelled with the precursor [^{99m}Tc(OH₂)₃(CO)₃]⁺. Although the organic chemistry of the derivatization of a biomolecule with cyclopentadienyl is demanding, the final derivative is reasonably stable even

in water. The corresponding half-sandwich complexes with ^{99m}Tc are stable over 24 h at 37°C without any decomposition.

10.1. KIT PREPARATION OF $[^{99m}Tc(OH_2)_3(CO)_3]^+$ WITHOUT FREE CO

As presented at the third Research Co-ordination Meeting for the first time, so called borano-carbonate $[H_3BCO_2H]^-$ (BC) is a very useful source for CO in aqueous solution. As a CO source, BC acts at the same time as a reducing agent since the important substructure BH_3 can be considered as the formerly used $[BH_4]^-$. The major problem in the application of BC until recent years lay in its synthesis, which started from highly pyrophoric diborane. We have developed in the meanwhile a synthesis starting from commercially available H_3BTHF which allows the preparation of BC on the gram scale [10.1]. The synthetic principle is given in scheme 1 shown in Fig. 10.1.

The behaviour of BC described is not so unexpected since its basic structure resembles that of metalla-carboxylic acids, which are also known to release water upon protonation. The CO which is formed intermediately is released in the case of the purely σ-bound CO in BC but usually remains bound to the metal in the case of a metalla-carboxylic acid.

In order to prove the so far unknown structure of BC it was possible to grow a crystal and to elucidate its X ray structure. An ORTEP (Oak Ridge thermal ellipsoid plot) presentation is given in Fig. 10.2.

10.1.1. Behaviour in water and kit preparation

Borano-carbonate is stable in water at a pH of more than 8 for weeks but decomposes rather rapidly below a pH of 6. For the development of a kit, some improvements of the formulation were required in order to achieve a reproducible yield of more than 98%. The final composition contains BC in milligram amounts and, in addition, $[B_4O_7]^{2-}$ as a buffering agent to keep the
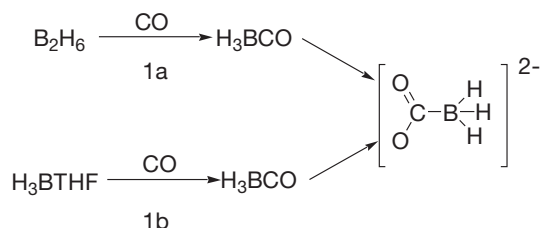
FIG. 10.1. Scheme 1 for the synthesis of BC starting from B_2H_6 or H_3BTHF.
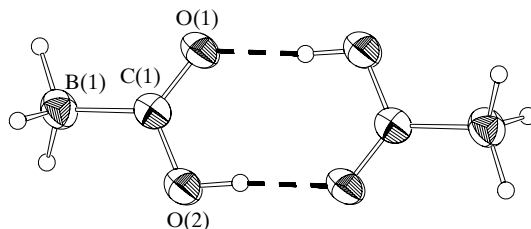
FIG. 10.2. ORTEP presentation of the [H₃BCO₂H]⁻ anion.

pH alkaline during the synthesis of $[^{99m}Tc(OH_2)_3(CO)_3]^+$. Additionally, a few milligrams of NaKtart are necessary in order to stabilize the intermediate oxidation states which must be formed during the (overall) six-electron reduction process. In a 10 mL vial up to 3 mL of generator elute can be transformed to $[^{99m}Tc(OH_2)_3(CO)_3]^+$ with this composition independently of the total activity. The former conditions of heating, for 30 min at 70°C, could be improved on as well. The new kit formulation allows a synthesis at 98°C, and completion is achieved usually after 15–20 min. A longer heating period does not interfere with the yield since, once formed, $[^{99m}Tc(OH_2)_3(CO)_3]^+$ is stable over a longer period of time at high temperature when not exposed to oxygen. After the synthesis the pH is about 9. If required, the solution can be neutralized by addition of an adequate buffer, or the biomolecule of interest can be added directly to the vial.

This procedure has been chosen for the labelling of the central nervous system (CNS) receptor ligands since they are in general not very sensitive for higher pH values (discussed later). If the biomolecule was not decomposed under reductive conditions, it was even possible to perform the complete labelling reaction with the biomolecule of choice in one single pot without initial preparation of the precursor $[^{99m}Tc(OH_2)_3(CO)_3]^+$ and subsequent labelling of the biomolecule.

10.2. LABELLING OF CNS RECEPTOR LIGANDS WITH THE *fac*-$[^{99m}Tc(CO_3)]^+$ MOIETY

During the project the introduction of novel ways for labelling biomolecules, in particular CNS receptor ligands, was considered to be of priority in our group. We did not focus on any particular biomolecule but rather elaborated alternative methods useful for all the participants of the project working with particular CNS receptor ligands. This strategy represents the prerequisite under which the chemistry to be described must be understood.

10.2.1. Labelling of biomolecules with an alternative mixed ligand 2 + 1 concept

One of the most important features in the labelling of CNS receptor ligands is the fine tuning of physico-chemical properties while keeping constant a large part of the radioconjugate. Changing the properties of a radioconjugate by changing the chelators means in many cases a complete change of the physico-chemical properties of the whole molecule, which leads to biological data difficult to compare with each other. It would be a significant advantage if a large part of the molecule could be kept constant while a small part is systematically replaced. This would allow a more systematic determination of the structure–activity relationship.

A mixed ligand concept is obviously useful to achieve such a systematic variation. However, it is of course also required that the mixed ligand complex be of high biological stability. Thus, the most labile part, usually the monodentate ligand, may not to be exchanged for competing groups, ubiquitously present in living systems. On the basis of the high (kinetic) stability of complexes formed with the $[Tc(CO)_3]^+$ moiety, we have developed an alternative mixed ligand concept. This method is based on a 2 + 1 or 1 + 2 mixing of ligands. 2 + 1 stands for a biomolecule attached to a monodentate ligand, wherein the bidentate ligand can be chosen as the variable parameter, whereas in 1 + 2 the inverse is the case. Both approaches have some advantages as will be seen later. The principal method is depicted in scheme 2 shown in Fig. 10.3.

It is highly important that the ligands used in these mixed ligand approaches be readily available (if possible commercially), cheap and convenient to handle. The bidentate ligand should have a structure which is not too large and which allows the bidentate ligand to co-ordinate only once, otherwise the remaining position, where the biomolecule should be attached, will be occupied in addition by the same ligand co-ordinating monodentate but not by the biomolecule. Furthermore, it is of advantage if the bidentate ligand is anionic. The ligand then compensates the monocationic charge of the precursor complex and the last position is easily available for a neutral ligand which bears the biomolecule. It is also possible to have a neutral bidentate ligand. The last position will then be occupied preferentially by a chloride, which can subsequently be exchanged for another incoming anionic ligand bearing the biomolecule or the CNS receptor ligand. Only the first case has been investigated during the time of the project.

(a)

(b)
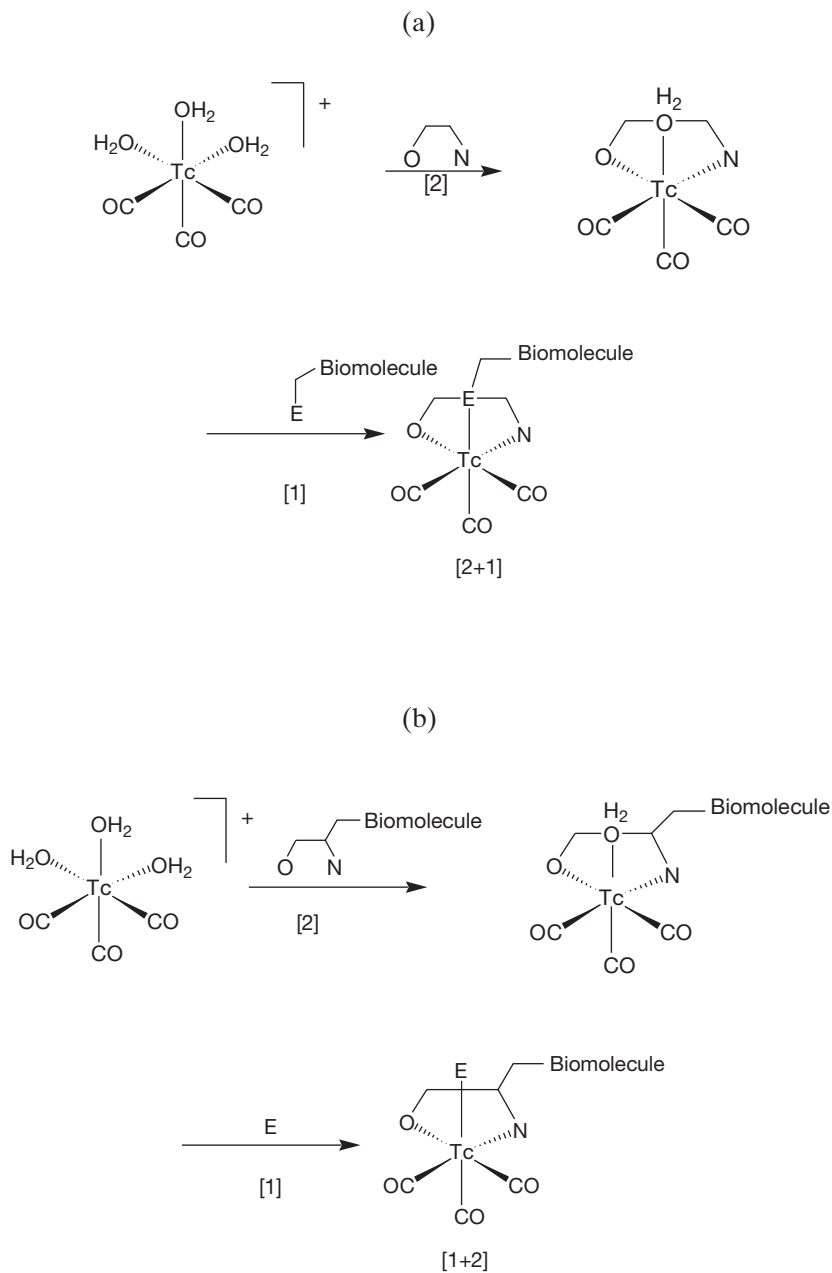
FIG. 10.3.   Scheme 2 for mixed ligand approaches: (a) the 2 + 1 concept; (b) the 1 + 2 concept.

(a)　　　　　　　　　(b)　　　　　　　　　(c)
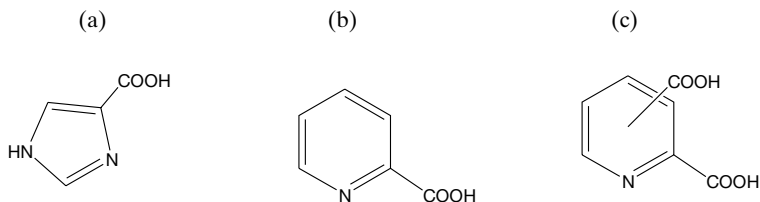
FIG. 10.4. Scheme 3 for bidentate ligands for the mixed ligand approach: (a) imidazole–carboxylic acid (imc), (b) picolinic acid (pic) and (c) dipicolinic acid (dipic).

The bidentate ligands depicted in scheme 3 shown in Fig. 10.4 were chosen for these studies.

10.2.1.1. *Synthesis of the precursor complexes*

For the 2 + 1 concept, the relevant precursor complex is of composition $[Tc(OH_2)(N\cap O)(CO)_3]$, where $N\cap O$ stands for the bidentate ligands picolinic acid or imidazolic acid. These complexes are easily prepared by the reaction of $[M(OH_2)_3(CO)_3]^+$ with the corresponding ligand at stoichiometric (M = Re, Tc) or at very low concentrations for ^{99m}Tc ($10^{-4} – 10^{-5}M$). The yield is quantitative after 20 min at 98°C. In order to prove the presence of a water ligand at the remaining position, the compounds were prepared with Re as well and the X ray structure could be elucidated for two precursors. The ORTEP presentations are given in Fig. 10.5.

(a)　　　　　　　　　　　　　　　　(b)
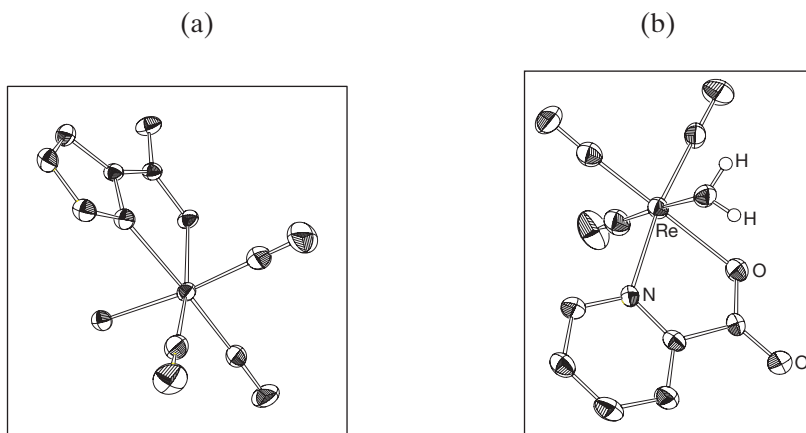
FIG. 10.5. ORTEP presentations of (a) [M(pic)(OH_2)(CO)_3] and (b) [M(imc)(OH_2)(CO)_3].

Comparison of the high performance liquid chromatography (HPLC) traces confirmed the composition of the corresponding ^{99m}Tc complex. All these complexes are stable in water for a very long time without any decomposition.

10.2.1.2. *Synthesis of the mixed ligand complex*

For the subsequent reactions with a monodentate ligand, the following characteristics seemed to be of importance for the later labelling of biomolecules such as CNS receptor ligands. The model ligand should be coupled easily to a biomolecule. It has to be as small as possible and neutral. Furthermore, lipophilicity is of importance since the final radioconjugate has to pass the blood–brain barrier (BBB). We have chosen pyridine, imidazole, primary amines and isocyanides. The imidazoles are conveniently derivatized at the non-coordinating nitrogen atom, for pyridine there exists a wide variety of derivatives, and isocyanides can be introduced into biomolecules by standard organic chemistry procedures. For the final choice of the ligand it is obviously of importance that the last water ligand be exchanged for the biomolecule as efficiently as possible; thus, a low concentration must be achieved. Since the electronic properties of the last ligand are not unambiguously clear, several types of acceptors and donors had to be tested.

We found that, in particular, the isocyanides fulfil these requirements. After the preparation of $[^{99m}Tc(OH_2)(N\frown O)(CO)_3]$, the water ligand could be substituted by a model isocyanide and by a CNS receptor ligand derivatized with an isocyanide (a WAY compound, received from H.-J. Pietzsch, Forschungszentrum Rossendorf, Dresden). Concentration levels as low as 10^{-5}M in WAY-NC allowed a complete coupling of the CNS receptor ligand to ^{99m}Tc with this method (Fig. 10.6). Depending on the concentrations, the temperature could be lowered; however, in very dilute systems, as mentioned above, high
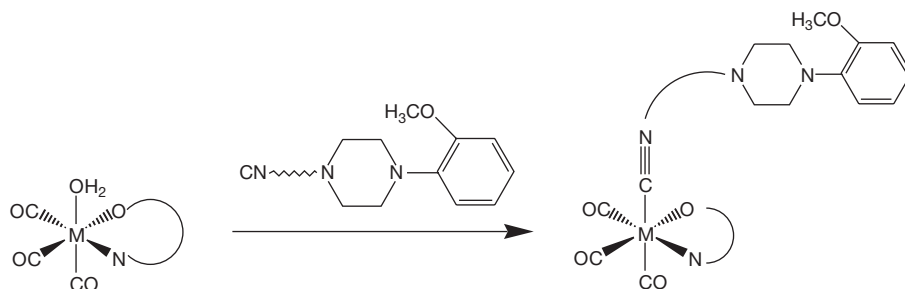
FIG. 10.6. Reactions (scheme 4) with WAY-NC with which concentrations of 10^{-5}M are possible.

(a)   (b)
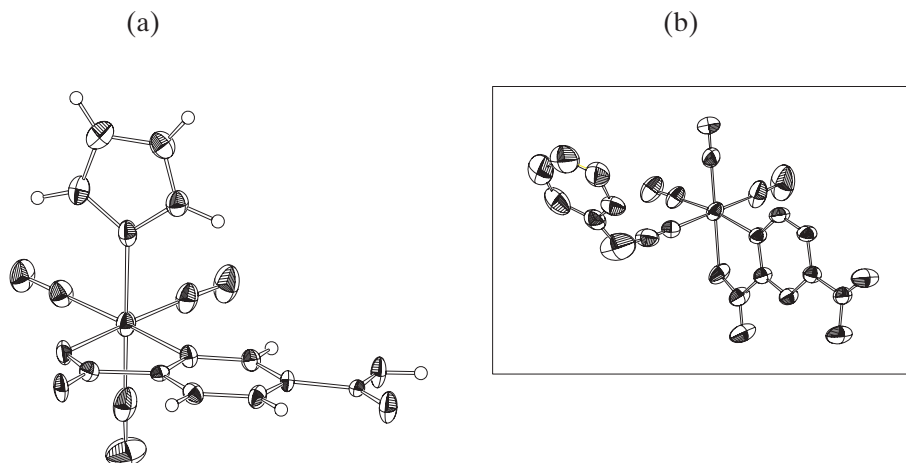
FIG. 10.7. ORTEP presentations of (a) [M(dipic)(im)(CO)₃] and
(b) [M(dipic)(C₆H₅CH₂NC)(CO)₃].

temperatures are required. The ORTEP presentations of two model complexes
are given in Fig. 10.7.

Imidazoles proved to be less efficient. Although very stable complexes
were formed as well, the concentrations required for complete labelling are
higher by a factor of about 5. Depending on the CNS receptor ligand and its
properties, imidazole also seems to be a versatile monodentate ligand provided
that the cold derivative does not cross the BBB.

Pyridine, on the other hand, was not as efficient as the other two ligands.
It seems that the electronic properties of the last site or the steric interactions
of the α-standing hydrogens interfere with the co-ordination ability. Pyridine is
at least ten times weaker and its use was not investigated further.

It can be concluded from these experiments that the properties of the last
positions favour a ligand atom with low donating but medium acceptor
properties. Isocyanides provide an excellent group for attaching a biomolecule
to this position.

10.2.1.3. One-pot synthesis

The above mentioned investigations included two different steps, first the
preparation of $[Tc(OH_2)(N \cap O)(CO)_3]$ and second its reaction with the
biomolecule. In order to show that the whole procedure is also possible in a
single step, all the components were mixed in a single vial, generator elute
added and the mixture heated to 98°C for 30–40 min. It was found that the

mixed ligand complex aimed for did form quantitatively under these conditions. Biological studies with mixed ligand complexes have not been performed so far.

In conclusion, the herein presented novel mixed ligand concept provides an additional possibility of screening systematically the biological behaviour of a particular CNS receptor ligand by varying smoothly the bidentate co-ligand. The advantage of the method is that all the steps are performed fully in water and no organic solvents are required at all. A further advantage of the system is the very high stability of the complexes (no decomposition or ligand exchange could be observed) and the fact that the labelling and the complex formation can be done in a single step. The method has a high potential which merits more detailed investigation.

10.2.2. Labelling of biomolecules with cyclopentadienyl derivatives

It need not be stressed that a potent and highly efficient ^{99m}Tc labelled CNS receptor should meet the following requirements: (a) it should be as small as possible, (b) it should be of low molecular weight and (c) it should be lipophilic. The manifold types of complexes tested so far satisfy one or more of these requirements but in general not all of them. It remains to be proved that all the requirements are really needed; however, in respect of the success achieved to date with ^{99m}Tc labelled CNS receptor ligands, it seems that they have indeed a high impact on the biological behaviour. Whereas iodinated compounds (iodide is relatively small) often show a high first pass extraction through the BBB, this factor is very low (usually below 1%) with ^{99m}Tc complexes. It is, in particular, difficult to obtain a small sized and low molecular weight complex. Figure 10.8 shows a comparison of the sizes of $[TcO(N_3S)]$ and $[CpTc(CO)_3]$ (Cp, cyclopentadiene).

In the literature, preparation of the so-called cymantren-like half-sandwich complexes with ^{99m}Tc has been an issue [10.2–10.7]. These half-sandwich compounds are small lipophilics and are of the lowest molecular
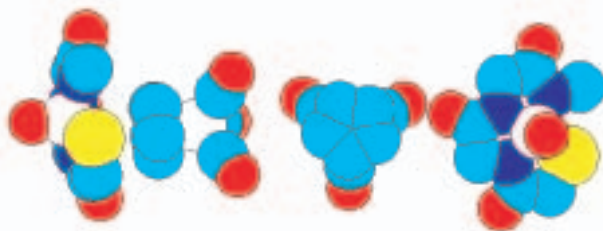
FIG. 10.8. Size comparison of [TcO(N₃S)] and [CpTc(CO)₃] along different axes.

weight. It has been shown, in particular with steroid hormones, that the rhenium analogues do not interfere with the receptor and lead to the highest possible retention of bioactivity [10.8–10.17]. However, many attempts to prepare the ^{99m}Tc analogue in a convenient way have failed so far. The attempts described in the literature are multistep syntheses based on classical synthetic organometallic chemistry, and are not very convenient for application to synthesis at all. A very recent approach requires, for example, CH_3OH at 160°C, which means that the reaction has to be performed in an autoclave. Furthermore, elements like chromium, which have a certain carcinogenic potential, are components of the synthesis.

10.2.2.1. Synthesis of cyclopentadienyl derivatives

In our opinion, the problem in the preparation of $[(R-Cp)Tc(CO)_3]$ complexes arises from the prohibitively high value of the dissociation constant pK_a of cyclopentadiene and its very low stability in water. We therefore sought for a derivative of cyclopentadiene with a better water stability and a pK_a value in the physiological range. To enhance the acidity of the cyclopentadiene, we introduced an acetyl group to achieve acetyl-cyclopentadiene (ACp). The synthesis is straightforward and has already been described in the early literature. The general approach to the synthesis of ACp and other derivatives is given in scheme 5 shown in Fig. 10.9.

The Na$^+$ salt of ACp can be isolated with a good yield and is stable at room temperature. The principle of the synthesis can be extended to other organic biomolecules which have attached to the carbonyl group not only a methyl group but also another substituent or even a CNS receptor ligand. We
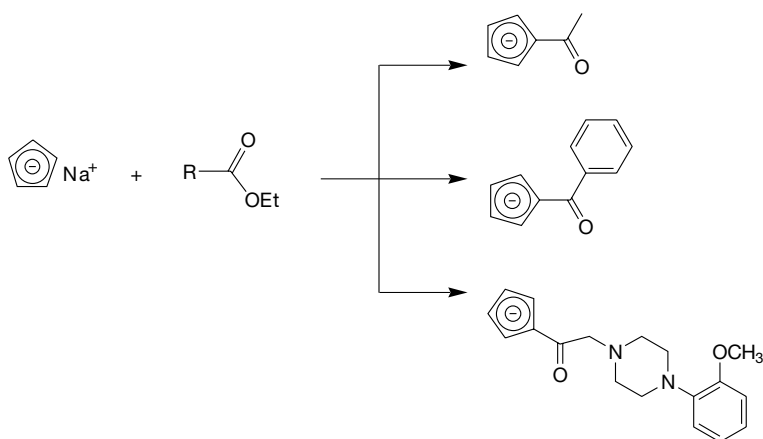
FIG. 10.9. General approach (scheme 5) to cyclopentadiene derivatized biomolecules.

have synthesized a number of such derivatives. Two derivatives of WAY have been prepared, in particular WAY1-Cp, which contains a single methylene group between the carbonyl function and the piperazine ring, and WAY4-Cp containing a butyl chain (see scheme 5 (Fig. 10.9) for WAY1-Cp).

10.2.2.2.   General synthesis for Na[(R-Cp)]

The ethyl N-(methylcarboxylate) derivative of WAY was prepared by alkylation of 1-(2-methoxyphenyl)piperazine (Fluka) with ethyl bromoacetate or bromo-butylacetate, respectively. Stirring for 24 h at room temperature in the presence of Hünig's base and purification on silica gel (CH_2Cl_2/ethylacetate, 4/1 vol./vol.) gave the precursors with a yield of 65–70%. NaCp was freshly prepared in situ from Na (0.3 g, 12.7 mmol) and the corresponding amount of freshly distilled dicyclopentadiene. To this solution the WAY precursor in tetrahydrofuran (THF) (1.8 g, 6.4 mmol) was added. Heating to about 60°C for 6 h gave in the case of the methylene spacer a precipitate, which could be isolated by filtration under N_2. The solid was washed several times with n-hexane to leave an almost colourless powder which was recrystallized from hot THF to give WAY1-Cp in an analytically pure quality. For the butyl spacer no precipitation took place. Instead, THF was evaporated to dryness after filtration from some precipitate and the whole mixture subjected to a preparative HPLC purification, which gave the compound WAY4-Cp in good quality. The fractions were lyophilized, leaving an almost white residue with the compound in about 98% purity. WAY4-Cp in the protonated form is stable in the cold as a solid, as the Na^+ salt is also at ambient conditions. Aqueous solutions of both compounds can be kept for days without significant decomposition. The analysis for WAY1-Cp yielded: ^{1}H NMR (200 MHz, D_2O): δ = 7.0 (m, 4 H); 6.60 (bs 2 H), 6.15 (bs, 1 H), 6.06 (bs, 1 H), 3.74 (s, 3 H), 3.50 (s, 2 H), 2.95 (bs, 4 H), 2.70 (bs, 4 H); ^{13}C NMR (300 MHz, D_2O): δ = 182.4, 150.4, 138.2, 122.5, 122.2, 119.1, 116.9, 116.5, 115.9, 114.2, 111.3, 109.7, 59.8, 53.0, 50.5, 48.1.

We determined the pK_a values of ACp and WAY1-Cp by simple potentiometric titration of the corresponding Na^+ salts. A titration curve for WAY1-Cp is shown in Fig. 10.10.

The pK_a values were found to be in the physiological range. The pK_a for ACp is 8.62(1) in 0.1M NaCl, which is an increase by about five orders of magnitude in comparison with the value for cyclopentadiene. The pK_a values for WAY1-Cp were found to be >12.5, 8.71(1) and 6.37(1), respectively. The dissociation constants pK_{a1} and pK_{a3} were assigned to the tertiary amine groups in the piperazine ring, while pK_{a2} represents the dissociation constant of the cyclopentadiene.
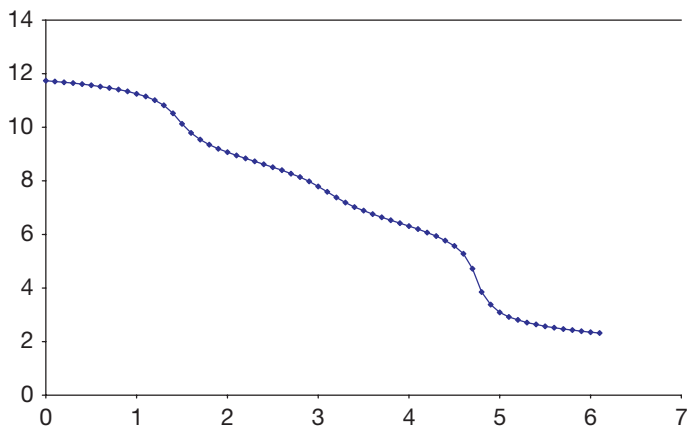
FIG. 10.10. *Potentiometric titration of WAY1-Cp in 0.1M NaCl.*

10.2.2.3. Preparation of the [(R-Cp)Tc(CO)₃] (M = Re, ⁹⁹Tc) complexes

To demonstrate the possibility of preparing complexes of the general composition [(R-Cp)Tc(CO)$_3$] (with M = Tc or Re) directly from water, the corresponding Cp derivatives were reacted in phosphate buffer at pH7.4 or in water with the Tc precursor. Within 2 h at 85°C, [(ACp)M(CO)$_3$] formed with a yield of 15–25% for Re and 40% for Tc. This was one of the first examples in which a Cp derivative reacts in water with an organometallic precursor to yield the corresponding half-sandwich complex. The yield is limited by the concerted formation of hydrolysis products, a reaction which will not occur on the no-carrier-added level. The composition of a number of half-sandwich complexes could be confirmed by X ray structure analysis, and ORTEP presentations are given in Fig. 10.11.

(a)   (b)
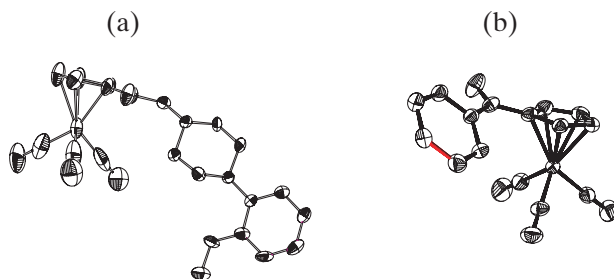
FIG. 10.11. *ORTEP presentations of (a) [(WAY1-Cp)Re(CO)₃] and (b) [(Bz-Cp)Re(CO)₃].*

10.2.2.4. Preparation of the [(R-Cp)Tc(CO)3] (M = 99mTc) complexes

To give a proof of principle, the same WAY precursors were reacted with $[^{99m}Tc(OH_2)_3(CO)_3]^+$. It was found that the corresponding half-sandwich complexes were formed within 30 min at 90°C in quantitative yield. A general labelling procedure is as follows:

For the general synthesis of $[(R\text{-}Cp)^{99m}Tc(CO)_3]$, the starting material $[^{99m}Tc(OH_2)_3(CO)_3]^+$ was prepared as described previously. An aqueous solution of WAY1-Cp or WAY4-Cp in water or phosphate buffer was added (with a final concentration of 10^{-3}–10^{-4}M). Subsequent heating to 95°C for 15 min afforded $[(R\text{-}Cp)^{99m}Tc(CO)_3]$ in yields greater than 95%. The HPLC retention times for R-Cp = ACp and WAY4-Cp are 21.9 and 20.5 min, respectively.

For the one-pot synthesis of $[(ACp)^{99m}Tc(CO)_3]$ a vial was charged with 4 mg of complex 10 and 5.5 mg of $Na_2B_4O_7$, sealed and flushed with dry N_2, after which 2 cm³ of generator elute containing $[^{99m}TcO_4]^-$ was added followed by an aqueous solution of complex 4. Heating to 90°C for about 40 min gave the half-sandwich complexes in high yields (≈80% complex 8, 20% reduced form). The yield and time course of the reaction were not influenced by the total amount of radioactivity (up to 20 GBq of ^{99m}Tc).

To prove the composition of the labelled compounds, the HPLC retention times were compared by co-injection of the Re and ^{99m}Tc complexes. An example of such a trace is given in Fig. 10.12, proving the identity of the ^{99m}Tc complex as a half-sandwich compound.
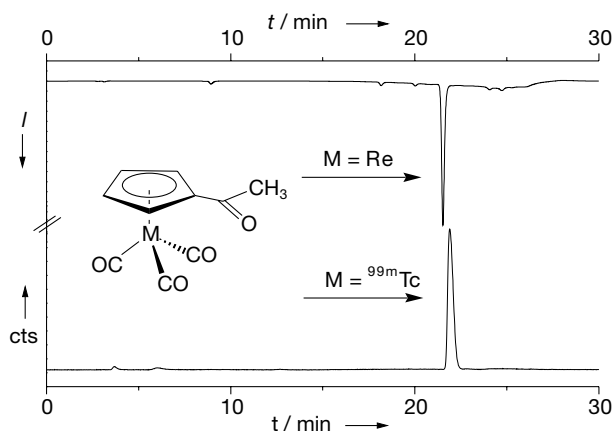
FIG. 10.12.   *Comparison of the HPLC traces of [(ACp)Re(CO)3] and [(ACp)99mTc(CO)3].*

Biological studies with the WAY compounds were carried out. The binding affinity for WAY1-Cp was low. This was to be expected since it is known that the spacer length between the piperazine group and the label should comprise at least three carbon atoms.

In conclusion, we could show that it is possible even in a single step to label a biomolecule with a half-sandwich complex directly from water. Since cyclopentadienyl complexes are in particular important for CNS receptor ligands, this methodology can be extended to a wide variety of other ligands, opening probably the possibility of a wide variety of new investigations.

10.3. SUMMARY AND OUTLOOK

At the end of the IAEA project, the Tc-CO strategy has reached a stage at which it is possible to have the starting material available in a reasonable form and quality from a simple kit. This will allow a systematic study not only of CNS receptor ligands but also of other biomolecules. We have, furthermore, introduced various methods to label CNS receptor ligands with the *fac*-$[Tc(CO)_3]^+$ moiety. This labelling can be based on the simple introduction of a bidentate or tridentate ligand into the biomolecule of interest, as reported earlier, or on the application of the mixed ligand concept, introduced at an advanced state as described in this report. The mixed ligand concept allows a systematic screening of biological behaviour as a function of the physico-chemical properties of the labelled biomolecules. Finally, it was possible for the first time to profit from the small cyclopentadienyl ligand. We could introduce a method with which half-sandwich complexes of ^{99m}Tc can be prepared fully in water and in quantitative yields.

The carbonyl method has the major advantages that the choice of ligands is extremely flexible, that all the reactions can be performed fully in water and that the compounds of interest are in general of high stability against decomposition and trans-metallation. It therefore not only offers a possibility of labelling a wide variety of biomolecules but also leads to new chemistry. Further publications of relevance [10.18–10.22] to the project are given in the references.

REFERENCES TO CHAPTER 10

[10.1] ALBERTO, R., ORTNER, K., WHEATLEY, N., SCHIBLI, R., SCHUBIGER, P.A., J. Am. Chem. Soc. **123** 13 (2001) 3135–3136.

[10.2] WENZEL, M., J. Labelled Compd. Radiopharm. **31** (1992) 641–650.

[10.3] SPRADAU, T.W., KATZENELLENBOGEN, J.A., Organometallics **17** (1998) 2009–2017.

[10.4] MINUTOLO, F., KATZENELLENBOGEN, J.A., J. Am. Chem. Soc. **120** (1998) 4514–4515.

[10.5] MINUTOLO, F., KATZENELLENBOGEN, J.A., Angew. Chem. Int. Ed. Engl. **38** (1999) 1617–1620.

[10.6] MINUTOLO, F., KATZENELLENBOGEN, J.A., Angew. Chem. **111** (1999) 1730–1732.

[10.7] SPRADAU, T.W., et al., Nucl. Med. Biol. **26** (1999) 1–7.

[10.8] JAOUEN, G., TOP, S., VESSIERES, A., ALBERTO, R., J. Organomet. Chem. **600** (2000) 23–36.

[10.9] JAOUEN, G., VESSIERES, A., BUTLER, I.S., Acc. Chem. Res. **26** (1993) 361–369.

[10.10] RYABOV, A.D., Angew. Chem. Int. Ed. Engl. **30** (1991) 931–941.

[10.11] RYABOV, A.D., Angew. Chem. **103** (1991) 945–955.

[10.12] DÖTZ, K.H., EHLENZ, R., Chem. Eur. J. **3** (1997) 1751–1756.

[10.13] SEVERIN, K., BERGS, V., BECK, W., Angew. Chem. Int. Ed. Engl. **37** (1998) 1634–1654.

[10.14] SEVERIN, K., BERGS, V., BECK, W., Angew. Chem. **110** (1998) 1722–1743.

[10.15] TOP, S., et al., J. Am. Chem. Soc. **117** (1995) 8372–8380.

[10.16] SALMAIN, M., GUNN, M., GORFTI, A., TOP, S., JAOUEN, G., Bioconjugate Chem. **4** (1993) 425–433.

[10.17] SPRADAU, T.W., KATZENELLENBOGEN, J.A., Bioconjugate Chem. **9** (1998) 765–772.

[10.18] KÜNDIG, M., Labelling of Biomolecules according to a New Mixed Ligand Concept, Diploma Thesis, University of Zürich (2001).

[10.19] ALBERTO, R., et al., J. Am. Chem. Soc. **120** (1998) 7987.

[10.20] ALBERTO, R., et al., J. Am. Chem. Soc. **25** (1999) 6076–6077.

[10.21] WALD, J., ALBERTO, R., ORTNER, K., CANDREIA, L., Angew. Chem. **113** 16 (2001) 3152–3156.

[10.22] WALD, J., ALBERTO, R., ORTNER., K., CANDREIA, L., Angew. Chem. Int. Ed. Engl. **40** (2001) 3062–3066.

Chapter 11

DEVELOPMENT OF NOVEL MIXED LIGAND TECHNETIUM COMPLEXES FOR IMAGING 5-HT$_{1A}$ NEURAL SYSTEM RECEPTORS

A.S. LEÓN, A. REY, E.T. LEÓN, M. PAGANO, J. GIGLIO
Cátedra de Radioquímica, Facultad de Química

E. MANTA
Cátedra de Química Farmacéutica, Facultad de Química

M.L. MALLO
Departamento de Radiofarmacia, Centro de Investigaciones Nucleares, Facultad de Ciencias

Universidad de la República
Montevideo, Uruguay

Abstract

The development of ^{99m}Tc complexes for imaging 5-HT$_{1A}$ neural system receptors using the 3 + 1 mixed ligand approach is described. Six novel complexes (I–VI) were designed using two different strategies. In complexes I–IV the pharmacophore 1-(2-methoxyphenyl)piperazine was attached to a monodentate thiol used as co-ligand and combined with tridentate dianionic aminothiols (SNS and NNS). On the other hand, complexes V and VI were obtained using thiophenol and 4-methoxy-thiophenol as co-ligand and a tridentate ligand (SNS) with the pharmacophore bound to the nitrogen through an alkyl chain. All complexes were prepared at tracer level using ^{99m}Tc-gluco-heptonate as precursor. Ligand and co-ligand concentration, reaction time and temperature were optimized to achieve high substitution yield and radiochemical purity. Structure was studied at carrier level through the corresponding rhenium complexes. Complexes I and II presented the expected ReOLK structure and a distorted trigonal bipyramidal geometry. The structure of the other four complexes has not been completely elucidated yet. Biodistribution studies of all the complexes demonstrated selective brain uptake and retention. Uptake of complex I in receptor-rich hippocampus was significantly higher than that of the cerebellum (P = 0.05) 1 h post-injection. Oxorhenium complexes I and II showed affinity for the 5-HT$_{1A}$ receptor binding sites, with IC$_{50}$ values in the nanomolar range. The results demonstrate the potential of the mixed ligand approach for the design of ^{99m}Tc complexes with the ability to bind neuroreceptors. However, the goal of imaging 5-HT$_{1A}$ receptors with technetium requires further development of complexes with improved biological profiles.

11.1. INTRODUCTION

Evaluation of the receptor function of the central nervous system (CNS) is an important field of radiopharmaceutical research, since abnormalities in density and activity of neuroreceptors are associated with a variety of neurological and psychiatric disorders. One of the serotonin receptor subtypes, 5-HT$_{1A}$, has, in particular, been implicated in depression, schizophrenia, dementia of the Alzheimer type, insomnia and anxiety [11.1–11.3].

The feasibility of studying receptors non-invasively in vivo has been demonstrated by positron emission tomography (PET) studies [11.4–11.6]. However, since single photon emission computed tomography (SPECT) is much more widely available than PET, many efforts have been focused on developing ^{99m}Tc agents for brain receptor imaging [11.7, 11.8].

A neuroreceptor imaging radiopharmaceutical must not only be able to bind selectively and with high affinity to the receptor but it should also reach its target by passing through the blood–brain barrier. The 3 + 1 mixed ligand approach [11.9], based on the simultaneous action of a dianionic tridentate ligand and a monodentate thiol as co-ligand on a suitable oxotechnetium precursor, offers easy and rational access to neutral Tc complexes, which are capable of crossing the intact blood–brain barrier [11.10]. Moreover, a wide variety of pharmacologically relevant groups [11.9, 11.11, 11.12] can be easily incorporated into the complex.

WAY 100635, a potent antagonist of pre- and post-synaptic 5-HT$_{1A}$ receptors, whose residue 1-(2-methoxyphenyl)piperazine is known to have a high affinity for 5-HT$_{1A}$ receptors, provides a good starting point for the development of potential radiotracers [11.13–11.15]. In order to imitate this prototypic organic compound, several neutral and lipophilic oxotechnetium complexes have been synthesized and evaluated as potential imaging agents for 5-HT$_{1A}$ receptors [11.16–11.18]. Fragments of WAY 100635 were combined with different tetradentate N$_2$S$_2$ chelates, such as amine amide dithiols or diamine dithiols, with different linkers between the receptor binding moiety, 1-(2-methoxyphenyl)piperazine, and the metal chelate. The major disadvantage of these compounds is their poor brain uptake in experimental animals, which precludes their usefulness as brain receptor imaging agents. This has been attributed mainly to their large molecular size.

The aim of this project was the design, synthesis, characterization and evaluation of novel neutral lipophilic ^{99m}Tc complexes for 5-HT$_{1A}$ receptor imaging. Two strategies were followed to achieve this objective: the 1-(2-methoxyphenyl)piperazine moiety of WAY 100635 was introduced either into the structure of the monodentate co-ligand or into the tridentate ligand.

The resulting co-ligand 1-(2-methoxyphenyl)-4-(2-mercaptoethyl)-piperazine (KH) was combined with four tridentate dianionic ligands (SNS and NNS) to produce complexes I–IV (Table 11.1).

The corresponding ligand 2-((2-mercaptoethyl)-(3-[4-(2-methoxy-phenyl)-piperazine-1-yl]propyl)amino)ethanethiol (L) was, on the other hand, co-ordinated to two commercially available aromatic monothiols, yielding complexes V and VI (Table 11.1).

TABLE 11.1. COMPLEXES STUDIED
(General formula: [(MO)LC] (M = Tc-o-Re))

Complex	Ligand	Co-ligand
I		
II		
III		
IV		
V		
VI		

11.2. MATERIALS

All laboratory chemicals were reagent grade and used without further purification. Solvents for chromatographic analysis were high performance liquid chromatography (HPLC) grade.

Sodium perrhenate was obtained from the Aldrich Chemical Co. $ReOCl_3(PPh_3)_2$ was prepared as described elsewhere [11.19]. $[^{99m}Tc]NaTcO_4$ was obtained from an Elumatic III generator (Cis Bio International, Gif-sur-Yvette, France). $[^3H]$-8-hydroxy-2-(di-N-propylamino)tetralin, $[^3H]$-8-OH-DPAT, of specific activity 124.9 Ci/mmol, was purchased from NEN Life Sciences Products, Inc. (Boston, MA).

HPLC analysis was performed on an LC-10 AS Shimadzu liquid chromatography system coupled to both an SPD-M10A Shimadzu photodiode array detector (UV trace for ^{99g}Tc, Re and ligands) and a Parken 3 in. × 3 in. (7.62 cm × 7.62 cm) NaI(Tl) crystal scintillation detector (gamma ray trace for ^{99m}Tc). Separations were achieved on a reverse phase µBondapack C18 column (3.9 mm × 300 mm), eluted with a binary gradient system at a flow rate of 1.0 mL/min. Mobile phase A is phosphate buffer pH7.4 with 2% triethylamine, while mobile phase B is methanol. The elution profile is: 0 min 0% phase B followed by a linear gradient to 85% phase B in 7 min; this composition was held for another 15 min.

Infrared spectra were obtained on a Bomen MB-102 FT-IR spectrophotometer. Elemental analysis was performed on a Carlo Erba EA 1108 analyser. Diffraction measurements were made on a Crystal Logic dual goniometer diffractometer. NMR spectra were obtained on a Bruker Avance 400 DPX spectrometer.

Activity measurements were performed either in a Capintec CRC-5R dose calibrator or in a scintillation counter, using a 3 in. × 3 in. (7.62 cm × 7.62 cm) NaI(Tl) crystal detector associated with an ORTEC monochannel analyser, or in a TRI-CARB 2100 TR beta counter.

11.3. METHODS

11.3.1. Synthesis and characterization of SNS and NNS ligands

The SNS ligands, N,N-bis(2-mercaptoethyl)-N′,N′ diethyl-ethylene-diamine (L_1) and N,N-bis(2-mercaptoethyl)-N′,N′-diisopropylethylene-diamine (L_2) were synthesized by reacting N,N-diethylethylene-diamine or N,N-diisopropyl-ethylene-diamine respectively, with ethylene sulphide in an autoclave at 110ºC, following the methods described by Corbin et al. [11.20].

The NNS ligands N-(2-mercaptoethyl)-N′,N′-diethylethylene-diamine (L$_3$) and N-(2-mercaptoethyl)-N′,N′-diisopropylethylene-diamine (L$_4$), which were also formed during the synthesis of L$_1$ and L$_2$, were purified by fractional distillation under high vacuum.

Each product was characterized by IR spectrometry, ^{1}H NMR and mass spectrometry.

11.3.2. Synthesis and characterization of the co-ligand with the pharmacophore moiety (K)

The synthesis of the co-ligand 1-(2-methoxyphenyl)-4-(2-mercaptoethyl)-piperazine (K) was done according to the same procedure described above by reacting 1-(2-methoxyphenyl)piperazine with ethylene sulphide in an autoclave at 110ºC. The product was purified by high vacuum distillation and characterized by IR spectrometry, ^{1}H NMR and mass spectrometry.

11.3.3. Synthesis and characterization of the ligand with the pharmacophore moiety (L)

The synthesis of the ligand 2-((2-mercaptoethyl)-(3-[4-(2-methoxy-phenyl)piperazine-1-yl]-propyl)-amino)-ethanethiol (L) was achieved by reacting 1-(2-methoxyphenyl)piperazine with 3-bromopropionitrile, followed by the reduction of the obtained nitrile with LiAlH$_4$.

The resulting amine was then reacted with ethylene sulphide in an autoclave at 110ºC, as described for the other ligands.

The SNS ligand with the pharmacophore moiety was purified in a chromatography column (silica gel 60 Fluka, 220–440 mesh), using ether and methanol in the ratio 2:1 as mobile phase.

11.3.4. Synthesis and characterization of the rhenium mixed complexes

Rhenium mixed ligand complexes were prepared by substitution using trichloro-bis-(triphenylphosphine rhenium) (V) oxide [ReOCl$_3$(PPh$_3$)$_2$], [11.19] as precursor. Table 11.1 shows the different complexes studied.

To a stirred suspension of 0.2 mmol of trichloro-bis-(triphenylphos-phine)-rhenium (V) oxide in methanol (10 mL), a 1N solution of CH$_3$COONa in methanol (2 mL, 2 mmol) was added. A mixture of 0.2 mmol of the corresponding ligand and 0.2 mmol of the co-ligand was added under stirring.

The solution was refluxed until the green yellow colour of the precursor turned to dark green. After cooling to room temperature, the reaction mixture was diluted with CH$_2$Cl$_2$ (30 mL) and then washed with water. The organic

layer was separated from the mixture and dried over MgSO$_4$. The volume of the solution was reduced to 5 mL, and then 5 mL of methanol was added.

Slow evaporation of the solvents at room temperature afforded the products of the reaction as green solids when ligands L$_1$ or L$_2$ were used. HPLC analysis of the crystals was performed and the UV–vis spectrum was recorded on-line. The IR spectrum was obtained from KBr pellets in the range 4000–200 cm^{-1}. Elemental analysis was also performed.

Thin layer chromatography (TLC) analysis of the organic layer using dichloromethane:methanol in the ratio 50:50 as eluting system was performed for complexes III and IV. Separation by a chromatographic column using silica gel 60 Fluka (220–440 mesh) and dichloromethane:methanol 50:50 was also developed.

11.3.5. Synthesis, evaluation and characterization of ^{99m}Tc complexes

Preparation of the complexes at tracer level was accomplished by using ^{99m}Tc-glucoheptonate as precursor. A vial containing a lyophilized mixture of 200 mg calcium glucoheptonate and 0.2 mg SnCl$_2$·2H$_2$O was reconstituted with 5 mL water, and 0.5 mL of this solution was mixed with [^{99m}Tc]NaTcO$_4$ (0.5–1 mL with an activity of 5–50 mCi (185–1850 MBq)). Substitution was performed at a co-ligand/ligand molar ratio of 1 for all the complexes, by adding the precursor (with radiochemical purity >95%) to a centrifuge tube containing a mixture of ligand and co-ligand in CH$_2$Cl$_2$. Different ligand and co-ligand concentrations (2×10^{-5}–0.2×10^{-7} mol) as well as temperatures and reaction times were assayed in order to optimize labelling conditions. The influence of the co-ligand/ligand ratio on the labelling was evaluated for complex IV. The mixture was agitated in a vortex mixer, the lipophilic species were extracted with CH$_2$Cl$_2$ and the organic layer was dried with MgSO$_4$, filtered and analysed by HPLC.

Characterization of the ^{99m}Tc complexes was accomplished by chromatographic correlation (HPLC) with the corresponding rhenium complexes.

Stability of the HPLC purified complexes in 25:75 methanol:saline was evaluated by HPLC using the above described conditions.

11.3.6. Biodistribution studies

Animal studies were approved by the Ethics Committee of the Faculty of Chemistry from the University of the Republic of Uruguay, Montevideo.

Normal mice (CD1, 25–30 g, four animals per group) were injected via a lateral tail vein with the HPLC purified ^{99m}Tc complexes I, II, III, V and VI reconstituted with 25:75 methanol:saline (0.1 mL, 2 µCi (0.074 MBq)). At

different intervals after injection (1–60 min) the animals were sacrificed by neck dislocation. Whole organs and samples of blood and muscle were collected, weighed and assayed for radioactivity. Total urine volume was collected during the biodistribution period and also removed from the bladder after sacrifice. The bladder, urine and intestines were not weighed. Corrections for different sample geometries were applied when necessary. Results were expressed as % dose/organ. The brain/blood ratio was calculated from the corresponding % dose/g values.

The biodistribution of radioactivity in various brain regions was developed in rats (Wistar, 250–300 g, three animals per group) at 5, 10, 60 and 120 min post-injection of the HPLC purified complexes (0.1 mL, 10 µCi (0.37 MBq)). The animals were sacrificed by neck dislocation, the whole brain was removed, and cortex, hippocampus and cerebellum were dissected, weighed and counted, and the % dose/g was calculated. Hippocampus/cerebellum and cortex/cerebellum ratios were also calculated from the corresponding % dose/g values. Student's test was applied to assess the significance of the differences in uptakes in different brain regions.

11.3.7. Receptor binding assays

11.3.7.1. Tissue preparation

Male Wistar rats (6 weeks old) were decapitated and their brains were rapidly chilled and dissected to obtain the hippocampi. The hippocampi were then homogenized in 50nM tris-HCl buffer pH7.6 (1:9, original wet weight:volume) using Ultra Turrax T-25 homogenizer (30 s, 20 000 rev./min). The tissue suspension was centrifuged (18 000g for 40 min at 4ºC) and the resulting pellet was resuspended in the same buffer. The process was repeated two additional times to wash the homogenate. The final pellet was resuspended in 5 mL and stored at –80ºC in 250 µL aliquots. The protein content was determined according to Lowry's method [11.21] using a protein determination kit containing bovine serum albumin as a standard.

11.3.7.2. In vitro binding studies

Competition binding experiments were performed in triplicates, using [^{3}H]-8-OH-DPAT as the radioligand. Briefly, aliquots (250 µL, corresponding to 50 µg of protein) of rat hippocampal homogenates were mixed with tris-HCl buffer (50mM tris-HCl, 0.1% ascorbic acid, 2mM CaCl$_2$, pH7.5), which contained 250 µL of [^{3}H]-8-OH-DPAT (0.14nM final concentration) and 250 µL of increasing concentrations (10^{-11}–10^{-6}M) of the competing rhenium

complexes (I and II). Non-specific binding was defined as the amount of activity bound in the presence of 10μM native 5-HT. After incubation for 20 min at 37ºC, a rapid filtration through GF/B glass fibre filters was performed on a Brandel Cell Harvester, and filters were rinsed four times with 3 mL of ice cold tris-HCl buffer (50mM tris-HCl, 154mM NaCl) and placed in a 10 mL scintillation cocktail. Radioactivity was measured by liquid scintillation using a beta counter (TRI-CARB 2100 TR with 60% efficiency). The results of competition experiments were subjected to non-linear regression analysis using the GraphPad computer software (Version 2.0) to calculate IC_{50} values.

11.4. RESULTS AND DISCUSSION

The 3 + 1 mixed ligand system was applied in order to synthesize neutral oxotechnetium complexes as potential 5-HT_{1A} receptor imaging agents. Two different design strategies according to the position of the 1-(2-methoxy-phenyl)piperazine moiety, the pharmacophore of the selective 5-HT_{1A} antagonist WAY 100635, were applied. One of them was to attach the pharma-cophore to a thiol group using an ethylene group as spacer, thus producing a monodentate co-ligand (K) which was combined with four different tridentate aminothiols. In the other approach a tridentate ligand was synthesized by attaching the 1-(2-methoxyphenyl)piperazine group to the nitrogen of an aminodithiol through an alkyl chain, and combined with monodentate aromatic thiols.

The analogous oxorhenium complexes were prepared by ligand exchange reaction in order to use them for structural characterization and in vitro binding assays. Complexes I and II were isolated as crystalline products in high yields (33 and 50%, respectively). They are neutral and lipophilic, as demon-strated by the quantitative extraction from the aqueous to the organic layer during the isolation process. Their IR spectra show characteristic peaks at 947 and 937 cm^{-1} for complex I and II, respectively, which can be attributed to metal–oxygen bond stretching [11.22–11.24]. The absence of bands associated with the SH stretching modes is a sign of the deprotonation of these groups upon complexation. Electronic absorption is characterized by an intense band in the region 380–400 nm probably due to S–Re charge transfer transitions [11.25], while absorption at shorter wavelengths corresponds to ligands and co-ligands. The results of ^{1}H NMR were consistent with the presence of one molecule of ligand and one of co-ligand per complex molecule. Elemental analysis results are also consistent with the proposed structures.
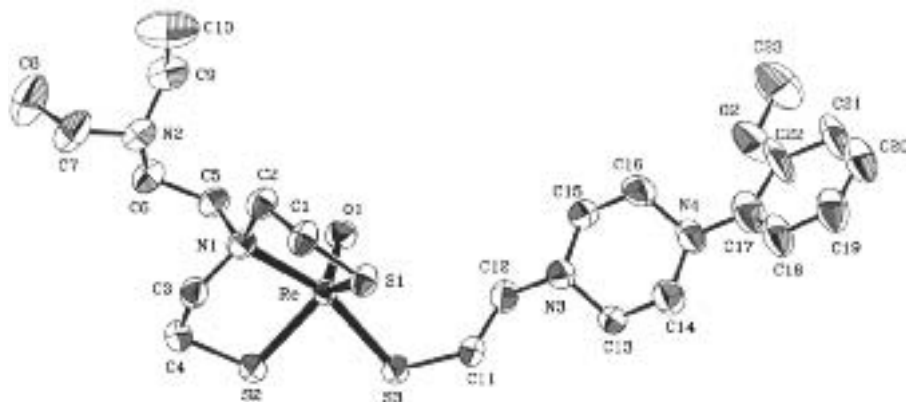
FIG. 11.1. ORTEP diagram of complex I.

X ray crystallographic studies were performed for complex I. An ORTEP (Oak Ridge thermal ellipsoid plot) diagram is given in Fig. 11.1. The sulphur atoms of the tridentate ligand and the oxo group are directed in the basal plane of a trigonal bipyramid, whereas the monodentate thiol and the nitrogen of the tridentate ligand occupy the apical positions. Ionization of the sulphur atoms led to a neutral compound.

Although crystals suitable for X rays were not obtained, previous experience with complexes with L_2 as ligands and aromatic thiols as co-ligands [11.26] suggests that complex II might have the same co-ordination geometry as complex I.

The oxorhenium complex III was prepared by combination of ligand L_3 and co-ligand K. TLC analysis showed two different species, which were separated by column chromatography. One of the complexes was isolated as a green powder with very low yield after evaporation from a mixture of methanol:isopropanol of 50:50. HPLC analysis revealed the presence of only one complex with ligand and co-ligand impurities. Recrystallization has not been possible so far and therefore the structure of this complex is still unknown.

Two different species were also formed by combination of L_4 and K (as demonstrated by TLC analysis). Column chromatography was also developed in order to separate them, but one of the complexes could not be eluted from the column while the other decomposed when it was left for crystallization.

The ^{99m}Tc complexes I, II and III were obtained in high yield (>80%, determined by dichloromethane extraction) and with high radiochemical purity (>90%, determined by HPLC), using a very low concentration of the

co-ligand that carries the pharmacophore group (Table 11.2). The radioactivity recovery from the column after injection of complexes was monitored and found to be quantitative.

Complex IV was prepared at tracer level using different co-ligand/ligand ratios (Table 11.2). In all these conditions three labelled species were formed, as shown by HPLC analysis. The radiochemical purities of all of them were very low. Consequently, studies with these species were not continued.

For complexes V and VI, dichloromethane extraction was higher than 80%, showing a main peak in HPLC with a radiochemical purity higher than 70%.

In order to establish the structural analogy between the ^{99m}Tc complexes with the respective oxorhenium complexes prepared in macroscopic amounts, comparison by HPLC adopting parallel radiometric and photometric detection was pursued. Thus, by co-injection of the oxorhenium and oxotechnetium-99m complexes, identical retention times were exhibited, revealing their structural analogy.

Stability studies of the HPLC purified ^{99m}Tc complexes reconstituted in 25:75 methanol:saline were developed as a previous step for biodistribution studies. No significant decomposition was observed for at least 2 h. Biological studies were performed within this period.

The biodistributions of ^{99m}Tc complexes I, II, III, V and VI were evaluated in mice between 1 and 60 min post-injection. Tables 11.3–11.6 show

TABLE 11.2. LABELLING CONDITIONS

Complex	Ligand (mol)	Co-ligand/ ligand ratio	Temperature (°C)	Yield (%)
I	2×10^{-7}	1	50–60	>90
II	2×10^{-6}	1	50–60	>90
III	2×10^{-6}	1	Room	>80
IV	2×10^{-6}	1	Room	>80
	2×10^{-6}	4	Room	>80
	2×10^{-6}	10	Room	>80
	2×10^{-6}	0.25	Room	>80
V	1×10^{-5}	1	Room	>80
VI	1×10^{-5}	1	Room	>80

TABLE 11.3. BIODISTRIBUTION RESULTS IN MICE (% DOSE/ORGAN ± σ) FOR ^{99m}Tc COMPLEX I AT VARIOUS TIMES POST-INJECTION

Region	1 min	5 min	30 min	60 min
Blood	21.5 ± 4.4	15.3 ± 2.9	11.7 ± 1.4	4.8 ± 0.8
Liver	23.6 ± 2.3	26.0 ± 1.9	33.9 ± 2.8	27.7 ± 2.0
Lungs	8.9 ± 1.8	5.6 ± 0.9	5.5 ± 0.8	3.8 ± 0.9
Thyroid	0.3 ± 0.08	0.4 ± 0.09	0.3 ± 0.08	0.2 ± 0.04
Intestines	7.9 ± 1.2	9.3 ± 0.6	15.2 ± 2.9	21.4 ± 2.7
Urine	0.8 ± 0.2	1.8 ± 0.7	6.3 ± 1.1	12.1 ± 1.1
Brain	0.5 ± 0.1	0.6 ± 0.2	0.5 ± 0.1	0.3 ± 0.1
Brain (% dose/g)	1.6 ±0.5	1.5 ± 0.3	1.6 ± 0.5	0.6 ± 0.1
Brain/blood	0.14	0.17	0.17	0.15

TABLE 11.4. BIODISTRIBUTION RESULTS IN MICE (% DOSE/ORGAN ± σ) FOR ^{99m}Tc COMPLEX II AT VARIOUS TIMES POST-INJECTION

Region	1 min	5 min	30 min	60 min
Blood	17.6 ± 3.6	8.2 ± 3.0	10.4 ± 2.4	8.1 ± 2.9
Liver	14.4 ± 4.1	19.2 ± 2.7	27.2 ± 3.1	24.5 ± 3.7
Lungs	8.0 ± 2.1	6.6 ± 1.8	5.2 ± 1.9	4.5 ± 2.3
Thyroid	0.6 ± 0.1	0.4 ± 0.1	0.18 ± 0.07	0.16 ± 0.05
Intestines	10.5 ± 1.4	13.4 ± 2.8	18.8 ± 2.4	29.1 ± 3.3
Urine	0.5 ± 0.05	1.0 ± 0.1	6.5 ± 0.2	10.6 ± 2.1
Brain	0.4 ± 0.1	0.3 ± 0.05	0.3 ± 0.06	0.2 ± 0.02
Brain (% dose/g)	0.9 ± 0.3	0.6 ± 0.1	0.6 ± 0.1	0.4 ± 0.1
Brain/blood	0.09	0.14	0.11	0.09

the results expressed as % dose/organ in the most significant organs as a function of time. All complexes have high initial blood, lung and liver uptakes, as expected from lipophilic compounds. Blood clearance is quite fast for complexes I, II, V and VI, while activity remains almost constant for complex III over the period studied. Excretion occurs mainly through the hepatobiliary tract with some urinary elimination. Thyroid activities are very low, indicating minimal in vivo reoxidation.

TABLE 11.5. BIODISTRIBUTION RESULTS IN MICE (% DOSE/ORGAN $\pm \sigma$) FOR ^{99m}Tc COMPLEX III AT VARIOUS TIMES POST-INJECTION

Region	1 min	5 min	30 min	60 min
Blood	28.1 ± 2.4	34.8 ± 5.7	38.1 ± 7.1	16.8 ± 5.5
Liver	16.6 ± 1.7	14.4 ± 1.9	16.3 ± 0.7	22.0 ± 2.3
Lungs	4.0 ± 0.75	2.6 ± 0.4	2.6 ± 0.2	2.3 ± 0.1
Thyroid	0.18 ± 0.04	0.16 ± 0.05	0.15 ± 0.04	0.18 ± 0.05
Intestines	6.2 ± 1.1	5.3 ± 1.2	5.8 ± 0.2	16.8 ± 0.05
Urine	0.7 ± 0.2	0.6 ± 0.1	1.9 ± 0.6	5.3 ± 2.5
Brain	0.55 ± 0.06	0.54 ± 0.05	0.38 ± 0.02	0.45 ± 0.04
Brain (% dose/g)	1.3 ± 0.1	1.3 ± 0.2	0.79 ± 0.01	1.0 ± 0.1
Brain/blood	0.07	0.06	0.04	0.09

TABLE 11.6. BIODISTRIBUTION RESULTS IN MICE (% DOSE/ORGAN $\pm \sigma$) FOR ^{99m}Tc COMPLEXES V AND VI AT VARIOUS TIMES POST-INJECTION

Region	Complex V				Complex VI	
	1 min	5 min	30 min	60 min	5 min	30 min
Blood	31.4 ± 0.5	14.3 ± 3.9	8.3 ± 0.3	7.8 ± 2.0	11.7 ± 1.6	8.7 ± 1.2
Liver	23.0 ± 6.7	22.4 ± 4.8	24.6 ± 2.5	33.2 ± 4.4	22.9 ± 2.8	21.9 ± 0.3
Lungs	5.3 ± 0.8	3.3 ± 1.0	2.1 ± 0.8	1.7 ± 0.3	1.9 ± 0.3	1.2 ± 0.2
Thyroid	0.6 ± 0.3	0.4 ± 0.1	0.4 ± 0.2	0.5 ± 0.1	0.4 ± 0.1	0.5 ± 0.1
Intestines	9.7 ± 2.4	8.9 ± 1.5	16.7 ± 3.1	33.2 ± 1.3	12.2 ± 0.4	18.0 ±1.3
Urine	0.26 ± 0.05	1.6 ± 0.6	3.6 ± 0.5	4.9 ± 2.5	1.4 ± 0.7	1.8 ± 0.1
Brain	0.6 ± 0.2	0.27 ± 0.07	0.21 ± 0.06	0.19 ± 0.07	0.19 ± 0.03	0.17 ± 0.01
Brain (% dose/g)	1.1 ± 0.4	0.6 ± 0.2	0.5 ± 0.2	0.5 ± 0.2	0.40 ± 0.06	0.36 ± 0.05
Brain/blood	0.14	0.08	0.10	0.10	0.11	0.11

Brain uptake and retention is significant for all the compounds studied. Complexes I and II show the highest brain uptake as well as the best brain/blood ratios. Consequently, regional brain uptake studies were performed in rats at between 5 and 120 min post-injection.

Percentage dose/g in receptor-rich brain regions such as hippocampus and cortex as well as in receptor-poor cerebellum are presented in Tables 11.7 and 11.8. Uptake in the hippocampus of complex I was significantly higher in comparison with cerebellum ($P = 0.05$) at one hour post-injection, resulting in a hippocampus/cerebellum ratio of 1.7. The uptake of complex II in hippocampus and cortex was not significantly higher in comparison to cerebellum ($P = 0.05$) from 1–120 min post-injection.

The differences in the distributions of these complexes in various brain regions may be attributed to their different rates of in vivo conversion by endogenous glutathione. It is known that the rate of this conversion is greatly influenced by small structural variations [11.27, 11.28]. Since the brain uptake of the complexes studied and their affinity for the 5-HT$_{1A}$ receptors are moderate, we did not proceed further to investigate the effect of the in vivo stability of these complexes on their in vivo behaviour.

TABLE 11.7. REGIONAL DISTRIBUTION OF ACTIVITY IN RAT BRAINS (% DOSE/g ± σ) FOR COMPLEX I AT VARIOUS TIMES POST-INJECTION

Region	5 min	15 min	60 min	120 min
Cerebellum	0.226 ± 0.005	0.181 ± 0.01	0.063 ± 0.005	0.036 ± 0.01
Hippocampus	0.216 ± 0.007	0.165 ± 0.02	0.104 ± 0.02	0.057 ± 0.02
Cortex	0.230 ± 0.02	0.188 ± 0.02	0.053 ± 0.003	0.038 ± 0.006
Hippocampus/cerebellum	0.95 ± 0.05	0.91 ± 0.07	1.67 ± 0.44	1.57 ± 0.12
Cortex/cerebellum	1.0 ± 0.07	1.04 ± 0.10	0.84 ± 0.05	1.05 ± 0.12

TABLE 11.8. REGIONAL DISTRIBUTION OF ACTIVITY IN RAT BRAINS (% DOSE/g ± σ) FOR COMPLEX II AT VARIOUS TIMES POST-INJECTION

Region	5 min	15 min	60 min	120 min
Cerebellum	0.086 ± 0.02	0.060 ± 0.009	0.062 ± 0.01	0.027 ± 0.003
Hippocampus	0.049 ± 0.01	0.038 ± 0.01	0.095 ± 0.02	0.025 ± 0.006
Cortex	0.065 ± 0.01	0.052 ± 0.007	0.089 ± 0.03	0.051 ± 0.004
Hippocampus/cerebellum	0.58 ± 0.10	0.62 ± 0.07	1.53 ± 0.35	0.93 ± 0.10
Cortex/cerebellum	0.77 ± 0.09	0.88 ± 0.14	1.43 ± 0.40	1.89 ± 0.07
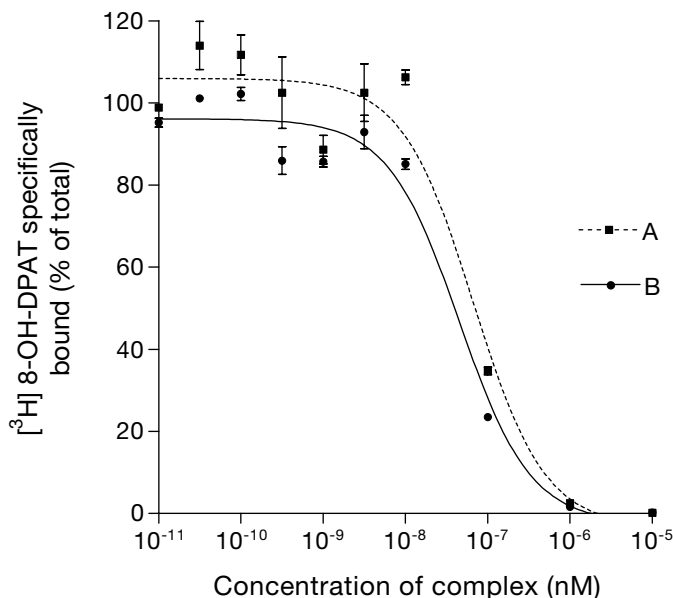
FIG. 11.2. Ability of the oxorhenium complexes I (curve A) and II (curve B) to inhibit binding of the agonist [^{3}H]-8-OH-DPAT in rat brain hippocampal homogenates.

The affinity of the rhenium complexes I and II for the 5-HT$_{1A}$ receptors was assessed in vitro on the basis of their ability to compete with the [^{3}H]-8-OH-DPAT binding to rat hippocampal tissue homogenate. The representative competition curves shown in Fig. 11.2 demonstrate that addition of increasing doses of both complexes induced a dose dependent displacement of the specific binding of [^{3}H]-8-OH-DPAT to 5-HT$_{1A}$ binding sites. The IC$_{50}$ values are 67 ± 4 and 45 ± 3nM for complexes I and II, respectively.

11.5. CONCLUSIONS

The 3 + 1 ligand system has been successfully applied, and six novel neutral mixed ligand oxorhenium and oxotechnetium-99m complexes carrying the 1-(2-methoxyphenyl)piperazine moiety, a fragment of the true 5-HT$_{1A}$ antagonist WAY 100635, either on the monodentate ligand or on the tridentate ligand, have been synthesized. Two of them have been fully characterized at carrier level. Characterization of the other complexes is being carried out.

Labelling procedures with ^{99m}Tc using very small concentrations of the co-ligand were developed and optimized for complexes I, II, III, V and VI. The expected complexes were obtained with high yield and radiochemical purity. All the ^{99m}Tc complexes studied were capable of penetrating the intact blood–brain barrier. Complex I showed a higher brain uptake, as well as significant accumulation in 5-HT$_{1A}$ receptor-rich hippocampus at one hour post-injection.

Oxorhenium complexes I and II showed an affinity for the 5-HT$_{1A}$ receptor binding sites with IC$_{50}$ values in the nanomolar range, as demonstrated by appropriate competition binding tests in rat hippocampal preparations.

Our results demonstrate the potential of the mixed ligand approach for the design of ^{99m}Tc complexes with the ability to bind neuroreceptors. However, the goal of imaging 5-HT$_{1A}$ receptors with technetium requires further development of complexes with improved biological profiles.

ACKNOWLEDGEMENTS

REFERENCES TO CHAPTER 11

[11.1] CORYELL, W., The treatment of psychotic depression, J. Clin. Psychiatry **1** (1998) 22–27.

[11.2] FRAZER, A., MAAYANI, S., WOLF, B., Subtypes of receptors for serotonin, Annu. Rev. Pharmacol. Toxicol. **30** (1990) 307–348.

[11.3] FULLER, R., Serotonin uptake inhibitors: Uses in clinical therapy and in laboratory research, Prog. Drug Res. **45** (1995) 167–204.

[11.4] FARDE, L., et al., Substituted benzamides as ligands for visualization of dopamine receptor binding in the human brain by positron emission tomography, Proc. Natl. Acad. Sci. **82** (1985) 3863.

[11.5] KIESEWETTER, D., et al., Preparation of ^{18}F-labelled muscarinic agonist with M2 selectivity, J. Med. Chem. **38** (1995) 5–8.

[11.6] WAGNER, H., et al., Imaging dopamine receptors in the human brain by positron tomography, Science **222** (1983) 1264–1266.

[11.7] KUNG, H., et al., Imaging of dopamine transporters in humans with technetium-99m TRODAT-1, Eur. J. Nucl. Med. **23** (1996) 1527–1530.

[11.8] LEVER, S., et al., Novel technetium ligands with high affinity for muscarinic cholinergic receptor, Nucl. Med. Biol. **21** (1994) 157–164.

[11.9] SPIES, H., PIETZSCH, H.-J., JOHANNSEN, B., "The "$n + 1$" mixed ligand approach in the design of specific technetium radiopharmaceuticals: Potential and problems", Technetium, Rhenium and other Metals in Chemistry and Nuclear Medicine (NICOLINI, M., MAZZI, U., Eds), SGE, Padua (1999) 101–108.

[11.10] PIRMETTIS, I., PAPADOPOULOS, M., CHIOTELLIS, E., Novel ^{99m}Tc aminobisthiolato/monothiolato "3 + 1" mixed ligand complexes: Structure–activity relationships and preliminary in vivo validation as brain blood flow imaging agents, J. Med. Chem. **40** (1997) 2539–2546.

[11.11] JOHANNSEN, B., Technetium (V) and rhenium (V) complexes for the 5-HT$_{2A}$ serotonin receptor binding: Structure–affinity considerations, Nucl. Med. Biol. **23** (1996) 429–438.

[11.12] PIRMETTIS, I., et al., Synthesis of oxorhenium (V) and oxotechnetium (V) [SN(R)S][S] mixed ligand complexes containing a phenothiazine moiety on the tridentate SN(R)S ligand, Bioorg. Med. Chem. Lett. **11** (2001) 1859–1862.

[11.13] WUST, F., SPIES, H., JOHANNSEN, B., Synthesis of "3 + 1" mixed ligand oxorhenium complexes containing modified 3,17β-estradiol, Bioorg. Med. Chem. Lett. **6** (1996) 2729–2734.

[11.14] CLIFFE, I., "The design of selective 5-HT$_{1A}$ receptor antagonists", Proc. 206th Natl. Mtg of the American Chemical Society, Chicago, IL, 1993 (abstract).

[11.15] FLETCHER, A., CLIFFE, I., DOURISH, C., Silent 5-HT$_{1A}$ receptor antagonists: Utility as research tools and therapeutic agents, TIPS **14** (1993) 441–447.

[11.16] KUNG, H., et al., "New TcO(III) and ReO(III)N$_2$S$_2$ complexes as potential CNS 5-HT$_{1A}$ receptor imaging agents", Technetium and Rhenium in Chemistry and Nuclear Medicine (NICOLINI, M., BANDOLI, G., MAZZI, U., Eds), SGE, Padua (1995) 293–298.

[11.17] MAHMOOD, A., et al., "Technetium (V) and rhenium (V) analogues of WAY 100635 5-HT$_{1A}$ receptor-binding complexes", Technetium, Rhenium and other Metals in Chemistry and Nuclear Medicine (NICOLINI, M., MAZZI, U., Eds), SGE, Padua (1999) 393–399.

[11.18] VANBILLOEN, H., CLEYNHENS, B., CROMBEZ, D., VERBRUGGEN, A.M., "Synthesis and biological evaluation of a conjugate of ^{99m}Tc-ECC with 1-(2-methoxyphenyl)-4-(2-pyridylamino)ethylpiperazine (WAY 100634)", ibid., pp. 479–484.

[11.19] CHATT, J., ROWE, G., Complex compounds of tertiary phosphines and a tertiary arsine with rhenium (V), rhenium (III) and rhenium (II), J. Chem. Soc. **4** (1962) 4019–4033.

[11.20] CORBIN, J., et al., Preparation and properties of tripodal and linear tetradentate N,S-donor ligands and their complexes containing the MoO$_2^{2+}$ core, Inorg. Chim. Acta. **90** (1984) 41–51.

[11.21] LOWRY, O., ROSEBROUGH, N., FARR, A., RANDALL, R., Protein measurement with the Folin phenol reagent, J. Biol. Chem. **193** (1951) 265–275.

[11.22] PAPADOPOULOS, M., et al., Syn–anti isomerism in a mixed-ligand oxorhenium complex, ReO[SN(R)S][S], Inorg. Chem. **37** 25 (1996) 7377–7383.

[11.23] REISGYS, M., SPIES, H., JOHANNSEN, B., LEIBNITZ, P., PIETZSCH, H., Synthesis and structural characterization of mixed-ligand oxorhenium (V) complexes containing bidentate dithioethers and monothiolato ligands, Ber. Recueil. **130** (1997) 1343–1347.

[11.24] ROUSCHIAS, G., Recent advances in the chemistry of rhenium, Chem. Rev. **74** 5 (1974) 531–566.

[11.25] FRANCESCONI, L., et al., Synthesis and characterization of neutral M^VO (M = Tc, Re) amine-thiol complexes containing a pendant phenylpiperidine group, Inorg. Chem. **32** (1993) 3114–3124.

[11.26] REY, A., et al., Oxorhenium and oxotechnetium [SNS/S] mixed ligand complexes having a pendant diisopropylaminoethyl-group: Synthesis, characterization and biodistribution studies, J. Labelled Compd. Radiopharm. **43** (2000) 347–358.

[11.27] NOCK, B., et al., Glutathione-mediated metabolism of technetium-99m SNS/S mixed ligand complexes, J. Med. Chem. **42** (1999) 1066–1075.

[11.28] SYHRE, R., SEIFERT, S., SPIES, H., GUPTA, A., JOHANNSEN, B., Stability versus reactivity of "3 + 1" mixed ligand technetium-99m complexes in vitro and in vivo, Eur. J. Nucl. Med. **25** (1998) 793–796.

LIST OF PARTICIPANTS

Alba, S.L.C.   Facultad de Química, Universidad de la República,
                                Gral Flores 2124, C.C. 1157, Montevideo, Uruguay

Alberto, R.   Paul Scherrer Institute,
                                Division of Radiopharmacy,
                                CH-5232 Villigen-PSI, Switzerland

Arencibia, J.C.   Centro de Isótopos,
                                Ave. Monumental y Carretera La Rada,
                                Guanabacoa, AP 22,
                                Havana, Cuba

Bodó, K.   Frédéric Joliot-Curie National Research Institute
                                    for Radiobiology and Radiohygiene,
                                Anna Strasse 5, P.O. Box 101,
                                H-1775 Budapest, Hungary

Carvalho, O.   Instituto de Pesquisas Energéticas e Nucleares,
                                Commissão Nacional de Energia Nuclear,
                                Travessa R, 400 Cidade Universitaria,
                                P.O. Box 11049, 05433-970 Pinheiros,
                                São Paulo, Brazil

He, Youfeng   China Institute of Atomic Energy, P.O. Box 275-39,
                                Beijing 102413, China

Johanssen, B.   Forschungszentrum Rossendorf,
                                Institut für Bioanorganische und
                                    Radiopharmazeutische Chemie,
                                Postfach 510119, D-01314 Dresden, Germany

Kyung Bae Park   Korea Atomic Energy Institute,
                                Radioisotope Department, Hanaro Centre,
                                P.O. Box 105, Yuseong,
                                Taejon 305-600, Republic of Korea

Narasimhan, D.V.S.   International Atomic Energy Agency,
                                Wagramerstrasse 5, P.O. Box 100,
                                A-1400 Vienna, Austria

Papadopoulos, M.   Demokritos National Centre
                                    for Scientific Research,
                                Radiopharmaceuticals Laboratory of the Institute
                                    of Radioisotopes and Radiodiagnostic Products,
                                GR-153 10 Aghia Paraskevi, Athens, Greece

Sivaprasad, N.

Board of Radiation and Isotope Technology,
Department of Atomic Energy, BARC Vashi
   Complex, Sector 20,
Navi Mumbai 400705, India